STANDARDIZING THE SPECIFICATIONS OF A BIOGAS RUN DUAL FUEL DIESEL ENGINE FOR STATIONARY APPLICATIONS

A Thesis
Submitted in Partial Fulfillment of the Requirements for
the Award of the Degree of

DOCTOR OF PHILOSOPHY

By

Bhaskor Jyoti Bora

DEPARTMENT OF MECHANICAL ENGINEERING
INDIAN INSTITUTE OF TECHNOLOGY GUWAHATI
GUWAHATI - 781039, INDIA
July, 2015

Dedicated to my Parents…

Ms. Anjana Bora

&

Mr. Debendra Nath Bora

Declaration

I hereby certify that the work presented in this thesis entitled '**STANDARDIZING THE SPECIFICATIONS OF A BIOGAS RUN DUAL FUEL DIESEL ENGINE FOR STATIONARY APPLICATIONS**' is entirely my own account of research performed under the guidance of Professor Ujjwal K. Saha. Any part of this work has not earlier been submitted for the award of any degree, diploma, associate-ship, fellowship or its equivalent to any University or Institution.

Date:

(Bhaskor Jyoti Bora)
Registration No. 11610309
Department of Mechanical Engineering
Indian Institute of Technology Guwahati
Guwahati – 781039, India

Department of Mechanical Engineering
Indian Institute of Technology Guwahati
Guwahati – 781039,
India

Certificate

It is certified that the work presented in the thesis entitled '**STANDARDIZING THE SPECIFICATIONS Of A BIOGAS RUN DUAL FUEL DIESEL ENGINE FOR STATIONARY APPLICATIONS**' submitted by **Mr. Bhaskor Jyoti Bora,** a student in the Mechanical Engineering Department**,** Indian Institute of Technology Guwahati, India for the award of the degree of Doctor of Philosophy has been carried out under my supervision. This work has not been submitted previously elsewhere for the award of any other degree or diploma.

Date:

(Ujjwal K. Saha)
Professor
Department of Mechanical Engineering
Indian Institute of Technology Guwahati
Guwahati – 781039, India

Abstract

Diesel engines have played an important role in the progress of humankind. They are the most reliable and efficient means of producing power. However, these engines are plagued by high emissions of oxides of nitrogen and soot that possess a serious threat to human health. In this context, dual fuel technology has been recognized as one of the panaceas to the above mentioned problem. Dual fuelling in diesel engines is a mode of combustion where a small pilot injection of high cetane fuel ignites a premixed high octane gaseous fuel and air mixture. The liquid fuel is called the pilot fuel and the gaseous fuel is called the primary fuel. Among the different types of primary fuel tested in dual fuel engines, biogas has emerged as a low cost renewable fuel. For conserving energy and protecting the global environment, biogas is a promising alternative fuel demonstrating high hydrogen to carbon ratio. The chief constituents of biogas are methane and carbon dioxide, which is produced by anaerobic digestion of biomass. Biogas has a higher octane number giving higher resistance to knock which allows it to be utilized in high compression ratio engines. Thus, biogas presents a promising prospect of utilizing dual fuel combustion in diesel engines which can significantly lower the oxides of nitrogen (NO_X) and soot emissions compared to that of tradition diesel engine. However, running biogas along with any liquid fuel at standard diesel setting will not offer the best performance. This is because the combination of biogas along with any liquid fuel does not have the same properties to that of diesel. Therefore, it becomes important to study and optimize the performance and emission characteristics of a biogas run dual fuel diesel engine at varied operating conditions, namely, load, compression ratio (CR) and injection timing (IT). The motivation behind this research work is to use dual fuel diesel engines for power generation in rural areas particularly for developing countries like India.

First of all, a comparative study of performance of three types of pilot fuel, namely palm biodiesel (PBD), Pongamia biodiesel (POBD) and rice bran biodiesel (RBB) is carried out to evaluate the best combination of pilot fuel with biogas. The selection of pilot fuel is based on the availability criteria related to the present geographical location. For experimentation, a 3.5 kW single cylinder, four-stroke, direct injection, naturally aspirated, water-cooled, variable compression ratio diesel engine diesel engine is converted into a biogas run dual fuel diesel engine by connecting a venturi gas mixer at its inlet manifold and installing a fuel control mechanism. The performance analyses evaluated are brake thermal efficiency, brake specific energy consumption, volumetric efficiency, exhaust gas temperature, liquid fuel

replacement and biogas flow rate. The combustion analyses include the cylinder pressure variation, ignition delay, net heat release rate and peak cylinder pressure. Finally, emission analysis is performed by measuring carbon dioxide, carbon monoxide, hydrocarbon and NO_X. The results indicated the combination of RBB-biogas is found to be superior in comparison to that of PBD-biogas and POBD-biogas at standard diesel setting.

This is followed by an investigation to standardize the operating parameters of the biogas run dual fuel diesel using diesel, RBB and emulsified RBB as pilot fuel. Initially, a two-phase stable water emulsion of RBB has been prepared by optimizing the factors such as water content (5%and 10%), surfactants (3%), and hydrophilic lipophilic balance values (4.3, 5, and 6). For engine test, a set of combinations comprising CR of 18, 17.5, and 17, and IT of 23°, 26°, 29°, and 32° BTDC at different loading conditions are considered. The optimum combinations for a biogas run dual fuel diesel engine using diesel, RBB and emulsified RBB as pilot fuel are found to be CR=18, IT=29° BTDC; CR=18, IT=32° BTDC and CR=18, IT=29° BTDC, respectively.

Lastly, a thermodynamic analysis for the aforementioned tests is carried out to unravel the effect of operating parameters on the energy and exergy distributions of the biogas run dual fuel diesel engine. It includes the first and second law analysis of the biogas run dual fuel diesel engine at different combinations CR and IT for the load where maximum brake thermal efficiency take place. The energy and exergy analyses reveal that the use of high CR along with advancement of IT of pilot fuel is a must for effectual utilization of fuel in a biogas run dual fuel diesel engine irrespective of the pilot fuel.

Keywords: Biogas, Biodiesel, Emulsion, Dual fuel diesel engine, Compression ratio, Injection timing, Exergy

Acknowledgements

The Ph.D tenure has been a great learning experience for me, which is full of support and encouragement from numerous individuals. They were beside me during the happy and hard moments to motivate me. It is an extreme pleasure to express my thanks to all those who contributed in many ways to made this thesis possible.

I take this opportunity to sincerely acknowledge the Indian Institute of Technology Guwahati for providing me with such as excellent environment for conducting my research. I would like to express my special appreciation and thanks to my supervisor Prof. Ujjwal K. Saha for his continuous support, encouragement and active guidance at every stage of this endeavour. His tremendous skill of organization, planning and management had enabled me to seek the absolute goal of the research. The best thing that I liked about him is his mesmerizing ability to give inspiration talks.

I wish to express my heartfelt gratitude to Prof. Anoop K. Dass (HOD, Mechanical Engineering Department) and Prof. Debrabrata Chakraborty (Dean, R & D) for providing all the research facilities and financial support. I have had the pleasure of association with the members of doctoral committee viz., Prof. Pinakeshwar Mahanta, Dr. Subrata K. Mazumder and Dr. Vinayak Kulkari who all have given me many useful suggestions. Their encouragement is highly acknowledged. It is my pleasure to thank Prof. Anoop K. Dass, Prof. Uday S. Dixit, Dr. Ashis Sen, Dr. Chandramohan Somayaji, Dr. Ganesh Natarajan and Dr. G. Madhusudhana for their excellent teaching during the course work. I am thankful to Dr. S. Kanagaraj, who has permitted me to work in Material Science Laboratory of Mechanical Engineering Department. Special thanks to Dr. Kaustubha Mohanty and Dr. Rajesh Kumar Upadhyay for allowing me to avail the facilities in the Petroleum Laboratory of Chemical Engineering Department.

I would like to thank all the faculty members, and staffs of Mechanical Engineering Department for rendering their whole hearted cooperation and support in the entire course of work. A word of appreciation goes to the senior technician and technical support staff of Mechanical Engineering Department viz., Mr. Dillip Chetri, Mr. Mrinal Sharma, Mr. Jaikrishna Saikia, Mr. Nip Bora, Mr. Saiffuddin Ahmed and Mr. Dhiren Huzuri of Centre for Energy. I am thankful to Scientific Officers, Mr. Rituraj Saikia and Mr. Pranjol Paul of Mechanical Engineering Department for their enthusiastic support for various apparatus

purchase and laboratory necessitates. Special thanks go to Mr. Vidya Sagar Nath (General Manager for Kirloskar Oil India Ltd., India) for his special assistance during engine troubleshooting. I would also like to thank Mr. Supratim Duwarah and Mr. Ratul Kumar Das for helping me in procuring biodiesel.

I am thankful to my seniors and my colleague Dr. Biplab K. Debnath, Dr. Pankaj Kalita, Dr. Sukanta Roy, Mr. Ashif Iqbal, Mr. Achinta Sarkar, Mr. Biplab Das, Ms. Debaleena Chakraborty, Mr. Debarshi Mallick, Mr. Hakeem Niyas, Mr. Kalpajyoti Borah, Mr. Maryom Dabi, Ms. Mayuri Baruah, Mr. Paragmoni Kalita, Mr. Prasenjit Mukherjee, Mr. Parag Kamal Talukdar, Mr. Rasmi Ranjan Bahera, Mr. Subra Sankar Kalita, Mr. Sumit Agarwal and Mr. Shuvayan Brahmachary for enriching my life with their bond of friendship. Their encouragement is greatly acknowledged.

I am grateful to MHRD, Govt. of India, for providing me financial support through DST to attend and present a technical paper in ASME 12th Biennial Conference on Engineering Systems Design and Analysis, held at Copenhagen, Denmark during June 25-27, 2014. I am thankful to the Defence Research Laboratory, DRDO, Assam, India, for funding my research.

I would like to thank my parents, Ms. Anjana Bora and Mr. Debendra Nath Bora for all their love and encouragement. I feel proud for them for their patience in times when I was unable to spend even a single week at a stretch with them during the last four years. Special thanks go to my sister Ms. Anupama Bora Dass, my brother-in-law Mr. Mridul Ranjan Dass, my sister-in-law Ms. Chinmayee Das Bora and my brother Mr. Manas Ranjan Bora for their continual support and love. I would also like to express my gratitude to my close friends, Mr. Dipal Baruah and Mr. Anup Kumar Bharali for their continuous inspiration and support. I would like to express appreciation to my beloved fiance Ms. Manashi Nath for her constant support in the moments when there was no one to answer my queries and encouraged me throughout this endeavour.

Lastly, I am and always be thankful to God for guiding me through this testing period of my life. I will be grateful to Him who has destined my life to be a part of Indian Institute of Technology Guwahati.

July, 2015

Bhaskor Jyoti Bora
Guwahati, India

CONTENTS

NOMENCLATURE

Abbreviations			
AFR	Air Flow Rate (kg /h)	HC	Hydrocarbon
ATDC	After Top Dead Centre	HHV	High Heating Value (MJ/kg)
BP	Brake Power (kW)	HLB	Hydrophilic Lipophilic Balance
BFR	Biogas Flow Rate (kg/h)	HRR	Heat Release Rate (J/Deg.CA)
BMEP	Brake Mean Effective Pressure (bar)	IC	Internal Combustion
BSCO	Brake Specific Carbon Monoxide (g/kWh)	ID	Ignition Delay (ms)
$BSCO_2$	Brake Specific Carbon Dioxide (g/kWh)	IT	Injection Timing (Deg.CA)
BSHC	Brake Specific Hydrocarbon (g/kWh)	KME	Karanja Methyl Ester
BSEC	Brake Specific Energy Consumption(kJ/s/kW)	LFR	Liquid Fuel Replacement (%)
BSFC	Brake Specific Fuel Consumption (kg/s/kW)	LHR	Low heat rejection
BSNO	Brake Specific Nitrous Oxide (g/kWh)	LHV_{bg}	Lower Heating Value of Biogas (MJ/kg)
BTDC	Before Top Dead Centre	LHV_{di}	Lower Heating Value of Diesel (MJ/kg)
BTE	Brake Thermal Efficiency (%)	LHV_{f}	Lower Heating Value of Fuel (MJ/kg)
CA	Crank Angle (Degree)	LHV_{p}	Lower Heating Value of Pilot Fuel (MJ/kg)
CH_4	Methane	LHV_{WIRBB}	Lower Heating Value of WIRBB (MJ/kg)
CFD	Computational Fluid Dynamics	NA	Naturally Aspirated
CI	Compression Ignition	NHRR	Net Heat Release Rate (J/Deg.CA)
CNG	Compressed Natural Gas	NO_X	Oxides of Nitrogen
CNT	Carbon Nano Tubes	PBD	Palm Biodiesel
CR	Compression Ratio	PCP	Peak Cylinder Pressure (bar)
DAD	Data Acquisition Device	PHRR	Peak Heat Release Rate (J/Deg.CA)
DI	Direct Injection	POBD	Pongamia Biodiesel
DFM	Dual Fuel Mode	Ppm	Parts per million
DFM1	Biogas Run Dual Fuel Mode using Rice Bran Biodiesel	RBB	Rice Bran Biodiesel
DFM2	Biogas Run Dual Fuel Mode using Pongamia Biodiesel	RBO	Rice Bran Oil
DFM3	Biogas Run Dual Fuel Mode using Palm Biodiesel	SI	Spark Ignition
EGR	Exhaust Gas Recirculation	TDC	Top Dead Centre
EGT	Exhaust Gas Temperature (^{o} C)	VCR	Variable Compression Ratio
FCM	Fuel Control Mechanism	WC	Water Column
FFA	Free Fatty Acids	WIRBB	Water in Rice Bran Biodiesel

Notations			
A	Availability (kW)	N	RPM
A_1	Area at the Inlet of the Gas Mixer	P	Instantaneous Cylinder Pressure (bar)
A_2	Area at the Throat of the Gas Mixer	P_1	Pressure at the inlet of the Gas Mixer
A_{den}	Density of Air (kg/m^3)	P_2	Pressure at the Throat of the Gas Mixer
C_d	Coefficient of Discharge	q_j	Diffusive Heat Flux
Cp	Specific Heat (kJ/kg K)	Q	Energy per unit time (kW)
d	Diameter of Orifice (m)	Q_H	Heat Source or Sink per unit volume
D	Engine Cylinder Diameter (m)	R	Universal Gas Constant (kJ/kg K)
f_u	Turbulent Viscosity Factor	R_e	Specific Gas Constant (kJ/kg K)
g	Acceleration due to Gravity (m/s^2)	S	Entropy Generation (kW/K)
h	Manometer reading across the orifice	S_i	External Force per unit mass
H_H	HLB of the Hydrophilic Surfactant	S_{ij}	Viscous Shear Stress Tensor
H_L	HLB of the Lipophilic Surfactant	T	Temperature (K)
k	Turbulent Kinetic Energy	ρ	Density (kg/m^3)
K	Number of cylinders	R	Dynamometer Arm Radius (m)
L	Engine Stroke Length (m)	TDC	Top Dead Centre
$\dot{m}$	Mass Flow Rate (kg/s)	V	Instantaneous Cylinder volume (m^3)
M	Molecular Weight	V_1	Velocity at the Inlet of the Gas Mixer
$\dot{m}_{bg}$	Mass Flow Rate of Biogas (kg/h)	V_2	Velocity at the Throat of the Gas Mixer
$\dot{m}_{di}$	Mass Flow Rate of Diesel (kg/h)	VE	Volumetric Efficiency (%)
$\dot{m}_f$	Mass Flow Rate of Fuel (kg/h)	W	Dynamometer Load (N)
$\dot{m}_p$	Mass Flow Rate of Pilot Fuel (kg/h)	W_{den}	Density of Water (kg/m^3)
n	Number of Revolution Per Cycle	W_H	Weight of the Hydrophilic Surfactant
Subscripts			
a	Air	in	Input
amb	Ambient	atm	Atmospheric Condition
c	Cooling Water	s	Shaft
bg	Biogas	u	Uncounted
bd	Biodiesel	w	Cooling Water
d	Destroyed	we	Water Flowing through Engine Jacket
di	Diesel	wic	Water Inlet to Calorimeter
e	Exhaust Gas	wie	Water Inlet to Engine
eic	Exhaust Gas Inlet to Calorimeter	woc	Water Outlet from Calorimeter
eoc	Exhaust Gas Outlet from Calorimeter	woe	Water Outlet from Engine
f	Fuel	II	Second Law
h	Hydrophillic		
Greek Symbols			
η	Efficiency (%)	θ_n	Nozzle Angle
β	Ratio between the Diameters of Throat and Inlet manifold	μ	Dynamic Viscosity Coefficient
γ	Specific Heat of the Combustion Gases (kJ/kgK)	μ_t	Turbulent Eddy Viscosity Coefficient
θ_1	Converging Angle (°)	θ_{CS}	Crank Angle at which combustion of the fuel starts (degree crank angle)
θ_2	Diverging Angle (°)	θ_{IN}	Crank Angle at which injection of fuel starts (degree crank angle)

LIST OF FIGURES

LIST OF TABLES

Chapter-1

Introduction

Overview:

There is no doubt that the world energy demand has recently witnessed a remarkable increase and is expected to reach a growth of 56% between 2010 and 2040. In the meantime, the energy market is facing bigger challenges, such as depletion of fossil fuel reserves, rise of population, lack of energy security, economic and urbanization growth. To overcome this future gap between energy supply and demand, as well as taking into consideration the risks from global climate change due to the greenhouse gas emissions and other pollutants from excessive fossil fuel combustion, a lot of attention is oriented to efficient harness the renewable energy sources. Among the renewable sources available, biogas seems to be an exciting prospect as a clean technology for power production in rural areas. The chapter briefly describes about world energy scenario, renewable fuel, biodiesel, emulsified fuel, biogas, dual fuel concept and emission norms. Finally, the chapter concludes with the objectives of the present investigation, the layout of the thesis and the Road map.

Chapter Outline:

1.1 The World Energy Scenario

The present energy scenario has stimulated active research interest in nonpetroleum, renewable, and non-polluting fuels. The world reserves of primary energy and raw materials are limited. According to an estimate, the reserves will last another 218 years for coal, 41 years for oil and 63 years for natural gas (Agarwal, 2007). Oil has no equal as an energy source for its intrinsic qualities of extractability, transportability, versality and cost. The oil being a burial product of biomass over 200 years and therefore, the amount of oil is limited. Moreover, burning of fossil fuels causes environmental concerns such as greenhouse gas emission, which is believed to be the major reason behind global warming. Hence, there is an urgent need to understand the world energy crisis and underlying science behind degradation of environment. To address this twin problem, a lot of effort has been made to explore renewable energy production technologies around the world like hydroelectric power, geothermal, wind, solar and biomass. The forecasting on renewable energy growth upto 2035 is illustrated in Figs. 1.1 and 1.2.

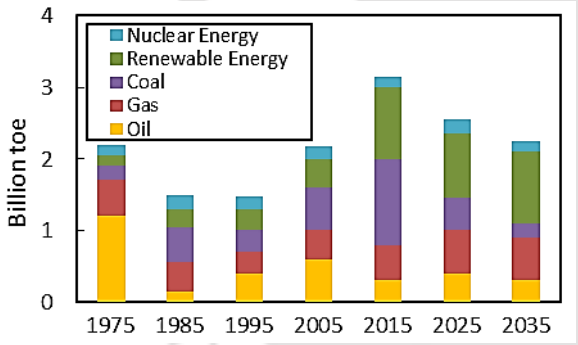

Fig. 1.1 Forecasting based on ten year increments by fuel (BP Energy Outlook 2035)

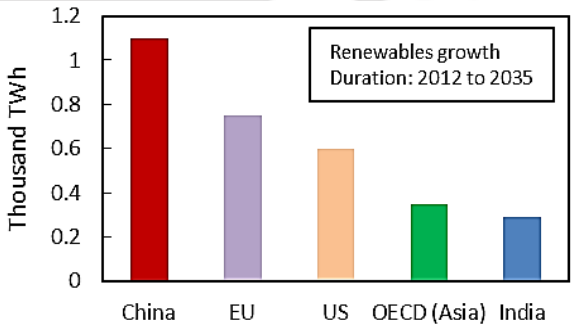

Fig. 1.2 Forecasting on renewable energy growth (BP Energy Outlook 2035)

1.2 Renewable Fuels

Renewable fuels are derived from resources that are regenerative. For this reason, renewable fuels are fundamentally different from fossil fuels, and do not contribute much greenhouse gases and other pollutants as fossil fuel combustion. Therefore, renewable fuels can be predominantly used as fuel for transportation and power generation applications. One feature of renewable energy is that they are well suited for developing decentralized power plants to meet the energy needs of rural and remote areas (Yaliwala *et al.*, 2014). Today, the use of renewable fuels `such as biomass derived biodiesel and biogas is more reliant for addressing rural power generation.

1.2.1 Biodiesel

Biodiesel can be produced from any material that contains fatty acids, either bonded to other molecules or present as free molecules. Thus, various vegetable fats and oils, animal fats, waste greases and edible oil processing wastes can be used as feedstock for biodiesel production. The choice of feedstock is based on such variables as local availability, cost, government support, and performance as a fuel. Different countries are looking for different types of fats and oils as feedstock for biodiesel. For example, soybean oil in United States, rapeseed and sunflower oils in Europe, coconut oil, palm oil, pongamia oil and rice bran oil in Asia (Cheng, 2010).

Biodiesel is mainly produced from oils and fats. The oil contains higher levels of unsaturated fatty acids and is liquids at room temperature. Their direct usages as fuel were tried more than 100 years ago. But problems with directly using oils as fuel are mostly associated their high viscosities, low viscosities and engine. Fats, however, contain more saturated fatty acids. They are solid at room temperature and cannot be used as fuel in a diesel engine. There are some problems associated using oil such as carbon deposits in the engine, engine durability and lubricating oil contamination. The oil and fats need to be converted to biodiesel them compatible for existing Compression Ignition (CI) engines. Biodiesel has minimal sulphur and aromatic content and higher flash point, lubricity, Cetane number, biodegradability and non-toxicity (Rakopoulos *et al*., 2014). It offers improved lubricity over certain low-sulphur petro-diesels and thus, can help to reduce wear of engine components (Pullen and Saeed, 2014). Biodiesel is also easy to handle due to its higher boiling point than that of diesel.

1.2.2 Emulsified Fuel

There are different workable techniques like engine combustion chamber modification and aftertreatment system to reduce the exhaust pollution such as particulate matter, smoke and the oxides of nitrogen (NOx). Besides these methods, there is a fundamental method to reduce the pollution from the source called emulsification (Lin and Wang, 2004). This technique enhances fuel efficiency and reduces emission of hazardous pollutants from diesel engines (Crookes *et al.*, 1997). In this technique, two or more immiscible liquid are mixed together such as diesel and water. In diesel engines, the emulsified fuel gets atomized into fine liquid droplets inside the cylinder with the help of the injector. As water has a lower boiling point than diesel, water droplets reach their boiling point earlier after soaking enough reaction heat. The fuel layer is then blown up by vaporization of water resulting in formation

of smaller fuel droplets, which increase the fuel's surface to volume ratio. This phenomenon is called ''micro-explosion''. This speeds up the reaction rate between the adjacent air and the fuel droplets. The water vaporization absorbs the heat of the combustion chamber resulting reduction in the adiabatic flame temperature. This is responsible for the reduced chemical reaction of nitrogen with oxygen to form nitric oxide which lowers NO_X emission. This technique can be used for biodiesel and bio-oil for controlling the NO_X emission.

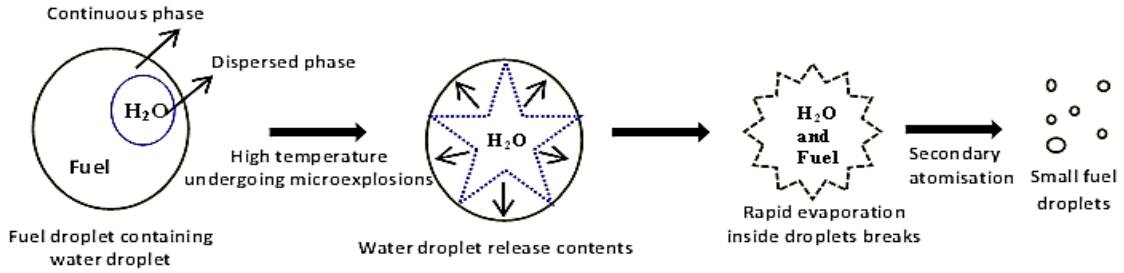

Fig. 1.3 Micro-explosion phenomenon (Sadhik Basha and Anand, 2011)

1.2.3 Biogas

Biogas can be produced by fermenting organic materials in absence of air with the help of bacteria to breakdown into intermediates such as alcohol and fatty acids and finally to methane, carbon dioxide and water (Mital, 1996). This process is called anaerobic fermentation. The anaerobic process consists of four main steps: hydrolysis, acidogenesis, acetogenesis and methanogesis (Cheng, 2010). Biogas has also been known as the swamp gas, sewer gas, fuel gas, marsh gas, wet gas and in India, commonly known as 'Gobar' gas. The main combustible component of biogas is methane. A period of 15 days enables anaerobic bacteria to convert organic matter to biogas. Animal and human wastes are excellent feedstock for anaerobic digestion. Biogas can be directly burned for heat generation or can be combusted in internal combustion engines for power generation.

1.2.4 Dual Fuel Concept

Dual fuel combustion is an effective technique for reducing pollutant emissions, especially soot and NOx, from direct injection diesel engines. In dual fuel diesel engine, a carburetted mixer of air and high octane index fuel is compressed like a conventional diesel engine. The compressed mixture of air and gaseous fuel does not auto ignite due to its high auto ignition temperature. Therefore, it is fired by a jet of liquid fuel which spontaneously ignites the charge at the end of compression. The gas–air mixture in the vicinity of the injected spray

ignites at number of places initiating a number of flame fronts (Ganesan, 2012). Thus, the combustion process starts smoothly and rapidly. The amount of liquid fuel needed for sufficient ignition is between 10% and 20% of the amount needed for operation on liquid fuel alone (von-Mitzlaff,1988). The advantage of this concept is that it uses a flammability difference of two used fuels. The disadvantage is the necessity to have liquid fuel available for the dual fuel engine operation (Sahoo, 2011). Thus, the dual fuel concept can be applied for efficient utilization of the available wide range of gaseous and liquid fuels.

1.3 Emission Standards

Emission standards are legal requirements governing air pollutants released into the atmosphere. Emission standards set quantitative limits on the permissible amount of specific air pollutants that may be released from specific sources over specific time frames. Emission may be divided into two categories: visible emissions and invisible emissions (Ganesan, 2012). Smoke and particulate matter is classified as visible emissions whereas carbon dioxide, carbon monoxide, oxides of nitrogen, unburnt hydrocarbons, carbon monoxide and aldehydes are classified as invisible emissions. They are generally designed to achieve air quality standards and to protect human health. The first measure to control vehicular air pollution was taken in USA in 1964. Since then there have been a large of numbers of amendments in forms of standards were implemented with the view to protect the environment. Currently, Euro 6 emission standards are implemented in most of countries across the globe as indicated in Table 1.1 and 1.2.

Table 1.1 European Standards for passenger cars, g/km (Pundir, 2010)

Description	Vehicle type	CO	HC	NO_x	HC + NO_x	Particulate matter
1992-Euro 1	All	2.72	-	-	0.97	0.14
1996-Euro 2	Gasoline	2.20	-	-	0.50	-
	Diesel	1.00	-	-	0.70	0.10
2000-Euro 3	Gasoline	2.30	0.2	0.15	-	-
	Diesel	0.64	-	0.50	0.56	0.05
2005-Euro 4	Gasoline	1.00	0.1	0.08	-	-
	Diesel	0.50	-	0.25	0.30	0.025
2009-Euro 5	Gasoline	1.00	0.1	0.06	-	-
	Diesel	0.50	-	0.18	0.23	0.025
2014-Euro 6	Gasoline	1.00	0.1	0.06	-	-
	Diesel	0.50	-	0.08	0.17	0.025

***** Particulate matter limits apply only to diesel cars

Table 1.2 Emission Standards for diesel and gas engines, g/kWh (Pundir, 2010)

Description	CO	Non-methane hydrocarbon	Methane[1]	NO_X	Particulate matter[2]
Euro 3. Oct. 1999	3	0.4	0.65	2	0.02
Euro 3. Oct. 2000	5.45	0.78	1.6	5	0.16
Euro 4. Oct. 2005	5.45	0.55	1.1	3.5	0.03
Euro 5. Oct. 2008	4	0.55	1.1	2	0.03
Euro 6. Jan. 2013	4	0.16[3]	0.5	0.4	0.01[4]

[1] For natural gas engines
[2] Not applicable for gas fuelled engines for approval to Euro 3 and Euro 4 standards
[3] Total hydro carbon limits apply for diesel
[4] Particle number limit apply to prevent ultra-fine particles from flow through filters

1.4 Objectives of the Present Investigation

The present contribution is focused to standardize the specifications of a biogas powered dual fuel diesel engine using different types of pilot fuel based on systematic experimental and theoretical approach. This is important because running biogas along with any liquid fuel at standard diesel setting will not offer the best performance. Therefore, it becomes necessary to study and optimize the performance, combustion and emission characteristics of a biogas run dual fuel diesel engine at varied operating conditions, namely, load, compression ratio and injection timing. The pilot fuels considered for this study are diesel, pongamia biodiesel, palm biodiesel, rice bran biodiesel, and emulsified rice bran biodiesel. For complete analysis, a thermodynamic study is carried out to unravel the effect of compression ratio and injection timing on the energy and exergy distributions for different types of pilot fuel. This study is very important for understanding the energy management of a biogas run dual fuel diesel engine. These types of studies have not been reported in archival literature. The motivation behind this research work is to use such biogas run dual fuel diesel engines for power generation in rural areas. The following objectives have been addressed in the present investigation:

- Selecting the biodiesel based pilot fuel for the biogas run dual fuel diesel engine based on performance and emission characteristics.

- Preparation of water in rice bran biodiesel (WIRBB) samples and their characterisation in order to select the optimum emulsion for the engine test.

- Standardization of the specification of a biogas run dual fuel diesel engine using diesel, rice bran biodiesel and emulsified rice bran biodiesel as pilot fuel.

- Energy and Exergy analysis of a biogas run dual fuel diesel engine using diesel, rice bran biodiesel and emulsified rice bran biodiesel as pilot fuel.

1.5 Organisation of Thesis and the Road Map

The thesis has been organized by focusing the concentration towards the clean and efficient power production from a biogas run dual fuel diesel engine using different types of pilot fuel. The thesis comprises of ten chapters, the details of which are summarized below:

Chapter 1 offers the motivation acquired towards the use of renewable fuel. This is followed by the objective of the dissertation. **Chapter 2** introduces the dual fuel engines, reviews on biogas run dual fuel diesel engines, the thermodynamic analysis, and discusses the scopes of work. **Chapter 3** refers to the variable compression ratio engine setup and its different measurement and instrumentation devices. This is followed by discussion regarding the modification carried out to make it suitable for dual fuel operations. **Chapter 4** compares the performance and emission characteristics of a biogas run dual fuel diesel engine for different types of pilot fuel at standard diesel settings. **Chapter 5** analyses the outcome of the experiments done for standardization of biogas run dual fuel diesel engine using diesel as pilot fuel at various compositions of load, CR, and IT. **Chapter 6** the outcome of the experiments done for standardization of biogas run dual fuel diesel engine using rice bran biodiesel as pilot fuel at various compositions of load, CR, and IT. **Chapter 7** elaborates preparation and characterization of emulsified rice bran biodiesel. It describe in brief about the surfactants used, hydrophilic lipophilic balance, ratio of emulsifying fluids, emulsion preparation procedure, measurement of droplet diameter and stability study of the emulsified rice bran biodiesel. **Chapter 8** analyses the outcome of the experiments done for standardization of biogas run dual fuel diesel engine using emulsified biodiesel as pilot fuel at various compositions of load, CR, and IT. **Chapter 9** compares the performance of the biogas run dual fuel diesel engine at the optimum operating parameter for different types of pilot fuel. **Chapter 10** explains the thermodynamic analysis covering both first law and second law study of the aforementioned works at a load where maximum efficiency prevailed. **Chapter 11** recaps the key findings of the experiments performed and the future works are proposed.

Road Map

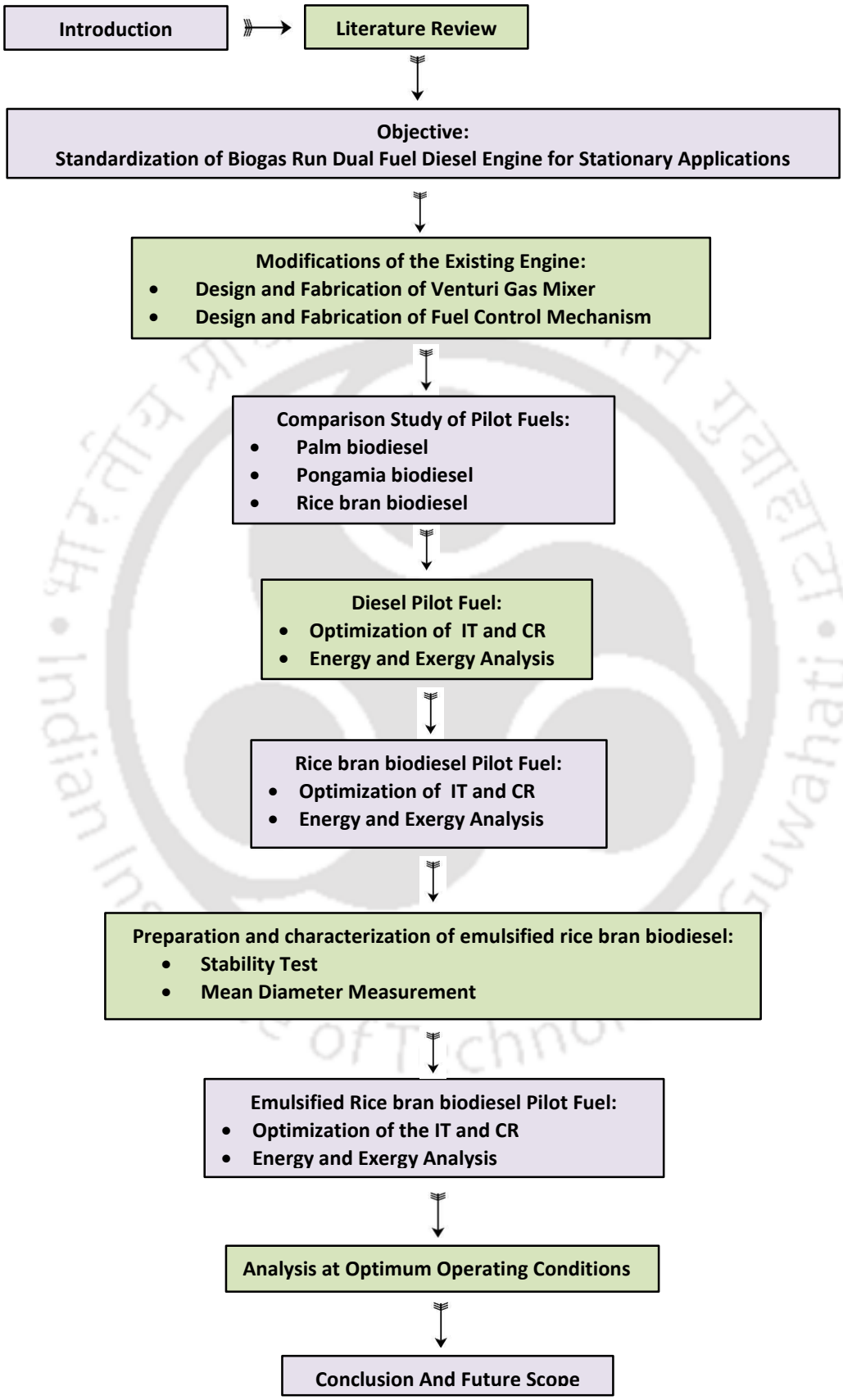

Fig. 1.4 Road map of the present study

Chapter-2

Literature Review

Overview:

Much of the early development of the Internal Combustion engines was based on employing gaseous fuel. At that time, the wide spread use of coal gas, produced by processing coal lead to the evolution of 'Dual Fuel Engines'. It was further revolutionised before World War-II in countries like Italy, Russia, Germany, Holland, the U.S.A and the U.K. During World War-II, there was much activity to utilize gaseous fuel engine applications as liquid fuels of right quality became scare especially in countries like Germany. The recent fossil fuel crisis and the rise of pollution have once again initiated active research in dual fuel engines using different test fuels. Nowadays, dual fuel engines are widely employed especially for stationary power generation applications. Biogas, a promising renewable fuel, has a great potential for dual fuel application. This chapter is dedicated towards a detailed literature review on biogas run dual fuel diesel engines. Besides, a discussion on thermodynamic potential study on diesel and dual fuel engines is incorporated. Finally, the objectives drawn in the earlier chapter are justified by identifying the key scopes of works from the literature review.

Chapter Outline:

2.1 Dual Fuel Diesel Engine

During the second half of 19th century, many different configurations of internal combustion (IC) engines were built and tested. These engines operated with variable success and fidelity using different mechanical system and engine cycles. The first practical engine was invented by J. J. E. Lenoir in 1860 (Pulkrabek, 2004). It was a single cylinder, two-stroke, double acting horizontal engine having a mechanical efficiency up to 5%. The next significant milestone achieved was the Otto and Lagen atmospheric or free piston engine in 1866. The main feature of this engine was that the fuel consumption was about half that of the Lenoir engine. Around the same time, the commercial exploitation of oil well have stated in USA. This led to the availability of liquid fuels. In 1876, the Otto silent engine commonly known as Spark Ignition (SI) engine based on four stroke cycle was patented and produced. The modern compression ignition (CI) was developed from the work of two people, Alkroyd Stuart and Rudolf Diesel. Alkroyd Stuart's engine was patented in 1890 and produced in 1892. It was a basically a four stroke compression ignition engine having a compression ratio of 3. The limitation of this engine was that the compression ratio was too low to provide spontaneous ignition of the fuel upon compression. This required an external heating system. Later on, Rudolf Diesel found a way to eliminate this limitation. Diesel's concept of compressing air to such an extent that fuel would spontaneously ignite after injection was published in 1890 and patented in 1892. The prototype ran with an efficiency of 25%, about twice the efficiency of any contemporary power plant (Stone, 1985).

There has been evolution of a different technology in the early part of 20th century for running gaseous fuel with the aid of liquid fuel in CI engines. These types of engines are known as dual fuel diesel engines. Dual fuel technology is used for efficient combustion of gaseous fuel like biogas, hydrogen, natural gas, producer gas, syngas, butane, etc. which have having low ignition characteristics (Thipse, 2010). The earliest experiment performed on dual fuel diesel engines by Cave dates back to 1929 using hydrogen gas. In 1939, the first commercial dual fuel engine fuelled by town gas was commercialised by the National Gas and Oil Engine Co. in Great Britain (Sahoo, 2011). The main driving force that initiated an active research in dual fuel engines was due to shortage of liquid fuel during World War-II. During this period, the versality of dual fuel engines enabled them to be used for military as well as for civil applications. The popularity gained by dual fuel engines during World War-

II plus the depletion of fossil fuels lead to their further development for different usage like power generation, on–road and off-road applications.

2.2 Working Principle

In dual fuel diesel engines, a gaseous high-octane fuel is usually inducted into a CI engine with incoming air through the intake manifold and then ignited by a small quantity of high-cetane liquid fuel. The high self-ignition temperature of the air-gaseous fuel mixture necessitates the use of a small quantity of a liquid fuel as an ignition source. The liquid fuel is called the pilot fuel. The gaseous fuel is called the primary fuel on which the engine mainly runs. The use of liquid fuel allows more potential ignition points to form throughout the charge as compared with a single point in case of SI engines (Korakianitis *et al*., 2011). The dual fuel engine initially follows the combustion pattern of a CI engine. However, in later stages, it follows the flame propagates akin to that of a SI engine. The advantage of this type of engine is that, it uses the difference of flammability of two used fuels. However, in case of lack of gaseous fuel, this engine runs according to the diesel cycle by switching from dual fuel mode (DFM). Another stand out of feature of dual fuel engine is that no cylinder modification is required. This dual fuel technology is an effective technique to control the NOx and soot emission. The alternative gaseous fuels that have been successfully tested under DFM include ethanol (Junior and Martins, 2015), hydrogen (Lata *et al*., 2012), liquefied petroleum gas (Selim, 2004), methane (Selim, 2004), natural gas (Selim, 2004), propane (Polk *et al*., 2014), producer gas (Banapurmath *et al*., 2009), syngas (Sahoo, 2011a) and biogas (Yoon and Lee, 2011).

2.3 Combustion Characteristics

The study carried out by Mansour *et al.* (2001) indicates that the dual fuel combustion is far more complex than pure diesel operation. Cylinder pressure data analysis is an important tool to diagnose the engine combustion behaviour as cylinder pressure history directly influences the engine performance and the emission characteristics. The combustion processes in CI engine comprises of four stages as shown in Fig. 2.1(a). They are as follows: AB is the ignition delay, BC is the uncontrolled combustion, CD is the controlled combustion and DE is the late combustion. Point ‘A’ is the start of injection whereas point ‘B’ is the point of initiation of combustion. However, in case of dual fuel engines, it comprises of five stages.

They are as follows: AB is the pilot fuel ignition delay, BC is the pilot premixed combustion phase, CD is the primary fuel ignition delay, DE is rapid combustion of primary fuel and EF is the diffusion combustion phase.

The critical analysis of *P-θ* diagram diagrams reveals the following points:

- The peak cylinder pressure of diesel mode is found to be higher than that of dual fuel mode.
- The pressure rise rate of diesel mode is found to be lower than that of dual fuel mode.
- The shift of peak cylinder pressure away from top dead centre (TDC) is more in case of dual fuel mode in comparison to that of diesel mode.
- The ignition delay of pilot fuel in case of dual fuel mode is longer than that of pure diesel operation. This is due to induction of large amount of gaseous fuel which reduces the amount of air and thereby, slowing down the combustion reaction.

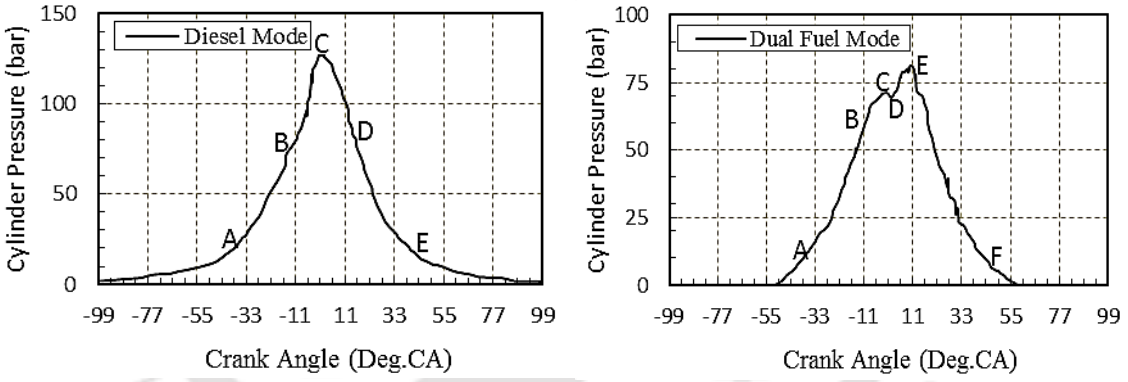

Fig. 2.1 Comparison of *P-θ* diagram for diesel and dual fuel mode (Mansour *et al.*, 2001)

2.4 Engine Modifications

A simple diesel engine can be easily converted into dual fuel diesel engine carrying out the following modifications as given below:

- ✓ Carburetor or a gas mixer needs to be connected at the inlet manifold for mixing of gaseous fuel and air (Walsh *et al.*, 1989). The carburetor or gas mixer should provide a homogeneous mixture of air and gaseous fuel taking into account of the appropriate air-fuel mixture.
- ✓ A control mechanism to be installed for maintaining the desired fuel setting on the injection pump (Walsh *et al.*, 1989).

- ✓ Advancement of injection timing of pilot fuel (Nijaguna, 2002). This is necessary to counter the late combustion phenomenon that is observed due to the difference of stoichiometric flame speed of primary fuel and pilot fuel.

2.5 Biogas Run Dual Fuel Diesel Engine

Biogas, a renewable gaseous fuel, can be successfully used in CI engines with minor modifications (Mustafi *et al*., 2013). This is particularly important in the case of developing countries where meeting the growing demand of fossil fuel is a major challenge. The carbon content in biogas is comparatively low to that of the conventional diesel fuel, resulting in a diminution in pollutants (Yoon and Lee, 2011). Besides, the high octane number of biogas makes it suitable for engines with high CR in order to maximize thermal efficiency (Henham and Makkar, 1998). The most positive aspect of using biogas in a CI engine is that there is no derating of power as observed in the case of a biogas run SI engine (Walsh *et al*., 1989; Bari, 1996). The reason behind this fact is that SI engines are very sensitive to biogas composition leading to high cycle to cycle variations (Bedoya *et al*., 2012). It is possible to achieve a substitution of diesel up to 85% by using biogas under DFM (von-Mitzlaff, 1988). Due to these advantages, it is economically and environmentally advantageous to use biogas in diesel engines. Biogas dual fuel combustion is a promising regime of the clean combustion for CI engine that offers potential for substantial reductions in both oxides of nitrogen and particulate matter emissions while still providing diesel like thermal efficiency. Due to this fact, there has been a continuous refinement of the biogas run dual fuel engines over the years. Many researchers have studied the performance and emission characteristics using different quality of biogas and different types of pilot fuel as summarised in Table 2.1.

2.6 Biogas Quality Limit

Biogas mainly contains methane (CH_4) and carbon dioxide (CO_2). The combustion value of any quality of biogas is directly related to its methane composition (Bedoya *et al*., 2009). However, presence of CO_2 up to 30% in biogas for dual fuel application can improved the performance of the engine. Biogas containing more than 40 % of CO_2 needs scrubbing. Conversely, biogas containing more than 45% of CO_2 results in harsh and irregular running of the engine (Bari, 1996). The properties of biogas used by different researchers for biogas run dual fuel applications are given in Table 2.2.

Table 2.1 Summary of the test engine, type of biogas and pilot fuel investigated for biogas run dual fuel diesel engine

Researcher(s)	Test Engine		Type of biogas	Pilot Fuel
Bari (1996)	Manufacturer	Nang Chang	Simulated Biogas	Diesel
	Model	2105		
	No. of cylinder	2		
	Stroke	2		
	Type	Water cooled , naturally aspirated with double combustion chamber		
	Rated power	16.8 kW at 1500 rpm		
Henham and Makkar (1998)	Manufacturer	Lister Petter	Simulated Biogas	Diesel
	Model	LPWS2		
	No. of cylinder	2		
	Stroke	4		
	Type	Water cooled, indirect injection		
Duc and Wattanavichien (2007)	Manufacturer	Kubota	Raw biogas	Diesel
	No. of cylinder	1		
	Stroke	4		
	Type	Single horizontal cylinder, naturally aspirated, water cooled		
	Swept volume	624 mm^3		
	Bore × stroke	94 mm × 90 mm		
	Compression ratio	21:1		
	Rated power	7.73 kW at 2400 rpm		
	Maximum torque	42N m at 1500 rpm		

Table 2.1 Summary of the test engine, type of biogas and pilot fuel investigated for biogas run dual fuel diesel engine (contd.)

Researcher(s)	Test Engine		Type of biogas	Pilot Fuel
Tippayawong *et al.*(2007)	Manufacturer	Mitsubishi	Raw biogas	Diesel
	Model	DI-800		
	No. of cylinder	1		
	Stroke	4		
	Type	Naturally aspirated, water cooled		
	Swept volume	411 cm^3		
	Bore × stroke	82 mm × 78 mm		
	Compression ratio	18:1		
	Rated power	5.5 kW @ 2400 rpm		
Bedoya *et al.* (2009)	Manufacturer	Lister Petter	Simulated biogas	Diesel, Palm oil biodiesel
	No. of cylinder	2		
	Type	DI, naturally aspirated, air cooled		
	Swept volume	1550 cm^3		
	Bore × stroke	98 mm × 101 mm		
	Compression ratio	15.5:1		
	Rated power	20 kW at 3000 rpm		
Luijten and Kerkhof (2011)	Manufacturer	Yangke	Simulated biogas	Diesel, Jatropaha oil
	No. of cylinder	1		
	Stroke	4		
	Type	12GF-SF		
	Swept volume	1.093 L		
	Bore × stroke	110 mm × 115 mm		
	Compression ratio	17:1		
	Rated power	12 kW		

Table 2.1 Summary of the test engine, type of biogas and pilot fuel investigated for biogas run dual fuel diesel engine (contd.)

Researcher(s)	Test Engine		Type of biogas	Pilot Fuel
Yoon and Lee (2010)	Type	Turbo charged, water cooled	Raw biogas	Diesel, Soybean biodiesel
	No. of cylinder	4		
	Bore × stroke	91.1 mm × 95 mm		
	Swept volume	2476 cm^3		
	Compression ratio	19:1		
	Maximum power	46 kW at 4000 rpm		
Sahoo *et al*. (2012)	Manufacturer	Kriloskar	Raw biogas	Diesel, Jatropha biodiesel
	Model	TV1		
	Type	DI, natural aspirated, water cooled		
	No. of cylinder	1		
	Bore × stroke	87 mm × 110 mm		
	Swept volume	661mm^3		
	Compression ratio	17.5		
	Rated power	5.5kW @1500 rpm		
Cacua *et al*. (2012)	Manufacturer	Lister Petter	Simulated biogas	Diesel
	Model	TR2		
	Type	DI, naturally aspirated, air cooled		
	No. of cylinder	2		
	Stroke	4		
	Displacement	1.55×10^{-3} m^3		
	Bore × stroke	0.098 m × 0.101m		
	Compression ratio	15.5:1		
	Rated power	20 kW at 3000 rpm		
	Maximum torque	76 N.m at 1800 rpm		

Table 2.1 Summary of the test engine, type of biogas and pilot fuel investigated for biogas run dual fuel diesel engine (contd.)

Researcher(s)	Test Engine		Type of biogas	Pilot Fuel
Mustafi *et al*. (2013)	Manufacturer	Lister Petter	Simulated biogas	Diesel
	Model	PHW1		
	Type	DI, water cooled		
	No. of cylinder	1		
	Bore × stroke	87.3 mm ×110 mm		
	Swept volume	659 cm^3		
	Compression ratio	16.5:1		
	Rated torque output	32.6 N.m at 1800 rpm		
Makareviciene *et al. (*2013)	Model	1Z	Simulated biogas	Diesel
	Type	DI, turbocharged, air cooled		
	No. of cylinder	4		
	Displacement	1896 cm^3		
	Bore × stroke	79.5 mm × 95.5 mm		
	Compression ratio	19.5:1		
	Rated power	66 kW at 4000 rpm		
Maizonnasse *et al.* (2013)	Rated power	3.1 kW	Raw biogas	Diesel
Barik and Murugan (2014a, 2014b)	Manufacturer	Kriloskar	Raw biogas	Diesel, Karanja biodiesel
	Model	TAF1		
	Type	DI, , air cooled, naturally aspirated		
	No. of cylinder	1		
	Bore × stroke	87 mm× 110 mm		
	Swept volume	661 mm^3		
	Compression ratio	17.5		
	Injection timing	23º BTDC		
	Rated power	4.4 kW @1500 rpm		

Table 2.2 Summary of Biogas properties

Researchers	Type of biogas	Composition	Calorific value (MJ/kg)	Air-fuel ratio	Boiling point (°C)	Density (kg/m^3)	Octane Number	Auto ignition temperature (°C)	Woobe Index (kWh/Nm^3)
Duc and Wattanavichien (2007)	Raw biogas	73% CH_4, 19% CO_2, 6.5% N_2, 1.5% O_2, 0.002% H_2S	26.17	17.2	-	0.91	-	-	-
Tippayawong *et al.* (2007)	Raw biogas	65.6% CH_4, 26.4% CO_2, 6% N_2,2% O_2	24.5	-	-	1.1	-	-	-
Bedoya *et al.* (2009)	Simulated biogas	60% CH_4, 40% CO_2	23.73	6.05	-	-	-	-	6.16
Luijten and Kerkhof (2011)	Simulated biogas-I	39.9% CH_4, 60.1% CO_2	-	-	-	-	-	-	-
	Simulated biogas-II	49.7% CH_4, 50.3% CO_2	-	-	-	-	-	-	-
	Simulated biogas-III	59.9% CH_4, 40.1% CO_2	-	-	-	-	-	-	-
	Simulated biogas-IV	70% CH_4, 30% CO_2	-	-	-	-	-	-	-
Yoon and Lee (2010)	Raw biogas	30-73% CH_4, 20-40 CO_2, 5-40 N_2,1-3H_2	26.17	17.2	180-330	0.65-0.91	130	632-813	-
Sahoo (2011)	Raw biogas	48% CH_4, 52% CO_2	15.74	-		1.2	-	-	-
Cacua *et al.* (2012)	Raw biogas	60% CH_4	23.73	-	-	-	-	-	-

Table 2.2 Summary of Biogas properties (contd.)

Researchers	Type of biogas	Composition	Calorific value (MJ/kg)	Air-fuel ratio	Boiling point (°C)	Density (kg/m^3)	Octane Number	Auto ignition temperature (°C)	Woobe Index (kWh/Nm^3)
Lacour *et al.* (2013)	Raw biogas	65% CH_4, 26% CO_2, 6% H_2O	-	-	-	-	-	-	-
Mustafi *et al.* (2013)	Simulated biogas-I	58% CH_4, 32% CO_2	-	-	-	-	-	-	-
	Simulated biogas-II	67% CH_4, 33% CO_2	-	-	-	-	-	-	-
	Simulated biogas-III	80% CH_4, 20% CO_2	-	-	-	-	-	-	-
Maizonnasse *et al.* (2013)	Simulated biogas-I	50% CH_4, 50% CO_2	17.22	4.6	-	-	-	-	-
	Simulated biogas-II	60% CH_4, 40% CO_2	20.67	6.08	-	-	-	-	-
	Simulated biogas-III	73% CH_4, 27% CO_2	25.14	8.54	-	-	-	-	-
Makareviciene *et al.* (2013)	Simulated biogas-I	65% CH_4, 35% CO_2	-	-	-	-	-	-	-
	Simulated biogas-II	85% CH_4, 15% CO_2	-	-	-	-	-	-	-
	Simulated biogas-III	95% CH_4, 5% CO_2	-	-	-	-	-	-	-
Debnath (2013)	Raw biogas	48% CH_4, 52% CO_2	15.74	-	-	-	-	-	-
Barik and Murugan (2014a, 2014b)	Raw biogas	-	27.53	17.2	-	1.2	130	600-650	-
			17.2	15.3	-	1.31	110	640-670	-

2.7 Effect of Different Parameters on the Performance of Biogas Run Dual Fuel Diesel Engines

The parameters include operating parameters, engine components, biogas quality, biogas inlet pressure and oxygenated combustion on the performance, combustion and emission characteristics of biogas run dual fuel diesel engines. Studies on operating parameters like load and speed reflect the manoeuvring capability of the engine. Investigations on engine components mainly include the air induction system and exhaust gas recirculation (EGR).

2.7.1 Brake Power, Torque and Brake Mean Effective Pressure

Effect of Load:

Sahoo (2011) demonstrates experimentally that brake power (BP) and torque increases with the increase of load at constant speed for both diesel and DFM as indicated in Fig. 2.2. Thus, both BP and torque have a linear relationship with load.

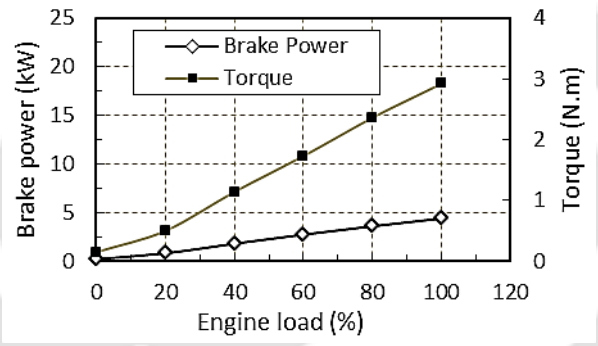

Fig. 2.2 Variation of BP and torque with load (Sahoo 2011)

Effect of Speed:

Duc and Wattanavichien (2007) carried out an experimental investigation on a dual fuel engine using synthetic biogas of different compositions. The results indicate that brake mean effective pressure (BMEP) and torque increases up to a particular rpm and then decreases as depicted in Fig. 2.3. In this particular study, the maximum BMEP and torque obtained were 844 kPa and 41.98 N.m, respectively at 1500 rpm. Tippayawong *et al.* (2007) tested an automobile engine to operate under DFM to generate electricity. Their study revealed that the power output of the engine was found to increase with increase of speed for both diesel and DFM as observed in Fig. 2.4.

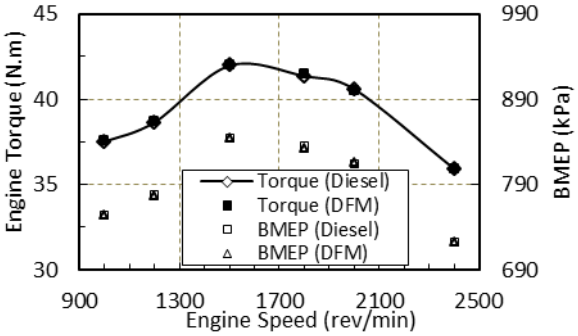

Fig. 2.3 Variation of torque and BMEP with speed (Duc and Wattanavichien, 2007)

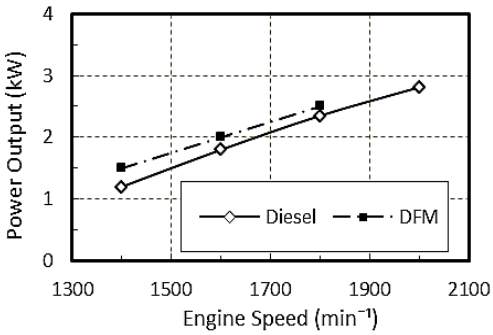

Fig. 2.4 Variation of power output with speed (Tippayawong *et al*., 2007)

2.7.2 Air-Fuel Ratio

Effect of Load:

The relative portion of the fuel and air are very vital from the viewpoint of combustion and efficiency of the engine. This is expressed either as a ratio of the mass of the fuel to that of the air or vice versa (Ganesan, 2012). The ratio of actual fuel-air ratio to stoichiometric fuel air ratio is called equivalence ratio. The air fuel ratio for SI engines ranges from 12 to 18. However, the air fuel ratio for CI engines ranges from 18 to 80 from full load to no load. However, the operation of dual fuel diesel engines can take place over wide range of air-fuel ratio. Yoon and Lee (2011) observed that the equivalence ratio under DFM is found to be higher in comparison to that of diesel mode. This is due to the fact that biogas is inducted into the engine through the air inlet manifold. This results in lowering of the volume of air entering into the combustion chamber. Barik and Murugan (2014a) found the stoichiometric air fuel ratio to decrease with the increase of load. This is due to the fact that as more amount of biogas flows needs to be supplied to the engine at higher load.

Effect of Speed:

Duc and Wattanavichien (2007) found that the air fuel ratio under DFM was lower than in comparison to diesel mode at different operating speeds. The results indicated that the air-fuel ratio was found to be maximum at 1800 rpm for both diesel and dual fuel modes (Fig. 2.5).

Effect of Air Induction System:

Bedoya *et al*. (2009) compared the performance of a biogas run dual fuel engine using two induction systems. The first one, SM1, comprises of a Kenics mixer and supercharger with a large mixing length (250 mm), while the second one, SM2, consists of a T-mixer and short

mixing length (25 mm). The pilot used for SM1 and SM2 were palm oil biodiesel and diesel, respectively. The tests indicated a lower air-fuel ratio found to be lower for SM1 in comparison to that of SM2 as depicted in Fig. 2.6.

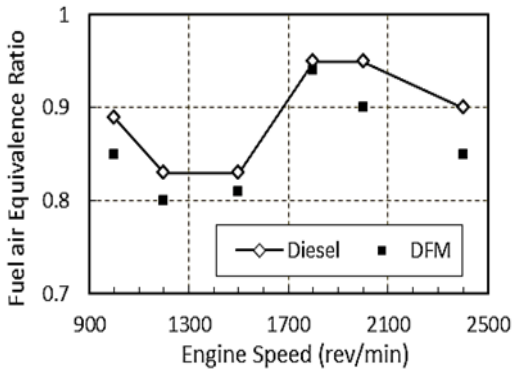

Fig. 2.5 Variation of equivalence ratio with engine speed (Duc and Wattanavichien, 2007)

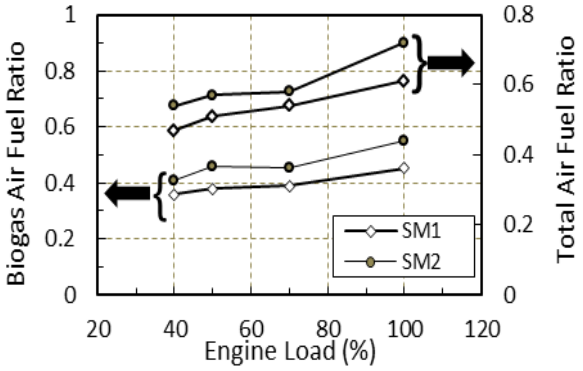

Fig. 2.6 Variation of air fuel ratio with engine load for different air induction systems (Bedoya *et al*., 2009)

Effect of Biogas Quality:

Luijten and Kerkhof (2011) investigated the effect of biogas quality on the performance of a dual fuel diesel engine. The study inferred that air fuel ratio was hardly got affected by low the quality of biogas.

Effect of Exhaust Gas Recirculation:

Makarevicience *et al*. (2013) conducted a comparison study on air-fuel ratio with EGR and without. The results showed a decrease of air fuel ratio with the use of EGR as indicated in Figs. 2.7 and 2.8. This is because the volume of air gets reduced due to induction of exhaust gases in the combustion chamber with the use of EGR.

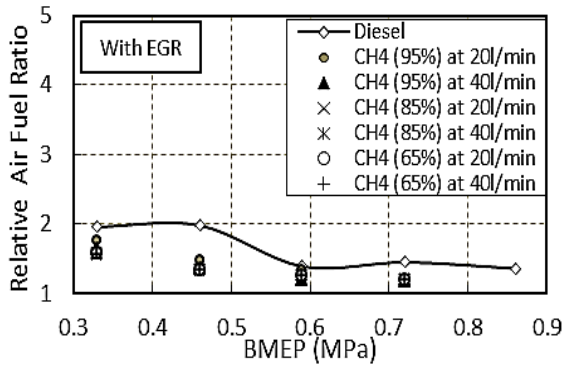

Fig. 2.7 Variation of relative air fuel ratio with BMEP with EGR (Makarevicience *et al*., 2013)

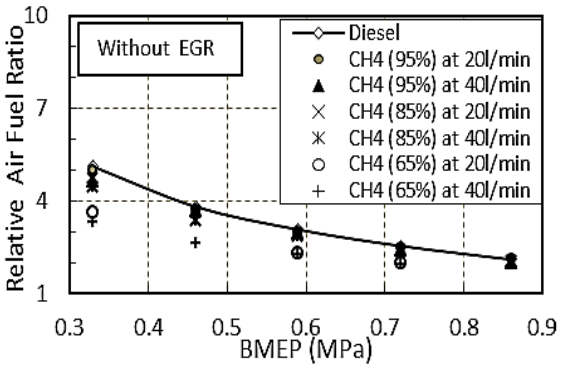

Fig. 2.8 Variation of relative air fuel ratio with BMEP without EGR (Makarevicience *et al*., 2013)

2.7.3 Volumetric Efficiency

Effect of Load:

Duc and Wattanavichien (2007) found that volumetric efficiency (VE) decreased with the increase of brake torque and load respectively for both lone and dual mode as shown in Fig. 2.9. Similar trend was observed by Barik and Murugan (2014a) for biogas run dual fuel diesel engine using karanja methyl ester (KME) as depicted in Fig. 2.10. This was due to the temperature of the exhaust gases increases with load which in turn preheats the incoming air and thereby, lowering the VE. The decrease in VE was more under DFM as compared to diesel mode as reported by Barik and Murugan (2014b). This was because the biogas substitution displaces a greater portion of air under DFM. For diesel mode, Sahoo (2011) reported that the maximum and minimum VEs found was about 85% and 81% at 0 and 100% loads, respectively. For the same loading conditions under DFM using diesel and jatropha biodiesel, these values were found to be 82% and 78%, and 82% and 77%, respectively.

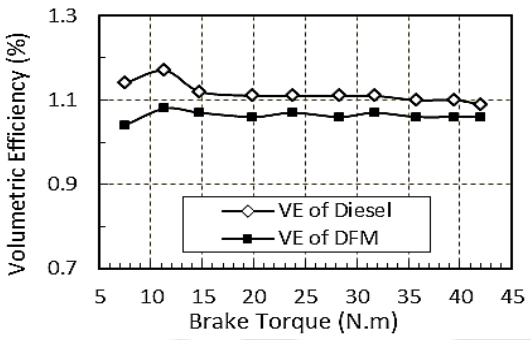

Fig. 2.9 Variation of VE with engine torque (Duc and Wattanavichien, 2007)

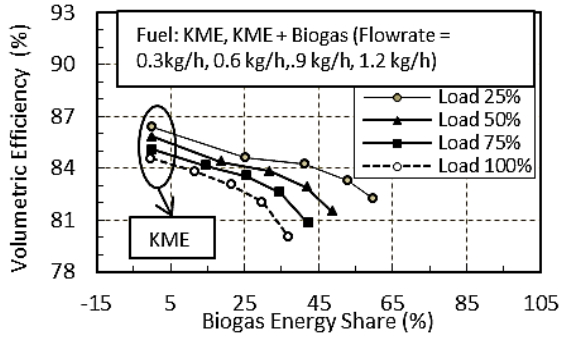

Fig. 2.10 Variation of VE with load for different BFRs (Barik and Murugan, 2014a)

Effect of Induction System:

Bedoya *et al*. (2009) found that there was a 6% drop in VE using the combination of Kenics mixer and supercharger along with a longer mixing length as compared to that of a T-mixer for the same biogas run dual fuel diesel engine (Fig. 2.11). At part load, the difference in VE between the two induction systems was observed to be less significant.

Effect of Biogas Quality:

Luijten and Kerkhof (2011) expressed VE as a function of the heat release fraction of pilot fuel and biogas quality. The quality of the biogas slightly affects the VE. Overall, the

decrease in VE was quite modest from 95% at zero substitution to 90–91% for maximum substitution even for the lowest quality of biogas as depicted in Fig. 2.12.

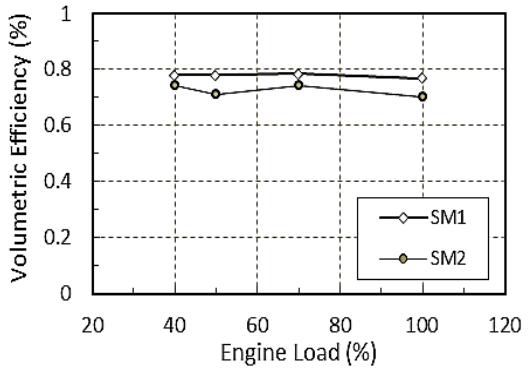

Fig. 2.11 Variation of VE with engine load (Bedoya *et al*. 2009)

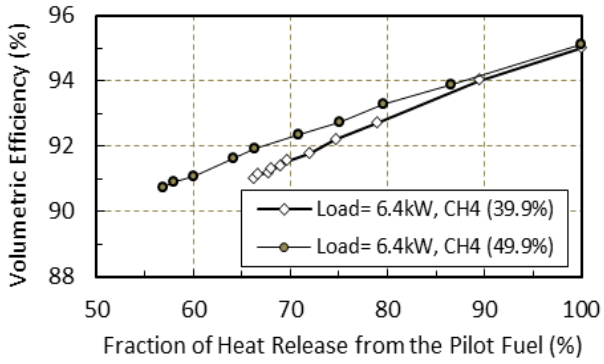

Fig. 2.12 Variation of VE with the fraction of heat release from the pilot fuel (Luijten and Kerkhof, 2011)

2.7.4 Brake Thermal Efficiency

Effect of Load:

The brake thermal efficiency (BTE) was found to increase with load for both diesel and DFM as shown in Figs. 2.13 and 2.14. However, the BTEs under DFM were found to be lower than diesel mode in all the test cases. This was mainly due to low calorific value of biogas as compared to that of diesel.

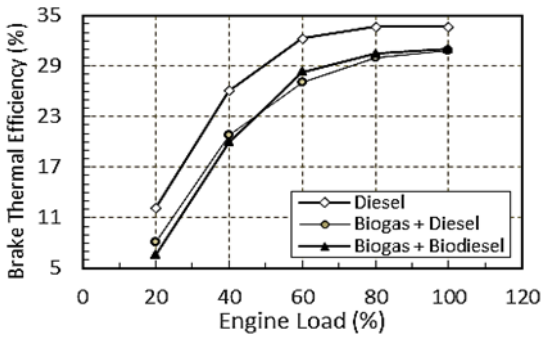

Fig. 2.13 Variation of BTE with engine load (Yoon and Lee, 2011)

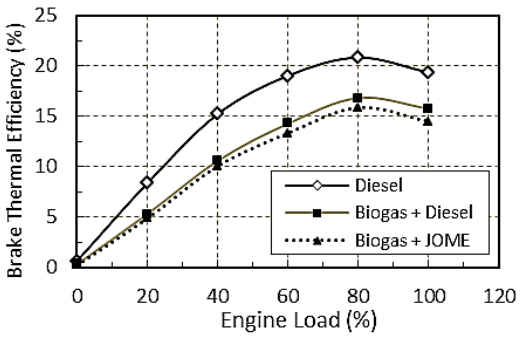

Fig. 2.14 Variation of BTE with engine load (Sahoo 2011)

The study done by Yoon and Lee (2011) and Sahoo (2011) revealed that using biodiesel as pilot fuel resulted in a lower BTE than diesel under DFM. The review on BTE highlighted an important fact that it was possible for a biogas run dual fuel diesel engine to achieve a high BTE around 32% as reported by Yoon and Lee, 2011.

Effect of Speed:

The review on the effect of the speed on BTE of biogas run dual fuel engines highlighted two contrasting findings. Firstly, Duc and Wattanavichien, 2007 indicated that the BTE under DFM was lower than that of diesel mode as depicted in Fig. 2.15. Further, the BTE kept on increasing upto a particular speed with the increase of speed. Secondly, the results of Tippayawong *et al*., 2007 inferred that the BTE under DFM was found to be higher than that of diesel mode as indicated in Fig. 2.16.

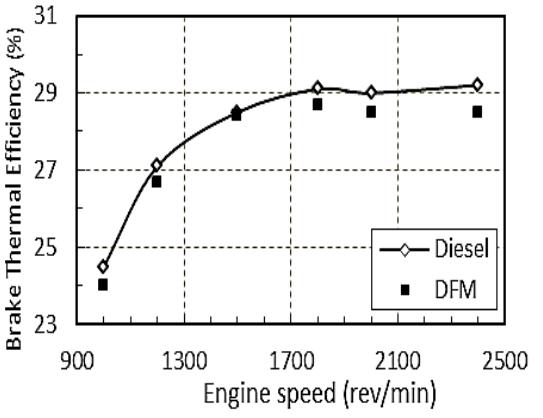

Fig. 2.15 Variation of BTE with speed (Duc and Wattanavichien, 2007)

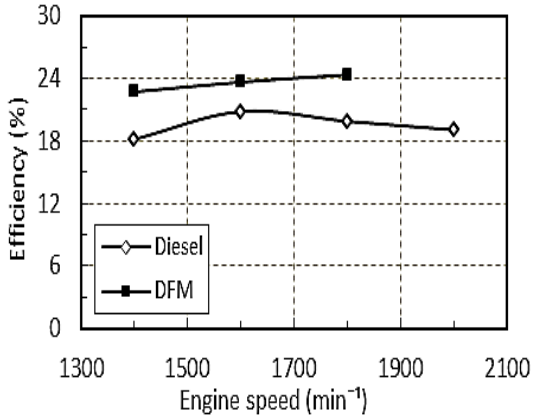

Fig. 2.16 Variation of BTE with speed (Tippayawong *et al*., 2007)

Effect of Air Induction System:

The test conducted by Bedoya *et al*. (2009) indicated that the combination of Kenics mixer and supercharger along with a longer mixing length (SM2) produced a better BTE in comparison to that of T-mixer along with a shorter mixing length (SM1) for the same biogas run dual fuel diesel engine. The BTE increased by 8% for the SM2 system in comparison to that of SM1 system.

Effect of Biogas Quality:

Henham and Makkar (1998) have conducted tests on the dual fuel diesel engine using synthetic biogas of various compositions. The test indicated that the overall efficiency falls with the increase of CO_2 content in the composition of synthetic biogas as indicated in Fig. 2.17. However, Luijten and Kerkhof (2011) found that the biogas quality has marginal effect on the BTE as evident from the Fig. 2.18.

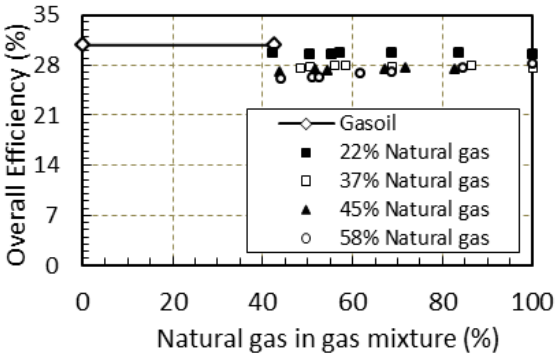

Fig. 2.17 Variation of overall efficiency with biogas quality (Henham and Makkar, 1998)

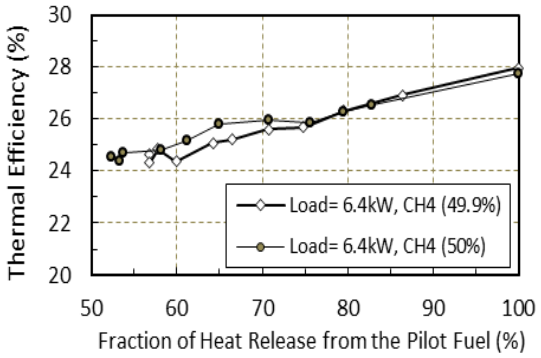

Fig. 2.18 Variation of BTE with biogas quality (Luijten and Kerkhof, 2011)

Effect of Exhaust Gas Recirculation:

At low loads, the BTE was found to be more for biogas run dual diesel engine using EGR in comparison to the same engine without EGR as depicted in Figs. 2.19 and 2.20. However, at high loads, the BTE was found to be lower for biogas run dual diesel engine using EGR in comparison to the same engine without EGR.

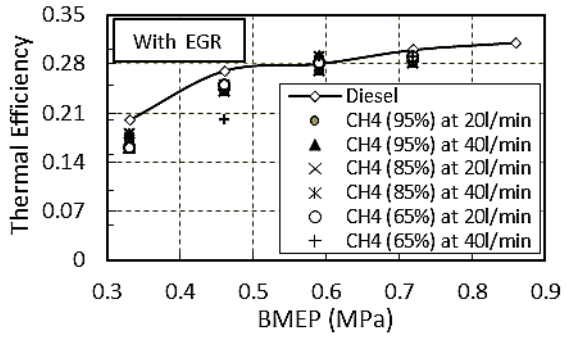

Fig. 2.19 Variation of BTE with EGR for different BMEPs (Makarevicience *et al.*, 2013)

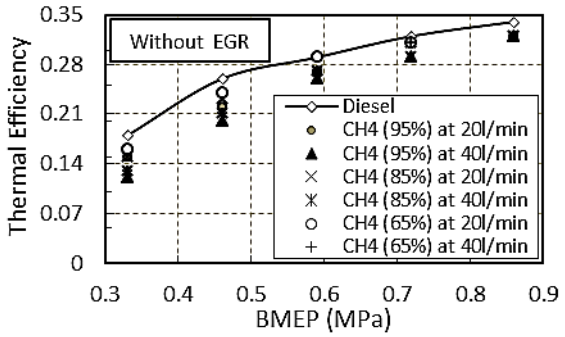

Fig. 2.20 Variation of BTE without EGR for different BMEPs (Makarevicience *et al.*, 2013)

Effect of Oxygenated Combustion:

The BTE under DFM was found to increase with increase of oxygen percentage in the inducted air. This was due to the increase in the activity of the partial oxidation reactions which resulted in an improved propagation of flame fronts of diesel. Thereby, results a better efficiency. The test conducted by Cacua *et al.* (2012) resulted in a maximum BTE of 18.8% at 70% load for 27% of oxygen in inducted air.

2.7.5 Brake Specific Fuel Consumption, Brake Specific Energy Consumption, Biogas Flow Rate and Liquid Fuel Replacement

Effect of Load:

From reported literature, the brake specific fuel consumption (BSFC) and brake specific energy consumption (BSEC) were found to decrease with the increase of load for both diesel and DFM as indicated in Figs. 2.21 and 2.22. The BSFC was found to be more under DFM in comparison to that of diesel mode for different loading conditions as observed by Yoon and Lee (2011). Their study showed that the BSFC of biodiesel-biogas was found to be lower than diesel-biogas under DFM. On the other hand, Sahoo (2011) reported that the BSEC of diesel-biogas was found to be lower than Jatropha-biogas. Their study indicated a maximum liquid fuel replacement (LFR) of 69% and 66 % with a biogas flow rate (BFR) 3.66 m^3/h and 4 m^3/h for diesel and jatropha pilot fuel, respectively at 100% load.

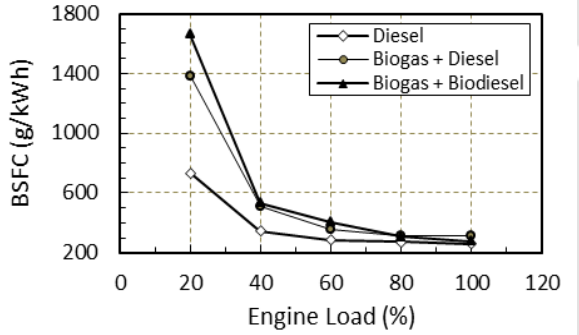

Fig. 2.21 Variation of BSFC of diesel with load (Yoon and Lee, 2011)

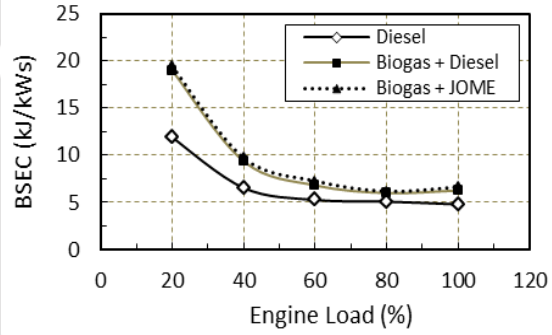

Fig. 2.22 Variation of BSEC of diesel with load (Sahoo, 2011)

For KME-biogas run dual fuel diesel engine, Barik and Murugan (2014a) found the BSEC respectively be to be 15.9 MJ/kWh, 17.3 MJ/kWh, 19.2 MJ/kWh and 21.5 MJ/kWh for BFR of 0.3 kg/h, 0.6 kg/h, 0.9 kg/h and 1.2 kg/h at full load as observed in (Fig. 2.23).

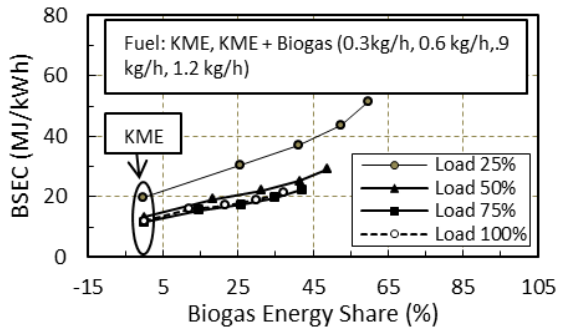

Fig. 2.23 Variation of BSEC with load for different BFRs (Barik and Murugan, 2014a)

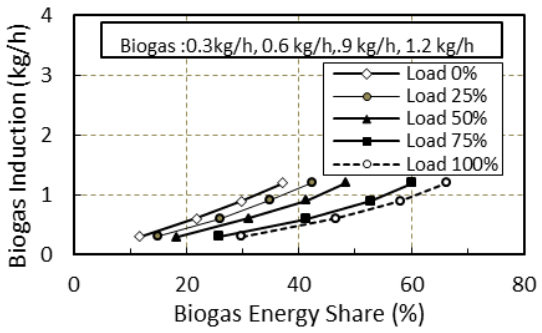

Fig. 2.24 Variation of biogas induction with load for different BFRs (Barik and Murugan, 2014a)

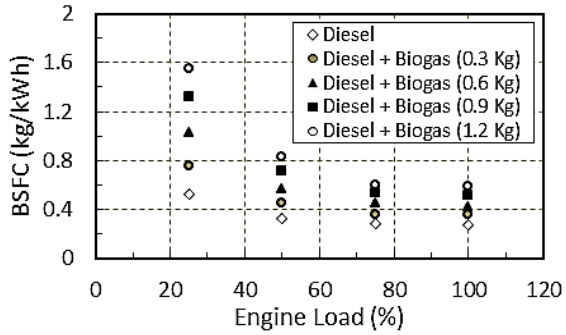

Fig. 2.25 Variation of BSFC with load for different BFR (Barik and Murugan, 2014b)

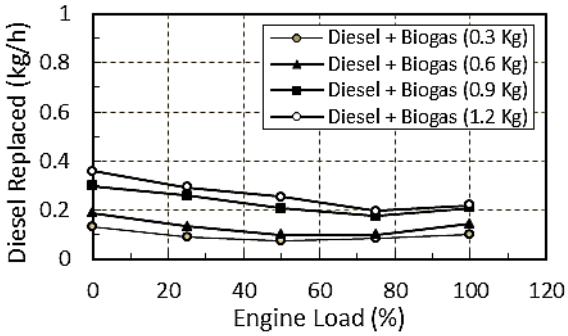

Fig. 2.26 Variation of diesel replacement with load for different BFRs (Barik and Murugan, 2014b)

The biogas energy share corresponding to these BFR values were found to be 11.8%, 21.8%, 30.2% and 37.4%, respectively as indicated in Fig. 2.24. In another study, Barik and Murugan (2014b) found the BSFC for diesel mode to be 0.27 kg/kWh at full load. Using diesel as pilot fuel under DFM for same loading conditions, the BSFC is 0.32 kg/kWh, 0.37 kg/kWh, 0.43 kg/kWh and 0.49 kg/kWh for BFR of 0.3 kg/h, 0.6 kg/h, 0.9 kg/h and 1.2 kg/h, respectively as shown in Fig. 2.25. For the same loading condition and BFRs, the LFRs were found to be 0.101 kg/h, 0.145 kg/h, 0.215 kg/h and 0.223 kg/h as depicted in Fig. 2.26.

Effect of Speed:

The BSFC was found to decrease with the increase of speed up to a particular speed as shown in Figs. 2.27 and 2.28. Tippayawong *et al*. (2007) reported that the BSFC to be 450 g/kW/h and 500 g/kW/h for diesel and DFM, respectively. Duc and Wattanavichien (2007) reported that the maximum diesel substitution was about 36% at the lowest speed. It reached a peak of about 48.8% at 1800 rpm before decreasing by 8% at rated speed.

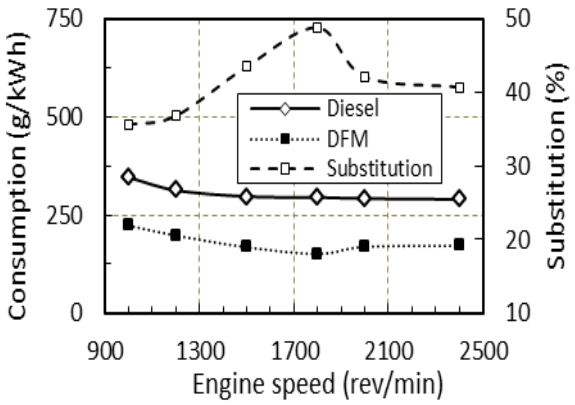

Fig. 2.27 Variation of BSFC and LFR with speed (Duc and Wattanavichien, 2007)

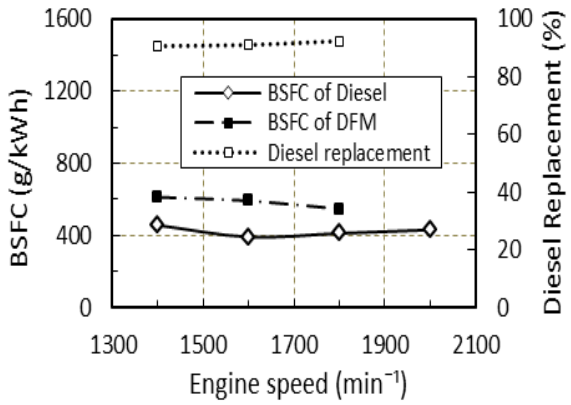

Fig. 2.28 Variation of BSFC and LFR with speed (Tippayawong *et al*., 2007)

Effect of Biogas Inlet Pressure:

Cheng-qui *et al.* (1989) studied the effect of biogas inlet pressure on performance of a biogas run dual fuel diesel engine. The results indicated that the BSFC of both diesel and biogas for a high pressure biogas run dual fuel diesel engine is higher than that of the low pressure biogas as shown in Figs. 2.29 and 2.30.

Effect of Biogas Quality:

Bari (1996) observes that the trend of BSFC rises as CO_2 increases in the biogas composition. This is due to the fact that as the CO_2 becomes higher in the biogas, CO_2 remains undissociated and acts as an inert gas. Addition of such inert gas affects the burning velocity leading to incomplete combustion, thereby increasing the BSFC and BFR.

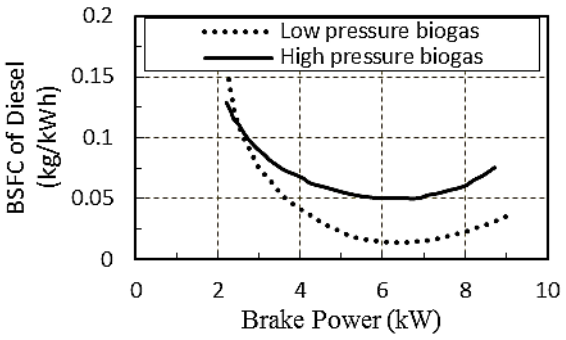

Fig. 2.29 Variation of BSFC of diesel with brake power for low and high pressure biogas (Cheng-qui *et al.*, 1989)

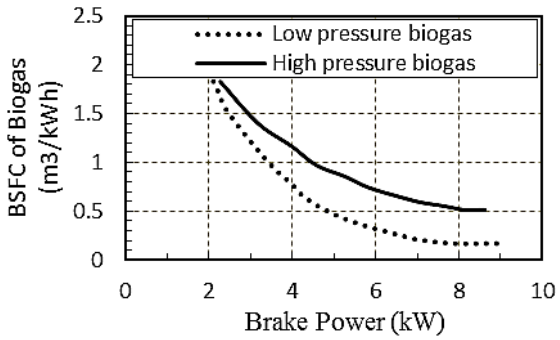

Fig. 2.30 Variation of BSFC of biogas with brake power for low and high pressure biogas (Cheng-qui *et al.*, 1989)

Mustafi *et al.*, (2013) found BSFC to be higher under DFM in comparison to that of diesel mode (Fig. 2.31). At the same loading conditions, the BSFC increased as the quantity of CO_2 in the biogas composition was increased.

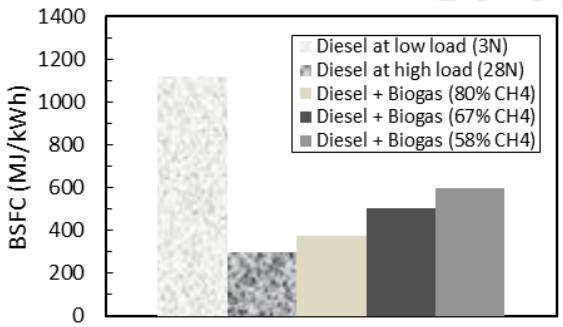

Fig. 2.31 Variation of BSFC with load for different biogas quality (Mustafi *et al.*, 2013)

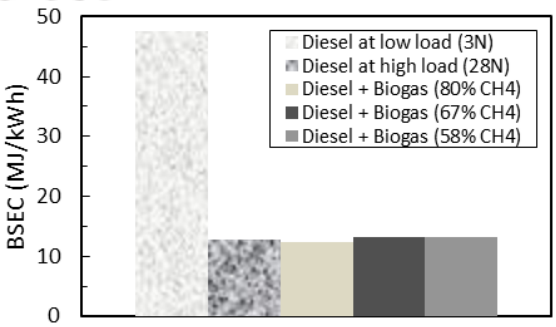

Fig. 2.32 Variation of BSEC with load for different biogas quality (Mustafi *et al.*, 2013)

However, there was no significant difference in BSEC between diesel and DFMs as indicated in Fig. 2.32. Analogous trend of variation of BSFC with biogas quality for a biogas run dual fuel diesel engine was reported by Maizonnasse *et al.* (2013) as shown in Fig. 2.33.

Effect of Oxygenated Combustion:

Cacua *et al.* (2012) observed that a higher oxygen concentration allows increasing the substitution level at 50% and 70% loads due to stable operation of the dual engine and a more uniform combustion. However, there were not significant differences at 40% of full load (Fig. 2.34).

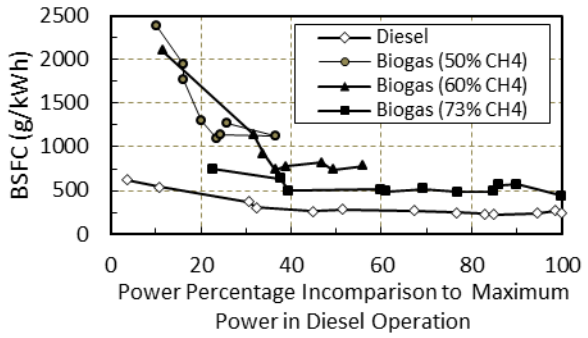

Fig. 2.33 Variation of BSFC with load for different types of biogas quality (Maizonnasse *et al.*, 2013)

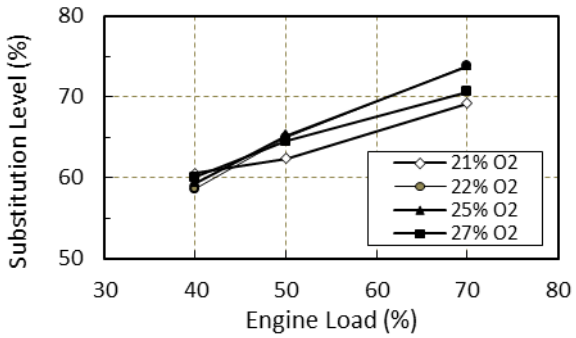

Fig. 2.34 Variation of BTE with the change of oxygen percentage in the inducted air (Cacua *et al.*, 2012)

Effect of Exhaust Gas Recirculation:

Makarevicience *et al.* (2013) found that the total specific fuel consumption with an operational EGR system was lower than when the engine ran without EGR at low BMEP (Figs. 2.35 and 2.36). The EGR rate decreased at an engine load of 0.6–0.7 MPa, which resulted in the same fuel consumption with and without the EGR system.

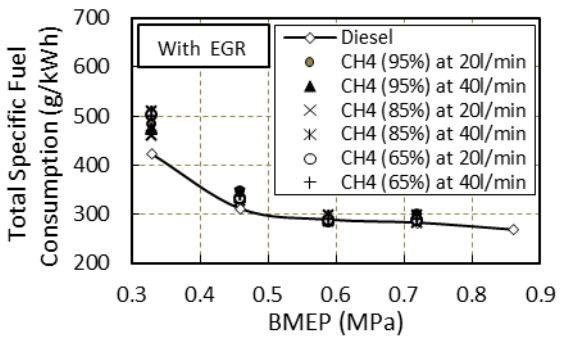

Fig. 2.35 Variation of total specific consumption with EGR for different BMEPs (Makarevicience *et al.*, 2013)

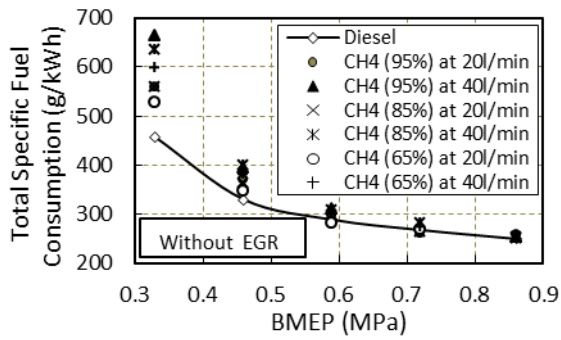

Fig. 2.36 Variation of total specific consumption without EGR for different BMEPs (Makarevicience *et al.*, 2013)

Combustion was less economically efficient at low engine loads because of the excessively high air/fuel ratios. The large quantity of oxygen in the mixture heated up during the combustion process and was later exhausted at high temperature, resulting in energy losses. As the engine load increased, the air/fuel ratio decreased, which increased the combustion efficiency.

2.7.6 Exhaust Gas Temperature

Effect of Load:

The exhaust gas temperature (EGT) is found to rise with the increase of load for both diesel and DFM. However, the review on EGT under DFM in comparison to diesel mode exhibited contrasting findings. Few studies (Yoon and Lee, 2011; Barik and Murugan, 2014a; Barik and Murugan, 2014b) reported a lower EGT under DFM whereas Sahoo (2011) reported a higher EGT under DFM in comparison to that of diesel mode (Figs. 2.37 and 2.38).

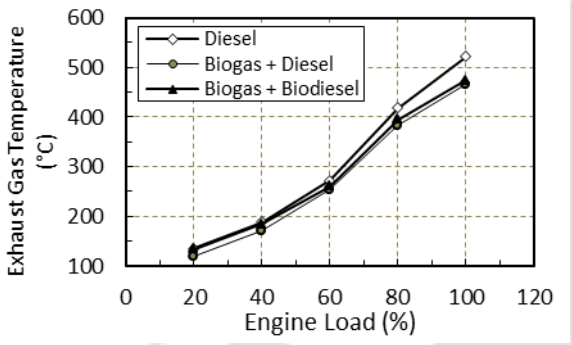

Fig. 2.37 Variation of EGT with load (Yoon and Lee, 2011)

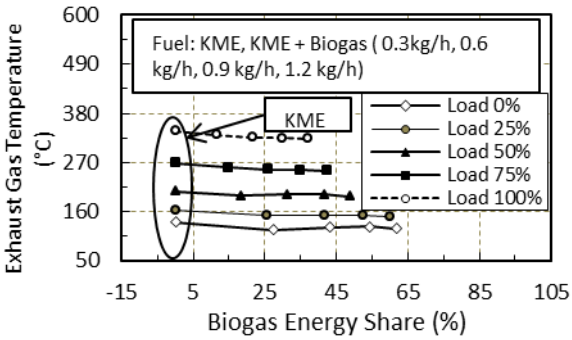

Fig. 2.38 Variation of EGT with load for different flow rate (Barik and Murugan, 2014a)

Effect of Speed:

Duc and Wattanavichien (2007) observe experimentally that the EGT rises with the increase of speed. At higher engine speeds, the higher combustion temperature would cause an increase in heat transfer to the cylinder head and cylinder wall, leading to a higher temperature of cooling water and lubricant oil. This resulted in a very high thermal load to the engine. However, the rise of EGT under DFM is lower than that of diesel mode as indicated in Fig. 2.39. As the combustion takes place closer to TDC, a larger fraction of the fuel energy is converted to work, to some extent, heat transfer. This leads to lower exhaust gas temperature, and hence, the loss of energy brought by exhaust gas decreased.

Effect of Air Induction System:

Bedoya *et al.*, (2009) reported that the combination of Kenics mixer and supercharger along with a longer mixing length produced a lower EGT in comparison to that of T-mixer along with a shorter mixing length for the same biogas run dual fuel diesel engine as shown in Fig. 2.40. This was due to the design of SM2 system which increased the mixing turbulence and thereby, resulted in better extraction of energy in power stroke. This caused a drop in EGT.

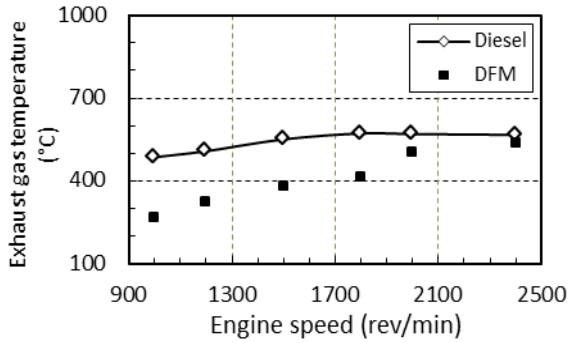

Fig. 2.39 Variation of EGT with speed (Duc and Wattanavichien, 2007)

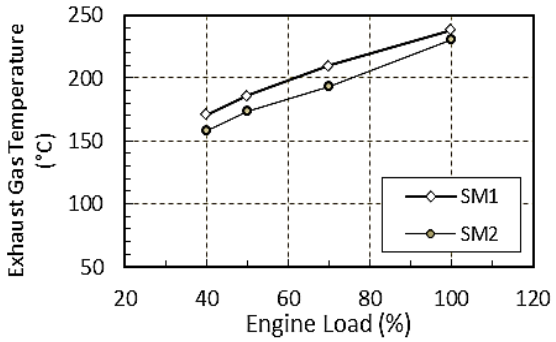

Fig. 2.40 Variation of EGT with load for different induction systems (Bedoya *et al.*, 2009)

Effect of Biogas Quality:

Henham and Makkar (1998) found that the EGT to be more affected by biogas substitution rather than biogas quality upto 45% replacement. At 58% replacement, EGT increased with the increase of CO_2 in biogas mixture.

2.7.7 Heat Release Rate

Effect of load:

Yoon and Lee (2011) reported the heat release rate (HRR) under DFM to be lower than diesel mode as indicated in Fig. 2.41. This was due to the low calorific value of biogas in comparison to diesel. At 100% loading condition, the net HRR under DFM for the combination of biogas-diesel is found to be more than biogas-biodiesel as indicated in Fig. 2.42 (Sahoo, 2011).

Effect of Air Induction System:

Bedoya *et al.*, (2009) found that the HRR in case of the combination of Kenics mixer and supercharger along with a longer mixing length is found to be less in comparison to that of T-

mixer along with a shorter mixing length for the same biogas run dual fuel diesel engine (Fig. 2.43). This may be due to the prolong delay period during which a large portion of pilot fuel mixed with air and producing a rapid release of energy in case of induction system having the combination of Kenics mixer and supercharger along with a longer mixing length.

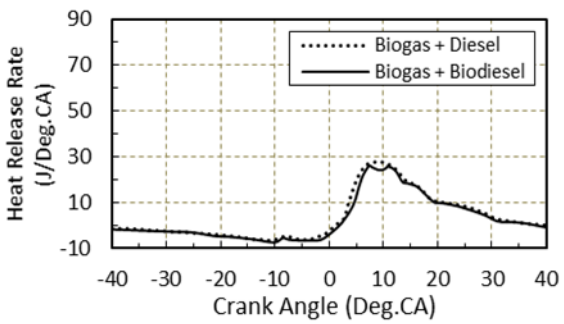

Fig. 2.41 Variation of HRR with crank angle (Yoon and Lee, 2011)

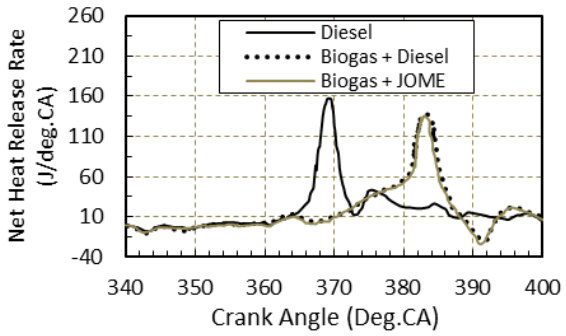

Fig. 2.42 Variation of net HRR with crank angle (Sahoo, 2011)

Effect of Biogas Quality:

Maizonnasse *et al.*, (2013) investigated the performance of a dual fuel diesel engine by using three types biogas quality along with diesel as pilot fuel. The biogas quality were 73% CH_4-27% CO_2, 60% CH_4-40% CO_2 and 50% CH_4-50% CO_2. The study indicated that HRR increased for the biogas having higher quality (i.e. 73% CH_4-27% CO_2) as depicted in Fig. 2.44. Further, the occurrence of peak of HRR shifted away from the TDC with decrease of biogas quality.

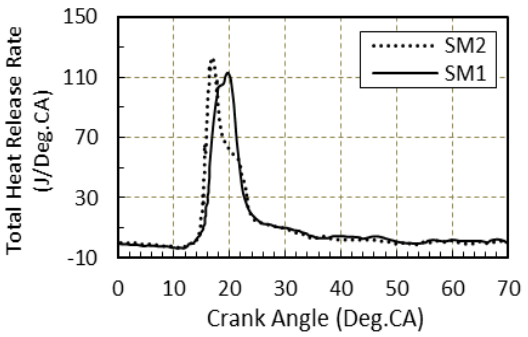

Fig. 2.43 Variation of HRR with crank angle for different induction systems at 100% load (Bedoya *et al.*, 2009)

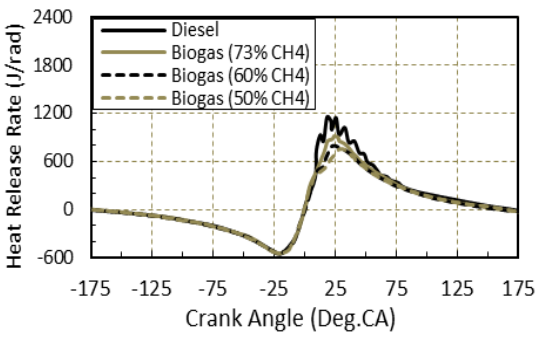

Fig. 2.44 Variation of HRR with crank angle (Maizonnasse *et al.*, 2013)

Effect of Oxygenated Combustion:

Cacua *et al.*, (2012) found that the HRR increased with the increase of oxygen percentage in the inducted air. The total heat release rate showed earlier premixed combustion and lower

diffusion with the increase of oxygen enrichment levels, which indicated a more efficient energy release.

2.7.8 Ignition Delay

Effect of Load:

The ignition delay (ID) is found to decrease with the increase of load for both diesel and DFM (Figs. 2.45, through and 2.48). However, the ID under DFM is found to be longer than diesel mode. This is due to high heat capacity of biogas, which results in the lowering of the combustion chamber temperature. Another important fact that got revealed about pilot fuel is that ID for the combination of biogas-biodiesel is found to be longer than biogas-diesel fuel as observed by Yoon and Lee (2011) and Sahoo (2011).

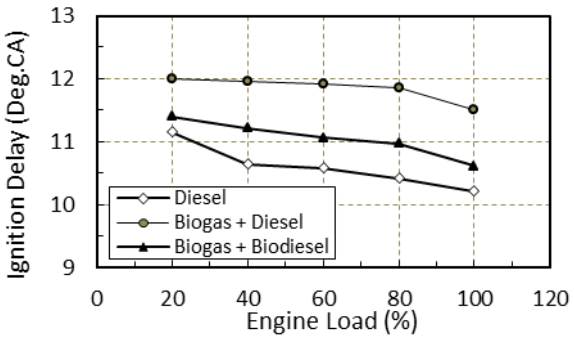

Fig. 2.45 Variation of ID with load (Yoon and Lee, 2011)

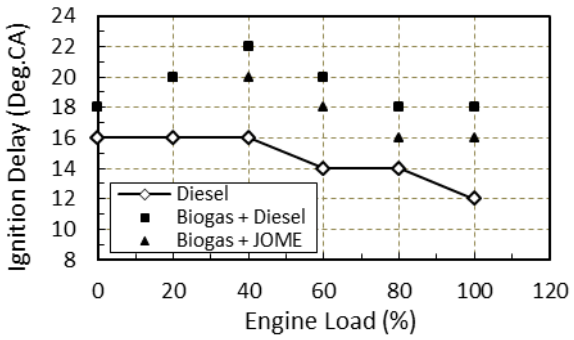

Fig. 2.46 Variation of ID with load (Sahoo, 2011)

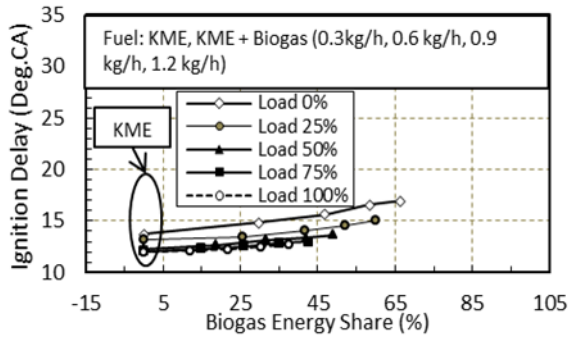

Fig. 2.47 Variation of ID with load (Barik and Murugan, 2014a)

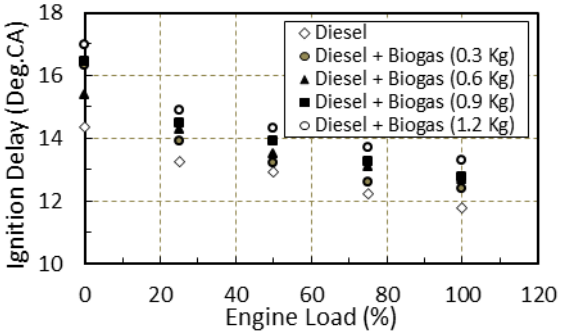

Fig. 2.48 Variation of ID with load for different BFR (Barik and Murugan, 2014b)

Effect of Oxygenated Combustion:

As reported, the ID of a biogas run dual fuel engine decreases with the increase of oxygen percentage in the inducted air as (Cacua *et al.* 2012). This is because of the increase in the

reactivity of fuel due to oxygen enrichment, which resulted in a higher flame propagation velocity and thereby, lowering the ID.

2.7.9 Cylinder Pressure

Effect of Load:

The peak cylinder pressure (PCP) was found to increase with the increase of load for both diesel and DFM as indicated in Fig. 2.49. Sahoo (2011) observed that the PCP under DFM is lower than diesel mode. Another important finding of this study was that there was a shift of PCP away from the top dead centre (TDC) under DFM as shown in Fig. 2.50. To add to it, another imperative fact that got unravelled about pilot fuel is that the PCP obtained using diesel is higher than that of jatropha biodiesel. However, Barik and Murugan (2014a, 2014b) reported that the PCP under DFM is higher than diesel mode.

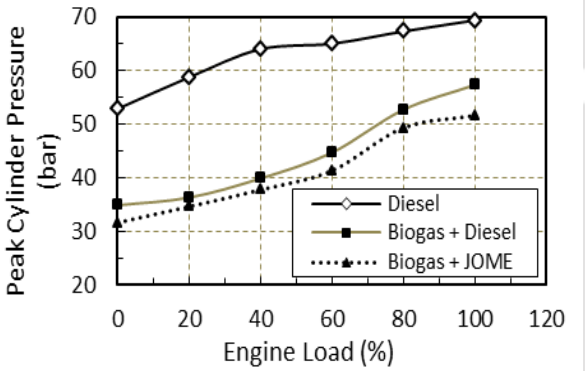

Fig. 2.49 Variation of PCP with load (Sahoo, 2011)

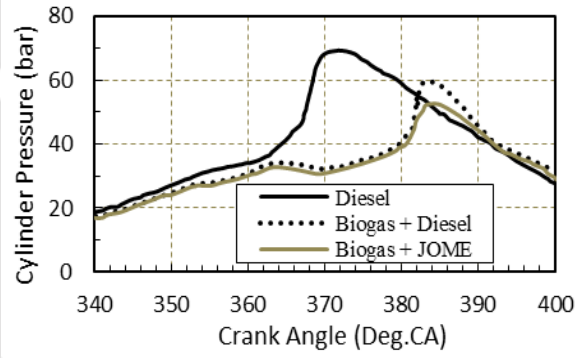

Fig. 2.50 Variation of PCP with crank angle at same loading condition (Sahoo, 2011)

Effect of Air Induction System:

The PCP increased approximately 5% greater and it occurred closer to TDC for the SM2 system compared with the SM1 system as indicted in Fig. 2.51. This fact suggested an increase in the reactivity of biogas-air mixture during premixed combustion period for the SM2 system.

Effect of Oxygenated Combustion:

The PCP corresponding to 22% oxygen enrichment of the inducted air was not as significant in comparison to atmospheric condition as observed by Cacua *et al.* (2012). However, the PCP corresponding to 25% and 27% oxygen enrichment was found to be higher in

comparison to that of atmospheric conditions for all loads as found in Fig. 2.52. This was due to increase in the reactivity of both fuels during premixed combustion stage and a decrease of ignition delay.

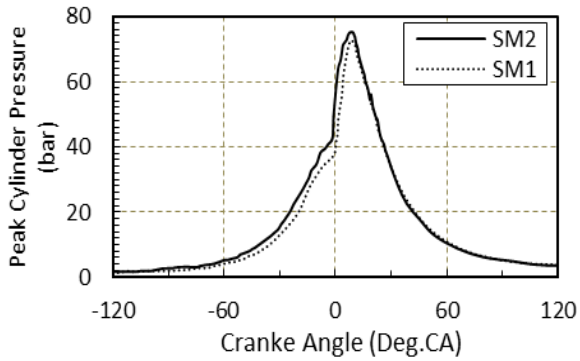

Fig. 2.51 Variation of HRR with crank angle for different induction systems at 100% load (Bedoya *et al.*, 2009)

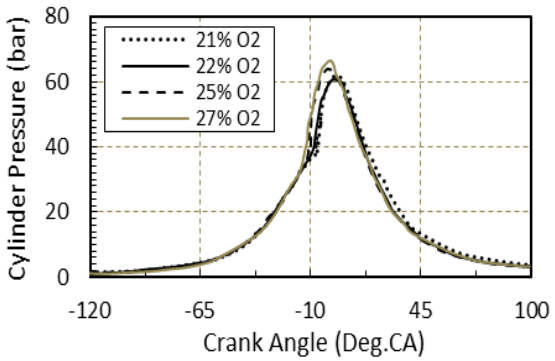

Fig. 2.52 Variation of PCP with the change of oxygen percentage in the inducted air (Cacua *et al.*, 2012)

Effect of Biogas Quality:

Mustafi *et al.* (2013) found that the PCP under DFM occurred later compared to that of diesel mode as depicted in Fig. 2.53. It was observed that addition of more CO_2 in gaseous fuel did not significantly affect the PCP, but the ignition and the peak of the cylinder pressures occurred slightly later in the cycle.

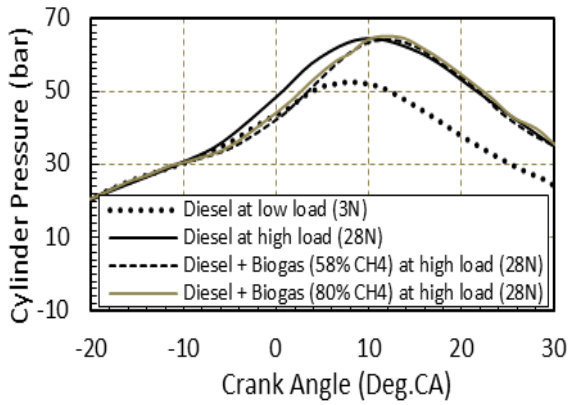

Fig. 2.53 Variation of PCP with different biogas quality (Mustafi *et al.*, 2013)

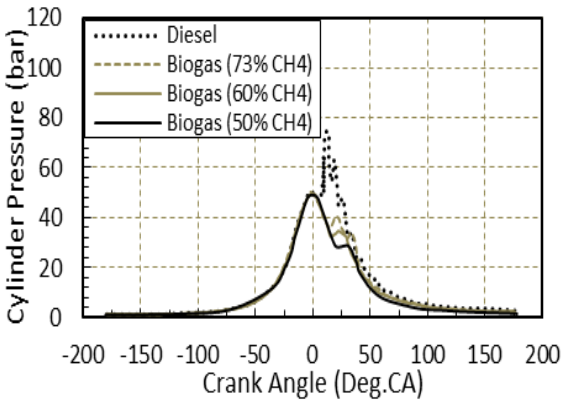

Fig. 2.54 Variation of PCP with different biogas quality (Maizonnasse *et al.*, 2013)

Maizonnasse *et al.* (2013) observed that the PCP increased with the improvement of biogas quality as indicated in Fig. 2.54. Further, there was a shift of PCP towards TDC with the improvement of biogas quality.

2.7.10 Carbon Monoxide Emission

Effect of Load:

Yoon and Lee (2011) found that the carbon monoxide (CO) emission to be more incase of DFM in comparison to that of diesel mode (Fig. 2.55). This was due to incomplete combustion caused by dilution of charge by the CO_2 present in biogas and deficiency of oxygen. Hence, the flame formed in the ignition region of the pilot fuel was normally suppressed, and did not proceed until the biogas fuel air mixture reached a minimum limiting value for autoignition. Conversely, Sahoo (2011) observed that there was a decrease of CO emission by 50% and 16% for biogas-diesel and biogas-jatropha biodiesel, respectively in comparison to diesel mode at 100% load as depicted in Fig. 2.56.

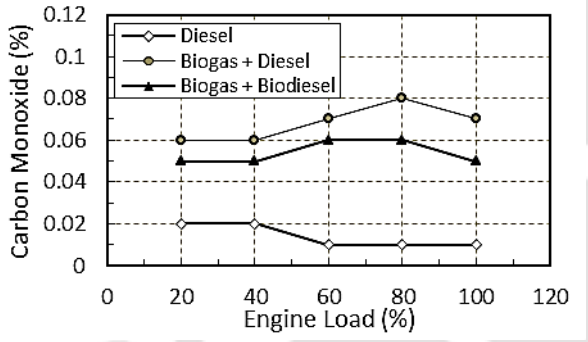

Fig. 2.55 Variation of CO emission with load (Yoon and Lee, 2011)

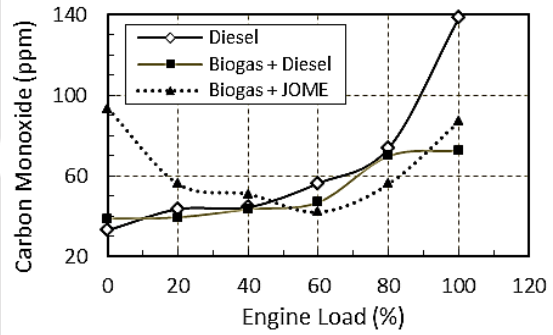

Fig. 2.56 Variation of CO emission with load (Sahoo, 2011)

Barik and Murugan (2014a) reported an increase of brake specific carbon monoxide (BSCO) emissions by 9%, 16.6%, 28.5% and 37.5% than KME operation for biogas energy shares of 11.8%, 21.8%, 30.2% and 37.4%, respectively at full load. Further, Barik and Murugan (2014b) observed that the CO emission to be higher by about 24% with biogas at the flow rate of 1.2 kg/h, in comparison with diesel at full load.

Effect of Air Induction System:

Bedoya *et al*. (2009) found that the CO emissions were produced more in the exhaust by using SM2 in comparison to that of SM1 (Fig. 2.57). At 40% load, CO emissions were increased with the SM2 system due to an increase in partial oxidation phenomena of methane, lower pilot fuel quantity and higher total fuel–air equivalence ratio. This occurred because the reactivity of biogas–air mixture on the compression stroke was increased, and the pilot fuel quantity was reduced with the SM2 system. At higher loads, CO emissions

increased for both the SM1 and the SM2 systems due to the reduction of unburned methane and lower oxygen availability at higher equivalence ratios. However, the SM2 system allowed a reduction in CO emissions in comparison with the SM1 system, close to 40% at 100% load. It was due to higher burning rates and higher availability of oxygen in later stages of combustion.

Effect of Biogas Quality:

Mustafi *et al.*, (2013) observed a slower increase of CO emissions as the percentage of CO_2 content increased in the fuel (Fig. 2.58). This may be due lowering of combustion efficiency as the amount of CH_4 got reduced with the decrease of biogas quality.

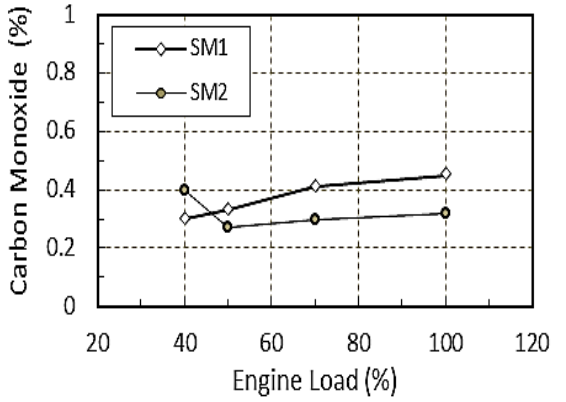

Fig. 2.57 Variation of CO emission with load for different induction systems (Bedoya *et al.*, 2009)

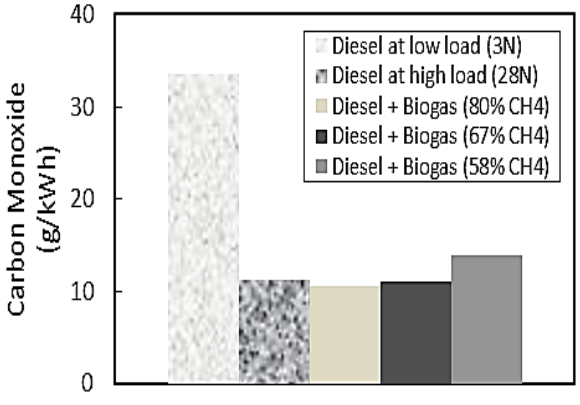

Fig. 2.58 Variation of CO emission with load for different biogas quality (Mustafi *et al.*, 2013)

Effect of Oxygenated Combustion:

Cacua *et al*. (2012) reported that at 40% of full load and 25% O_2, CO decreased by 19.5% in comparison to that of atmospheric air (21% O_2). This was due to a decrease in fuel/air equivalence ratio and an increase in preignition reactions of biogas. At 50% of full load, CO emissions increased up to 11% for 22% oxygen and up to 7.5% for 25% oxygen. This was caused by an increase in partial oxidation of biogas and higher substitution levels in comparison to that of atmospheric air (21% O_2).

Effect of Exhaust Gas Recirculation:

Makarevicience *et al*. (2013) found that the engine operated with the EGR system under DFM, the CO concentration increased significantly by 3–20 times, as compared to engine operation under diesel mode (Figs. 2.59 and 2.60). Such results were obtained because the

CO_2 gases present in biogas along with exhaust gases reduced the amount oxygen in air-fuel mixture. Conversely, when the EGR system was off, the carbon in the fuel was combusted more efficiently because the air fuel ratio was higher, and the proportion of the CO pollutants in the exhaust gas was three times lesser than when the EGR was operational.

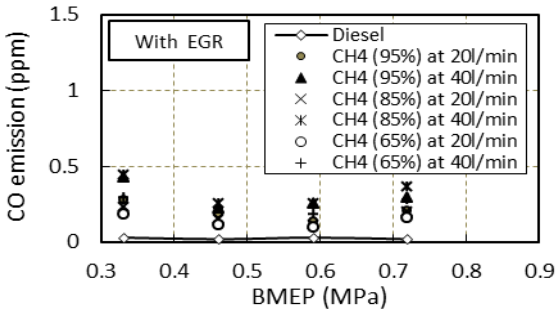

Fig. 2.59 Variation of CO emission with EGR for different BMEPs (Makarevicience *et al*., 2013)

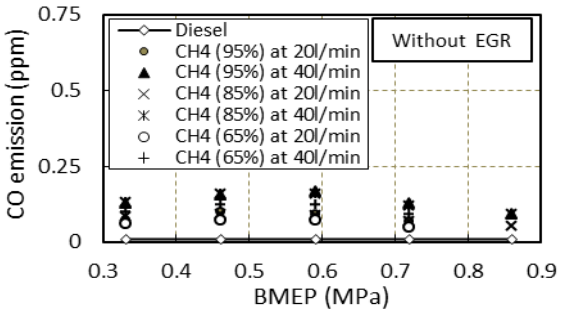

Fig. 2.60 Variation of CO emission without EGR for different BMEPs (Makarevicience *et al*., 2013)

2.7.11 Carbon Dioxide Emission

Effect of Load:

The carbon dioxide (CO_2) emission is found to increase with the increase of load for both diesel and DFM. However, the CO_2 emission is found more in case of DFM in comparison to that of diesel mode. This is because biogas mainly contains methane and CO_2. Yoon and Lee (2011) found that the combination of biogas-biodiesel emitted more CO_2 in comparison to biogas-biodiesel. Conversely, Sahoo (2011) reported that the combination of biogas-diesel emitted more CO_2 emission than biogas–biodiesel especially at higher loads.

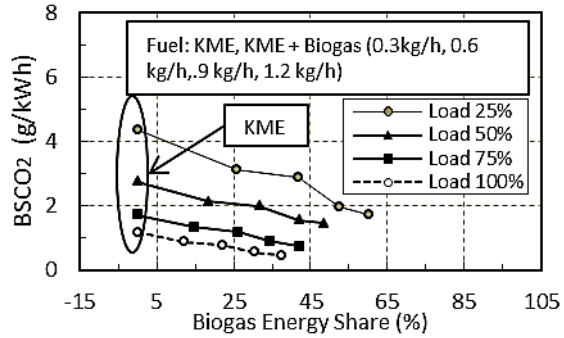

Fig. 2.61 Variation of CO_2 emission with load for different biogas share (Barik and Murugan, 2014a)

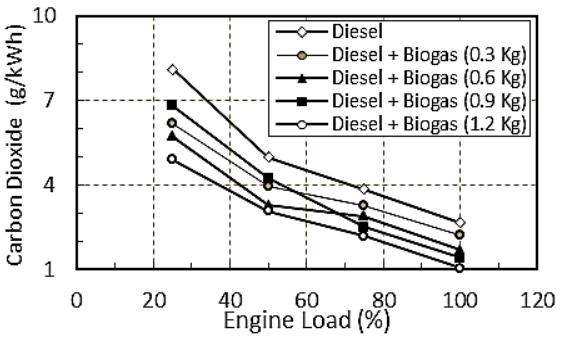

Fig. 2.62 Variation of CO_2 emission with load for different BFRs (Barik and Murugan, 2014b)

In another study, Barik and Murugan (2014a) used KME as pilot fuel under DFM (Fig. 2.61). The test indicated that the brake specific carbon dioxide ($BSCO_2$) decreased with the increase in the biogas energy share. The biogas energy share of 11.8%, 21.7%, 30.2% and 37.4% produces a drop of $BSCO_2$ by 25%, 33%, 52% and 60% respectively, than that of KME at full load. This reduction in the $BSCO_2$ emission under DFM was attributed to the lower volumetric efficiency and higher CO_2 in biogas. The same group of authors observed that the CO_2 emission rises with the increase in biogas flow rate for the same loading conditions using diesel as pilot fuel (Fig.2.62).

Effect of Exhaust Gas Recirculation:

Makarevicience *et al*. (2013) found that the CO_2 emissions did not vary linearly when EGR was operational for higher loads (Fig. 2.63). Conversely, the CO_2 emissions drop by two times when EGR was turned off as indicated in Fig. 2.64. This behaviour may be attributed to the sudden change in air-fuel ratio when the EGR was turned off.

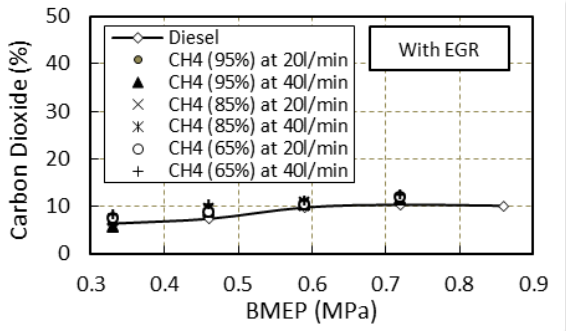

Fig. 2.63 Variation of CO_2 emission with EGR for different BMEPs (Makarevicience *et al*., 2013)

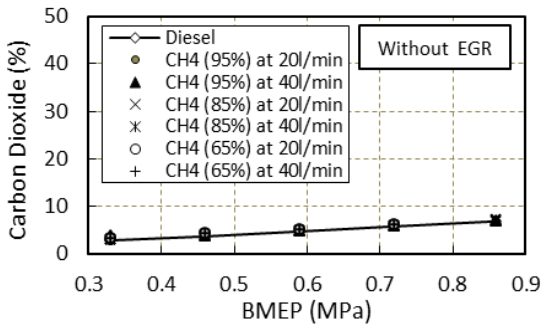

Fig.2.64 Variation of CO_2 emission without EGR for different BMEPs (Makarevicience *et al*., 2013)

2.7.12 Hydrocarbon Emission

Effect of Load:

Yoon and Lee (2011) found a decrease of hydrocarbon (HC) emission with the increase of load for both diesel and DFM as shown in Fig. 2.65. However, Sahoo (2011) observed that the HC emissions were higher at low loads as the combustion chamber temperature was low. This gradually decreases at medium loads and then increases at high loads as depicted in Fig. 2.66. Barik and Murugan (2014b) reported an increase of HC emission increases with load for high biogas flow rate.

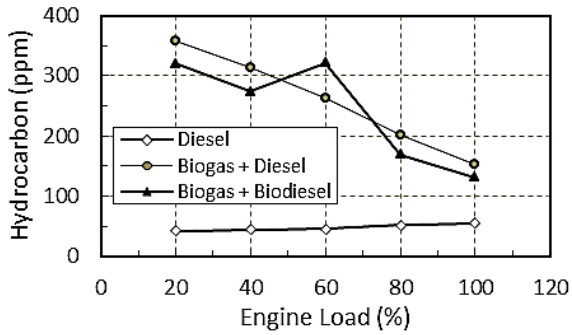

Fig. 2.65 Variation of HC emission with load (Yoon and Lee, 2011)

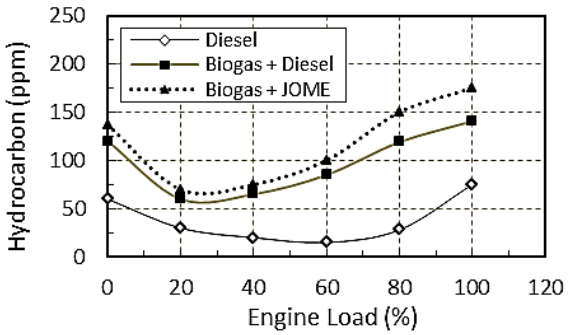

Fig. 2.66 Variation of HC emission with load (Sahoo, 2011)

Effect of Air Induction System:

Bedoya *et al.* (2009) reported that the methane emission dropped by 34% using the SM2 system in comparison to that of SM1 system at 40% load as indicated in Fig. 2.67. At full load, the effect of dual fuel system on methane emissions was less than at part load as the equivalence ratio was closer to the stoichiometric value for both the SM1 and the SM2 systems.

Effect of Biogas Quality:

The HC emission is found to increases with the increase of CO_2 in the biogas composition as observed by Mustafi *et al.* (2013) as shown in Fig. 2.68. This is due to the fact that with the increase of CO_2 in the biogas composition, the turbulent flame propagation from the ignition regions of the pilot fuel is suppressed further due to the low combustion chamber temperature and low air-fuel ratio.

Effect of Oxygenated Combustion:

Cacua *et al*. (2012) observed that the methane emissions decreased by 35% for 27% O_2 for all loads. The most noticeable change was presented at 50% of full load and 25% O_2, where a decrease of 38% in methane emissions was reached.

Effect of Exhaust Gas Recirculation:

The HC concentration in the exhaust gas was directly proportional to the methane concentration in the fuel mixture as observed by Makarevicience *et al*. (2013). The test indicated that the HC concentration at a low engine speed was considerably lower when the

EGR system was turned off than when the EGR system was on. However, as the engine load was increased, the same HC concentration was observed when the EGR system was on and off (Figs. 2.69 and 2.70).

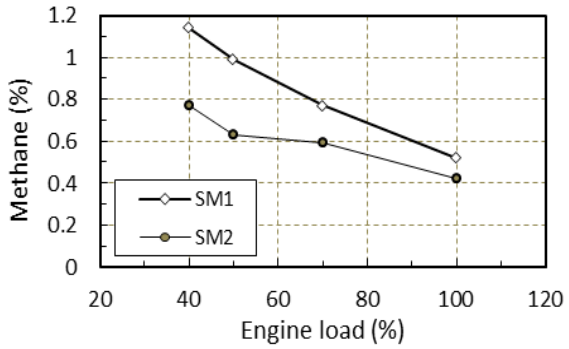

Fig. 2.67 Variation of HC emission with load for different induction systems (Bedoya *et al.*, 2009)

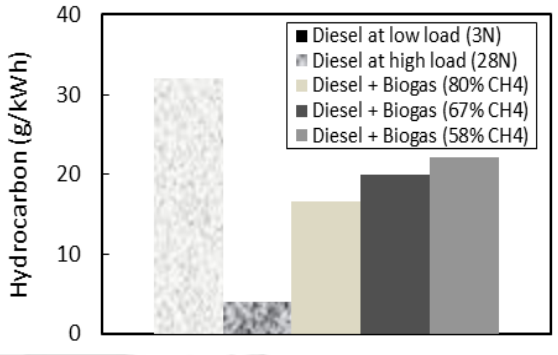

Fig. 2.68 Variation of HC emission with load for different biogas quality (Mustafi *et al.*, 2013)

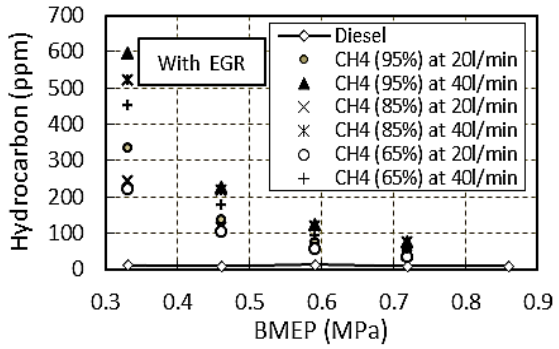

Fig. 2.69 Variation of HC emission with EGR for different BMEPs (Makarevicience *et al.*, 2013)

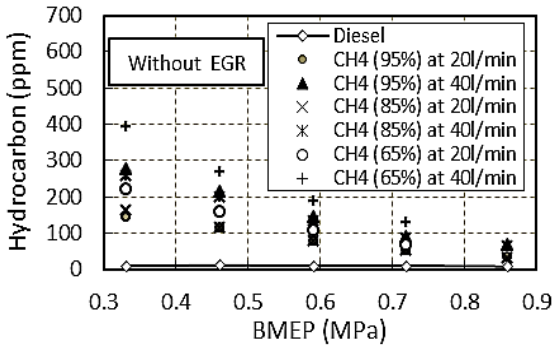

Fig. 2.70 Variation of HC emission without EGR for different BMEPs (Makarevicience *et al.*, 2013)

2.7.13 Oxides of Nitrogen Emission

Effect of Load:

The oxides of nitrogen (NO_X) emission mainly depend upon combustion chamber temperature which in turn depends on the applied load (Heywood, 1988). Therefore, there is an increase in NO_X emission with the increase of load for both diesel and DFMs (Figs. 2.71 and 2.72). However, the NO_X emission is lower in case of dual fuel operations. This is due to the fact the presence of CO_2 in biogas lowers the combustion temperature. Yoon and Lee (2011) reported that diesel-biogas produced lower NO_X emission than soybean biodiesel-biogas for the same dual fuel engine. In a different pilot fuel study, Sahoo (2011) found that diesel-biogas produced higher NO_X emission than jatropha biodiesel-biogas.

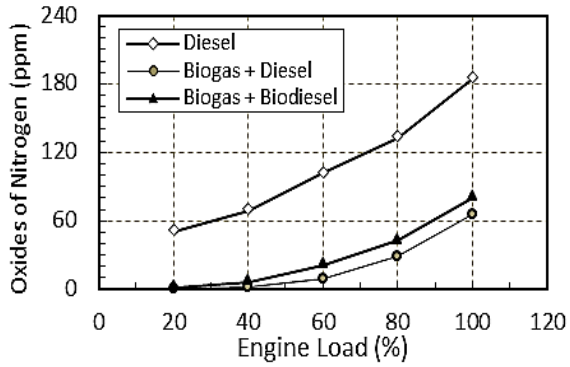

Fig. 2.71 Variation of NO_X emission with load (Yoon and Lee, 2011)

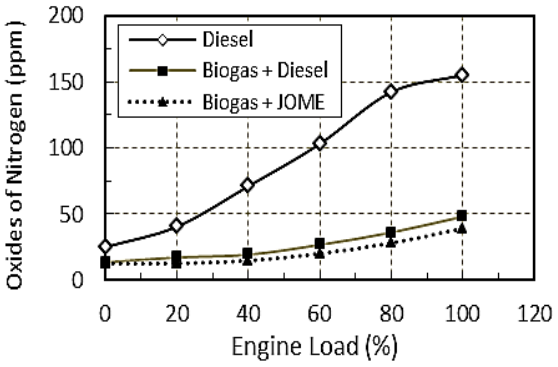

Fig. 2.72 Variation of NO_X emission with load (Sahoo, 2011)

Barik and Murugan (2014a) carried out a comparison of brake specific nitrous oxide (BSNO) emission for a biogas run dual fuel diesel engine for different biogas energy share. The results indicated a reduction of 24%, 29%, 34% and 39.5% in the BSNO emission under DFM with the biogas energy share of 11.8%, 21.8%, 30.2% and 37.4% respectively, in comparison to KME in lone mode at full load (Fig. 2.73). In another study, the same group of authors observed the NO emission to be lowers by 42.8% as compared to that of diesel for a BFR of 1.2 kg/h lowers at full load as depicted in Fig. 2.74.

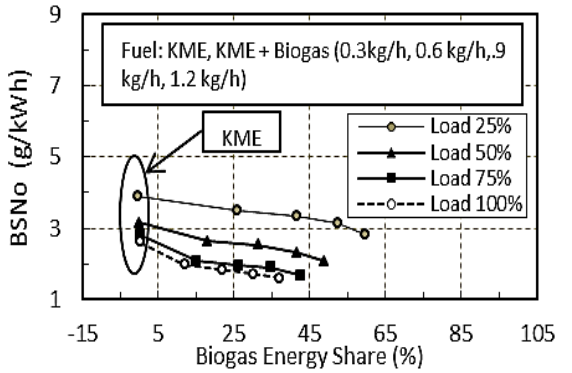

Fig. 2.73 Variation of NO emission with load for different BFRs (Barik and Murugan, 2014a)

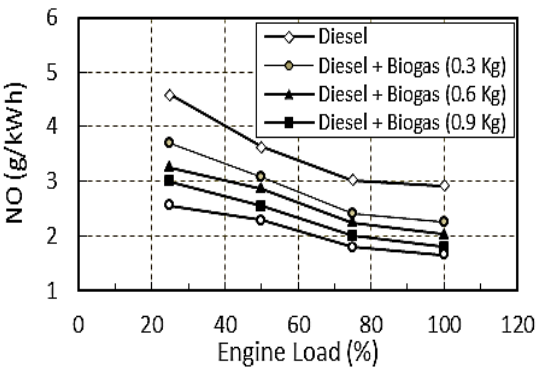

Fig. 2.74 Variation of NO emission with load for different BFRs (Barik and Murugan, 2014b)

Effect of Biogas Quality:

The NO_X emission decreased with the increase of CO_2 in biogas composition as observed by Mustafi *et al.* (2013). The increase of CO_2 in biogas caused more gaseous fuel to escape the combustion process, which affected oxygen concentration followed by a decrease in overall cycle temperature. Therefore, NO_X formation reduced with the degradation of the biogas quality.

Effect of Exhaust Gas Recirculation:

Makarevicience *et al*. (2013) found that the NO_X emission increased more rapidly with increase of BEMP when EGR was not operational than when EGR was on as depicted in Figs. 2.75 and 2.76. At BMEP = 0.7 bar, the NO_X emission with EGR turned off was twice as high as when EGR was on.

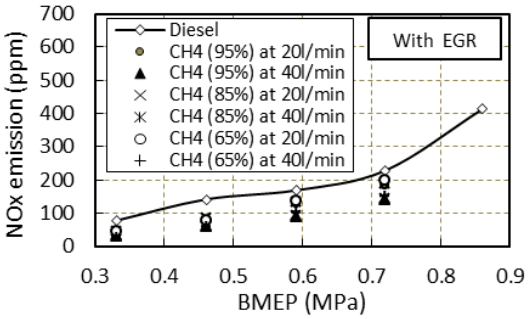

Fig. 2.75 Variation of NO_X emission with EGR for different BMEPs (Makarevicience *et al*., 2013)

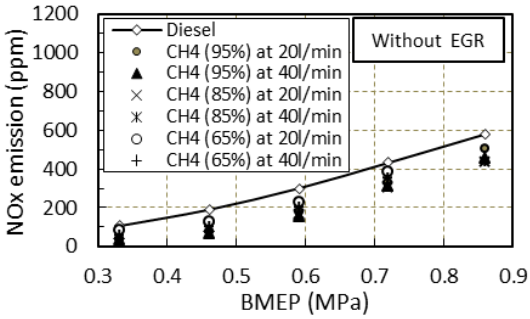

Fig. 2.76 Variation of NO_X emission without EGR for different BMEPs (Makarevicience *et al*., 2013)

2.7.14 Soot, Particulate Matter and Opacity Emission

Effect of Load:

Yoon and Lee (2011) observed that the values of filtered soot number increased with the increase of load for both diesel and dual fuel modes. However, the filtered soot number was found to be lower under DFM in comparison to diesel mode. These values were found to be significantly lower for biodiesel-biogas combination as indicated in Fig. 2.77. The drop in soot emission can be attributed to the absence of aromatics and the low sulphur content. For the same loading conditions, Barik and Murugan (2014a) found that the smoke opacity reduced with the increase of biogas flow rate as depicted in Fig. 2.78. This was due to the presence of methane in biogas, which possessed very small tendency to produce soot. In general, the reduction of smoke is attributed to flame temperature reduction and increased oxidation of soot precursors in the soot forming region by the enhanced concentration of O and OH around the flame produced from the CO_2 in biogas. The CO_2 concentration in the fuel causes a reduction in overall cycle temperature, which lowers the smoke formation. The dual fuel operation using KME as pilot fuel with the biogas energy share of 11.8%, 21.8%, 30.2%, and 37.4% drops the smoke emission by 4.5%, 12.9%, 14.5% and 22.5%, respectively in comparison to KME at full loading conditions. In another study, the same group of authors

used diesel as pilot fuel under DFM. Their results indicated a drop of 30%, 41%, 49% and 62% for biogas flow rates of 0.3 kg/h, 0.6 kg/h, 0.9 kg/h and 1.2 kg/h, respectively, at full load in comparison to that of diesel mode.

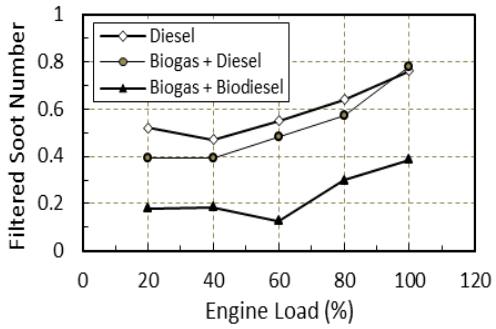

Fig. 2.77 Variation of filter soot number with load (Yoon and Lee, 2011)

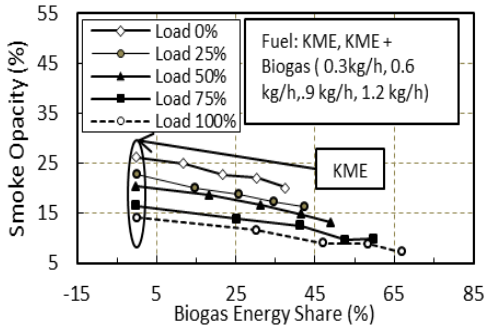

Fig. 2.78 Variation of opacity with load for different biogas share (Barik and Murugan, 2014a)

Effect of Biogas Quality:

Mustafi *et al.* (2013) observed that the presence of more CO_2 in biogas resulted in a greater reduction of particulate matter soot emission. The presence of higher CO_2 concentration in biogas resulted in a decrease of overall cycle temperature. However, in case of diesel mode, the cycle temperature was higher which resulted in formation of more soot particulate matter.

Effect of Exhaust Gas Recirculation:

Makarevicience *et al.* (2013) observed that the smokiness reduced significantly when EGR was turned off in comparison to the engine with EGR as indicated by Figs. 2.79 and 2.80. This was because the air fuel ratio improved greatly when EGR was turned off.

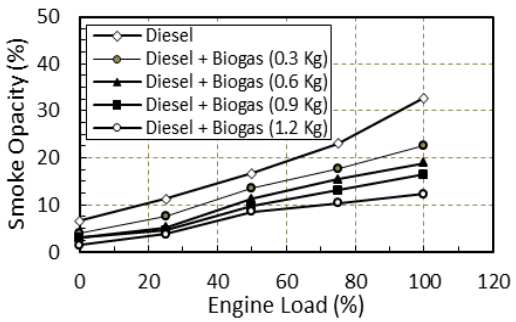

Fig. 2.79 Variation of opacity with load for different biogas share (Barik and Murugan, 2014b)

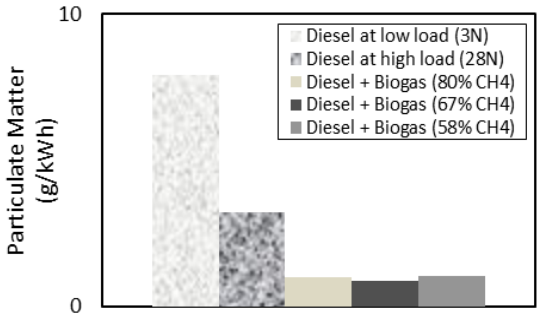

Fig. 2.80 Variation of particulate matter with load (Mustafi *et al.*, 2013)

2.8 Exergy Analysis

In order to evaluate the inefficiency associated with various engine processes, the analysis of second law of thermodynamics is cardinal. The key concept of the second law of thermodynamics is termed as 'exergy or availability'. Exergy or availability of a system is defined to be its work potential with reference to a prescribed environment (Som and Datta, 2008). The term 'work potential' represents the maximum theoretical work accessible if the system and the prescribed environment interact with each other and reach the equilibrium. Unlike energy, exergy can be destroyed by a number of phenomena such as combustion, friction, mixing and throttling during engine operation. The destruction of exergy is termed as irreversibility which represents the defective exploitation of fuel into useful mechanical work. The reduction of irreversibility can lead to improved performance through effective utilisation of fuel. There has been limited work on reported on energy and exergy analysis on biogas run dual fuel diesel engine. To establish this fact, a brief literature survey in the field of energy and exergy analysis on diesel and dual fuel diesel engines was carried out in the two upcoming subsections.

2.8.1 Exergy Analysis on Diesel Engines

Several studies have been carried out on the effect of different parts of diesel engines on energy and exergy analysis. The exergy analysis carried out by AL-Najem and Diab (1992) on a turbo-charged, diesel engine indicated that 50% of the chemical availability of the fuel was destroyed due to uncounted factors. Rakopoulos and Giakoumis (1997a) conducted an exergy analysis of a turbocharged diesel engine using a single-zone thermodynamic model. The study revealed that the throttling, friction and thermal mixing losses encountered in the turbocharger and inlet-exhaust manifold destructions contributed a significant amount to the total irreversibilities. Nakonieczny (2002) found that the turbine effective area ratio had the greatest impact on the total entropy generation rate during the exergy analysis of a diesel engine turbocharging system. Ghazikhani *et al.* (2010) studied the effect of EGR on total in-cylinder irreversibility of a diesel engine. The results of this study indicated that the total in-cylinder irreversibility increased with the use of EGR due to the extension of the flame region. Further, Hatami *et al.* (2015) carried out an exergy analysis of a vortex generator heat exchanger for an OM314 diesel engine. This investigation revealed that high engine loads

and low water mass flow rates were more suitable from the second law view point to maximize the exergy recovery in the heat exchanger.

Few studies on exergy analysis have been conducted on low heat rejection (LHR) diesel engines. One of these studies investigates the effect of insulated combustion chamber surfaces on the performance of a turbocharged, direct injection (DI) LHR diesel engine by Parlak *et al.* (2005). They revealed that the available exhaust gas energy of the standard diesel engine was 3–27% lower in comparison to that of the LHR engine. In a separate work, Parlak (2005) found a higher amount of available energy of the exhaust gas stream for a LHR engine at the optimum IT in comparison to its standard IT. Giakoumis (2007) found that the combustion irreversibilities with the application of insulation in a LHR diesel engine decreased by 23% as compared to non-insulated configuration. Zeng and Caton (2012) reported that exergy transfer due to heat transfer, blow-by and unburned fuel of a LHR engine were found to be the function of EGR level and IT.

Studies on lighter fuel like methane, oxygenated fuel (i.e. methanol and biodiesel) and low cetane number fuels reported a higher value of exergetic efficiency in comparison to petroleum diesel (Rakopoulos and Kyritsis, 2001; Tat, 2011; Lopez *et al.*, 2014; Jena and Misra, 2014). A good number of investigations on operational parameters demonstrate a decrease of combustion irreversibilities with the increase of torque, speed, load, CR and at retarded IT (Rakopoulos and Giakoumis 1997b, 1997c ; Debnath *et al.*, 2013a, 2014a; Ozkan *et al.*, 2013; Ghazikhani *et al.*, 2014). Furthermore, Caliskan *et al.* (2009) reported an increase of exergetic efficiency with the lowering of dead state temperature.

2.8.2 Exergy Analysis on Dual Fuel Diesel engines

The following section gives an overview on the work reported in the field of exergy analyses on dual fuel diesel engines for last two decades. The primary fuels considered in these investigations were natural gas, hydrogen, ethanol, landfill gas, syngas and biogas as indicated in Table 2.3. The analyses were done mainly to study the effect of hydrogen addition, speed, EGR, load and variation of percentage water ethanol mixture on exergy efficiency of dual fuel diesel engine. Rakopoulos and Kyritsis (2006) investigated the influence of hydrogen enrichment to natural gas and landfill gas under DFM. The study indicated that the hydrogen combustion resulted in a monotonic decrease in combustion irreversibilities. In contrast, the hydrocarbon combustion significantly increased the entropy

by converting molecules of relatively complicated structure to a mixture of relatively light `gaseous fragments. Analogous finding for hydrogen enrichment in case of natural gas under DFM was reported by Rakopoulos *et al.* (2008). Hosseinzadeh *et al.* (2010) compared the thermal, radical and chemical effect of the EGR gases for a natural gas run dual fuel diesel engine using availability analysis at part load conditions. The study revealed that the thermal and radical effects have a positive impact on the work availability. However, the chemical effect of EGR has a negative impact on work availability as the unburnt chemical availability increases. Costa *et al.* (2012) formulated a mathematical model based on the thermodynamics concepts for energetic and exergetic analysis of a natural gas run dual fuel diesel engine. The energy efficiency ranged from 15.7% to 37.9% in diesel mode, whereas 10.02% to 55.13% under DFM for a change of power from 10 to 150 kW. For a similar change of power, the exergetic efficiency ranged from 14.6% to 35.4% in diesel mode and from 9.57% to 52.38% under DFM. Chintala and Subramanian (2014) estimated the maximum available work potential of a hydrogen run dual fuel diesel engine. The test indicated that the maximum work increased with hydrogen addition due to reduction of irreversibility. The maximum work at the rated load increased from 29% in diesel mode to 31.7% under DFM, whereas the irreversibility decreased from 41.2% in diesel mode to 39.3% under DFM. Jafarmadar (2014) carried out the energy and exergy analysis for hydrogen run dual fuel diesel engine with a constant diesel fuel amount (6.48 mg/cycle) at different fuel-air ratios (0.3, 0.4, 0.5, 0.6, 0.7, and 0.8). The computational study revealed that with an increase of gas fuel-air ratio from 0.3 to 0.8, the exergy efficiency decreased from 43.7% to 34.5%. Morsy (2015) studied the effect of variation of percentage of ethanol-water mixture and speed on the exergy efficiency of a dual fuel diesel engine. The test indicated that at a low speed of 600 rpm, the highest improvement in exergy efficiency of 2.36% and 2.32% was obtained for 25% and 50% ethanol water mixture, respectively. Sahoo *et al.* (2011a) experimentally investigated the effect of both hydrogen addition and load level on exergy analysis of syngas run dual fuel diesel engine. It was found that the cumulative work availability with the increase of hydrogen quantity. This enhancement was due to a better combustion process caused by hydrogen addition. Furthermore, the dual fuel cumulative work availability was found to increase at higher loads. The same group of investigators (Sahoo *et al.*, 2012) carried out an exergy balance of a biogas run dual fuel diesel engine for two different pilot fuels, namely, diesel and jatropha biodiesel. The pilot fuel study showed a reduction of maximum exergy efficiency approximately by 2% for jatropha biodiesel in comparison to that of diesel fuel.

Table 2.3 Summary on the exergy analysis of dual fuel diesel engines

Researchers	Primary Fuel	Pilot Fuel	CR	IT (BTDC)	Observation	Objective of the Exergy Analysis
Rakopoulos and Kyritsis (2006)	Natural gas, landfill gas	Not specified	18:1	23°	CR and IT were fixed	To analyse the hydrogen enrichment of the primary fuels
Rakopoulos *et al.* (2008)	Natural gas	Not specified	18:1	-	CR was fixed, IT was not specified	To analyse the hydrogen enrichment of the natural gas
Hosseinzadeh *et al.* (2010)	Natural gas	Diesel	16.1:1	16°	CR and IT were fixed	To compare the thermal, radical and chemical effects of EGR gases at part load
Sahoo *et al.* (2011a)	Syngas	Diesel	17.5:1	23°	CR and IT were fixed	To analyse the variation of hydrogen in the composition of syngas
Sahoo *et al.* (2012)	Biogas	Diesel, Jatropha biodiesel	17.5:1	23°	CR and IT were fixed	To investigate the effect of different types of pilot fuel
Costa *et al.* (2012)	Natural gas	Diesel	-	-	CR and IT were not specified	To investigate the performance characteristics of a diesel engine
Chintala and Subramanian (2014)	Hydrogen	Diesel	19.5:1	-	CR was fixed, IT was not specified	To assess the maximum reversible work and irreversibility
Jafarmadar (2014)	Hydrogen	Diesel	17.5:1	-	CR was fixed, IT was not specified	To analyse the air-fuel ratio at various loads
Morsy (2015)	Ethanol	Diesel	17.5:1	-	CR was fixed, IT was not specified	To explore the effects of using ethanol/water mixtures fumigation

2.9 Scope of Work

The literature review suggests that there has been a considerable research on biogas run dual fuel engines especially in the area of power production applications. Still, there are areas that need to explore to make biogas run dual fuel diesel engine more efficient. The following gaps are found out from exhaustive literature survey:

- The standardization of the operating parameters (viz. compression ratio and injection timing of pilot fuel) of a biogas run dual fuel diesel engine have not been reported. This is very important because the operating parameters of a diesel engine are standardized based on the chemical and physical properties of diesel fuel. Therefore, running biogas under dual fuel mode at standard diesel setting will not offer the best performance. Hence, the operating parameters need to be adjusted in order to obtain efficiency comparable to that diesel fuel.

- The use of emulsified fuel as a pilot fuel for a biogas run dual fuel diesel engine is not found in any archival literature. This is important as the use of emulsified fuel as pilot fuel may further lower the NO_X and soot emissions.

- The effect of compression ratio and injection timing on the energy and exergy distribution of a biogas run dual fuel diesel engine is not known. This is vital as the second law analysis determines the availability loss or destroyed in the various parts of an engine, and thereby estimates the maximum possible performance of a thermodynamic system.

2.10 Summary

To sum up, the review of the earlier work have clearly suggested that several factors operating parameters, engine components, biogas quality, biogas inlet pressure and oxygenated combustion have effects on the performance, combustion and emission characteristics of the biogas run dual fuel diesel engines. However, the investigation of two most critical operating parameters i.e. CR and IT on performance of biogas run dual fuel diesel engines have not been reported. Besides, the influence of CR and IT on the energy and exergy distributions of such type of engines is not clear. These findings will surely help in reducing the losses to improve the performance of the engine in terms of efficiency and emission characteristics.

Chapter-3

Variable Compression Ratio Engine Test Setup

Overview:

The objective of present study is to standardize the operating parameters, namely, compression ratio and injection timing of a biogas run duel fuel diesel engine using different types of pilot fuel. In order to achieve this objective, the existing engine test setup needs to be modified to a biogas run dual fuel diesel engine. The existing test setup is a 3.5 kW single cylinder, four stroke, direct injection, naturally aspirated, water-cooled, variable compression ratio diesel engine. The present chapter discusses the details specification of the engine, devices and instruments used for conducting these experiments. The discussion includes air and fuel flow measurement, P-θ measurement, temperature measurement, compression ratio variation control injection timing variation control and performance measurement. Further, the specifications along with the working principle of the flue gas analyser are also described. Thereafter, the modifications carried out for converting the existing setup to biogas run dual fuel engine are briefly explained. Finally, the experimental procedure used for both diesel and dual fuel mode is elaborately discussed.

Chapter Outline:

3.1 The VCR Engine Test Setup

The experimental setup consists of 3.5 kW single cylinder, four stroke, direct injection (DI), naturally aspirated (NA), water-cooled, variable compression ratio (VCR) diesel engine as indicated in Fig. 3.1. It is connected to an eddy current and water-cooled dynamometer for loading on crankshaft with the help of electromagnetic force. A tilting cylinder block arrangement is used for varying the CR without stopping the engine and without altering the combustion chamber geometry. The fuel injector in the engine has three circular holes having 0.3 mm diameter which spray fuel with a spray angle of 120º. The piston top of the engine is bowl type. Hence, the combustion chamber is of hemispherical type when piston reaches TDC. The liquid fuel reaches engine fuel pump from fuel tank by gravity. A regulator, fixed on the panel box, controls electric supply for load variation. The load sensor, fitted with the dynamometer, sends the load signal to the digital display in kg. Instruments for combustion pressure and crank-angle measurement are provided along with the setup. The signals are interfaced to computer through engine indicator for pressure-crank angle (*P*-θ) and pressure volume (*P*-*V*) diagrams for each of 360° rotation of crank. There are provisions for measuring the airflow, fuel flow and temperatures. Rotameters are used for cooling water and calorimeter water flow extent. The cooling water flows through the jackets of the engine block and cylinder head to remove excess heat produced during combustion. The fuel injection pressure can be varied between 200 to 220 bar. The specification of the engine is given in Table 3.1. The specification of the engine is added in Table 3.1.

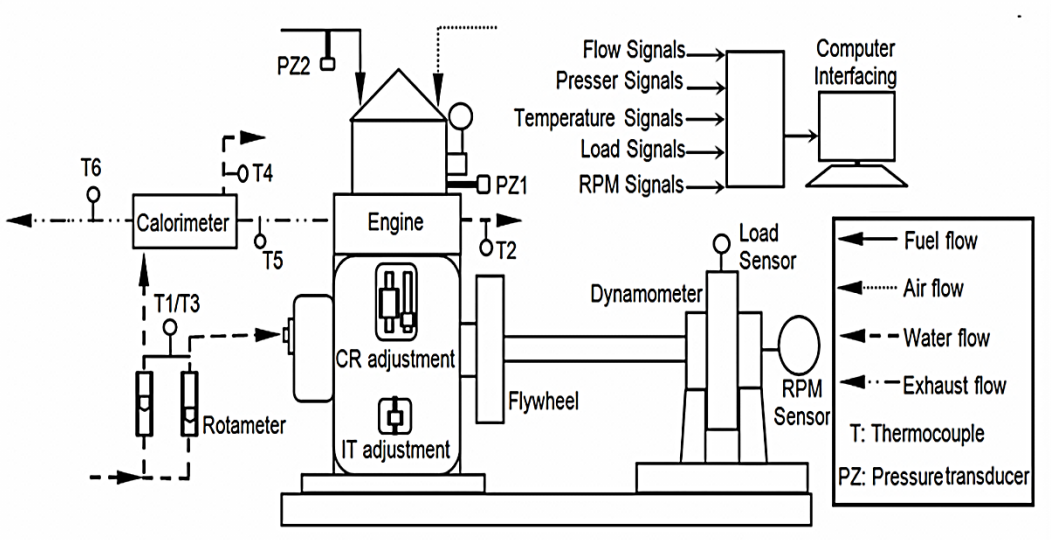

Fig. 3.1 The schematic diagram of the VCR diesel engine setup

Table 3.1 The specification of VCR diesel engine

System specifications	
Parameter	Specification
Make and model	Kirloskar, Model TV1
Product	Research engine test setup, Code 240
Type	Single cylinder, four stroke, DI, NA, VCR diesel engine
Power	3.5 kW (@ 1500 ± 50 rpm)
Type of cooling	Water cooled
CR range	12:1 – 18:1
Injection	variation 0 – 25º BTDC
Combustion chamber	Hemispherical bowl in piston type
Dynamometer	Eddy current type, water cooled with loading unit
Air box	MS fabricated with orifice meter and manometer (100 - 0 - 100)
Type of air induction	Naturally aspirated
Fuel tank Capacity	15 lit with measuring tube (0-450 ml)
Calorimeter	Pipe in pipe type
Rotameters	Engine cooling 40-400 lph, calorimeter 25-250 lph
Data acquisition Software	'Enginesoft' engine performance analysis software
Transmitters, sensors and indicators	
Fuel flow transmitter	DP transmitter, range 0-500 mm WC
Air flow transmitter	Pressure transmitter (-) 250 mm WC
Pressure sensors	Piezo type, range 5000 psi, with low noise cable
Temperature sensors and Transmitters	PT100 (RTD) type, range 0-100º C, output 4-20 mA (4 nos), K (ungrounded) type, range 0-1200º C, output 4-20 mA (2 nos)
Load sensor and indicator	Strain gauge type load cell with digital indicator, range 0-50 kg
Speed sensor and indicator	Resolution 1º, range (5500 rpm) with TDC pulse
Data acquisition device	NI USB-6210, 16-bit, 250 kS/s
Setup constants	
Pulse per revolution	360º
No. of cycles	10
Fuel measuring interval	60 s
Speed scanning intervals	2000 ms
Bore × Stroke	87.5 mm × 110 mm
Capacity	661 cc
Orifice diameter	20 mm
Dynamometer arm length	185 mm
Connecting rod length	234 mm
Theoretical constants	
Orifice coefficient of discharge	0.6
Specific heat of exhaust gas	1.00 – 1.25 kJ/kg-K
Specific heat of water	4.186 kJ/kg-K

3.2 Instrumentations for Measurements

The VCR research diesel engine setup is consists of a several sensors, transmitters and indicators. These are interfaced with the data acquisition device (DAD) through a computer for automatic measurement of almost all of the direct and indirect performance parameters.

3.2.1 Air and Fuel Flow Measurement

Both air and fuel flow measurement can be performed manually and automatically. Manual airflow measurement is carried out by recording the difference in height of water column in the manometer. It is interconnected across the orifice meter, through which air comes into the engine panel box, before leaving towards the engine manifold. Manual measurement of fuel is executed by transferring fuel from the tank through the measuring tube for known duration. Airflow transmitter (WIKA Instruments Ltd.) and differential pressure transmitter (Yokogawa Electrical Corporation) that are lined with DAD assess the automatic air and fuel flow amount.

3.2.2 *P-θ* Measurement

The PCB Piezotronics made two dynamic pressure sensors are fitted on the cylinder head and fuel injector. Both of them has identical specification and capable of distinguish pressure of compression, combustion, explosion, pulsation, cavitation, blast, pneumatic, hydraulic, fluidic etc. An optical crank angle sensor (Kubler make) is used to measure each degree rotation of crank with TDC pulse.

3.2.3 Temperature Measurement

Four PT100 temperature sensors measure the inlet and outlet temperatures of engine cooling water flow and calorimeter water flow. The inlet and outlet temperatures of exhaust gas to calorimeter are measured by two K type thermocouples. All of these are interfaced with computer for automatic data recording. The thermocouples used in this work, have a response time more than 0.08 seconds (for the constant speed engine around 1500 rpm). Hence, they cannot show the pulsation nature of the exhaust gas in the form of temperature readings and are found almost steady after a certain time (nearly 5 minutes) at a particular load.

3.2.4 Compression Ratio Variation Control

The VCR diesel engine has provisions for eight step CR variation from 12 to 18. This is done by tilting cylinder head with the help of locknut and adjuster arrangement. However, the engine starting should be done at the standard CR (17.5) and later on, the CR can be changed online. There are six socket headed vertical allen bolts fitted on two supporting blocks on the two sides of the cylinder, which needed to be loosen for CR variation. The appropriate value of CR should be entered manually in the software for data acquisition.

3.2.5 Injection Timing Variation Control

The IT of the liquid fuel can be tuned online by rotating the locknut of the screw, which changes the relative distance camshaft and plunger of the fuel pump. The updated timing is learnt from the fuel pressure data at the certain crank angle displayed by the 'Engine soft software'. The fuel injection point on the plot shifts horizontally to retard or advance the injection point depending on the way of rotation of the adjusting nut.

3.2.6 Performance Measurement

The measurement of the performance parameters are done automatically by collecting the data from the computerized system after setting the running engine at particular load level. The density and the calorific value of the respective fuel are included according to the requirement. The parameters evaluated are air and fuel flow rates, air fuel ratio, power, mean effective pressure, efficiencies and heat balance. The basic correlations used for estimating the above parameters are included in Appendix-A.

3.2.7 Emission Measurement

The emission analysis is carried out by using a Testo 350S/M/XL Testo flue gas analyser. The resolution, accuracy and range of these emission parameters are shown in Table 3.2. The calibration of the instrument is performed automatically by measuring oxygen quantity in the air, each time it is restarted. Carbon monoxide (CO) and oxides of nitrogen (NO_X) are measured through electrochemical measurement cells; whereas, carbon dioxide (CO_2) and hydrocarbon (HC) are measured by Infrared and Pellistor Heat Affect Detector, respectively. The analyser uses ASTM-D6522 standard for emission measurement. The working principle of the gas analyser is as follows. During steady engine operation, the flue gas is allowed to

surge through a probe and dried out by a condensation trap. Thereafter, each of the CO_2, CO, HC, and NO_X emission concentrations in the flue gas is analyzed by individual sensors and readings are then displayed on the screen of the control unit.

Table 3.2 The specifications of Testo 350 S/M/XL flue gas analyser

Sl. No.	Measured gas	Resolution	Accuracy	Range
1	O_2	0.1%	± 0.8%	0 – 25%
2	CO	1 ppm	± 10 ppm < 200 ppm	0 – 10000 ppm
3	CO_2	0.01% vol. < 25% 0.1% vol. > 25%	± 0.3% vol. < 25% ± 0.5% vol. > 25%	0 – 50%
4	NO	1 ppm	± 5 ppm < 100 ppm	0 – 3000 ppm
5	NO_2	0.1 ppm	± 5 ppm < 100 ppm	0 – 500 ppm
6	HC	1 ppm	400 ppm < 4000 ppm	0 – 40000 ppm

3.3 Dual Fuel Modifications

The VCR engine test setup was modified to a biogas run dual fuel setup by connecting a venturi gas mixer at its in let manifold as depicted in Fig. 3.2. The existing setup and the components of the modified setup are shown in Fig. 3.3.

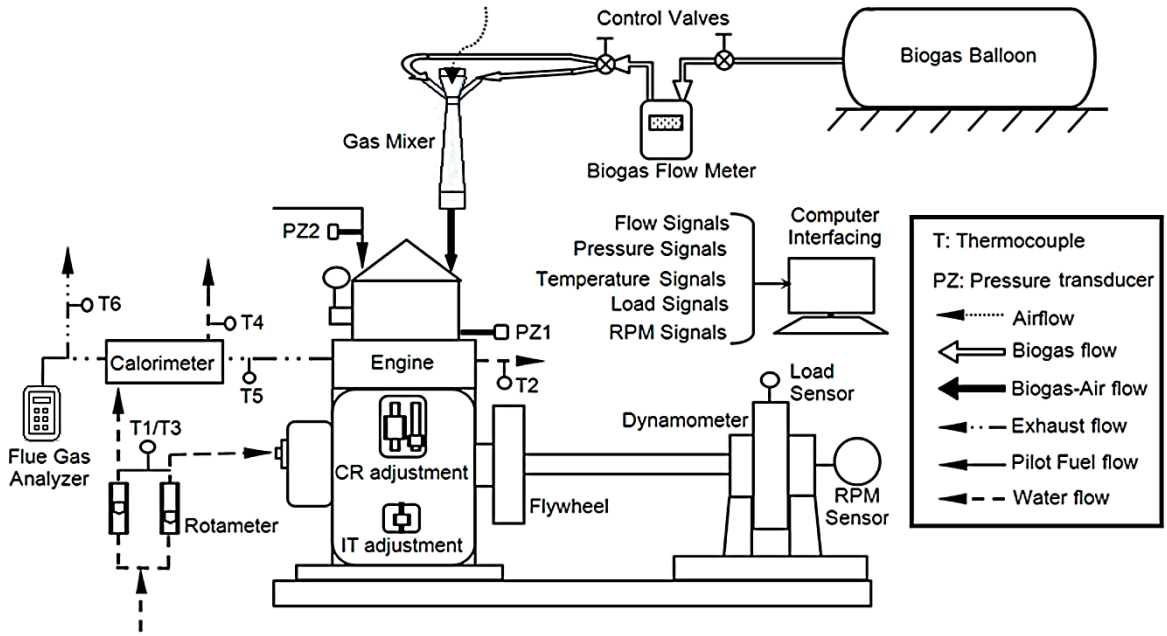

Fig. 3.2 The schematic diagram of the modified dual fuel VCR diesel engine setup

(a) Test setup

(b) Modified test setup

(c) Venturi gas mixer

(d) Y-connector

(e) Fuel control mechanism

Fig. 3.3 Experimental facility and key components

The pressure drop created at the throat of the venturi gas mixer due to its geometry facilitates the induction as well as mixing of the biogas and air. The liquid fuel supply is controlled by using fuel control lever mechanism (FCM), which is connected to fuel shut off valve of the fuel pump. The design and mechanism of the venturi gas mixer and FCM is explained in Appendix-B. The biogas flow rate is measured by a biogas flow meter (Siya Instruments make, India). The biogas is procured from a fixed dome type biogas digester having a capacity of 3 m^3. The cowdung is used as raw material for the production of biogas. The

pressure of the biogas at the outlet of the digester was found to be 1.06 bar. The biogas was collected in the biogas balloon at the same pressure. The composition of biogas used for this work is found out through gas chromatography.

3.4 Experimental Procedure

The VCR engine is first run with diesel at standard diesel specification of compression ratio of 17.5 and IT of 23^{o}BTDC. The engine is initially run at no load condition for some time so that warm up is optimum for a proper combustion of fuel. During the experiments, the engine is tested with 20%, 40%, 60%, 80%, and 100% load. As the load is increased, the engine speed reduces. In order to maintain a constant BP, the engine consumes more fuel resulting a higher heat release, and hence, a higher temperature inside cylinder. This increases temperatures at the outlet of the cooling water and exhaust gas. At any particular specified load condition, the engine is allowed to run for few minutes and the temperatures at the outlet of cooling water and exhaust gas are monitored closely at the computer display until it reaches a steady state condition. This indicates that the combustion inside the cylinder becomes steady and the engine is ready for data acquisition. The readings of temperatures, air and fuel flow rate, speed, cylinder and fuel pressure variation are automatically recorded by the DAD. At a particular load of the dual fuel operation, initially, the rpm of the engine under diesel mode is noted. Biogas supply valve is then opened very slowly. As biogas flows into the engine, the speed of the engine increases. The speed increases due to additional energy that the engine gets due to combustion of biogas. The flow of biogas is slowly increased till the rpm does not rise any further. In the meantime, the governor tries to lower the speed of engine. However, to perfectly match the rpm at any particular load in diesel mode, the pilot fuel that is diesel in this case is slowly reduced by the fuel control mechanism. The pilot fuel supply is then reduced till original rpm run on diesel mode is achieved. The engine is allowed to run for few minutes and then readings are recorded. Biogas flow rate is then noted from the biogas flow meter. The same procedure is followed for various combinations of CR and IT using different test pilot fuels under DFM.

The specification of the instrument and uncertainty analysis of the entire experimental investigation is given in Table 3.3 and 3.4. The detailed calculation for uncertainty analysis is given in Appendix-C.

Table 3.3 Specification of the instruments

Instrument	Make	Type	Accuracy	Resolution	Range
Biogas flow meter	Siya Instruments	Mechanical	2%	0.001 m^3	10,000 m^3/hr
Fuel flow transmitter	Yokogawa Electrical Corporation	DP transmitter	-	0.1cc	0-500 mm of water column
Air flow transmitter	WIKA Instruments Ltd	Pressure transmitter	2%	1mm	(-) 250 mm of water column
Pressure sensors	PCB Piezotronics	Piezo type with low noise cable	2%	0.1 psi	5000 PSI
Temperature sensors and transmitters	-	PT100 (RTD) type	-	-	0-100º C
		K type	-	-	0-1200º C
Load sensor and indicator	Sensortronics	Strain gauge type load cell with digital indicator	-	-	0-50 kg
Speed sensor and indicator	Kubler	-	-	1º	5500 rpm
Data acquisition device	National Instruments	NI USB-6210	-	-	16-bit, 250 kS/s

Table 3.4 Uncertainties of independent variables

SL No	Independent variable	Relative error
1	Engine speed	0.5%
2	Biogas flow rate	2%
3	LHV of diesel fuel	1%
4	LHV of RBB fuel	1%
5	LHV of WIRBB fuel	1%
6	LHV of gaseous fuel	1%

Table 3.5 Uncertainties of performance parameters

SL No	Performance parameter	Diesel mode error	DFM error
1	Brake thermal efficiency	± 1.5%	± 2.7%
2	Air flow rate	± 0.5%	± 0.5%
3	Air fuel ratio	± 1%	± 2.3%
4	Emission	± 5%	± 5%

3.5 Summary

This chapter briefly discusses about the engine setup, devices, and equipment required for experimentation. The brief specifications and the schematic diagrams of the both existing setup and modified setup are included. Further, the important specifications of the flue gas analyser are also tabulated. Finally, the experimental procedure for both diesel and dual fuel mode is elaborately discussed.

Chapter-4

Selection of Pilot Fuel

Overview:

Increased industrialization and the growing transport sectors worldwide face major challenges in terms of energy demand as well as increased environmental concerns. The rising demand and the limited availability of mineral oil provide incentives for the development of alternative fuels from renewable sources with less environmental impact. However, the widespread production and the use of such alternative fuels are hindered by its uncompetitive price against the petroleum based fuels. There is now an intensifying search for cheaper raw material for biodiesel production. One of the possible alternatives is the use of fuels from plant based origin like rice bran biodiesel (RBB), pongamia biodiesel (POBD) and palm biodiesel (PBD). The use of these types of biofuel as a renewable source combines the advantages of almost unlimited availability and ecological benefits such as integrated closed carbon cycle. The present chapter discusses the investigations of using RBB, POBD and PBD as pilot fuel for the biogas run dual fuel diesel engine. At standard diesel setting, the most suitable pilot fuel is selected on the basis of performance, combustion and emission characteristics.

Chapter Outline:

4.1 Pilot Fuel and its Importance

The pilot fuel has a tremendous influence on the dual fuel combustion as it elicits the combustion process. The combustion process of a biogas run dual fuel diesel engine is more complex than single fuel combustion. Prior to ignition of pilot fuel, the biogas air mixture undergoes pre-ignition chemical reaction during the relatively longer compression stroke. The preignition reaction results in the formation of active radicals and partial combustion products that are believed to affect the ignition of the injected pilot fuel (Yoon and Lee, 2011). Most of the studies on biogas have been conducted with diesel fuel as the pilot fuel. The study of different types of pilot fuel for biogas run dual fuel diesel engine is of immense importance taking in consideration of recent fuel crisis. The different pilot fuels studied for biogas run dual fuel engine are diesel (Henham and Makkar, 1998; Yoon and Lee, 2011; Sahoo, 2011; Bari, 1996; Cheng-qui *et al*., 1989; Duc and Wattanavichien, 1998; Tippayawong *et al*., 2007; Bedoya *et al*., 2009; Cacua *et al*., 2012; Mustafi *et al*., 2012; Makareviciene *et al*., 2013; Barik and Murugan, 2014), Soybean biodiesel (Yoon and Lee, 2011); Jatropha biodiesel (Sahoo, 2011); Palm oil biodiesel (Bedoya, 2009) and Jatropha oil (Luijten and Kerkhof, 2011). Thus, few studies have been reported on biogas dual fuel combustion using biodiesel as pilot fuel.

4.2 Experimental Matrix and Properties of Test Fuel

The pilot fuels considered for this investigation are rice bran biodiesel (RBB), pongamia biodiesel (POBD) and palm biodiesel (PBD). The experimental matrix and properties of the test fuel are given in Tables 4.1 and 4.2. The variations of load are performed from no-load to full-load (12 kg) with an increment of 2.4 kg (20%). The diesel and dual fuel modes compared at standard diesel setting (i.e. Compression ratio =17.5 and Injection timing = 23º BTDC). The performance and combustion analysis are performed based on theoretical equations given in Appendix-A. The performance analyses evaluated are brake thermal efficiency (BTE), brake specific energy consumption (BSEC), volumetric efficiency (VE), exhaust gas temperature (EGT), liquid fuel replacement (LFR) and biogas flow rate (BFR). The combustion analyses include the cylinder pressure variation, ignition delay (ID), net heat release rate (NHRR) and peak cylinder pressure (PCP). Finally, emission analysis includes measurement of carbon dioxide (CO_2), carbon monoxide (CO), hydrocarbon (HC) and oxides of nitrogen (NO_X). The higher heating values of the biodiesels are determined through bomb calorimeter available in the Centre for Energy, IIT Guwahati.

Table 4.1 Experimental Matrix of the Biodiesel-Biogas Run Dual Fuel Diesel Engine

Mode	Fuel used		CR	IT	Loading conditions (%)
Diesel	100% Diesel		17.5	23° BTDC	20, 40, 60, 80, 100
Dual	DFM1	Pilot Fuel : RBB Primary Fuel: Biogas			
	DFM2	Pilot Fuel : POBD Primary Fuel: Biogas			
	DFM3	Pilot Fuel : PBD Primary Fuel: Biogas			

Table 4.2 Fuel Properties

Properties	Diesel	RBB	POBD	PBD	Biogas
Chemical Composition	$C_{12}H_{26}$ (Sahoo *et al.*, 2011)	$C_{18.05}H_{34.9}O_2$*	$C_{17.69}H_{32.94}O_2$*	$C_{18.07}H_{34.93}O_2$ (Debnath, 2013)	60% CH_4, 40% CO_2 (volume)*
Density(kg/m^3)	840 (Sahoo *et al.*, 2011)	880*	890*	870*	0.91*
Lower calorific value (MJ/kg)	42 (Sahoo *et al.*, 2011)	39.54*	39.14*	38.84*	20.67*
Cetane number	45-55 (Sahoo *et al.*, 2011)	56.3 (Giakoumis, 2013)	55.4 (Giakoumis, 2013)	56.5 (Giakoumis, 2013)	-
Auto-ignition Temperature (K)	553 (Sahoo *et al.*, 2011b)	-	-	-	1087 (Sahoo *et al.*, 2011)
Stoichiometric air fuel ratio	14.92 (Sahoo *et al.*, 2011)	12.5*	12.05*	12. 48 (Debnath *et al.*, 2013b)	10 (Sahoo *et al.*, 2011)

*Calculated value

4.3 Performance Analysis

The BTE increases with the increase in load for both diesel and dual fuel mode as indicated in Fig. 4.1(a). However, BTEs are found to be lower for all three cases of dual fuel mode in comparison to diesel mode due to low calorific value of biogas. In addition, the other factors like biogas residual, combusted residual gases, low combustion temperature and low flame propagation speed, higher total fuel flow rate during combustion, increased negative compression work caused by induction of large biogas air mixture are contributing to the low thermal efficiency in dual fuel mode. The three cases of dual fuel modes viz. RBB-biogas, POBD-biogas and PBD-biogas are abbreviated as DFM1, DFM2 and DFM3, respectively. At 100% load, the BTEs are found to 19.97%, 18.4% and 17.4% for DFM1, DFM2 and DFM3 respectively as compared to 27.76% for diesel mode. The marginal higher calorific value of RBB than POBD and PBD results in obtaining a slightly more BTE. The BSEC reduces with the increase of load for diesel and DFM as indicated in Fig. 4.1(b). However, the BSEC for all the three cases of dual fuel mode are higher in comparison to diesel mode. At low loads, the difference of BSEC between dual fuel mode and diesel is quite high due to low conversion of gaseous fuel to work. However, at high thermal load (over 80%), there is a considerable improvement in BSEC of dual fuel mode due to high thermal load imposed on the engine. This facilitates the high conversion of biogas fuel into work. At 100% load, the BSEC increased by 38.89%, 50.83% and 58.33% for DFM1, DFM2 and DFM3, respectively in compared to diesel mode. The VE decreases as load increases for both diesel and dual fuel mode as observed from Fig. 4.1 (c). The temperature of exhaust gases increases with load, which in turn, preheats the incoming air, and thereby lowering the VE. In dual fuel mode, the biogas substitution displaces a greater portion of air with the increase of load. Hence, the VE in DFM is lower than the diesel mode. The low VE also contributes for the low BTE under DFM. At 100% load, the VEs are found to be 71%, 70.11%and 69.13% for DFM1, DFM2 and DFM3, respectively in comparison to 79.69% in diesel mode. The EGT follows a linear relationship with load for both diesel and DFM. The EGT for all cases of dual fuel mode is found to be higher than diesel mode [Fig. 4.1 (d)]. This is due to late combustion of biogas which shortens the duration of extraction of power by the engine from fuel. As a result, the combustion products in the form of gases come out at higher temperature. At 100% load, there is an increase of 13.2%, 15.09% and 16.98% of EGT for DFM1, DFM2 and DFM3 respectively in compared to diesel mode at 23^{o} BTDC. The BFR and LFR increases with the increase in load for DFM1, DFM2 and DFM3, respectively as depicted in Figs. 4.1 (e) and

4.1 (f). At 100% load, the BFR is found to be 2.73 kg/h, 2.83 kg/h and 3 kg/h for DFM1, DFM2 and DFM3, respectively. For the same loading condition, the maximum LFR is found to be 79%, 78% and 77%, respectively for DFM1, DFM2 and DFM3.

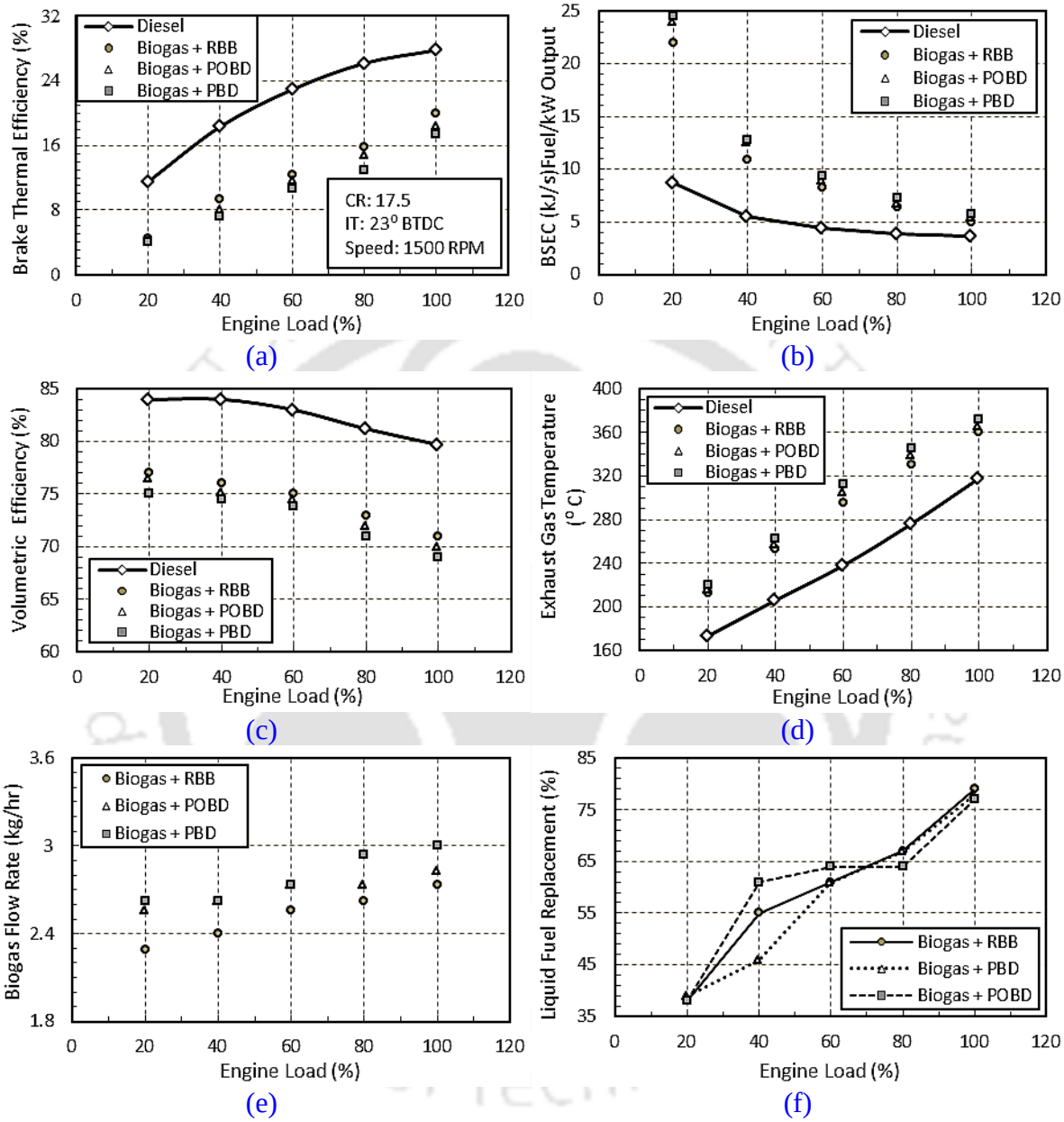

Fig. 4.1 Performance analysis for biogas run dual fuel diesel engine using RBB, POBD and PBD as pilot fuel

4.4 Combustion Analysis

The combustion analysis has been carried out in the form of ID, PCP and NHRR. The ID gradually decreases as load increases for both diesel and DFM as observed in Fig. 4.2 (a). At low load condition of 20%, the combustion chamber temperature being low resulted in longer ID. However, at high load of 80%, the combustion chamber temperature being high which

reduced the ID. The ID under the dual fuel mode is found to be longer than the diesel mode. The reason behind this linger ID for dual fuel mode is due to larger amount of biogas fuel in the intake and compression processes and reduction of charge temperature compared to diesel mode. The high overall heat capacity of biogas results in lowering the charge temperature. This delays the ignition of pilot fuel significantly. At 100% load, the ID is found to be 20° CA, 21° CA and 21.5° CA for DFM1, DFM2 and DFM3, respectively in comparison to 14° CA in diesel mode. The heat release is more in diesel mode in comparison to DFM. This is due to high calorific value of diesel as compared to biogas.

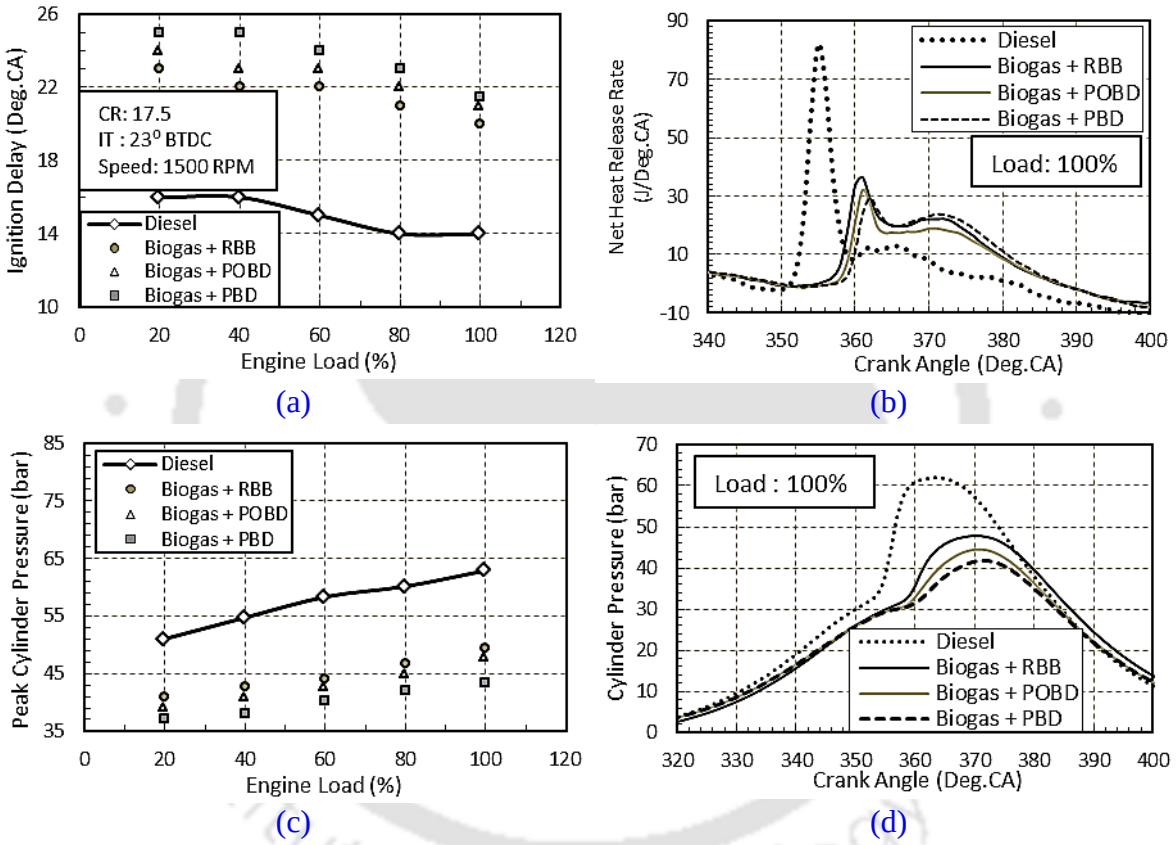

Fig. 4.2 Combustion analysis for biogas run dual fuel diesel engine using RBB, POBD and PBD as pilot fuel

At 100% load, the maximum NHRR is found to be 36.42 J/deg.CA, 32 J/deg.CA and 29.67 J/deg.CA for DFM1, DFM2 and DFM3, respectively in comparison to 82.02 J/deg.CA in diesel mode as indicated in Fig. 4.2 (b). The PCP increases with the increase in load for both diesel and DFM as indicated in Fig. 4.2 (c). However, the rise of pressure under all the three cases of dual fuel mode is less than diesel mode. At 100% load, the average drop in PCP is found to be 47.78 bar, 44.55 bar and 41.86 bar for DFM1, DFM2 and DFM3, respectively in comparison to 62.93 bar for diesel mode. It can be observed from the *P-Θ* diagram that there

is a shift of PCP away from TDC in dual fuel mode as observed in Fig. 4.2(d). At 100% load, the crank angle corresponding to PCP is found to be 11^{o} ATDC, 13^{o} ATDC and 13^{o} ATDC for DFM1, DFM2 and DFM3, respectively in comparison to 3^{o} ATDC in diesel mode.

4.5 Emission Analysis

The CO_2 emission increases with the increase of load for both diesel and DFM as observed in Fig. 4.3(a). This is due to the fact that the amount of fuel consumes increases with for high loading conditions. However, CO_2 emission is higher for all the three cases of dual fuel mode in comparison to diesel mode. This is because biogas contains large amount of CO_2 (i.e. around 40% by volume). Further, the presence of oxygen (around 11%) in biodiesel also expedites the oxidation process. Sahoo (2011) also reported a higher CO_2 emission under DFM as compared to diesel mode. On an average, there is an increase of CO_2 emission by 40.55%, 31.18% and 27.64% for DFM1, DFM2 and DFM3, respectively in compared to diesel mode. CO is generally formed due to deficiency of oxygen. At low loads, CO emissions are high which then decreases at medium load, and again increases at high load as indicated in Fig. 4.3(b). This is because initially, at low load, the cylinder temperature is low, and as a result the combustion of fuel is not proper. At high load, more amount of fuel needs to be supplied. Hence, after a particular load, the fuel air mixture becomes too rich to undergo complete combustion. However, the CO emissions are higher for all the three cases of DFM in comparison to diesel mode. This is due to the fact that biogas displaces air under DFM, and therefore, there is not enough oxygen is available for complete combustion. On an average, there is an increase of CO emission by 46.46%, 62.15% and 68.92% for DFM1, DFM2 and DFM3, respectively in compared to diesel mode. In this study, the lower flame velocity of biogas contributes to the formation of HC more in dual fuel mode in comparison to diesel mode as observed in Fig. 4.3(c). Initially, at low load of 20%, the HC emission is high due to improper combustion as combustion chamber temperature is low in DFM. The HC emission gradually decreases as load increases upto load of 80%. At 100% load, the fuel air mixture become rich due to reduction of oxygen availability which resulted in emission of more hydrocarbons. On an average, there is an increase in HC emission by 411.57%, 466.31% and 491.57% for DFM1, DFM2 and DFM3, respectively in compared to diesel mode. NO_X are mainly composed of mainly NO and small amount of NO_2. The NO_X formation is a temperature dependent phenomenon. NO_X is formed in the high temperature combustion gases inside the cylinder mainly through oxidation of nitrogen present in the

inducted air. In this investigation, the NOx emission increases with load as more amount of fuel needs to be supplied with increase of load which results in increase of temperature of combustion chamber. However, the NO_X emission in the diesel mode is much higher in comparison to all the three cases of DFM as depicted in Fig. 4.3(d). This is because the temperature of the combustion chamber in case of diesel is much more as diesel has a high calorific value as compared to biogas. Moreover, the presence of inert CO_2 in biogas results in lowering the temperature of combustion chamber. On an average, there is a reduction in NOx emission by 72.83%, 77.06% and 83.03% for DFM1, DFM2 and DFM3, respectively in compared to diesel mode. The CO and HC emissions are within the limits as specified by the Government of National Capital Territory of Delhi, India (2014).

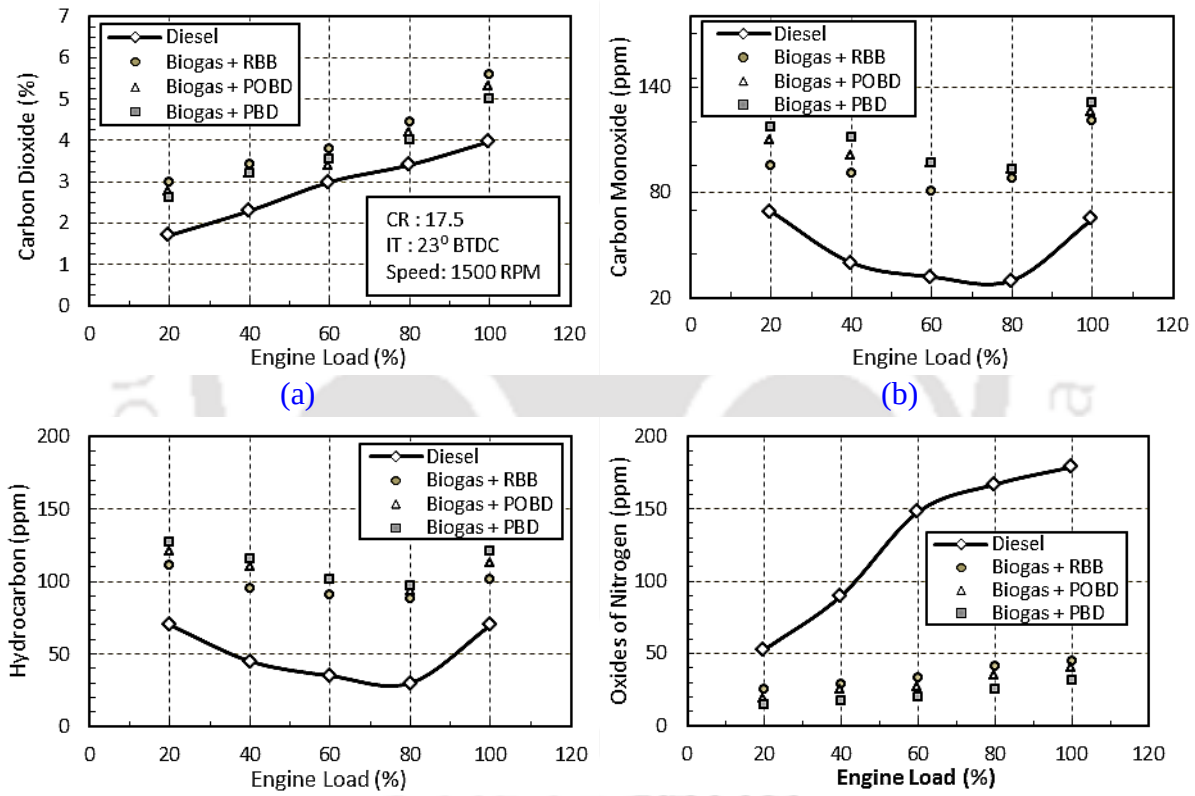

Fig. 4.3 Emission analysis for biogas run dual fuel diesel engine using RBB, POBD and PBD as pilot fuel

4.6 Summary

The present study investigated the possibility of using rice bran biodiesel (RBB), pongamia biodiesel (POBD) and palm biodiesel (PBD) as pilot fuel for a biogas run dual fuel diesel engine particularly in rural areas. The results of this pilot fuel study under DFM indicated that RBB-biogas produced a maximum BTE of 19.97% in comparison to 18.4% and 17.4% for

POBD-biogas and PBD-biogas, respectively at 100% load. At the same loading condition and under same mode, the maximum liquid fuel replacement is found to be 79%, 78% and 77% for RBB-biogas, POBD-biogas and PBD-biogas, respectively. The emission study divulged that under DFM, there is an increase of CO emission by 25.74% and 32.58% for POBD-biogas and PBD-biogas, respectively in comparison to RBB-biogas. Furthermore, the HC emissions for POBD-biogas and PBD-biogas increased by 11.73% and 16.27%, respectively in comparison to RBB-biogas. On the other hand, there is a decrease in NOx emission by 5.8% and 14% for POBD-biogas and PBD-biogas, respectively in comparison to RBB-biogas. The CO_2 emission for POBD-biogas and PBD-biogas also decreased by 23.1% and 31.83%, respectively in comparison to RBB-biogas. From the above analysis, it is quite clear that the rice bran biodiesel performs better as a pilot fuel in comparison to pongamia oil biodiesel and palm oil biodiesel for a biogas run dual fuel diesel engines. However, further research needs to be done on rice bran biodiesel -biogas run dual fuel diesel engine to raise the efficiency at par with diesel through suitable adjustment of operational parameters. Therefore, the rice bran biodiesel has been selected for the next course of research in the upcoming chapters.

Chapter-5

Results of Diesel - Biogas Run Dual Fuel Engine

Overview:

The prime objective of this chapter is to standardize the operating parameters of a biogas run dual fuel diesel engine using diesel as pilot fuel. Therefore, in this chapter, the experimental observation performed in the VCR engine is analysed to find out its optimum performance. The engine is run at a constant speed of 1500 ± 50 rpm and rated power output of 3.5 kW. The overall analyses are segregated into performance, combustion and exhaust gas emissions of the biogas run dual fuel diesel engine. In each of these sections, explanations are provided based on compression ratio and injection timing variations. The outcome of the experimental study is compared with respect to the diesel run engine at standard setting for quantitative and qualitative assertion.

Chapter Outline:

5.1 Diesel as Pilot Fuel

Most of the studies reported on biogas run dual fuel diesel engine used diesel as pilot fuel. The analyses were done mainly to study the effect of speed (Henham and Makkar, 1998; Duc and Wattanavichien, 2007; Tippayawong, 2007), load (Cheng-qui *et al*., 1989; Yoon and Lee, 2011; Sahoo, 2011; Barik and Murugan, 2014a), air induction system (Bedoya *et al*., 2009), oxygenated combustion (Cacua *et al*., 2012), effect of biogas quality (Bari, 1996; Mustafi *et al*., 2013; Maizonnasse *et al*., 2013) and exhaust gas recirculation (Makareviciene *et al*., 2013). The review of literature on biogas run dual fuel diesel engines confirms that, until now, the performance, combustion and emission characteristics of biogas dual fuel diesel run engine using diesel as pilot fuel under variable compression ratio (CR) and injection timing (IT) are not transparent. Hence, this chapter explores on the behaviour of a biogas run dual fuel diesel engine for a set of CR and IT using diesel as pilot fuel.

5.2 Experimental Design

The experimental matrix consists of sixteen combinations of CR and IT as indicated in Table 5.1. The CRs are varied from 16 to 17, 17.5, and 18, where ITs are set at 23º, 26º, 29° and 32º BTDC. The variations of load are performed from no-load to full load (12 kg corresponding brake mean effective pressure of 4.2 bar) with an increment of 2.4 kg (20%). The standard diesel specification is CR=17.5 and IT=23º BTDC and used as a baseline for comparison with the findings with biogas dual fuel diesel run engine. The experiments are performed at a constant speed of 1500±50 rpm.

Table 5.1 Experimental Matrix of the Diesel-Biogas Run Dual Fuel Diesel Engine

Mode	Fuel used	CR	IT (BTDC)	Loading conditions (%)
Diesel	100% Diesel	17.5	23°	20, 40, 60, 80, 100
Dual Fuel Mode	Pilot Fuel: Diesel Primary Fuel: Biogas	18, 17.5, 17, 16	23°, 26°, 29°, 32°	

5.3 Performance Analysis

The performance analyses evaluated are brake thermal efficiency (BTE), brake specific energy consumption (BSEC), exhaust gas temperature (EGT), biogas flow rate (BFR) and

liquid fuel replacement (LFR). The combustion analyses include the cylinder pressure variation, ignition delay (ID), peak cylinder pressure (PCP) and net heat release rate (NHRR). Finally, emission analysis is performed by measuring carbon dioxide (CO_2), carbon monoxide (CO), hydrocarbon (HC) and oxides of nitrogen (NO_X). The theoretical equations, based on which performance and combustion analysis are executed, are included in Appendix-A. In this study, the EGT, BFR, ID, PCP and emission characteristics analysis are carried out on average basis for considering the effect of all loading conditions. The CR variations are made for biogas run dual fuel diesel engine for a constant IT. Therefore, the plots of each performance parameter for constant ITs are clubbed together with diesel mode for comparison. The results are discussed with respect to the two design and performance parameters, namely, CR and IT.

5.3.1 Effect of Compression Ratio

The BTE under DFM is found to be lower in comparison to diesel mode due to a low calorific value of biogas as depicted in Fig. 5.1. At 23° BTDC with 100% load, the BTEs under DFM are found to 20.04%, 18.25%, 17.07% and 16.42% for CRs of 18, 17.5, 17 and 16, respectively as compared to 27.76% for diesel mode. The BTE under DFM improves for high CR. This is due to the fact that the temperature and the pressure rise with the increase in CR. This, in turn, increases the probability of more amount of biogas to undergo complete combustion. Similar trend of rise of BTE with increase of CR was reported earlier (Jindal *et al.*, 2010). The BSEC during diesel mode is found to be lower than dual fuel mode (Fig. 5.2). This is because diesel is having higher calorific value than biogas. The BSEC drops with the increase of CR. At 100% load, the BSEC reduces by 19.38% as CR increased from 16 to 18. This is due to better combustion of biogas at high CR. The EGT for all cases of DFM is found to be higher than diesel mode (Fig. 5.3). This is due to late combustion of biogas which shortens the duration of extraction of power. As a result, the combustion products in the form of gases come out at higher temperature. At 23° BTDC, the EGT increases by 13.54%, 20.39%, 22.13% and 26.09% for CRs of 18, 17.5, 17 and 16, respectively as compared to diesel mode. The burning velocity of the biogas air mixture increases with the increase of CR. Therefore, the time required for complete combustion reduces and this produces lower EGT. This means, combustion of biogas starts early in case of high CR. Analogous trend of drop of EGT with the rise of CR was reported earlier (Raheman and Ghadge, 2008). At 23° BTDC with 100% load, the BFR is found to be 2.73 kg/h, 2.8 kg/h, 2.88 kg/h and 3.02 kg/h

for CRs of 18, 17.5, 17and 16, respectively as indicated in Fig. 5.4. Thus, the BFR decreases at high CR at same loading condition.

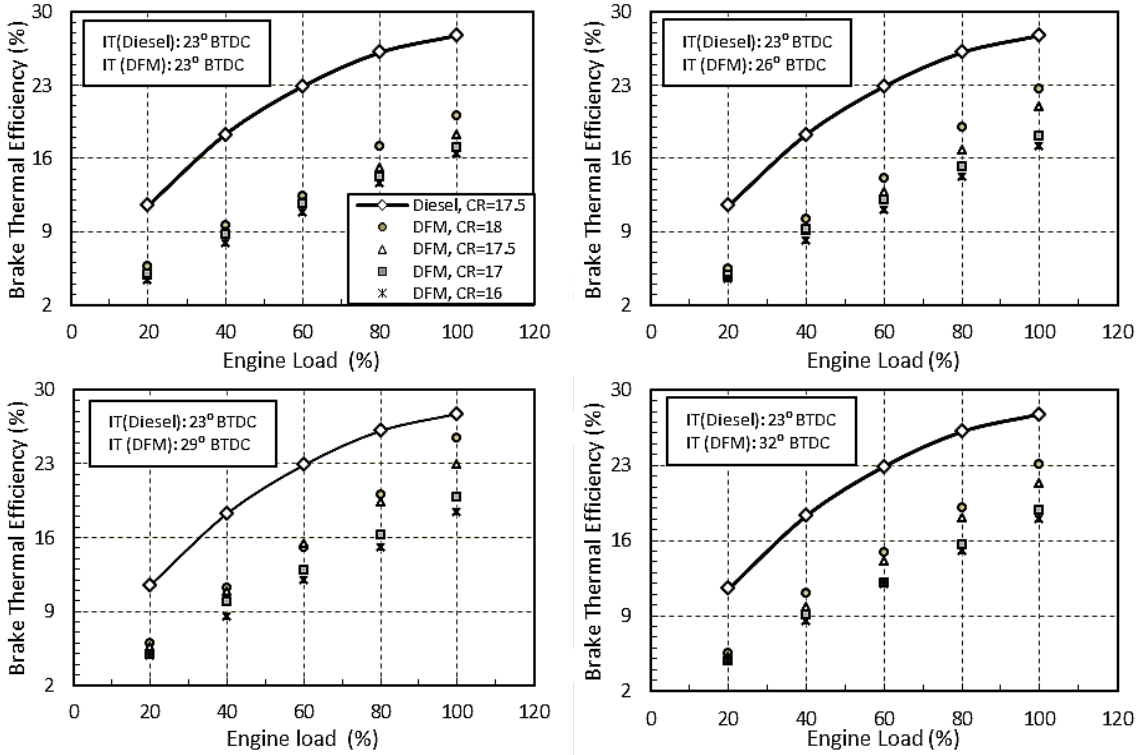

Fig. 5.1 Variation of BTE with load, CR and IT

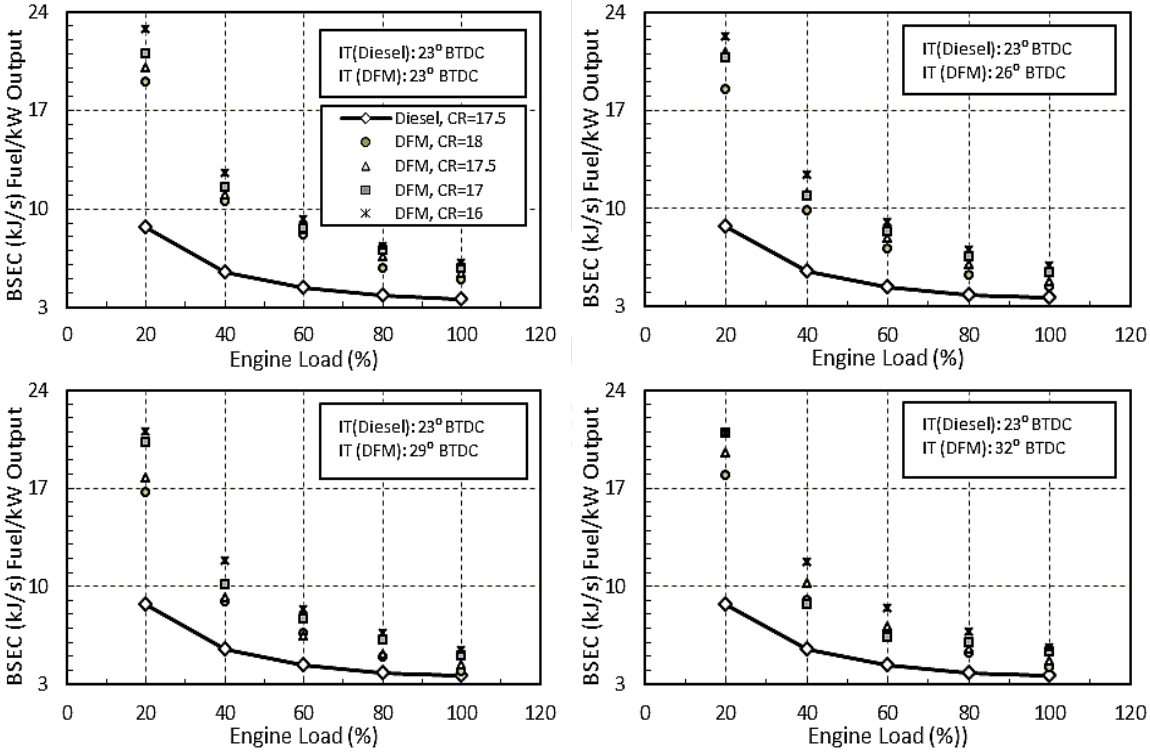

Fig. 5.2 Variation of BSEC with load, CR and IT

On an average, there is a reduction of 15.23% in BFR by increasing the CR from 16 to 18 at 23° BTDC. At 23° BTDC with 100% load, the LFR is found to be 79.46%, 76.1%, 74% and 72% for CRs of 18, 17.5, 17 and 16, respectively as depicted in Fig. 5.4. Thus, the LFR marginally improves with the increase of CR.

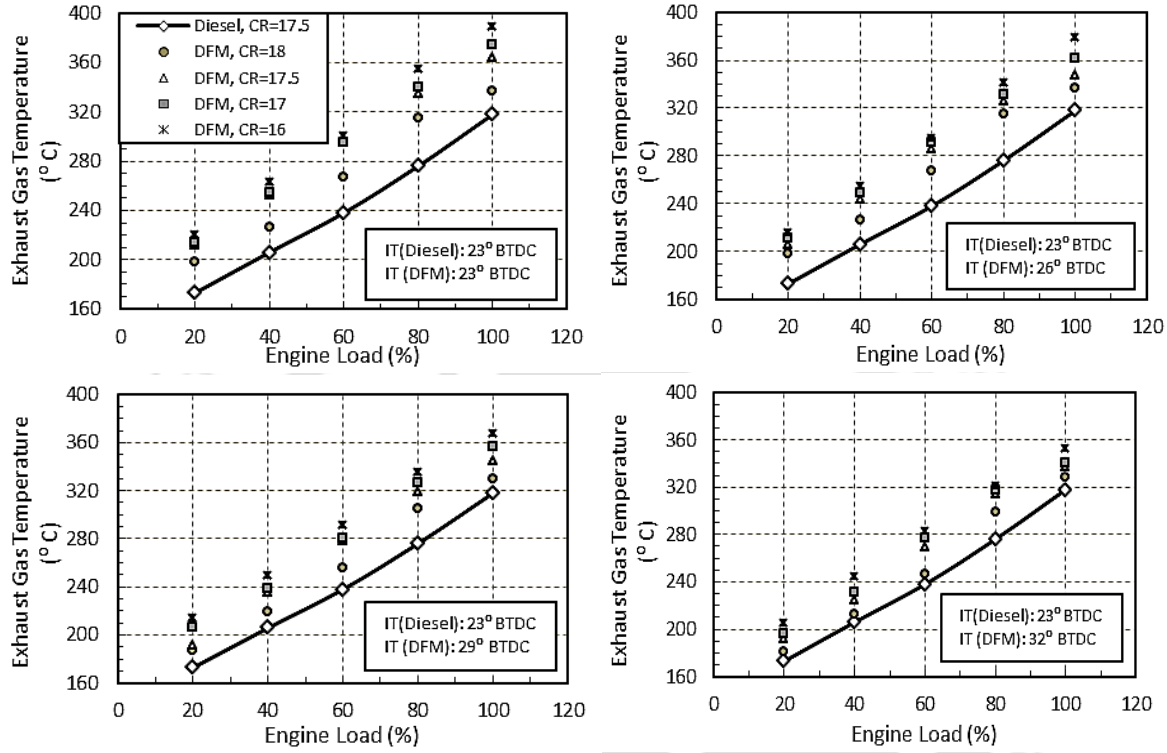

Fig. 5.3 Variation of EGT with load, CR and IT

5.3.2 Effect of Injection Timing

For CRs of 18, 17.5, 17 and 16 with 100% load, the BTEs is found to be 22.68%, 20.99%, 18.15 and 17.12% at 26° BTDC in comparison to 25.44%, 22.99%, 19.89 and 18.35% at 29° BTDC. However, at 32° BTDC, the BTEs are found to be 23.06%, 21.25%, 18.86% and 17.96% for CRs of 18, 17.5, 17 and 16, respectively. From the above analysis, it is quite evident that the BTE of the biogas run dual fuel diesel engine for this particular study improves with the advancement of IT of pilot fuel up to IT of 29° BTDC. The advancement of IT results in injection of diesel earlier into biogas-air mixture than its standard IT, thereby giving sufficient time for the complete combustion of biogas. This increases the probability of a better combustion of biogas. Similar trend of in BTE with the advancement of IT was observed by Raheman and Ghadge (2008) for a biodiesel run diesel engine. On an average, for CRs of 18, 17.5, 17 and 16, the BSEC drops by 6.6%, 1.61%°C, 3.67% and 2.56% at 26°

BTDC in comparison to 14.7%, 16.7%, 8.42% and 8.2% at 29° BTDC. Further advancement of IT to 32° BTDC lowers the BSEC to 10.88%, 8.52%, 12.24% and 8.07% for CRs of 18, 17.5, 17 and 16, respectively. For CRs of 18, 17.5, 17 and 16, the EGT rises by 10.9%, 16.43%°C, 19.24% and 22.7% at 26° BTDC in comparison to 7.1%, 12.96%, 16.43% and 20.23% at 29° BTDC. Further advancement of IT to 32° BTDC increases the EGT to 4.7%, 10.4%, 12.55% and 16.1% for CRs of 18, 17.5, 17 and 16, respectively. Thus, the EGT decreases with the advancement of pilot fuel IT under DFM. On an average, there is a reduction of 18.51% in BFR is achieved on advancing IT from 23° BTDC to 32° BTDC for CR of 18. For the same range of IT, there is a drop of 12.66%, 10.64% and 7.22% in BFR for CRs of 17.5, 17 and 16, respectively. For CRs of 18, 17.5, 17 and 16 with 100% load, the LFR is found to be 83.17%, 80.67%, 76.06% and 75.22% at 26° BTDC in comparison to 82.67%, 80.70%, 76.06 and 75.22% at 29° BTDC. However, at 32° BTDC, the LFR is found to be 79.32%, 78.4%, 76.13% and 76.1% for CRs of 18, 17.5, 17 and 16, respectively.

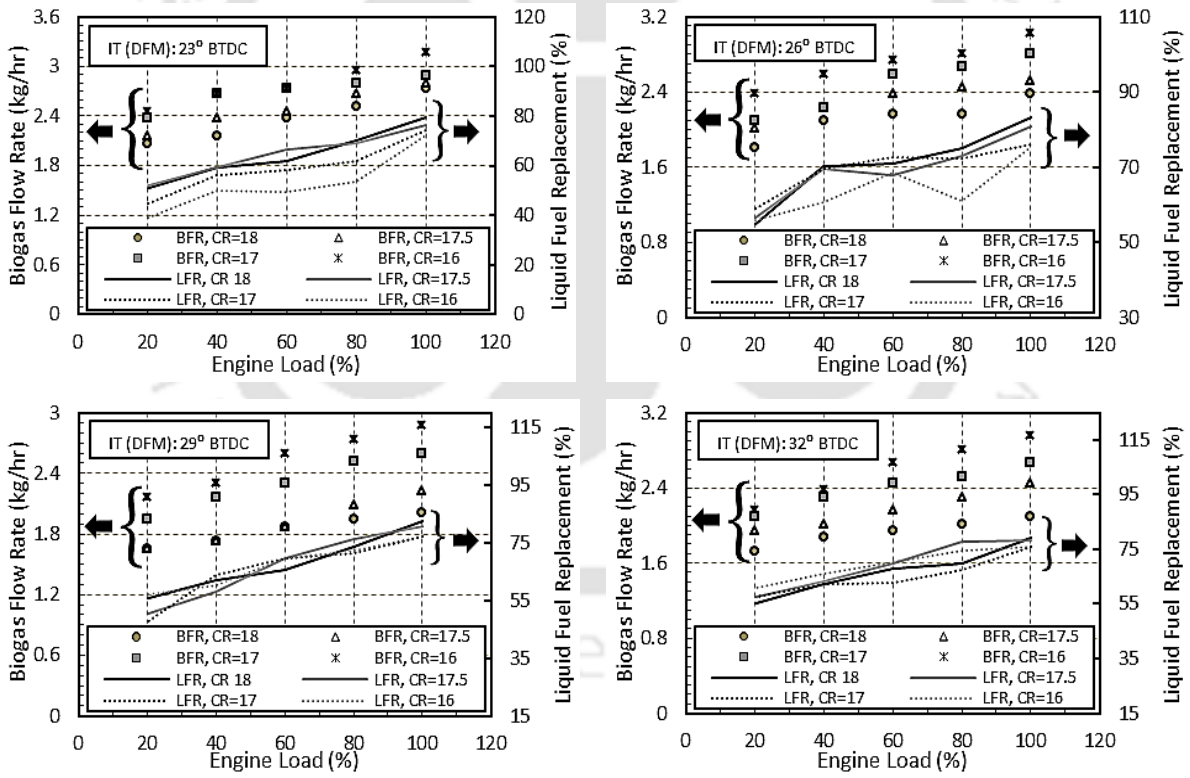

Fig. 5.4 Variation of BFR and LFR with load, CR and IT

5.4 Combustion Analysis

The combustion analysis has been carried out in the form of variation of cylinder pressure, ID, PCP and NHRR. Similar to the performance study, the parametric variation of CRs for

particular ITs are clubbed together. The effects of load, CR and IT on combustion are investigated in following sections.

5.4.1 Effect of Compression Ratio

The ID under the DFM is found to be longer than the diesel mode as observed from Fig. 5.5. The reason behind this prolonged ID for DFM is due to large amount of biogas fuel in the intake and compression processes and reduction of charge temperature compared to diesel mode. The high overall heat capacity of biogas results in lowering the charge temperature. This delays the ignition of pilot fuel significantly. It is observed that ID decreases for high CR in DFM. At the end of compression, the temperature and pressure of biogas air mixture becomes higher as the CR is increased. This enhances the preignition reactions that are believed to affect the ignition of the injected pilot fuel. The average drop in the ID with rise of CR from 16 to 17, 17 to 17.5 and 17.5 to 18 are 3.2 %, 1.6% and 3.4%, respectively.

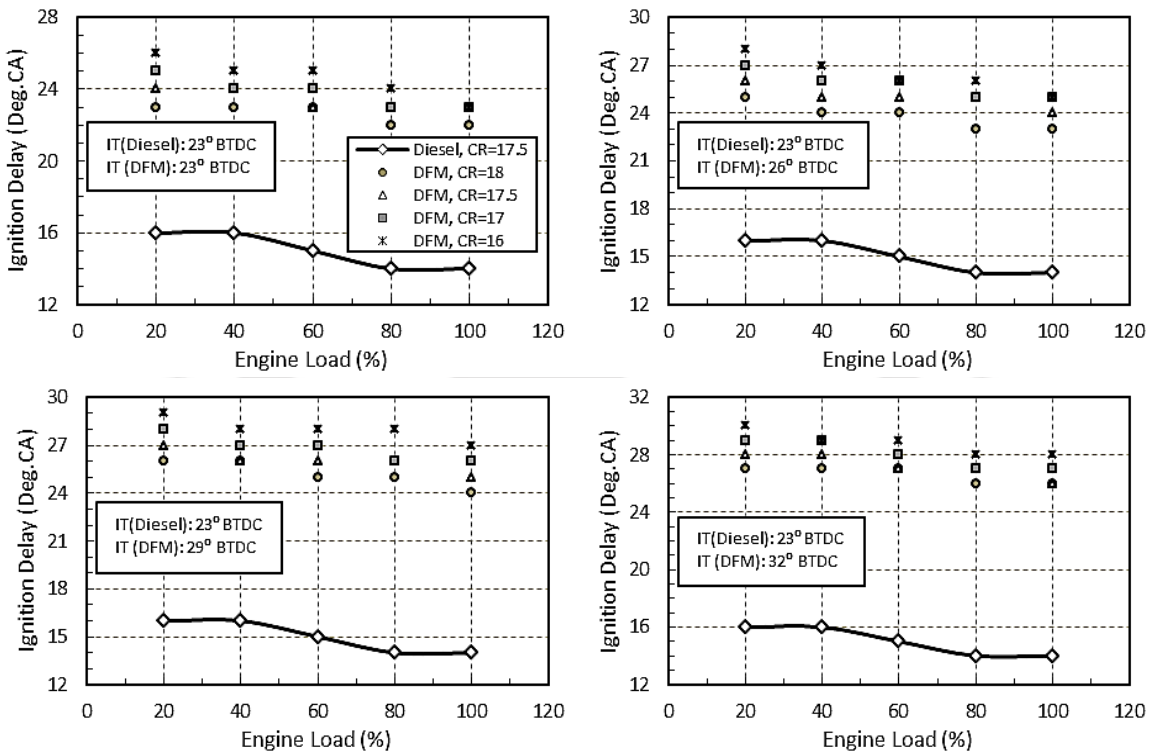

Fig. 5.5 Variation of ID with load, CR and IT

The NHRR is more in diesel mode in comparison to DFM. This is due to a high calorific value of diesel with respect to biogas. At 23° BTDC with 100% load, the maximum NHRR under DFM reduces by 44.33%, 47.13%, 52.51% and 54.71% for CRs of 18, 17.5, 17 and 16, respectively in comparison to diesel mode as indicated in Fig. 5.6 Thus, the maximum NHRR

under DFM increases with use of high CR. From the *P-Θ* diagram, it can be observed that there is a shift of PCP towards the TDC with the increase of CR in DFM as found in Fig. 5.7. At 23° BTDC with 100% load, the crank angle corresponding to PCP under DFM is found to be 9°, 9°, 9°and 12°ATDCs for CRs of 18, 17.5, 17 and 16, respectively in comparison to 3°ATDC in diesel mode. The PCP under DFM is low as compared to diesel mode as indicated in Fig. 5.8. At 23° BTDC, the PCP under DFM is found drop by 40.03%, 36.42%, 30.05%, and 27.24% for CRs of 18, 17.5, 17 and 16, respectively in comparison to diesel mode. Similar drop of ID and rise in PCP with the increase of CR was reported by El_Kassaby and Nemit_allah (2013).

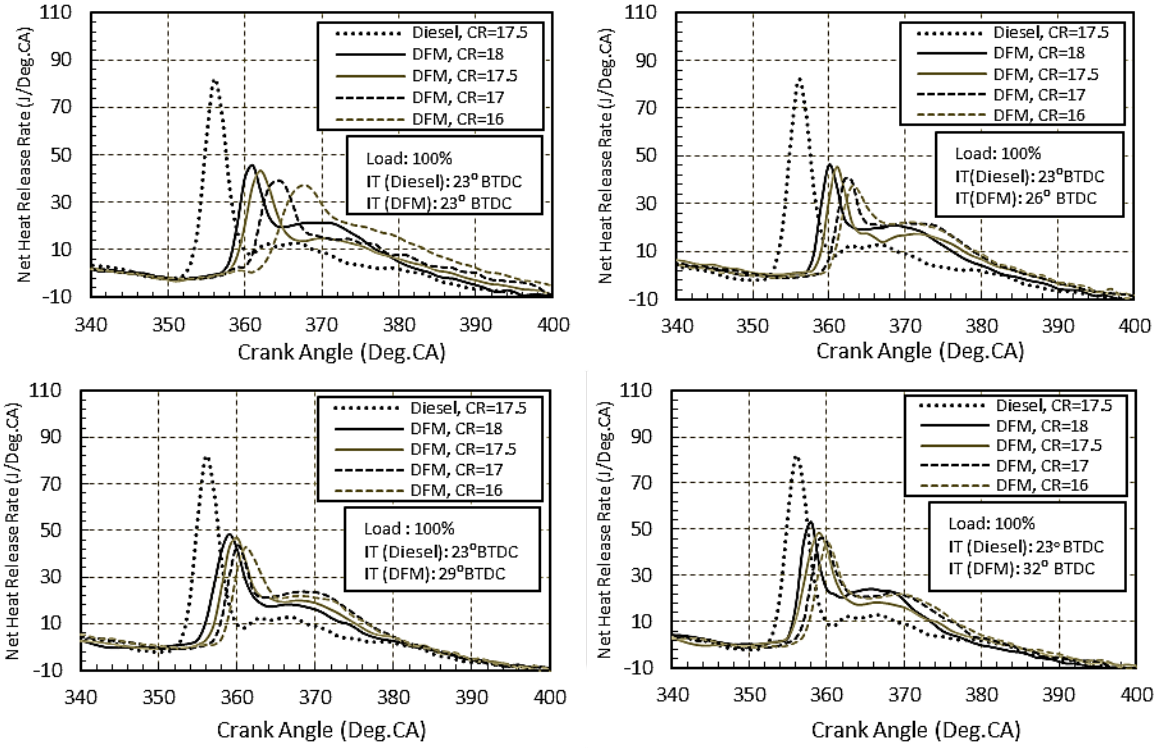

Fig. 5.6 Variation of NHRR with CR and IT at 100% load

5.4.2 Effect of Injection Timing

Advancing IT of pilot fuel resulted in injecting the fuel in a low gas temperature environment which caused in longer ID. The advancement of IT by 3°, 6° and 9° causes an average rise of IDs by about 6.99%, 12.28% and 17.16%, respectively. This goes well with the findings of Ryu (2013) for a compressed natural gas run dual fuel diesel engine. For CRs of 18, 17.5, 17 and 16 with 100% load, the maximum NHRR drops by 52.19%, 52.09%, 44.13%, 52.09% and 43.20% at 26° BTDC in comparison to 48.23%, 46.79%, 42.9% and 41.30%at 29°

BTDC. However, for same loading conditions, the maximum NHRR decreases by 45.74%, 44.35%, 41.35% and 35.83% for CRs of 18, 17.5, 17 and 16, respectively at 32° BTDC.

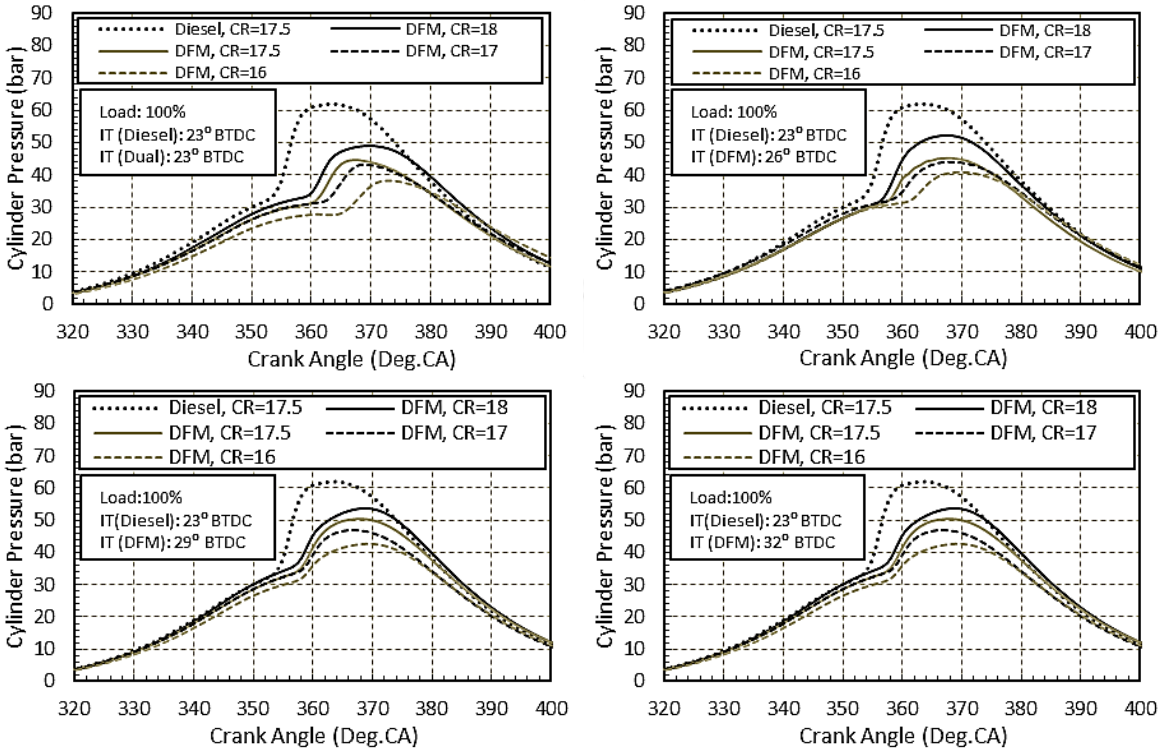

Fig. 5.7 Variation of PCP with CR and IT at 100% load

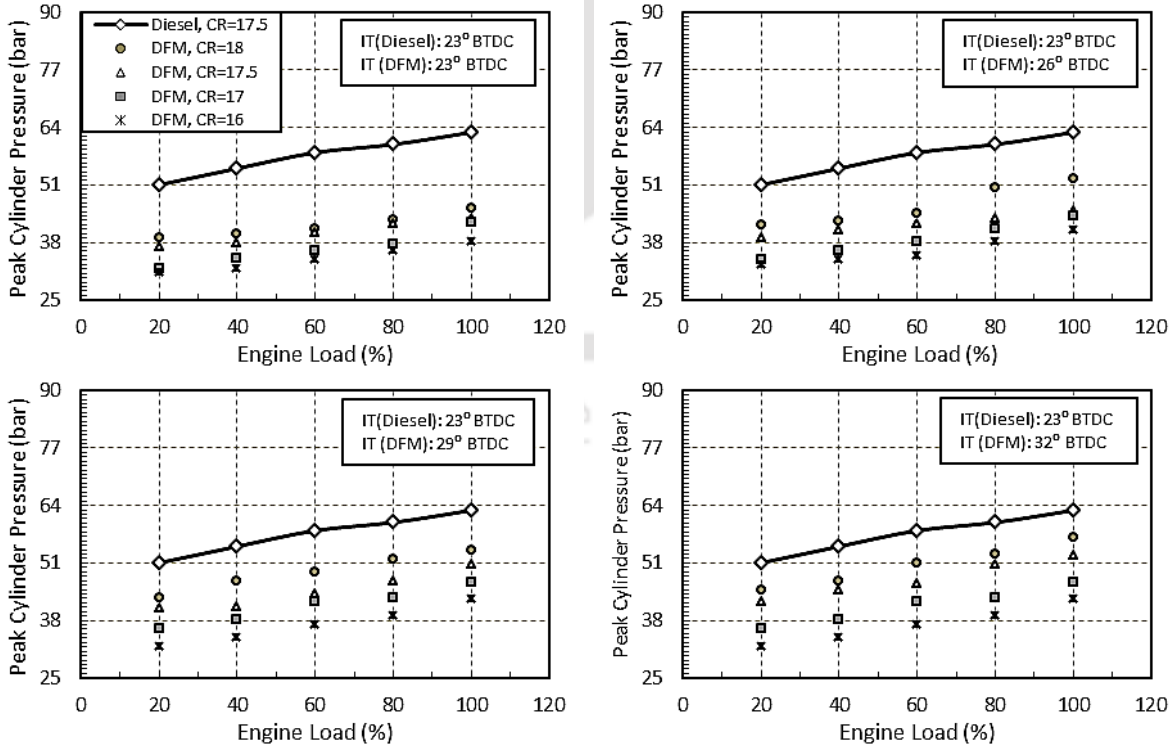

Fig. 5.8 Variation of PCP with load, CR and IT

For CRs of 18, 17.5, 17 and 16 with 100% load, the crank angle corresponding to PCP is found to be 8°, 8°, 9°and 10°ATDCs at 26°BTDC in comparison to 8°, 8°, 9° and 9° ATDCs at 29° BTDC. However, the crank angle corresponding to PCP is found to be 6°, 7°, 8° and 8° ATDCs for CRs of 18, 17.5, 17 and 16, respectively at 32° BTDC. On an average, for CRs of 18, 17.5, 17 and 16, the PCP decreases by 19.27%, 26.6%, 32.66% and 36.96% at 26° BTDC in comparison to 14.92%, 22.28%, 28.26% and 35.49% at 29° BTDC. Further advancement of IT to 32° BTDC drops the PCP by 12.04%, 17.66%, 22.24% and 28.5% for CRs of 18, 17.5, 17 and 16, respectively. Similar trend of rise of PCP with the advancement of IT of pilot fuel was observed for a natural gas dual fuel diesel engine (Papagiannakis *et al*., 2007).

5.5 Emission Analysis

The components of exhaust gas are measured by using Testo flue gas analyzer. The measured quantities are CO_2, CO, HC and NO_X. The effect of CR and IT variations on these emission parameters are discussed in following sections.

5.5.1 Effect of Compression Ratio

In this investigation, CO_2 emission is higher in DFM in comparison to diesel mode as found in Fig. 5.9. This is due to the presence of a large amount of CO_2 (i.e. around 40% by volume) in biogas. The CO_2 emission increases for high CR. As CR increases, the clearance volume decreases, which in turn surges the temperature and pressure of the charge during the end of the compression stroke. The increased temperature results in better combustion of fuel and the outcome is CO_2 emission increases. Therefore, on an average, there is an increase of 27.18% in CO_2 emission while increasing the CR from 16 to 18 at 23° BTDC. Similar trend of increase in CO_2 emission with the increase of CR was reported earlier (El_Kassaby and Nemit_allah, 2013). The CO emission is found to be higher under DFM in comparison to diesel mode as shown in Fig. 5.10. The CO emission decreases for high CR. High CR results more growth of temperature during the compression stroke which results in better combustion. This leads to lower formation of CO for higher CR. On an average, there is a reduction of 26.22% in CO emission by increasing the CR from 16 to 18 at 23° BTDC. This goes well with the findings on CO emission with the change of CR as reported earlier (Papagiannakis *et al*., 2007; Jindal *et al*., 2010; Sayin and Gumus, 2011; El_Kassaby and Nemit_allah, 2013). In this analysis, the lower flame velocity of biogas contributes to the formation of HC more under DFM in comparison to diesel mode as observed in Fig. 5.11.

The HC emission decreases with the increase of CR. Therefore, on an average, there is a reduction of 41.97% in HC emission is achieved by increasing the CR from 16 to 18 at 23° BTDC. The explanation for these findings is similar to that of CO emission. Analogous trend of drop in HC emissions with the rise of CR was reported by Sayin and Gumus, 2011. In this study, the NO_X emission in the diesel mode is much higher in comparison to DFM as depicted in Fig. 5.12. This is because the formation of NO_X depends on the temperature of the combustion chamber. The combustion chamber temperature in case of diesel is much more as diesel has a high calorific value as compared to biogas. Moreover, the presence of inert CO_2 in biogas results in lowering the temperature of the combustion chamber. The NO_X emission increases for high CR. On an average, an increase of 38.81% in NO_X emission is resulted by increasing the CR from 16 to 18 at 23° BTDC. Similar results of increased NO_X emission with the increase of CR were reported earlier (Sayin and Gumus, 2011; El_Kassaby and Nemit_allah, 2013).

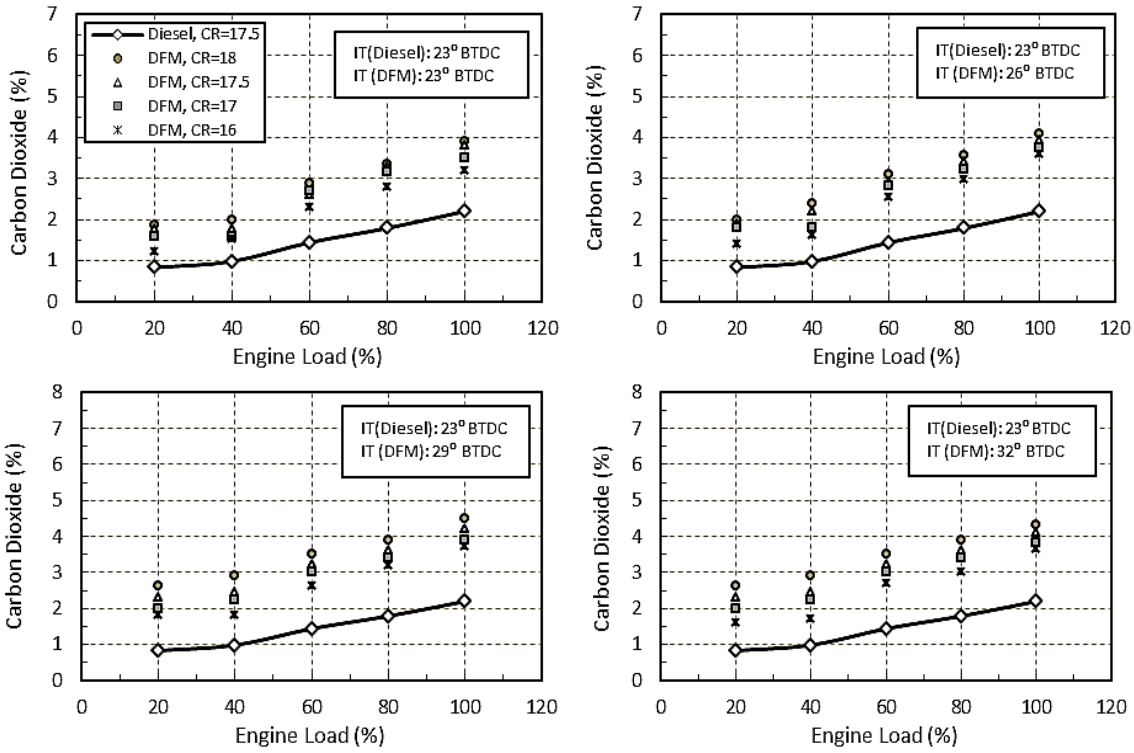

Fig. 5.9 Variation of carbon dioxide emission with load, CR and IT

5.5.2 Effect of Injection Timing

It is found that advancing IT resulted in better combustion of biogas which caused an increase of CO_2 emission. Therefore, on an average, there is an increase of 23.23% in CO_2 emission on advancing IT from 23° to 32° BTDC for CR of 18. For the same range of IT, on

an average, there is an increase of 18.18%, 15.37% and 14.97% respectively in CO_2 emission for CR of 17.5, 17 and 16. This goes well with the finding obtained by Sayin *et al.* (2008). The CO emission decreases with advancement of IT. This resulted from the increase of CO oxidation mechanism which is due to the increased time interval during the expansion stroke for which high temperature persists in the cylinder. This along resulted in more complete oxidation of CO. On an average, there is a reduction of 5.59% in CO emission on advancing IT from 23° to 32° BTDC for CR of 18.

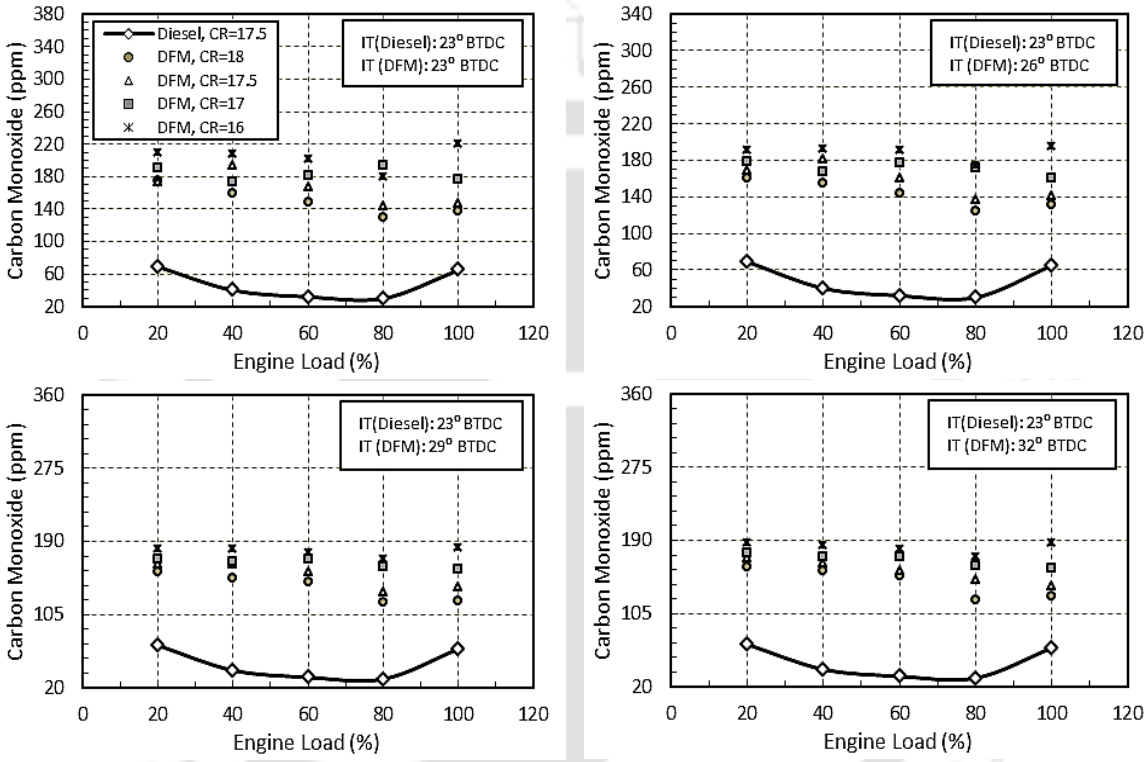

Fig. 5.10 Variation of carbon monoxide emission with load, CR and IT

For the same range of IT, on an average, there is a reduction of 6.56%, 8.64% and 10.7% respectively in CO emission for CR of 17.5, 17 and 16. Similar trend of CO emission with variation of IT was reported by Sayin and Canakci (2009). Advancing the IT causes earlier start of combustion relative to the TDC. This results in a relatively higher combustion chamber temperature as the charge being compressed as the piston moves to the TDC and lowers the HC emissions. On an average, there is reduction of 9.54% in HC emission is achieved on advancing IT from 23° to 32° BTDC for CR of 18. For the same range of IT, on an average, there is a reduction of 10.03%, 13.83% and 8.98% respectively in HC emission for CRs of 17.5, 17 and 16. Analogous results on HC emission with the variation of CR and IT was reported earlier (Raheman and Ghadge, 2008; Sayin *et al.*, 2008).

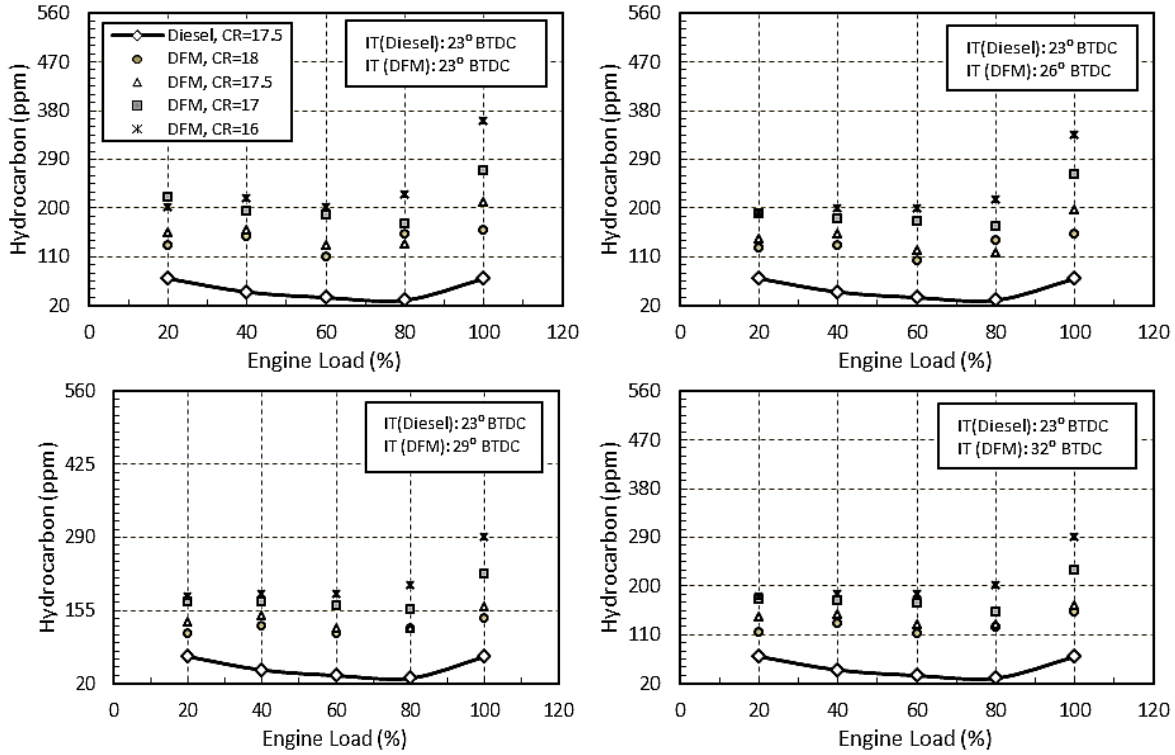

Fig. 5.11 Variation of hydrocarbon emission with load, CR and IT

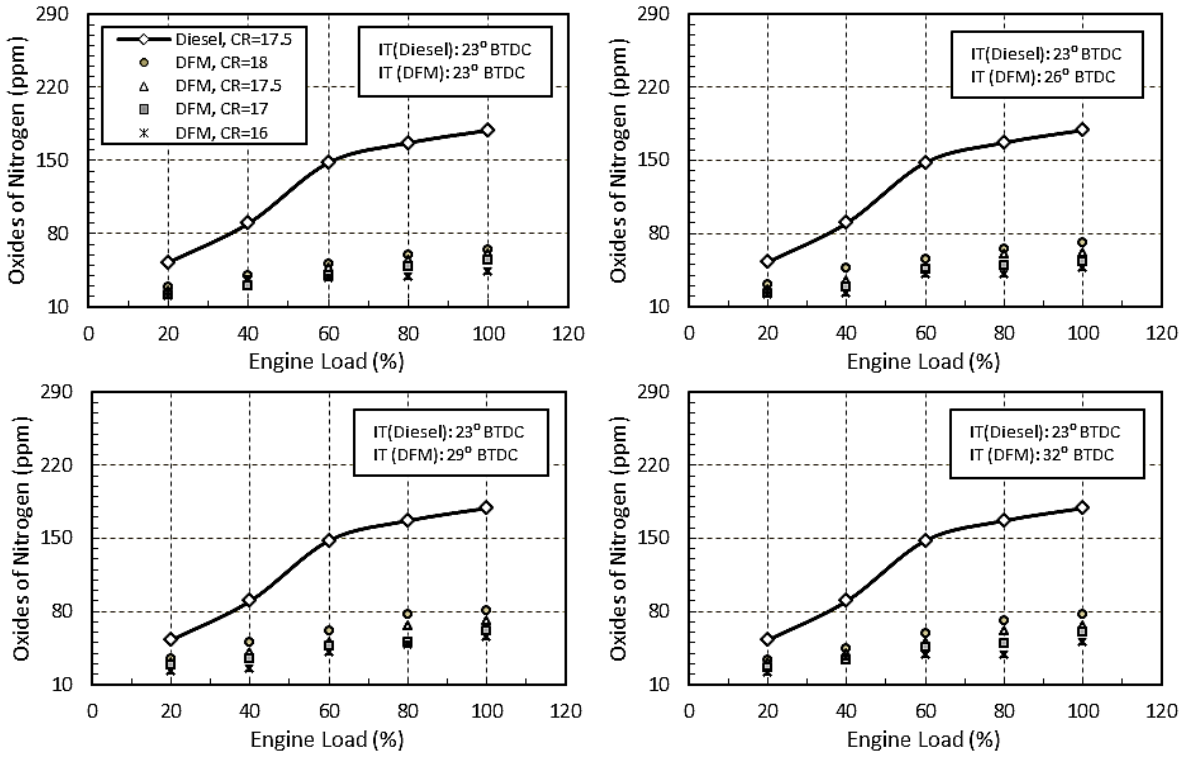

Fig. 5.12 Variation of oxides of nitrogen emission with load, CR and IT

The combustion chamber temperature increased with the advancement of IT due to better combustion of biogas. This resulted in higher emission of NOx. On an average, there is an increase of 15.91% in emission is achieved on advancing IT from 23° BTDC to 32° BTDC

for CR of 18. For the same range of IT, on an average, there is increase of 10.76%, 9.7% and 4.2% respectively in NO_X emission for CR of 17.5, 17 and 16. This goes well with the findings of previous work (Sayin and Canakci, 2009; Ryu, 2013).

5.5 Summary

- The BTE of the biogas run dual engine is found to increase with the use of high CR of 18. However, with the advancement of pilot fuel IT, the performance improves up to a particular IT. The maximum BTE of 25.44% is obtained for a combination of CR=18 and IT=29° BTDC.

- The BSEC is found to be increase with the use of high CR of 18. Conversely, with the advancement of pilot fuel IT, the BSEC drops up to a particular IT. The maximum fall in BSEC of 14.7% is obtained for a combination of CR=18 and IT=29° BTDC.

- The EGT is found to drop with the use of high CR of 18. The advancement of pilot fuel IT results in further drop of EGT. The maximum drop in EGT is attained for a combination of CR=18 and IT=32° BTDC.

- There is an average reduction of 15.23% in BFR by increasing the CR from 16 to 18 at 23° BTDC. On an average, there is a reduction of 18.51% in BFR is achieved on advancing IT from 23° BTDC to 32° BTDC for CR of 18. For the same range of IT, there is a drop of 12.66%, 10.64% and 7.22% in BFR for CRs of 17.5, 17 and 16, respectively.

- At 23° BTDC with 100% load, the LFR is found to be 79.46%, 76.1%, 74% and 72% for CRs of 18, 17.5, 17 and 16, respectively. For CRs of 18, 17.5, 17 and 16, the LFR is found to be 83.17%, 80.67%, 76.06% and 75.22%, respectively at 26° BTDC in comparison to 82.67%, 80.70%, 76.06 and 75.22% at 29° BTDC. However, at 32° BTDC, the LFR is found to be 79.32%, 78.4%, 76.13% and 76.1% for CRs of 18, 17.5, 17 and 16, respectively.

- The average drop in the ID with rise of CR from 16 to 17, 17 to 17.5 and 17.5 to 18 are 3.2 %, 1.6% and 3.4%, respectively. The advancement of IT by 3°, 6° and 9° causes an average rise of IDs by about 6.99%, 12.28% and 17.16%, respectively.

- The maximum NHRR and the PCP increases with use of high CR and advancement of IT of pilot fuel. The maximum NHRR and the PCP is attained for a combination of CR=18 and IT=32° BTDC.

- On an average, there is an increase of 23.23% in CO_2 emission on advancing IT from 23° to 32° BTDC for CR of 18. For the same range of IT, there is an increase of 18.18%, 15.37% and 14.97% in CO_2 emission for CR of 17.5, 17 and 16, respectively. Therefore, there is an increase of 27.18% in CO_2 emission while increasing the CR from 16 to 18 at 23° BTDC.

- There is a reduction of 26.22% in CO emission by increasing the CR from 16 to 18 at 23° BTDC. There is a reduction of 5.59% in CO emission on advancing IT from 23° to 32° BTDC for CR of 18. For the same range of IT, there is a reduction of 6.56%, 8.64% and 10.7% in CO emission for CR of 17.5, 17 and 16, respectively.

- There is a reduction of 41.97% in HC emission is achieved by increasing the CR from 16 to 18 at 23° BTDC. There is reduction of 9.54% in HC emission is achieved on advancing IT from 23° to 32° BTDC for CR of 18. For the same range of IT, on an average, there is a reduction of 10.03%, 13.83% and 8.98% in HC emission for CRs of 17.5, 17 and 16, respectively

- There is an increase of 38.81% in NO_X emission is resulted by increasing the CR from 16 to 18 at 23° BTDC. there is an increase of 15.91% in emission is achieved on advancing IT from 23° BTDC to 32° BTDC for CR of 18. For the same range of IT, there is increase of 10.76%, 9.7% and 4.2% in NO_X emission for CR of 17.5, 17 and 16, respectively.

Therefore, it can be concluded from the above discussion that the CR=18 and pilot fuel IT = 29° BTDC is the optimum combination for this particular specification of a biogas run dual fuel diesel engine using diesel as pilot fuel.

Chapter-6

Results of Rice Bran Biodiesel - Biogas Run Dual Fuel Engine

Overview:

The main objective of this chapter is to standardize the operating parameters of a biogas run dual fuel diesel engine using rice bran biodiesel as pilot fuel. Rice bran biodiesel, a bio-origin alternative fuel, also known as rice bran oil methyl ester, is considered for the study. Therefore, in this chapter, the experimentation conducted in a biogas run dual fuel diesel engine is examined to find out its optimum performance. The investigation is based on performance, combustion and emission analysis of the biogas run dual fuel diesel engine. In each analysis, explanations are provided based on compression ratio and injection timing variations. Alongside, a comparison with baseline test under diesel mode at standard setting is carried out for quantitative and qualitative assertion. The purpose of this investigation is to comprehend the behaviour of a biogas run dual fuel diesel engine using rice bran biodiesel as pilot fuel under various combinations of compression ratio and injection timing.

Chapter Outline:

6.1 Rice Bran Biodiesel as Fuel

Rice bran oil (RBO) is extracted from rice bran, which is a by-product of rice milling process. Crude RBO can be extracted from rice bran and refined to make edible oil. However, RBO with free fatty acids (FFA) higher than 10% is considered as inedible. Only a small portion (<10%) of the total production of RBO is processed into edible oil (Zullaikah *et al*., 2005). Therefore, RBO with high FFA can be utilised as a feedstock for biodiesel. As rice production is a renewable process, the availability of rice bran biodiesel (RBB) is also renewable in nature (Pandey, 2009).

Several investigations have been carried out to test the suitability RBB and its blends with diesel as a diesel engine fuel. Saravanan *et al*. (2009) carried out a feasibility analysis of RBB blend with diesel as a stationary and automotive diesel engine fuel. The study revealed that hourly fuel cost of RBB blend when used in a stationary engine increases by 50% while that in an automotive engine increases by 45% as compared to diesel. The combustion characteristics of a stationary diesel engine fuelled with a blend RBB was investigated by Saravanan *et al*. (2010). The results revealed that the blend of RBB produced lower smoke intensity and higher oxides of nitrogen (NO_X) emission in comparison to that of diesel. MohamedMusthafa *et al*. (2011) compared the performance and emission characteristics of fly ash coated low heat rejection engine with uncoated engine fuelled with RBB. The test indicated a significant reduction of both brake specific fuel consumption and NO_X emission for fly ash coated engine in comparison to that of non-coated engine. Saravanan and Nagarajan (2014) found fuel injection pressure to be the most influencing factor among injection timing and exhaust gas recirculation in reducing NOx emission for a RBB run diesel engine. The review of literature confirms that, until now, the performance, combustion and emission characteristics of biogas dual fuel diesel run engine using RBB as pilot fuel under variable compression ratio (CR) and injection timing (IT) has not been explored. Hence, this chapter investigates the behaviour of a biogas run dual fuel diesel engine for different combinations of CR and IT using RBB as pilot fuel.

6.2 Experimental Design

The experimental matrix consists of twelve combinations of CR and IT as indicated in Table 6.1. The CRs comprise of 17, 17.5, and 18, where ITs consist of 23º, 26º, 29° and 32º BTDC. The variations of load are performed from no-load to full load (12 kg corresponding brake

mean effective pressure of 4.2 bar) with an increment of 2.4 kg (20%). The standard diesel specification is CR=17.5 and IT=23º BTDC and used as a baseline for comparison with the findings with RBB-biogas dual fuel diesel run engine. The experiments are performed at a constant speed of 1500±50 rpm.

Table 6.1 Experimental Matrix of the RBB-Biogas Run Dual Fuel Diesel Engine

Mode	Fuel used	CR	IT (BTDC)	Loading conditions (%)
Diesel	100% Diesel	17.5	23°	20, 40, 60, 80, 100
Dual Fuel Mode	Pilot Fuel: RBB Primary Fuel: Biogas	18, 17.5, 17	23°, 26°, 29°, 32°	

6.3 Performance Analysis

The performance analyses includes brake thermal efficiency (BTE), brake specific energy consumption (BSEC), exhaust gas temperature (EGT), biogas flow rate (BFR) and liquid fuel replacement (LFR). The combustion analyses include ignition delay (ID), peak cylinder pressure (PCP) and net heat release rate (NHRR). Finally, emission analysis is performed by measuring carbon dioxide (CO_2), carbon monoxide (CO), hydrocarbon (HC) and oxides of nitrogen (NO_X). The theoretical equations, based on which performance and combustion analysis are executed, are included in Appendix-A. In this investigation, the EGT, BFR, ID, PCP and emission characteristics analysis are carried out on average basis for considering the effect of all loading conditions. The CR variations are made for RBB-biogas run dual fuel diesel engine for a constant IT. Therefore, the plots of each performance parameter for constant ITs are group together with diesel mode for comparison. The results are discussed with respect to the two design and performance parameters, namely, CR and IT

6.3.1 Effect of Compression Ratio

The BTE increases with the increase in load for both diesel and DFM as indicated in Fig. 6.1. However, BTE is found to be lower under DFM in comparison to diesel mode. This is due to a low calorific value of both biogas and RBB. At 23° BTDC with 100% load, the BTEs under DFM are found to be 20.27%, 19.97% and 18.39% for CRs of 18, 17.5 and 17, respectively as compared to 27.76% for diesel mode. Thus, the BTE under DFM improves for high CR.

This is due to the surge in temperature with the increase in CR. This, in turn, increases the probability of more amount of biogas to undergo complete combustion. Analogous trend of the increase of BTE with increase of CR was reported by Jindal *et al.* (2010).

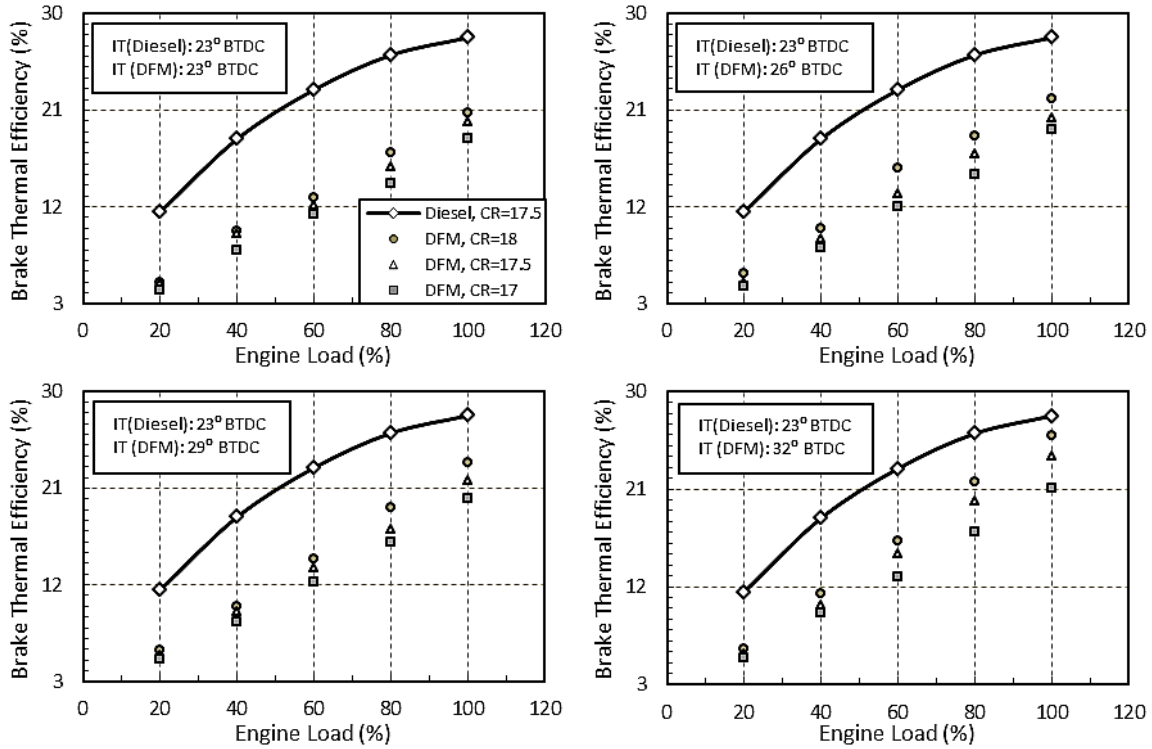

Fig. 6.1 Variation of BTE with load, CR and IT

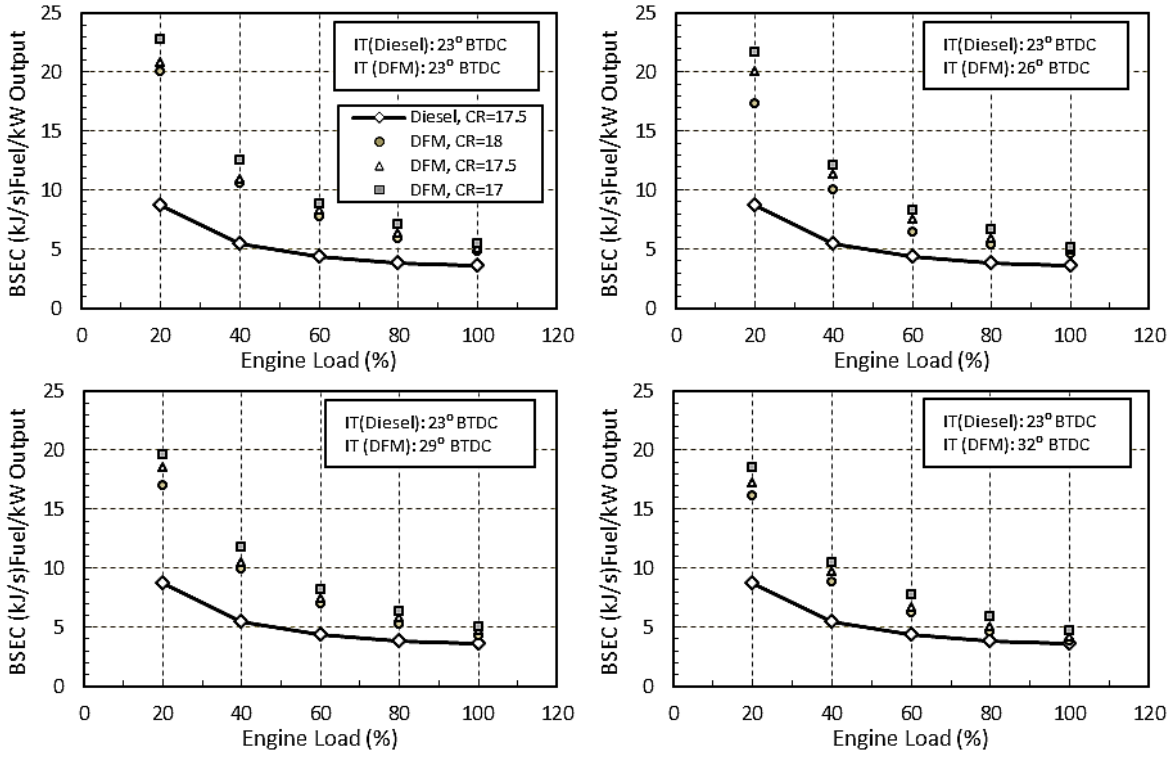

Fig. 6.2 Variation of BSEC with load, CR and IT

The BSEC during diesel mode is found to be lower than DFM (Fig. 6.2). On an average, the BSEC reduces by 13.53% as CR increased from 17 to 18. The EGT follows a linear relationship with load. The EGT for all cases under DFM is found to be higher than diesel mode (Fig. 6.3). This is due to late combustion of biogas, which results the combustion products in the form of gases come out at a higher temperature. At 23° BTDC, there is a rise of EGT by 13.04%, 19.81% and 22.54% at CRs of 18, 17.5 and 17, respectively as compared to diesel mode. This is due to the increase in burning velocity of the biogas air mixture with the rise of CR. Therefore, the time required for the complete combustion reduces and this lowers the EGT. Similar trend of drop of EGT with the increase of CR was observed by Raheman and Ghadge (2008). At 23° BTDC with 100% load, the BFR is found to be 2.82 kg/h, 3 kg/h and 3.12 kg/h for CRs of 18, 17.5 and 17, respectively. At 23° BTDC, there is a reduction of 8.36% in BFR by increasing the CR from 17 to 18 as depicted in Fig. 6.4. The liquid fuel replacement (LFR) increases with the increase of load. At 23° BTDC for 100% load, the LFR is found to be 80%, 79% and 78.26% for CRs of 18, 17.5 and 17, respectively.

6.3.2 Effect of Injection Timing

For CRs of 18, 17.5 and 17 with 100% load, the BTEs under DFM are found to be 22.04%, 20.3% and 19.19%, respectively at 26° BTDC in comparison to 23.36%, 21.7% and 20.09% at 29° BTDC. With the further advancement of IT to 32° BTDC, the BTEs under DFM are found to be 25.88%, 24% and 21.08% for CRs of 18, 17.5 and 17, respectively. This particular study reveals that the BTE of the RBB-biogas run dual fuel diesel engine improves with the advancement of IT of pilot fuel. With the advancement of IT, biodiesel is injected earlier into the biogas-air mixture than its standard IT, thereby giving ample time for the combustion of biogas. This burns the biogas more efficiently. Similar trend of the increase of BTE with the advancement of IT was reported earlier. (Agarwal *et al*., 2013; Raheman and Ghadge, 2008). For CRs of 18, 17.5 and 17, the BSEC drops by 10.81%, 3.08%°C, and 4.7%, respectively at 26° BTDC in comparison to 11.44%, 8.5% and 10.25% at 29° BTDC. Further advancement of IT to 32° BTDC lowers the BSEC to 19.29%, 16.7% and 16.4% for CRs of 18, 17.5 and 17, respectively. For CRs of 18, 17.5 and 17, the EGT rises by 10.5%, 16.67% and 19.15% respectively at 26° BTDC in comparison to 7.18%, 12.72% and 16.27% at 29° BTDC. However, at 32° BTDC, the EGT is increases by 4.46%, 10.23% and 12.72% for CRs of 18, 17.5 and 17, respectively. An analogous finding on the variation of EGT with advancement of IT was observed by Sayin *et al*. (2008).

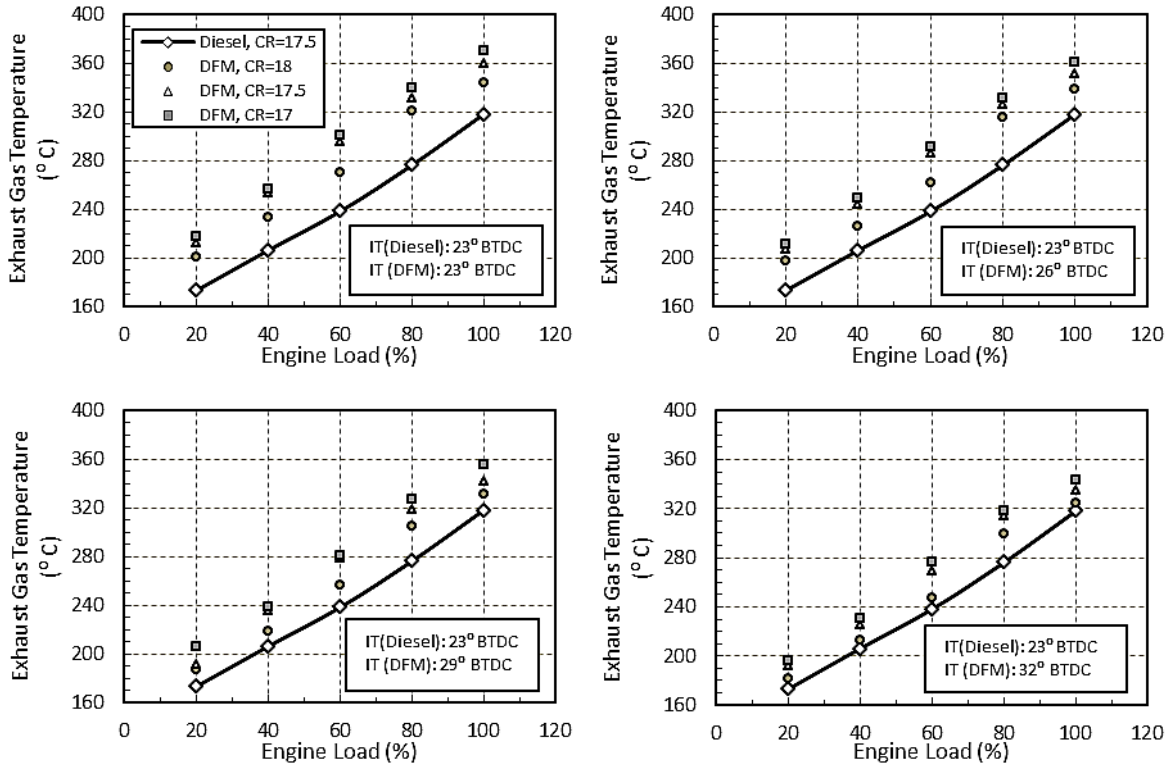

Fig. 6.3 Variation of EGT with load, CR and IT

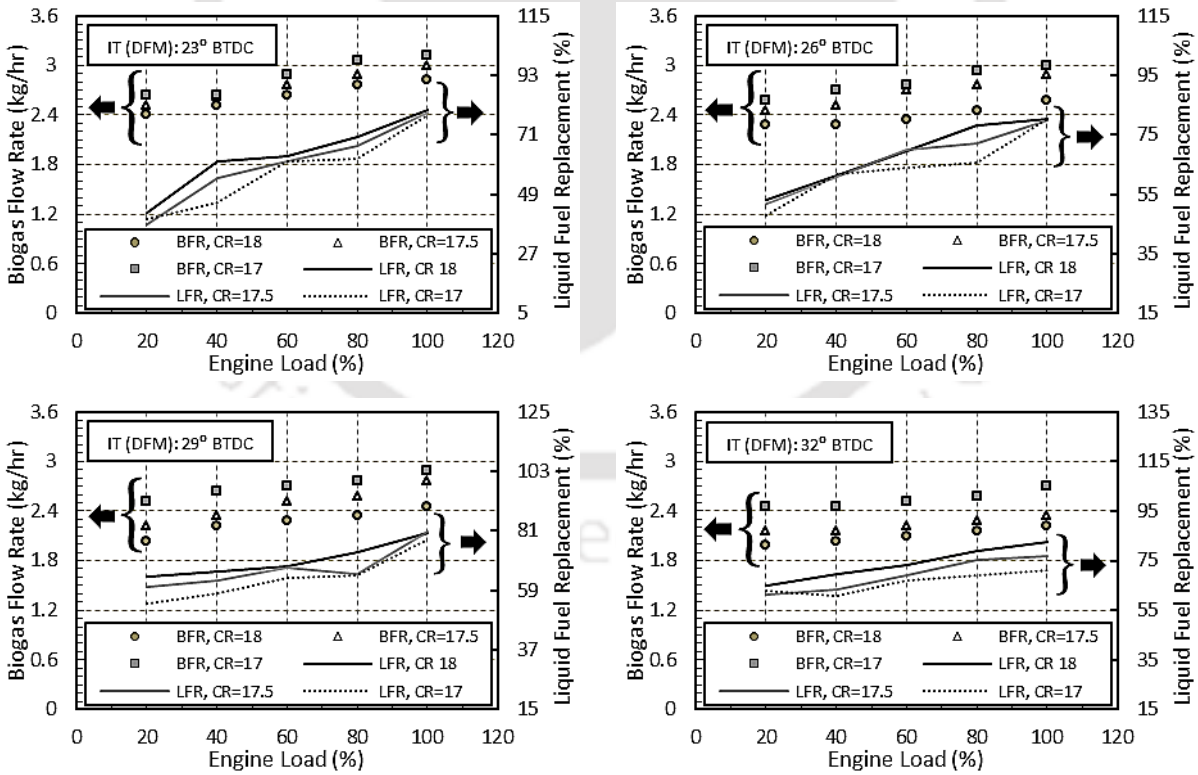

Fig. 6.4 Variation of BFR and LFR with load, CR and IT

On advancing IT from 23° to 32° BTDC for CR of 18, there is a drop of 20.09% in BFR. For the same range of IT, there is a drop of 19.07% and 11.27%, respectively in BFR at CRs of

17.5 and 17. For CRs of 18, 17.5 and 17 with 100% load, the LFR is found to be 80%, 80% and 80.25%, respectively for at 26° BTDC in comparison to 80.51%, 80.51% and 77.71% at 29° BTDC. However, the LFR is found to be 82.75%, 72.51% and 71% for CRs of 18, 17.5 and 17, respectively at 32° BTDC. The LFR increases slightly with the advancement of IT particularly for CR of 18.

6.4 Combustion Analysis

The combustion analysis has been carried out in the form of variation of ID, PCP and NHRR. Similar to the performance study, the parametric variation of CRs for particular ITs are clubbed together. The effects of load, CR and IT on combustion are investigated in following sections.

6.4.1 Effect of Compression Ratio

The ID gradually decreases as load increases for both diesel and DFM as observed from Fig. 6.5. The ID under the DFM is found to be longer than the diesel mode. The large amount of biogas during intake and compression process results in lowering of the charge temperature under DFM. This is due to high overall heat capacity of biogas. This delays the ignition of pilot fuel significantly. It is observed that ID decreases at high CR under DFM. At the end of compression, the temperature and pressure of biogas air mixture becomes higher as the CR is increased. This enhances the preignition reactions that are believed to affect the ignition of the injected pilot fuel. The average drop in ID with the rise of CR from 17 to 17.5 and 17.5 to 18 are 3.7% and 4.4%, respectively. The NHRR is more in diesel mode in comparison to DFM as indicated in Fig. 6.6. This is due to a high calorific value of diesel with respect to biogas. At 23° BTDC with 100% load, the maximum NHRR under DFM reduces by 53.18%, 55.91% and 64.31% for CRs of 18, 17.5 and 17, respectively in comparison to diesel mode. Thus, it can be observed that the maximum NHRR in DFM increases with the increase in CR. From the *P-Θ* diagram, it can be observed that there is a shift of PCP towards the TDC with the increase of CR under DFM as observed in Fig. 6.7. At 23° BTDC with 100% load, the crank angle corresponding to PCP under DFM is found to be 11°, 12° and 12° after top dead centres (ATDCs) for CRs of 18, 17.5 and 17, respectively in comparison to 3° ATDC in diesel mode. The PCP increases with the increase in load for both diesel and DFM as indicated in Fig. 6.8. However, the pressure rise is low in case of DFM as compared to diesel mode. AT 23° BTDC, the PCP reduces by 22.02%, 24.96% and 30.05% for CRs of 18, 17.5

and 17, respectively in comparison to diesel mode. Similar trend of variation of ID, NHRR and PCP with CR was reported by Debnath *et al.* (2014b).

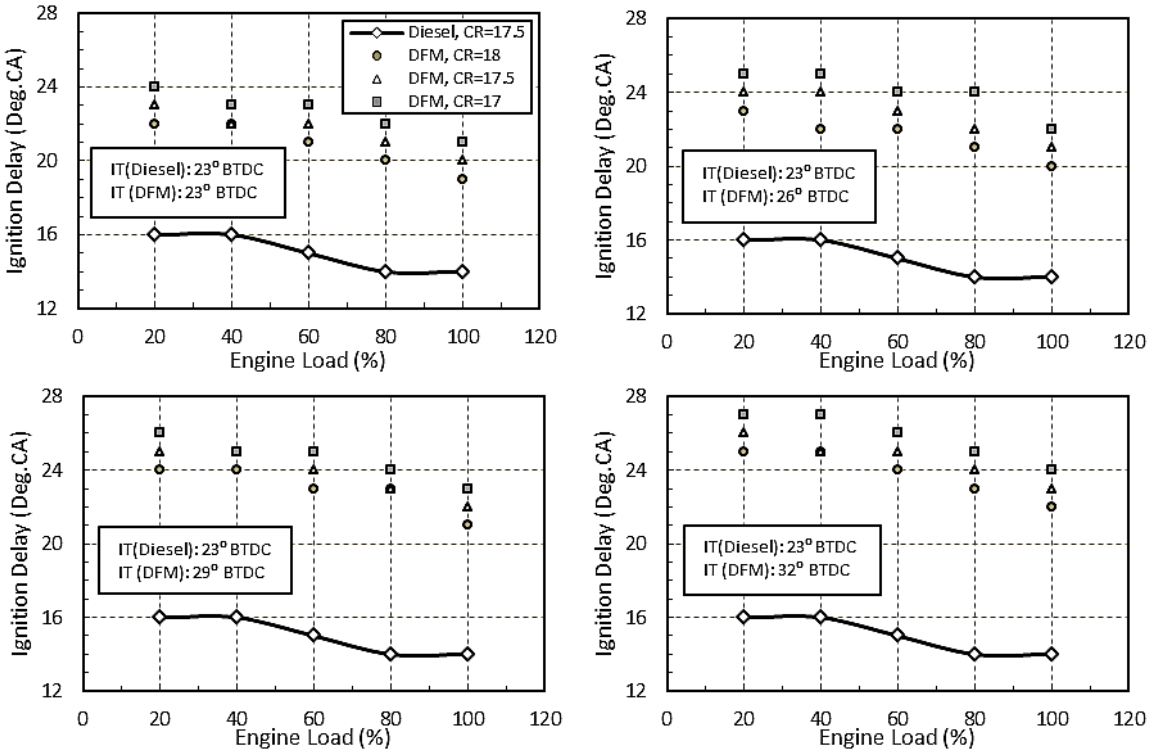

Fig. 6.5 Variation of ID with load, CR and IT

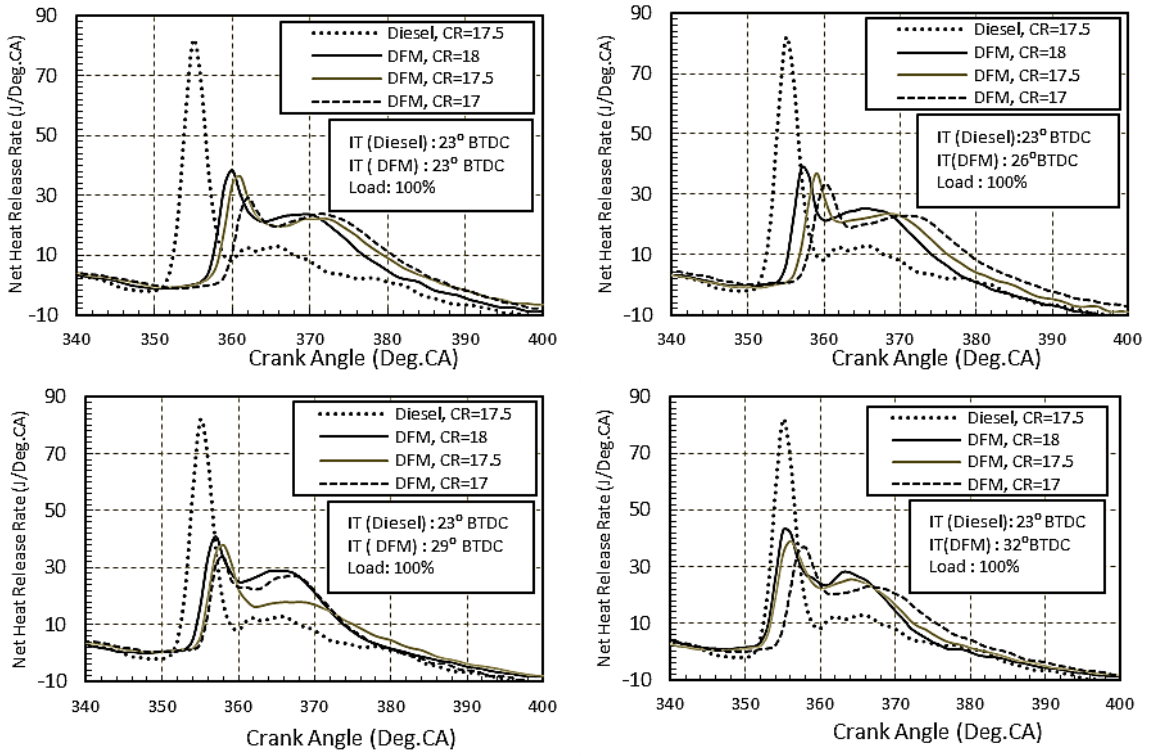

Fig. 6.6 Variation of NHRR with CR and IT at 100% load

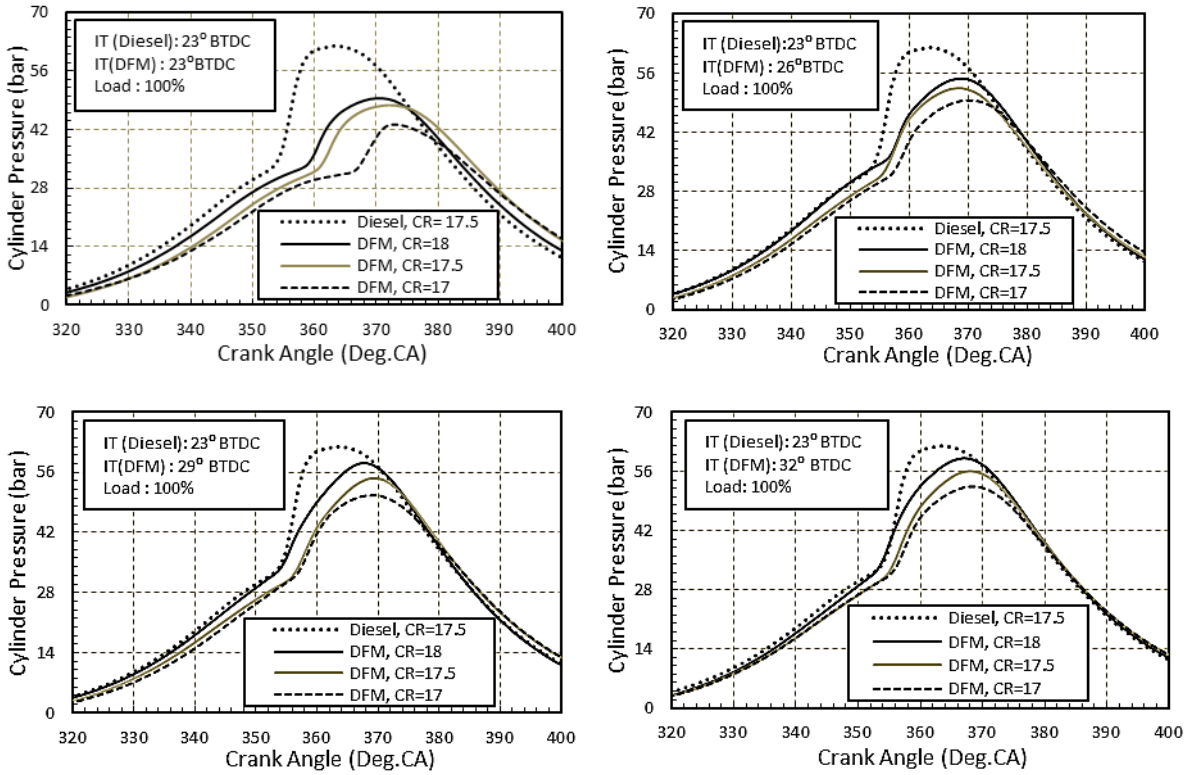

Fig. 6.7 Variation of PCP with CR and IT at 100% load

6.4.2 Effect of Injection Timing

The advancement of IT of pilot fuel resulted in injecting the fuel in a low gas temperature environment which caused in longer ID. For CR of 18, 17.5 and 17, the advancement of IT by 3°, 6° and 9° resulted in an average rise of IDs by about 14.42%, 13.88% and 14.15%, respectively. For CRs of 18, 17.5 and 17 with 100% load, the maximum NHRR drops by 52.84%, 54.91% and 59.44% at 26° BTDC in comparison to 50.01%, 53.67%, and 58.23% at 29° BTDC. However, for same loading conditions, the maximum NHRR decreases by 47.73%, 52.37% and 55.12% for CRs of 18, 17.5 and 17, respectively at 32° BTDC. Thus, the maximum NHRR under DFM increases with the advancement of IT. For CRs of 18, 17.5 and 17 with 100% load, the crank angle corresponding to PCP under DFM is found to be 9°, 9° and 10° ATDCs at 26° BTDC in comparison to 8°, 9° and 10°ATDCs at 29° BTDC. However, the crank angle corresponding to PCP under DFM is found to be 6°, 8° and 8° ATDCs for CRs of 18, 17.5 and 17, respectively at 32° BTDC. Thus, it can be observed that there is a shift of the pressure curve towards TDC with the advancement of IT. For CRs of 18, 17.5 and 17 with 100% load, the PCP drops by 15.97%, 19.79% and 23.45% at 26° BTDC in comparison to 11.2%, 15.92%, and 20.89% at 29° BTDC. However, at 32° BTDC, the PCP decreases by 11.2%, 12.92%, and 18.46% for CRs of 18, 17.5 and 17, respectively.

Analogous trend of variation of ID, NHRR and PCP with IT was observed by Agarwal *et al.* (2013)

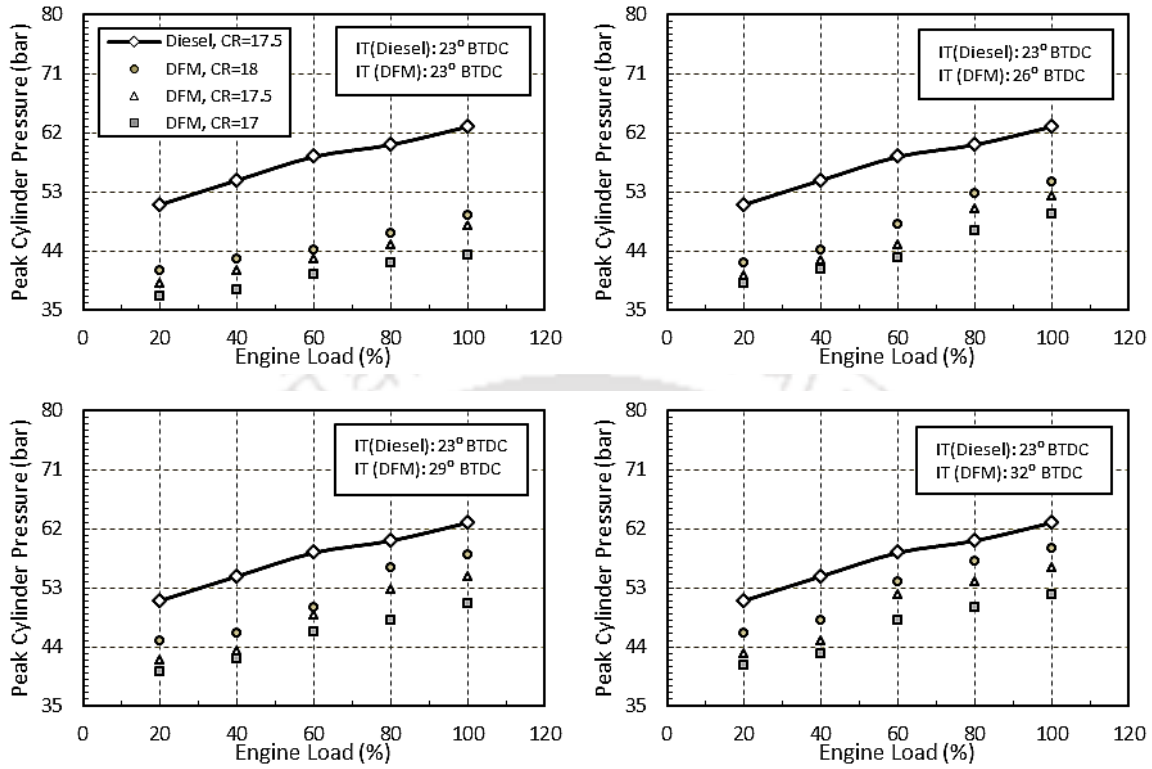

Fig. 6.8 Variation of PCP with load, CR and IT

6.5 Emission Analysis

The samples are investigated inside the flue gas analyzer and visualize the respective concentrations of CO, CO_2, HC and NO_X emissions on the display of control unit.

6.5.1 Effect of Compression Ratio

In this investigation, CO_2 emission is found to be higher under DFM in comparison to diesel mode as found in Fig. 6.9. The CO_2 emission under DFM rises with the increase in CR. The clearance volume decreases with the increase of CR, which in turn increases the temperature of the charge at the end of the compression stroke. The increased temperature results in better combustion of fuel and thereby, CO_2 emission increases. Therefore, there is rise of CO_2 emission by 13.78% on increasing the CR from 17 to 18 at 23° BTDC. The CO emission is found to be higher under DFM in comparison to diesel mode as shown in Fig. 6.10. The CO emission decreases for high CR under DFM. High CR results more growth of temperature which causes better combustion. This leads to lower formation of CO for higher CR. On an

average, there is a reduction of 17.67% in CO emission by increasing the CR from 17 to 18 at 23° BTDC. This goes well with the findings on both CO_2 and CO emission with the change of CR as reported earlier (Sayin and Gumus, 2011; Jindal *et al*., 2010).

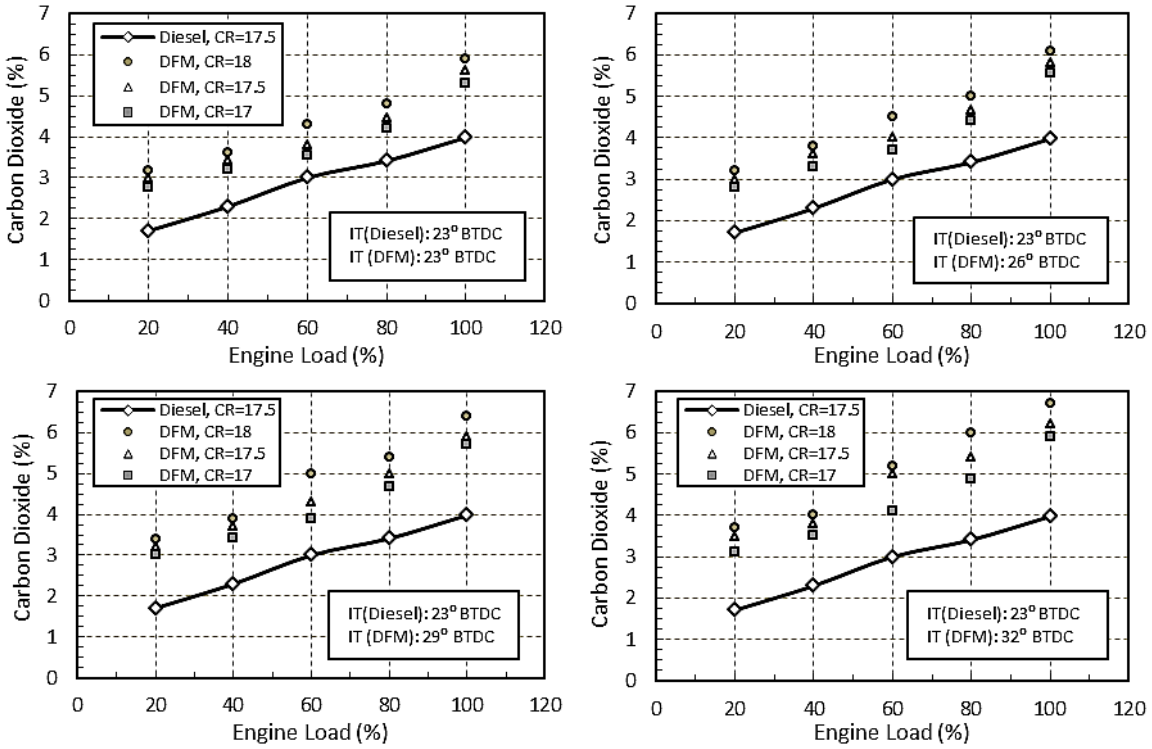

Fig. 6.9 Variation of carbon dioxide with load, CR and IT

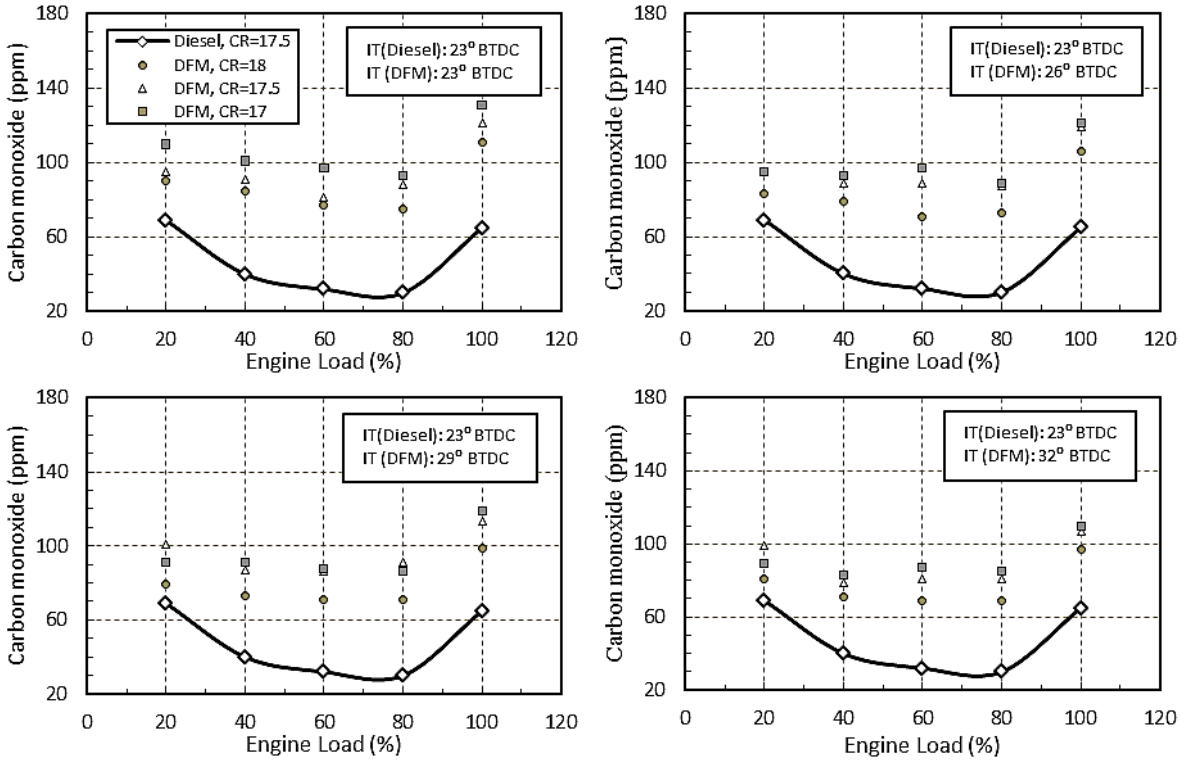

Fig. 6.10 Variation of carbon monoxide with load, CR and IT

In this analysis, the lower flame velocity of biogas leads to the formation of HC more under DFM in comparison to diesel mode as observed in Fig. 6.11. Therefore, on an average, there is a reduction of HC emission by 17.67% is achieved on increasing the CR from 17 to 18 at 23° BTDC. The explanation for these findings is similar to that of CO emission. In this study, the NO_X emission in the diesel mode is much higher in comparison to DFM as depicted in Fig. 6.12. This is because the formation of NO_X depends on the temperature of the combustion chamber. The rise in combustion chamber temperature is much more in case of diesel as compared to biogas due to high calorific value of diesel. Moreover, the presence of inert CO_2 in biogas results in lowering the temperature of the combustion chamber. On an average, an increase of 42% in NO_X emission is resulted by increasing the CR from 17 to 18 at 23° BTDC under DFM. Similar trend of variation of HC and NO_X emission with the increase of CR was reported by Debnath *et al*. (2014b).

6.5.2 Effect of Injection Timing

It is found that advancing IT resulted in better combustion of biogas which caused an increase of CO_2 emission. Advancing IT caused created high combustion chamber temperature and this increased the chemical reaction speed as reported by Sayin *et al*. (2008). Therefore, on an average, there is an increase of 17.43% in CO_2 emission on advancing IT from 23° to 32° BTDC for CR of 18. For the same range of IT, on an average, there is an increase of 17.14% and 12.21% respectively in CO_2 emission for CR of 17.5 and 17. The CO emission decreases with advancement of IT. This resulted from the increase of CO oxidation mechanism which is due to the increased time interval during the expansion stroke for which high temperature persists in the cylinder. This along resulted in more complete oxidation of CO. On an average, there is a reduction of 11.64% in CO emission on advancing IT from 23° to 32° BTDC for CR of 18. For the same range of IT, on an average, there is a reduction of 6% and 3.38% respectively in CO emission for CR of 17.5 and 17. Advancing the IT causes earlier start of combustion relative to the TDC. This results in a relatively higher combustion chamber temperature as the charge being compressed as the piston moves to the TDC and lowers the HC emissions. On an average, there is a reduction of 15.24% in HC emission is achieved on advancing IT from 23° to 32° BTDC for CR of 18 under DFM. For the same range of IT, on an average, there is a reduction of 13.14% and 14.27% respectively in HC emission for CRs of 17.5 and 17. Similar trend of CO and HC emissions with variation of IT was reported by Sayin *et al*. (2009).

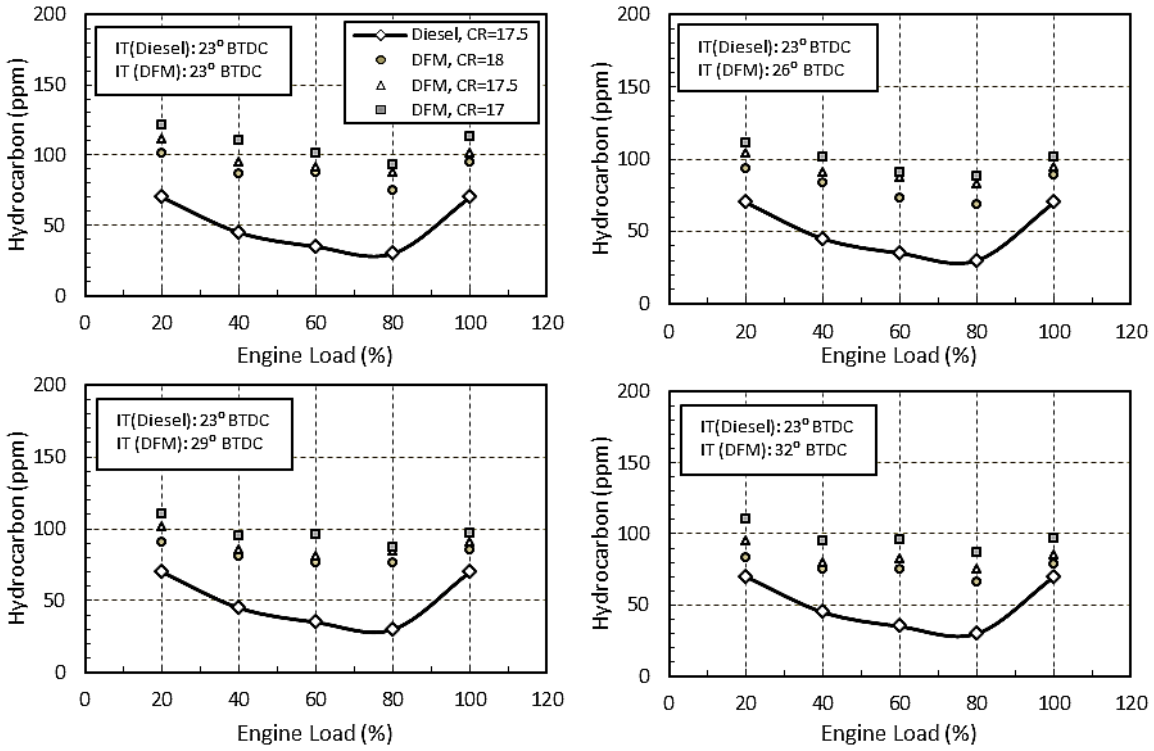

Fig. 6.11 Variation of hydrocarbon emission with load, CR and IT

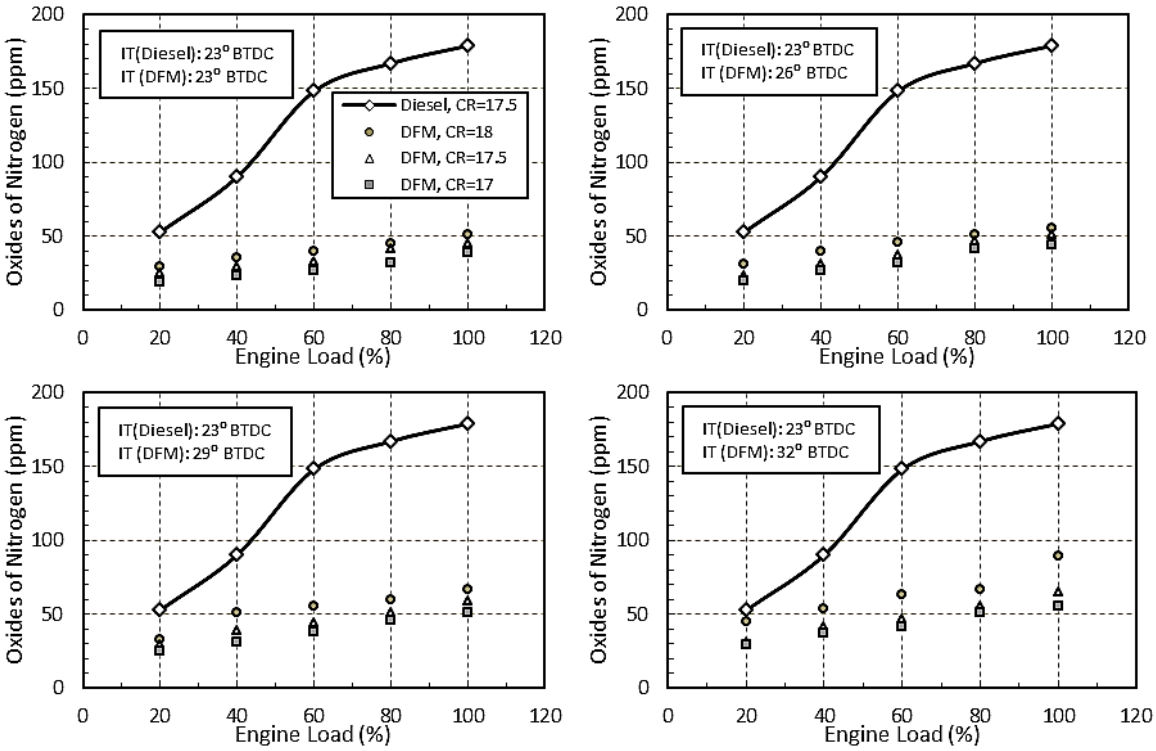

Fig. 6.12 Variation of oxides of nitrogen emission with load, CR and IT

The combustion chamber temperature increased with the advancement of IT due to better combustion of biogas. This resulted in higher emission of NOx. On an average, there is an increase of 39% in emission is achieved on advancing IT from 23° to 32° BTDC for CR of 18

under DFM. For the same range of IT, on an average, there is an increase of 41.42% and 52.14% respectively in NO_X emission for CR of 17.5 and 17. This goes well with the findings of Ganapathy *et al*. (2011).

6.6 Summary

- The BTE of the RBB-biogas run dual engine is found to be increase with the use of high CR of 18. The performance improves further with the advancement of pilot fuel IT. The maximum BTE of 25.88% is obtained for a combination of CR=18 and IT=32° BTDC.

- The BSEC is found to be decrease with the use of high CR of 18. Conversely, with the advancement of pilot fuel IT, the BSEC drops up to a particular IT. The maximum drop in BSEC of 19.29% is obtained for a combination of CR=18 and IT=32° BTDC.

- The use of high CR and advancement of IT results in a drop of EGT. The maximum drop of EGT is obtained for the combination of CR=18 and IT=32° BTDC.

- There is an average reduction in BFR by 8.36% for increasing the CR from 17 to 18. On advancing IT from 23° to 32° BTDC for CR of 18, there is a reduction of BFR by 20.09%. For the same range of IT, there is a drop of 19.07% and 11.27% in BFR at CRs of 17.5 and 17, respectively.

- At 23° BTDC with 100% load, the LFR is found to be 80%, 79% and 78.26% for CRs of 18, 17.5 and 17, respectively. For the same loading conditions at CRs of 18, 17.5 and 17, the LFR is found to be 80%, 80% and 80.25% at 26° BTDC in comparison to 80.51%, 80.51% and 77.71% at 29° BTDC. However, the LFR is found to be 82.75%, 72.51% and 71% for CRs of 18, 17.5 and 17, respectively at 32° BTDC.

- The average fall in ID with the rise of CR from 17 to 17.5 and 17.5 to 18 are 3.7% and 4.4%, respectively. The advancement of IT by 3°, 6° and 9° resulted in an average rise of IDs by about 14.42%, 13.88% and 14.15% for CR of 18, 17.5 and 17, respectively.

- The maximum NHRR and the PCP increases with use of high CR and advancement of IT of pilot fuel. The maximum NHRR and the PCP is attained for a combination of CR=18 and IT=32° BTDC.

- There is an average rise in CO_2 emission by 13.78% on increasing the CR from 17 to 18 at 23° BTDC. Therefore, there is a rise of 17.43% in CO_2 emission on advancing IT from 23° to 32° BTDC for CR of 18. For the same range of IT, on an average, there is an increase of 17.14% and 12.21% in CO_2 emission for CR of 17.5 and 17, respectively.

- There is an average drop in CO emission by 17.67% on increasing the CR from 17 to 18 at 23° BTDC. There is a reduction of 11.64% in CO emission on advancing IT from 23° to 32° BTDC for CR of 18. For the same range of IT, on an average, there is a reduction of 6% and 3.38% in CO emission for CR of 17.5 and 17, respectively.

- There is an average reduction in HC emission by 17.67% on increasing the CR from 17 to 18 at 23° BTDC. On an average, there is a reduction of 15.24% in HC emission is achieved on advancing IT from 23° to 32° BTDC for CR of 18 under DFM. For the same range of IT, on an average, there is a reduction of 13.14% and 14.27% in HC emission for CRs of 17.5 and 17, respectively.

- There is an average increase in NO_X emission by 42% on increasing the CR from 17 to 18 at 23° BTDC. There is an increase of 39% in emission is achieved on advancing IT from 23° to 32° BTDC for CR of 18 under DFM. For the same range of IT, there is a rise of 41.42% and 52.14% in NO_X emission for CR of 17.5 and 17, respectively.

Based on the above findings, it can be concluded that the optimum combination for a biogas run dual fuel diesel engine using rice bran biodiesel as pilot fuel is found to be CR=18 and IT=32° BTDC.

Chapter-7

Characterisation of Emulsified Rice Bran Biodiesel

Overview:

Emulsification is one of the proven techniques to control the pollutants of the diesel engines. Most studies on emulsions are conducted in diesel engines under lone mode only. The effect of use of emulsified biodiesel as a pilot fuel for dual diesel engine, particularly for biogas, is not known. This may lower the ignition delay of pilot fuel due to the occurrence of phenomenon called 'microexplosion', which may expedite the entire combustion process. Alongside, proper adjustment of operating parameter may enhance the performance and emission characteristic of a biogas run dual diesel engine using emulsified fuel as pilot fuel. With the intention to realize this fact in the work, the emulsion of water in biodiesel (rice bran biodiesel) has been explored in a modified variable compression ratio biogas run dual fuel diesel engine. In this chapter, the preparations of water emulsions of rice bran biodiesel (WIRBB) with various specifications are discussed elaborately.

Chapter Outline:

7.1 Emulsified Fuel

A growing interest in the potential of utilizing emulsified fuel, in various combustion systems, has been evident throughout the last two decades. The desire to improve the combustion efficiency with simultaneous reduction in smoke and soot particles and the oxides of nitrogen emitted from diesel engines and gas turbines has been the main driving force. The study on biodiesel emulsion is very limited in open literature. Keeping this vista in mind, the central idea of this investigation is to explore the emulsification characteristics and fuel properties of water in rice bran biodiesel (WIRBB) emulsions prepared by ultrasonic wave to be used as a pilot fuel for a biogas run dual fuel diesel engine. An emulsion that will be used as an engine fuel should have the water dispersed evenly and stable for suitable time. However, before going deep into subject, it is essential to get acquainted with some terms associated with characterization of emulsion. The terms include continuous phase (Lin and Wang, 2004), dispersed phase (Lin and Chen, 2006), surfactant (Becher, 1965), Hydro lipophilic balance (Guo *et al.*, 2006), ratio of emulsifying fluids (Abu-Ziad, 2004) and stability (Lin and Wang, 2003) which are discussed in the upcoming section of this chapter.

7.2 Characterisation of Emulsification

The emulsion prepared for this study is a two-phase water in rice bran biodiesel emulsion. It is prepared by intruding a phase called the dispersed phase into another phase called the continuous phase. The continuous phase is having the greater volume. In this particular case, rice bran biodiesel (RBB) will be the continuous phase and the water will be the dispersed phase as the application of the prepared emulsion is as an alternative fuel for diesel engine.

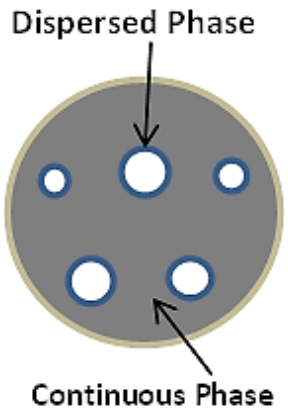

Fig. 7.1 The physical structure of two phase of water in oil emulsion (Lin and Chen, 2006)

7.2.1 Surfactant and Hydrophilic Lipophilic Balance

The surfactant reduces the surface tension between two immiscible liquids i.e. water and oil, maximizing their superficial contact area, and activating their surfaces. The measurement of this activation force is determined by a parameter called hydrophilic lipophilic balance (HLB). HLB can be defined as the measure of the degree to which a liquid molecule is hydrophilic or lipophilic. Lipophilic molecule dissolves in fats, oils, lipids and non-polar solvents, whereas hydrophilic molecules are those, which interact with or dissolved by water and other polar substances. Griffin (1949) defined HLB by following mathematical expression,

$$HLB = 20 \times (M_h/M) \qquad \text{Eq. (7.1)}$$

where, M_h and M are the molecular weights of hydrophilic molecules and the whole molecule, respectively.

Based on Eq. (7.1), Griffin formulated a 'scale' of HLB, ranging from '0' to '20' (non-dimensional value). The HLB number of all the hydrophilic, lipophilic surfactants or combination of both, are measured within this range. In the water in oil emulsion, the HLB number should lie within 4–6, whereas for oil in water emulsion it is 8–18. The HLB for emulsion having both types of surfactants is calculated by:

$$HLB = (H_L \times W_L + H_H \times W_H)/(W_L + W_H) \qquad \text{Eq. (7.2)}$$

where, HLB is the hydrophilic lipophilic balance of the total emulsion prepared. H_L and H_H are the HLB and W_L and W_H are the weights of the lipophilic and hydrophilic surfactants respectively.

To observe the effect of variation of HLB, its range is fixed from 4.3 to 6 as described for lipophilic dominating emulsion (Debnath *et al.*, 2014b). The surfactants selected for the emulsification of RBB with water are the commonly used sorbitan monoleate (SPAN 80) and polyoxyethylene sorbitan monoleate (TWEEN 80). However, to prepare emulsion of HLB 4.3, only SPAN 80 is used. The quantity of surfactant is maintained at 3% of the total solution. The specifications of the surfactants and the detailed matrix of the emulsion samples is included in Tables 7.1 and 7.2, respectively.

Table 7.1 Specifications of the surfactants

Type	HLB	Specific gravity
Sorbitan monoleate (SPAN 80)	4.3	0.98
Polyoxyethylene sorbitan monoleate (TWEEN 80)	15	1.08

Table 7.2 Matrix for emulsion composition for 1000 ml

HLB	4.3	5	6	4.3	5	6
Water quantity	5%			10%		
RBB (ml)	920	920	920	870	870	870
Water (ml)	50	50	50	100	100	100
TWEEN 80 (g)	0	2.2	5.1	0	2.2	5.1
SPAN 80 (g)	29.4	27.5	24.7	29.4	27.5	24.7

7.2.2 Ratio of Emulsifying Fluids

The ratio of emulsifying fluids plays an important role in the stabilization of the emulsion. The proper dispersion of the water in RBB, the diameters of the dispersed water bubbles and separation depends on the quantity of water used for emulsification. In the present study, the volumetric quantity of water is taken on 5% and 10% based on a previous investigation (Debnath *et al*., 2014b).

7.3 Preparation of Water in Rice Bran Biodiesel Emulsion and Stability Study

7.3.1 Ultra Bath Sonication Machine

The ultrasonic vibration technique is deemed an excellent choice for effectively preparing tiny particles in a solution at a high speed. The ultrasonic vibration technique is widely applied in medical sciences, biochemistry and pharmaceutical industries. Strong physical and chemical reactions can be created when applying violent ultrasonic waves at a rather high frequency. It produces a huge amount of tiny air bubbles with the result that the surrounding liquid becomes well stirred. A phenomenon called cavitation takes place when a continuous production and consequent collapse of the air bubbles occurs. Positive and negative pressure waves can be formed alternatively by the motion of the ultrasonic wave. When the

corresponding hydrostatic pressure of the surrounding liquid is lower than the pressure produced by the ultrasonic wave, the particles of the liquid will be twisted and hollowed out, resulting in the formation of cavities. Much energy is released through this process, which is transferred to the liquid solution thereby producing a strong mechanical stirring effect. An emulsification of two immiscible liquids can thus be made more homogeneously and create a more effective emulsification (Lin and Chen, 2006). The brief specification of the ultrasonic bath sonication machine used in this work is given in Table 7.3.

Table 7.3 Specification of the ultrasonic bath sonication machine (Buehler, 1993)

Parameter	Specification
Power Capacity (W)	80
Operating voltage (V)	115
Operating frequency (Hz)	60
Tank dimension (cm^3)	12.7×12.7×7.6
Transducer tank material	Stainless Steel

7.3.2 Emulsion Preparation Procedure

In this study, an ultrasonic emulsification method is used to prepare the two-phase WIRBB emulsion. To prepare WIRBB of HLB 4.3, only lipophilic surfactant is used. The quantities of surfactants are measured by using Eq. (7.2). RBB is initially mixed with surfactant (SPAN 80) with the aid of a magnetic stirrer. The RBB surfactant mixture is then placed in an ultrasonic bath and sonication is done. Thereafter, the surfactant (TWEEN 80) mixed distilled water is gently added into the RBB surfactant mixture and sonicated for three hours. The samples are checked at 15, 30, 60, 90, 120, 150, and 180 min intervals to ensure proper mixing and detect minor deposition. A similar method is followed for other HLBs, surfactant, and 10% volume of water.

7.3.3 Measurement of Mean Droplet Diameter

The mean droplet diameter of the dispersed phase of the emulsion in the continuous phases is photographed and measured by an optical electron microscope named Axioscope equipped with software called Axiovision 4.2. The microscope has a magnification of 50X. After each 15, 30, 60, 90, 120, 150 and 180 min, the droplets of emulsion prepared are taken on micro

slides, observed and analysed under the microscope accordingly. The mean droplet diameter measured for total six samples are shown in Fig. 7.2. The variation of the mean droplet diameters for each HLB of 4.3, 5 and 6 of each 5% and 10% water content with emulsification time is given in Figs. 7.3(a) and 7.3(b). This analysis highlights the fact that the lower mean droplet diameter of the emulsion can be achieved with longer emulsification time. In all the figures, the maximum to minimum range of the mean droplet diameter lies within 5–1μm. This is in good agreement for the criteria set by Becher (1965) for micro emulsions. Fig. 7.3(c) shows a comparison of mean droplet diameter of different composition of emulsions. The value of the minimum mean droplet diameter is obtained for HLB 6 and 5% water is 1.64 μm. The study of mean droplet diameter disclosed an important fact that the emulsion having high HLB value with less water quantity and prepared by dual surfactant has the lowest mean droplet diameter. The reason for HLB 6 and 5% water having lower than the WIRBB produced with same HLB with 10% water is that with higher water quantity encapsulated inside biodiesel. This increases the chance of cohesion of water droplets scattered throughout the solution. As a result, the cohesive forces among the water droplets are forced to come closer, and form bigger droplets. Therefore, the presence of the proper surfactant combination and right emulsification method can shrink the mean droplet diameter.

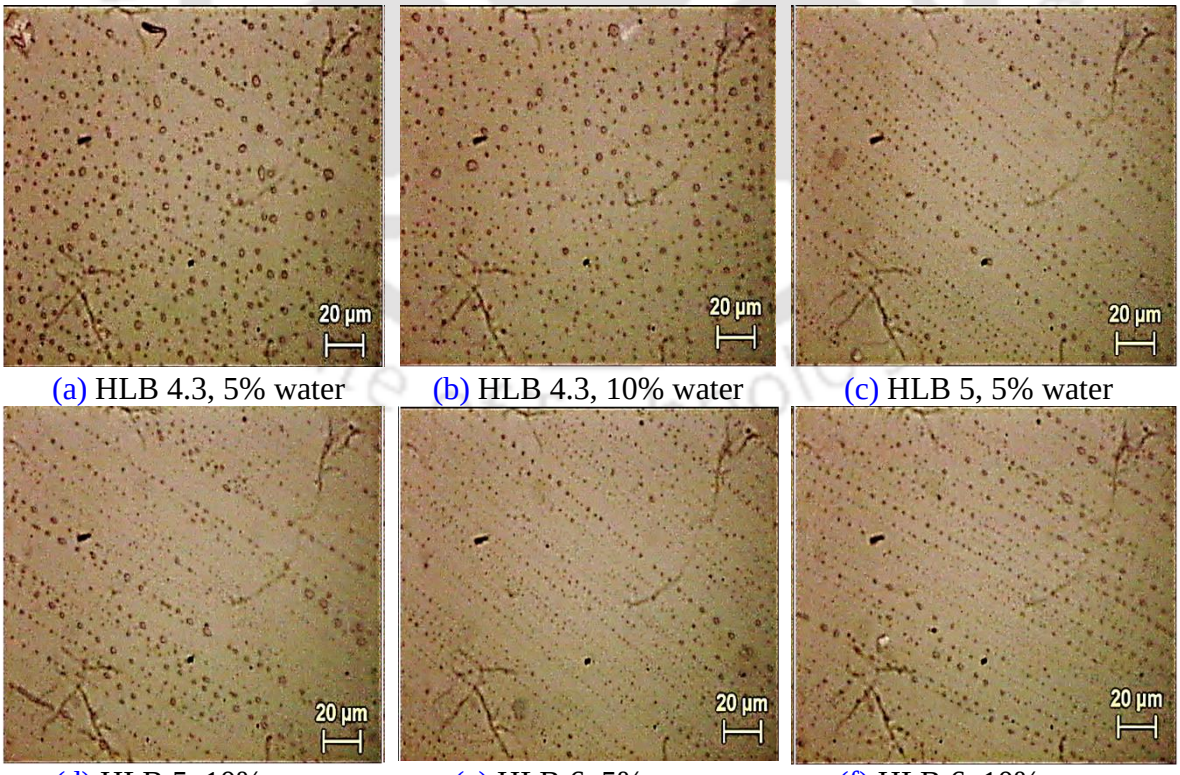

(a) HLB 4.3, 5% water (b) HLB 4.3, 10% water (c) HLB 5, 5% water

(d) HLB 5, 10% water (e) HLB 6, 5% water (f) HLB 6, 10% water

Fig. 7.2 Images of droplet for different compositions of WIRBB emulsion

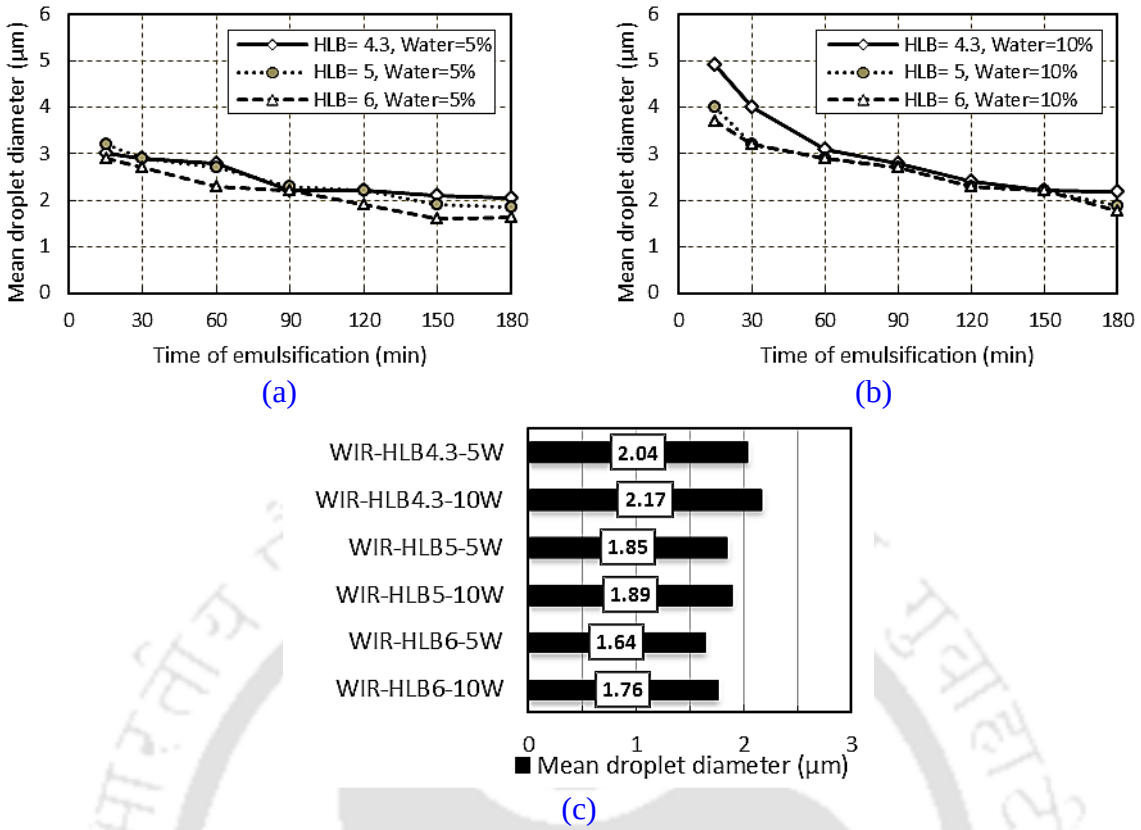

Fig. 7.3 Assessment of mean droplet diameter for different compositions of WIRBB emulsion

7.3.4 Stability Analysis

In this study, the emulsion stabilities of the two-phase WIRBB samples are found based on the percentage of separation of the emulsion as depicted in Fig. 7.4. The stability of the emulsion is checked by keeping the solutions motionless in measuring test tubes for three hours. The volumetric deposition of WIRBB sediment layer and water from an unaffected emulsion layer is recorded after 1 h interval. For HLB 4.3 and 5% WIRBB emulsion, the separation plus fully separated water quantity is less than 3.8% of the total volume, whereas it is around 5.2% for 10% WIRBB emulsion. The tendency of water to agglomerate rises with the increase in percentage of water in emulsion. For HLB 5 and 6, the agglomeration and separation is lesser in comparison to HLB 4.3. The stability analysis revealed that the WIRBB prepared with both hydrophilic and lipophilic surfactant has a better stability than only lipophilic surfactant. The emulsion having composition of 5% WIRBB with 3% surfactant of 6 HLB is found to be the most stable sample prepared. Hence, 5% WIRBB with 3% surfactant of 6 HLB is considered for the experimental engine. Prior to the conduct of experiments, the petroleum property 5% WIRBB with 3% surfactant of 6 HLB is carried out as shown in Table 7.4.

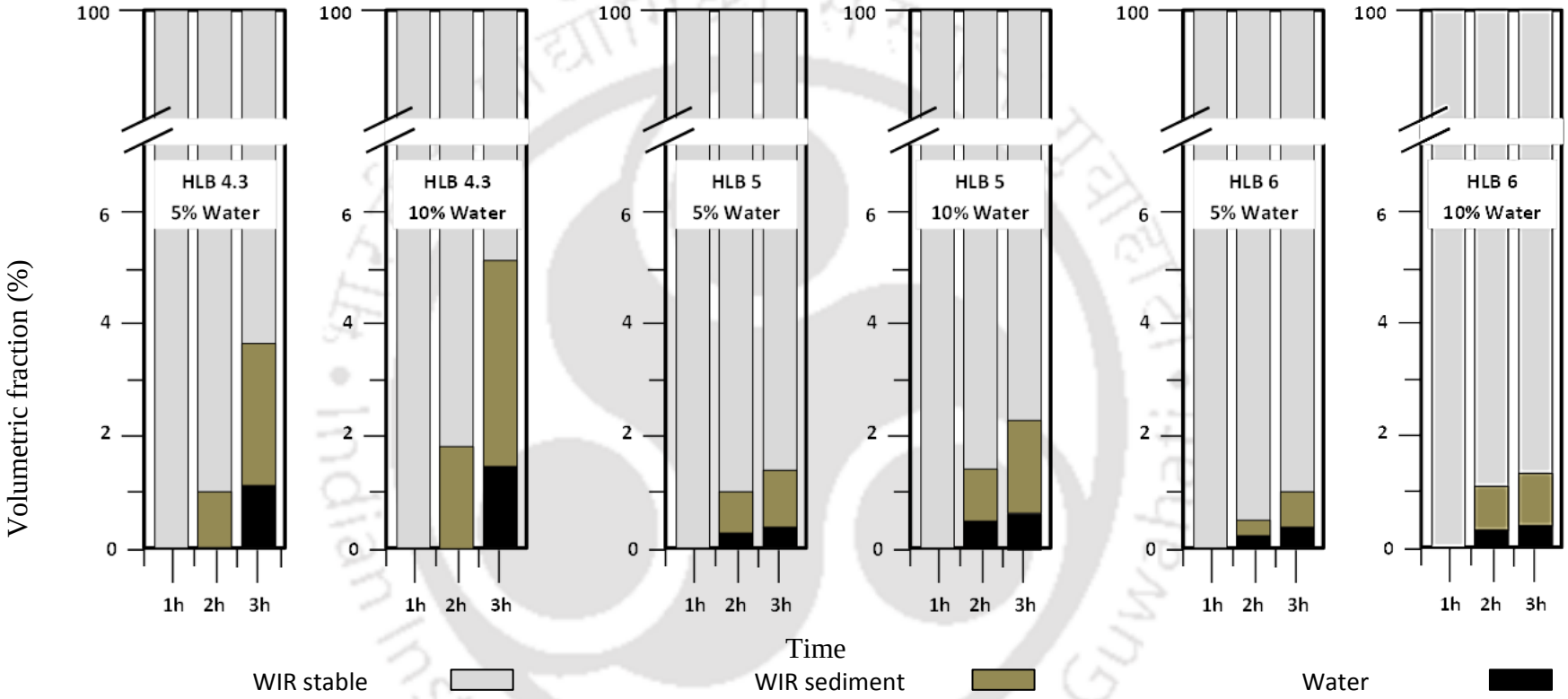

Fig. 7.4 Variation of stability with time for different compositions of WIRBB emulsion

Table 7.4 Fuel Properties

Properties	Diesel	RBB	5% WIRBB	Biogas
Chemical Composition	$C_{12}H_{26}$	$C_{18.05}H_{34.9}O_2$*	5% H_2O, 2.48% SPAN, 0.52% TWEEN, 92% $C_{18.05}H_{34.9}O_2$	60%CH_4, 40% CO_2 (volume)*
Density(kg/m^3)	840	880*	893*	0.91*
Lower calorific value (MJ/kg)	42	39.05*	38.33*	20.67*
Cetane number	45-55	56.3 (Giakoumis, 2013)	-	-
Auto-ignition Temperature (K)	553	-	-	1087 (Sahoo, 2011)
Flash point (K)	348	427*	-	-
Fire point (K)	358	442*	-	-
Stoichiometric air fuel ratio	14.92	12.48*	11.02*	10 (Sahoo, 2011)

*Calculated value

7.4 Summary

This chapter describes the preparation of WIRBB in the laboratory with two commercially available surfactants with their suitable HLB values. It is observed that longer the emulsification time, lower is the mean droplet diameter. It is also seen that the highest amount of surfactant with 5% water provides lower mean droplet diameter. The presence of hydrophilic surfactant, in double surfactant emulsions, lowers the separation, agglomeration and sedimentation rates than the single surfactant ones. Finally, the thermodynamic, physical and petroleum properties of the optimized sample are measured and tabulated.

Chapter-8

Results of Emulsified Rice Bran Biodiesel - Biogas Run Dual Fuel Engine

Overview:

Emulsions have long been considered as an alternative fuel for diesel engines in order to achieve better fuel economy and pollution reduction. This is basically due to occurrence of a physical phenomenon called 'micro-explosion'. Several studies have carried out on emulsified fuel in diesel engines under lone mode. However, limited research has been reported under dual fuel mode, particularly for biogas run dual fuel diesel engines. The present chapter attempts to unravel the effect of injection timing (IT) of pilot fuel and compression ratio (CR) for an emulsified rice bran biodiesel - biogas run dual fuel diesel engine.

Chapter Outline:

8.1 Emulsified Fuel

Research work on emulsified fuel have advanced significantly in the last two decades using different test fuels like fuel oil, diesel, soybean biodiesel, rapeseed biodiesel, and palm oil biodiesel. They can be of two-phase or three-phase based on the method of preparation which can be used in diesel engines in lone mode or dual fuel mode (DFM). In lone mode, Sjogren (1977) found from experiments that the role of water in the emulsion during the combustion process was not chemical but physical. It caused a secondary atomisation of the oil droplets which leads to the formation of smaller droplets in the combustion chamber. This resulted in faster and cleaner combustion without particulate emission. Greeves *et al.* (1977) observed from experiment that injecting water along with diesel reduced nitrous oxide (NO), hydrocarbon (HC) and smoke emission by 70%, 50% and 50%, respectively. Nazha and Crookes (1985) reported that 5% by volume of water in diesel emulsion was the optimum value for maximum reduction in soot concentration. Abu-Zaid (2004) found from experiment that the average increase in brake thermal efficiency (BTE) for 20% water diesel emulsion was approximately 3.5% over diesel mode. Lin and Wang (2004) experimentally found that using three–phase emulsion in diesel engine lowered the exhaust gas temperature (EGT) significantly. Ghojel *et al.* (2006) found that the use of emulsion resulted in a retarded injection timing along with reduction of oxides of nitrogen (NO_X) emission. Lin and Chen (2006) examined the engine performance and emission characteristics of a three-phase diesel emulsions prepared by an ultrasonic emulsification method. Their study indicated three–phase diesel emulsion produced a low NO emission, low soot formation and high brake specific fuel consumption (BSFC). Lin and Lin (2007) conducted experiments to study the engine performance and emission characteristics of a three-phase soybean biodiesel emulsions produced by peroxidation. The study indicated a low carbon dioxide (CO_2) and NO_X emission with a high fuel consumption rate for three-phase soybean biodiesel emulsions. Lin and Chen (2008) compared the fuel properties and emission characteristics of two and three-phase emulsions. The results indicated that the two phase emulsion produced lower BSFC and smoke opacity in comparison to three phase emulsion. Qi *et al.* (2010) demonstrated the use of ethanol-soybean biodiesel-water micro-emulsions for a direct injection, compression ignition engine. The engine tests indicated a long ignition delay, low brake specific energy consumption and a drastic reduction of smoke. Alahmer *et al.* (2010) experimentally found that diesel emulsion fuel emitted higher amount of CO_2 in comparison to neat diesel. Sadhik Basha and Anand (2010) investigated the combustion, performance and

emission characteristics of the neat diesel, water diesel emulsion and carbon nano tubes (CNT) blended water diesel emulsion for the constant speed diesel engine. The study indicated at the full load, the BTE for the neat diesel, water diesel emulsion and CNT blended water diesel emulsion were found to be 28%, 25.7% and 25.1%, respectively. The effect of diesel, biodiesel and biodiesel-diesel-ethanol (diestrol) water micro emulsion fuels on performance, emission and combustion characteristics of a diesel engine were investigated by Kannan and Anand (2011). The results indicated that biodiesel and micro emulsion fuels had a higher BSFC than diesel. However, the emission characteristics like carbon monoxide (CO), CO_2, HC, NO and smoke for biodiesel and micro emulsion fuels were lower than diesel fuel at all load conditions. Lei *et al.* (2012) developed a novel emulsifier to improve the physical stability of the emulsion for a wide range of temperature. The engine test with the emulsifier and ethanol diesel blend resulted in improvement in BTE and reduction of NO_X emission. Alahmer (2013) investigated the influence of using emulsified diesel fuel on the performance and pollutants of a diesel engine. The results indicated that the maximum value of torque and brake power produced by engine was obtained at 5% water emulsion. Further, the NO_X emission was found to decrease with the increase of water content in the emulsion. Zhang *et al.* (2013) found that the use of emulsified fuel along with oxygen rich air greatly reduced the NO_X and smoke emission without any serious penalty in BSFC. Debnath *et al.* (2014b) adjusted the operating parameters of an emulsified palm biodiesel run diesel engine. The test revealed that the combination of compression ratio (CR) of 18 and injection timing (IT) of 20° BTDC produced an overall 11% higher BTE for emulsified palm biodiesel in comparison to diesel mode. Chen *et al.* (2015) examined the performance and emissions of diesel engines by a novel emulsified diesel fuel. The results indicated that the BTEs of emulsified diesel and pure diesel were comparable at 75% and 100% load. On the part of emission, CO and soot reduced significantly with the use of the emulsified diesel in comparison to neat diesel.

There has a limited amount of investigation done in dual fuel engines using emulsified fuel. The emulsified fuels investigated under DFM include rapeseed biodiesel (Namasivayam *et al.*, 2010; Korakianitis *et al.*, 2010) and waste cooking oil (Kumar and Jaikumar, 2014). Namasivayam *et al.* (2010) studied the application of emulsified rapeseed biodiesel as a pilot fuel for natural gas run dual fuel diesel engine. The emulsified pilot fuels produced similar BTE as neat biodiesel. On the part of emissions, emulsified biodiesel did not perform well with the rise in CO and HC emission. Korakianitis *et al.* (2010) conducted experiments on a

hydrogen run dual fuel diesel engine using emulsified rapeseed biodiesel as pilot fuel. The study indicated that the emulsified pilot fuel resulted in an increase of BTE at high speed and low NOx at low speed as compared to neat biodiesel. Kumar and Jaikumar (2014) investigated the effect of hydrogen induction on performance, emission and combustion behaviour of a dual fuel engine using emulsified waste cooking oil as pilot fuel. The results showed that the use of emulsified pilot fuel along with hydrogen addition under dual fuel mode resulted in a BTE similar diesel mode at high loads. The literature survey on emulsified fuel highlights three major findings. Firstly, most studies were done in lone mode using diesel fuel. Secondly, there has been a limited research on the use of biodiesel as emulsified fuel. Finally, the effect of using emulsified biodiesel as pilot fuel for biogas run dual fuel diesel engine is not known. Keeping this view in mind, the prime objective of this investigation is to enhance the performance and emission characteristics for an emulsified biodiesel–biogas run dual fuel diesel through suitable adjustment of injection timing and compression ratio. The pilot fuel considered for this study is a two-phase stable emulsion of water in rice bran biodiesel (WIRBB). The preparation and characterisation of WIRBB has been discussed in Chapter 7.

8.2 Experimental Design

The experimental matrix consists of twelve combinations of CRs 17, 17.5, and 18; and ITs of 23º, 26º, 29° and 32º BTDCs at different loading conditions as indicated in Table 8.1. The standard diesel specification is CR=17.5 and IT=23º BTDC and used as a baseline for comparison with the findings with WIRBB-biogas dual fuel diesel run engine. The experiments are conducted at a constant speed of 1500±50 rpm. The method of experimentation is followed in the similar manner as discussed in section 3.4.

Table 8.1 Experimental Matrix of the WIRBB-Biogas Run Dual Fuel Diesel Engine

Mode	Fuel used	CR	IT (BTDC)	Loading conditions (%)
Diesel	100% Diesel	17.5	23°	20, 40, 60, 80, 100
Dual Fuel Mode	Pilot Fuel: WIRBB Primary Fuel: Biogas	18, 17.5, 17	23°, 26°, 29°, 32°	

8.3 Performance Analysis

The performance analyses include brake thermal efficiency (BTE), brake specific energy consumption (BSEC), exhaust gas temperature (EGT), biogas flow rate (BFR) and liquid fuel replacement (LFR). The combustion analyses include ignition delay (ID), peak cylinder pressure (PCP) and net heat release rate (NHRR). Finally, emission analysis is performed by measuring carbon dioxide (CO_2), carbon monoxide (CO), hydrocarbon (HC) and oxides of nitrogen (NO_X). The theoretical equations used for performance and combustion analysis are given in Appendix-A. In this investigation, the EGT, BFR, ID, PCP and emission characteristics analysis are carried out on average basis for considering the effect of all loading conditions. The CR variations are made for WIRBB-biogas run dual fuel diesel engine for a constant IT. Therefore, the plots of each performance parameter for constant ITs are group together with diesel mode for comparison. The results are discussed with respect to the two design and performance parameters, namely, CR and IT.

8.3.1 Effect of compression ratio

The BTE under DFM is found to be lower in comparison to diesel mode due to lower calorific values of both biogas and WIRBB as depicted in Fig. 8.1. In addition, the other factors like biogas residual, combusted residual gases, low combustion temperature and low flame propagation speed, higher total fuel flow rate during combustion and increased negative compression work caused by induction of large biogas air mixture are contributing to the low thermal efficiency. With 100% load, at 23° BTDC, the BTEs under DFM are found to be 19.84%, 18.07% and 17.4% for CRs of 18, 17.5 and 17, respectively as compared to 27.76% for diesel mode. The BTE under DFM improves for high CR. This is due to the fact that the temperature and the pressure rise with the increase in CR. This resulted in occurrence of fast microexplosion, which initiates the earlier ignition of pilot fuel by appropriate mixing of air and pilot fuel, thereby giving sufficient time for the combustion of biogas. This increases the probability of a better combustion of biogas. The BSEC during diesel mode is found to be lower than DFM (Fig. 8.2). On an average, the BSEC reduces by 11.01% as CR increased from 17 to 18. The EGT for all cases of DFM is found to be higher than diesel mode (Fig. 8.3). This is owing to late combustion of biogas which reduces the duration of extraction of power. As a result, the combustion products in the form of gases come out at a higher temperature. Further, it seems that the cooling effect of microexplosion produced by the emulsified pilot fuel has a marginal effect on the rise of EGT in comparison to late

combustion of raw biogas as engine mainly run on biogas under DFM. At 23° BTDC, there is an increase of 7.23%, 12.26% and 14.78% of EGT at CRs of 18, 17.5 and 17, respectively as compared to diesel mode. The burning velocity of the biogas air mixture increases with the increase of CR.

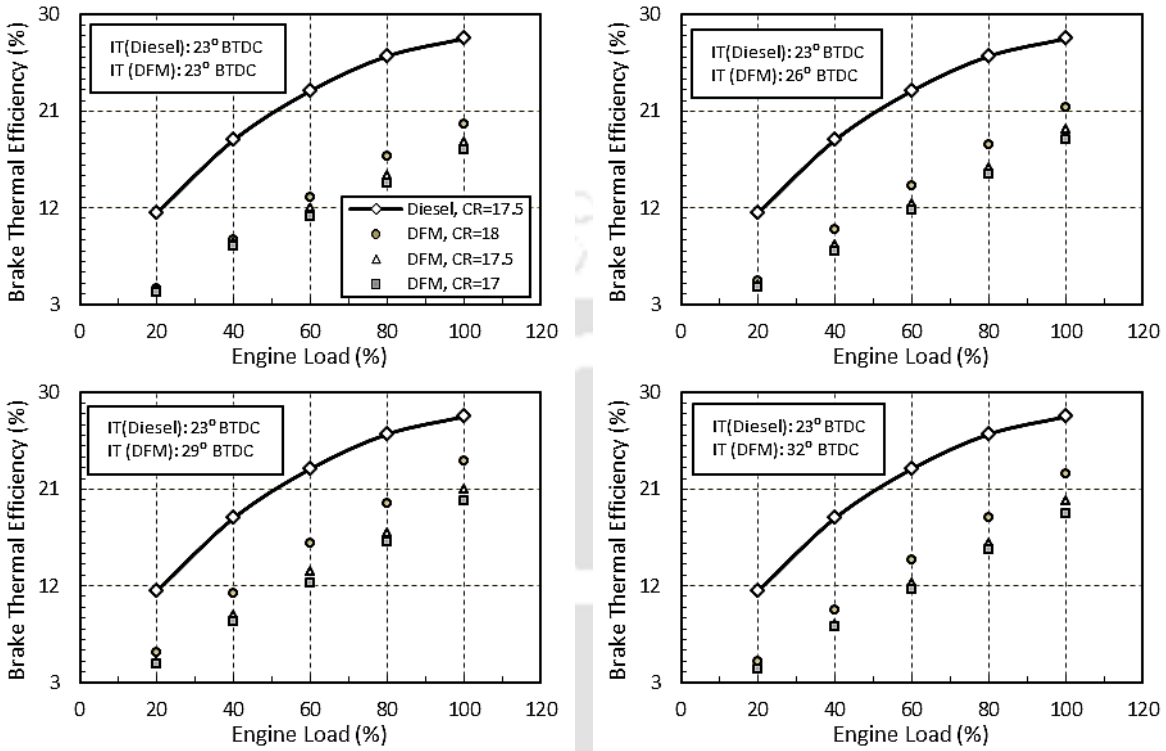

Fig. 8.1 Variation of BTE with load, CR and IT

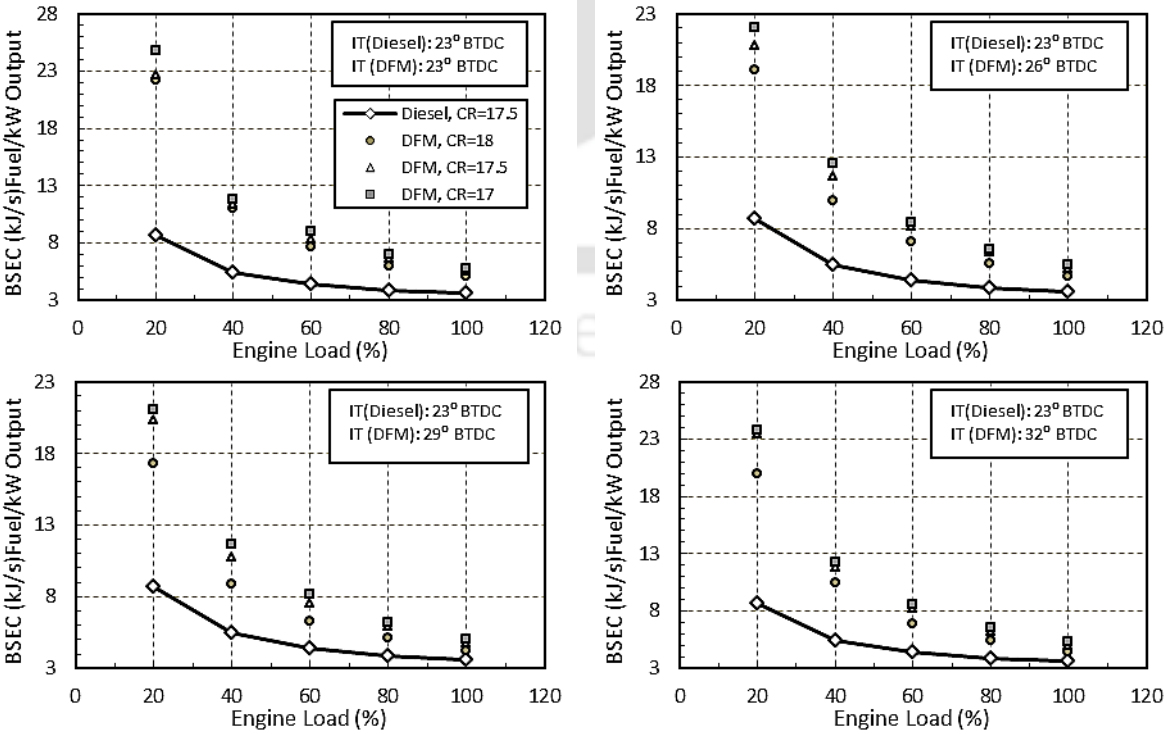

Fig. 8.2 Variation of BSEC with load, CR and IT

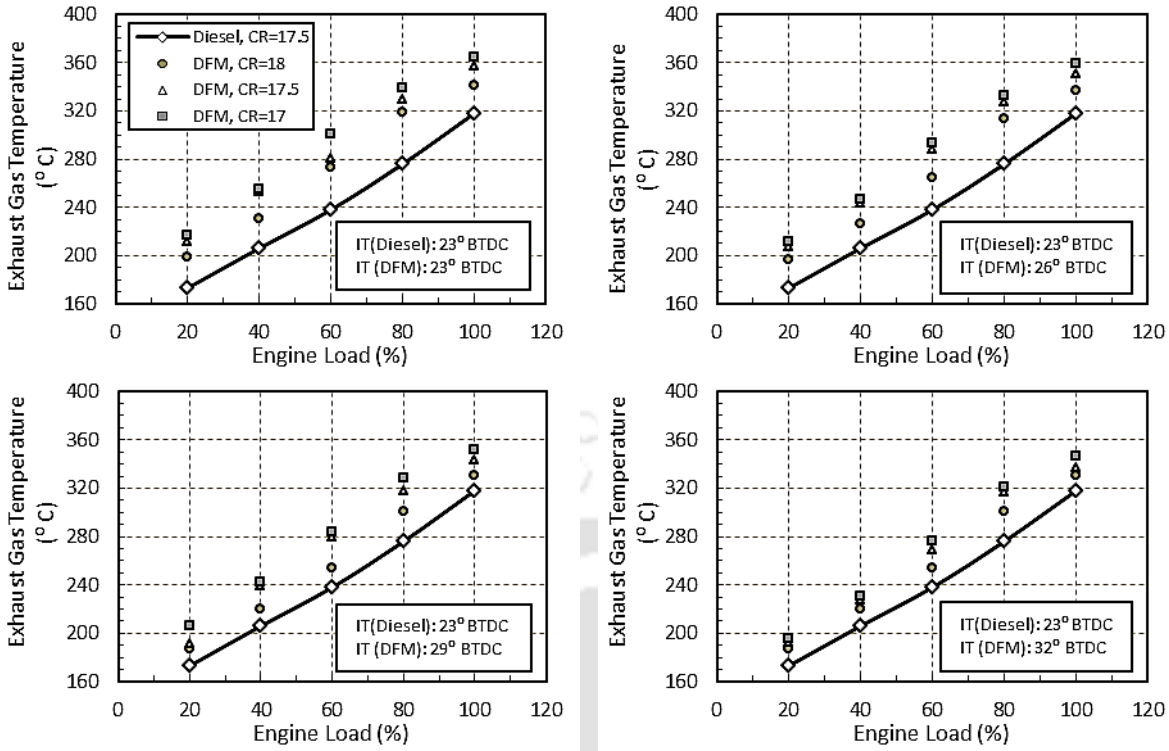

Fig. 8.3 Variation of EGT with load, CR and IT

Therefore, the time required for the complete combustion shortens and this produces lower EGT. This means, combustion of biogas starts early in case of high CR. With 100% load, at 23° BTDC, the BFR is found to be 2.67 kg/h, 2.95 kg/h and 3.06 kg/h for CRs of 18, 17.5 and 17, respectively as indicated in Fig. 8.4. Thus, the BFR decreases at high CR at same loading condition. At 23° BTDC, there is a reduction of 15.84% in BFR by increasing the CR from 17 to 18 at 23° BTDC. With 100% load, at 23° BTDC, the liquid fuel replacement (LFR) is found to be 79.25%, 77.77% and 76.79% for CRs of 18, 17.5 and 17, respectively as depicted in Fig. 8.4. Thus, the LFR increases marginally for high CR. Analogous trend of rise of BTE and drop of EGT with increase of CR for different test fuels was reported earlier (Raheman and Ghadge, 2008; Jindal *et al*., 2010).

8.3.2 Effect of Injection Timing

For CRs of 18, 17.5 and 17, with 100% load, the BTEs are found to be 21.36%, 19.29% and 18.35% at 26° BTDC in comparison to 23.62%, 20.97% and 19.89 % at 29° BTDC. However, at 32° BTDC, the BTEs are found to be 22.36%, 19.91% and 18.27% for CRs of 18, 17.5 and 17, respectively. From the above investigation, it is quite evident that the BTE of the biogas run dual fuel diesel engine for this particular study improves with the advancement of pilot fuel IT upto IT of 29° BTDC. The advancement of IT results in injection of WIRBB

earlier into the combustion chamber than its standard IT, thereby giving ample time for the WIRBB to form a homogeneous mixture with air and biogas. This results in more efficient burning of biogas air mixture. For CRs of 18, 17.5 and 17, the BSEC drops by 10.55%, 4.57%˚C, and 5.77%, respectively at 26° BTDC in comparison to 19.66%, 9.56% and 10.9% at 29° BTDC. Further advancement of IT to 32° BTDC lowers the BSEC to 9.05%, 4.21% and 3.42% for CRs of 18, 17.5 and 17, respectively. On an average, for CRs of 18, 17.5 and 17, the EGT rises by 5.97%, 10.37% and 12.89% at 26° BTDC in comparison to 4.08%, 7.86% and 10.69% at 29° BTDC. However, at 32° BTDC, the EGT is increases by 2.83%, 5.97% and 9.11% for CRs of 18, 17.5 and 17 respectively. Thus, the EGT under DFM drops with the advancement of IT. Researcher (Raheman and Ghadge, 2008, Debnath *et al*., 2014b) observed similar trend of EGT with the advancement of IT for different test fuels.

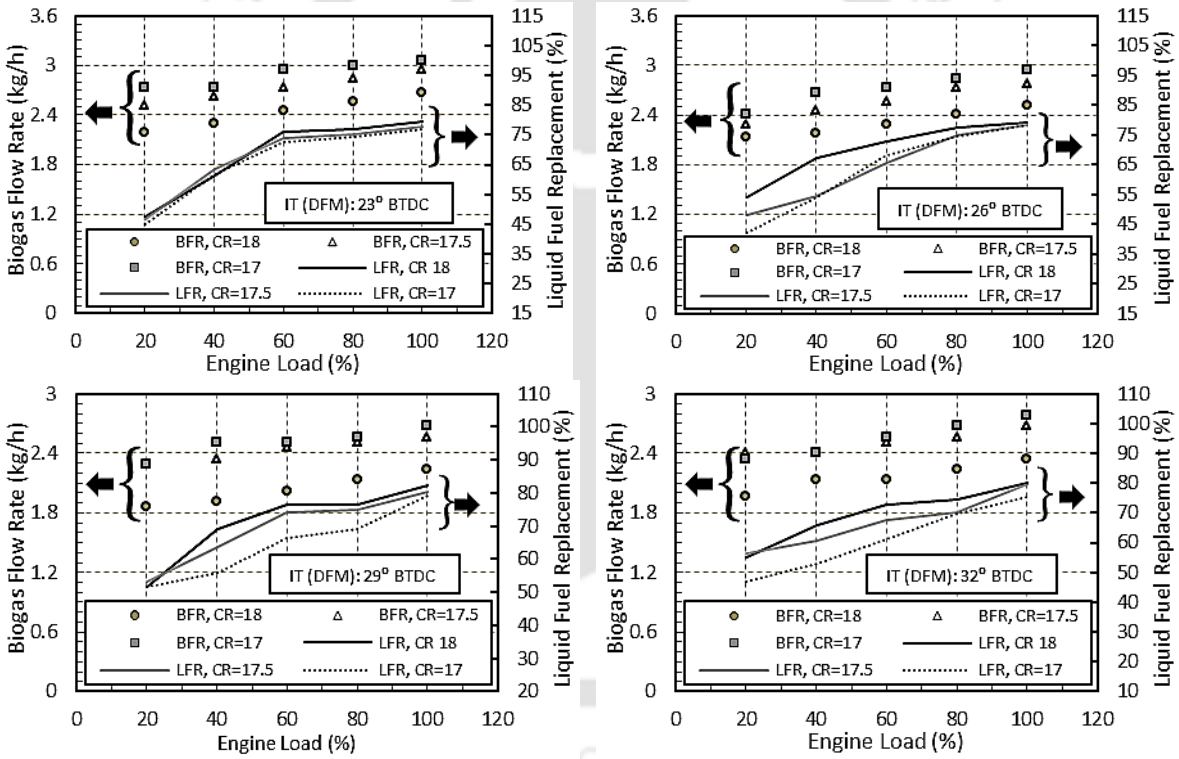

Fig. 8.4 Variation of BFR and LFR with load, CR and IT

On advancing IT from 23° to 32° BTDC for CR of 18, there is a reduction of 11.21% in BFR. `For the same range of IT, there is a drop of 8% and 11.7%, respectively in BFR at CRs of 17.5 and 17. For CRs of 18, 17.5 and 17 with 100% load, the LFR is found to be 79.47%, 78.27% and 78.21% at 26° BTDC in comparison to 82.22%, 80.24% and 79.25% at 29° BTDC. However, at 32° BTDC, the LFR is found to be 80.24%, 79.75% and 75.46% for CRs of 18, 17.5 and 17, respectively.

8.4 Combustion Analysis

The combustion analysis has been carried out in the form of variation of ID, PCP and NHRR. Similar to the performance study, the parametric variation of CRs for particular ITs are clubbed together. The effects of load, CR and IT on combustion are investigated in following sections.

8.4.1 Effect of Compression Ratio

The ID under the DFM is found to be longer than the diesel mode as observed from Fig. 8.5. The reason behind this prolonged ID is due to the high overall heat capacity of biogas as well as cooling effect produced by emulsified pilot fuel results in lowering the charge temperature. It is observed that ID decreases for higher CR. At the end of compression, the temperature and pressure of biogas air mixture becomes higher as the CR is increased. This enhances the preignition reactions that are believed to affect the ignition of the injected pilot fuel. The average drop in the ID with the rise of CR from 17 to 17.5 and 17.5 to 18 are 1.7% and 3.5% respectively. The NHRR is found to be more in diesel mode in comparison to DFM. This is due to a high calorific value of diesel with respect to biogas.

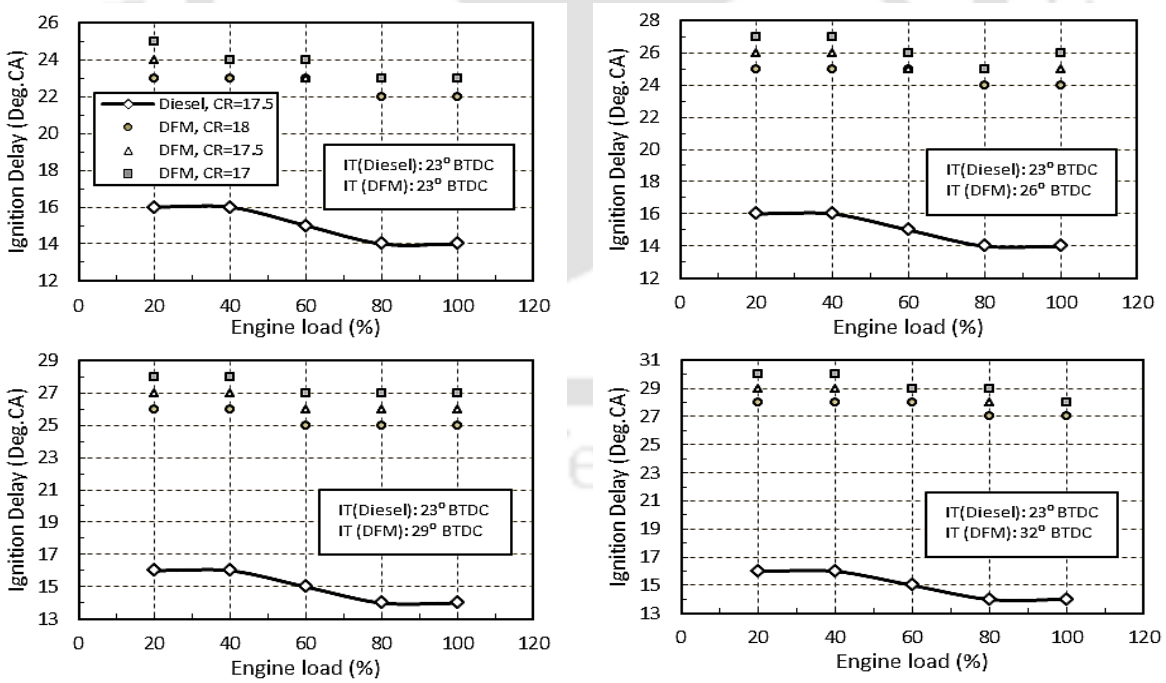

Fig. 8.5 Variation of ID with load, CR and IT

With 100% load, at 23° BTDC, the maximum NHRR under DFM were found to be 30.32 J/deg.CA, 27.93 J/deg.CA and 23.59 J/deg.CA for CRs of 18, 17.5 and 17, respectively in

comparison to 82.05 J/deg.CA diesel mode as indicated in Fig. 8.6. From the *P-Θ* diagram, it can be observed that there is a shift of PCP towards the TDC with the increase of CR in DFM as found in Fig. 8.7. With 100% load, at 23° BTDC, the crank angle corresponding to PCP under DFM is found to be 10°, 11°and 11° after top dead centres (ATDCs) for CRs of 18, 17.5 and 17, respectively in comparison to 3° ATDC in diesel mode. The PCP under DFM is low as compared to diesel mode as indicated in Fig. 8.8. AT 23° BTDC, the PCP reduces by 26.97%, 29.66% and 36.61% for CRs of 18, 17.5 and 17, respectively in comparison to diesel mode. Similar trend of decrease of ID and rise of both NHRR and PCP with the increase of CR was reported earlier (El_Kassaby and Nemit_allah, 2013; Sharma and Murugan, 2015).

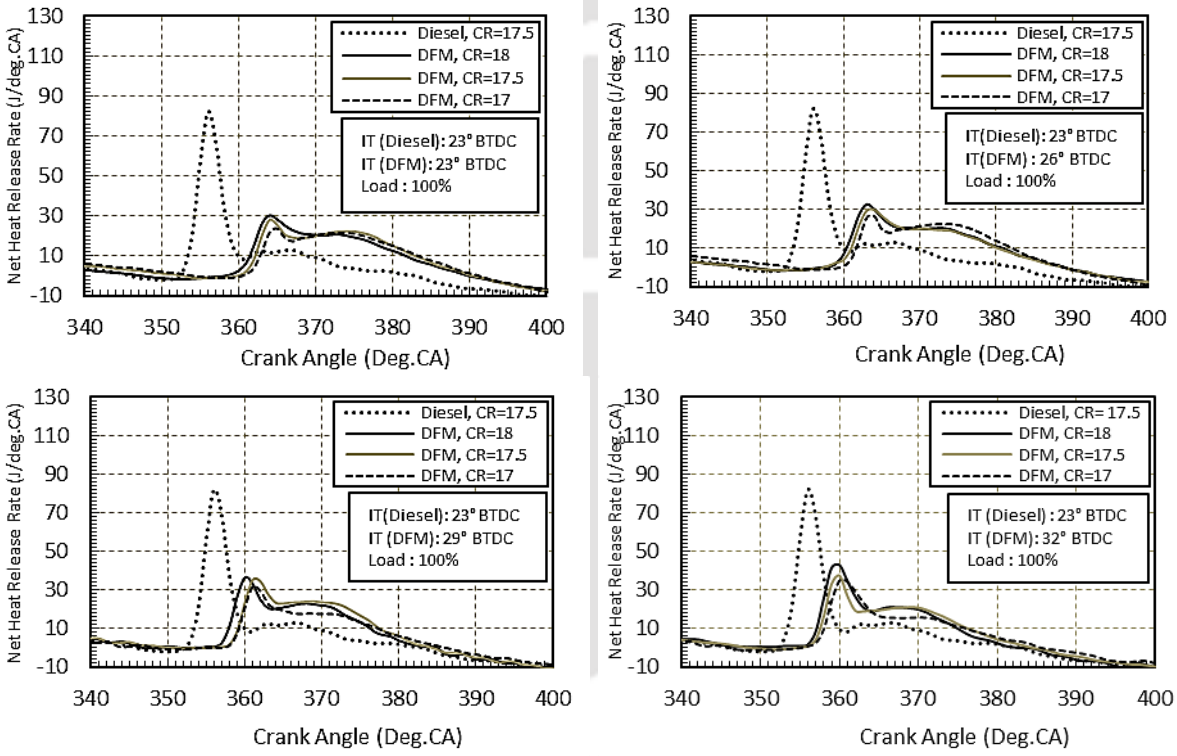

Fig. 8.6 Variation of NHRR with CR and IT at 100% load

8.4.2 Effect of Injection Timing

Advancing IT of pilot fuel resulted in injecting the fuel in a low gas temperature environment which caused in longer ID. The advancement of IT from 23° to 32° BTDC causes an average rise of IDs by about 20.42%, 22.22% and 22.68% for CRs 18, 17.5 and 17, respectively. For CRs of 18, 17.5 and 17, with 100% load, the maximum NHRR were found to be 32.26 J/deg.CA, 29.25 J/deg.CA and 26.58 J/deg.CA at 26° BTDC in comparison to 36.56 J/deg.CA, 34.39 J/deg.CA and 31.64 J/deg.CA at 29° BTDC.

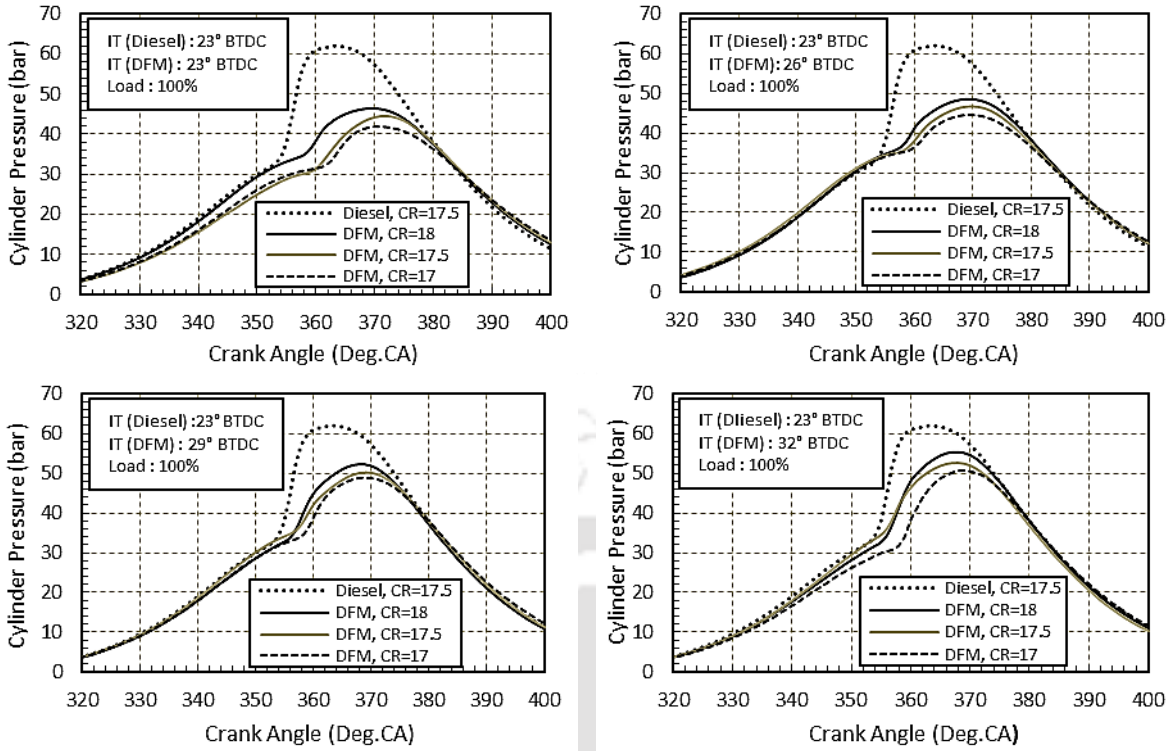

Fig. 8.7 Variation of PCP with CR and IT at 100% load

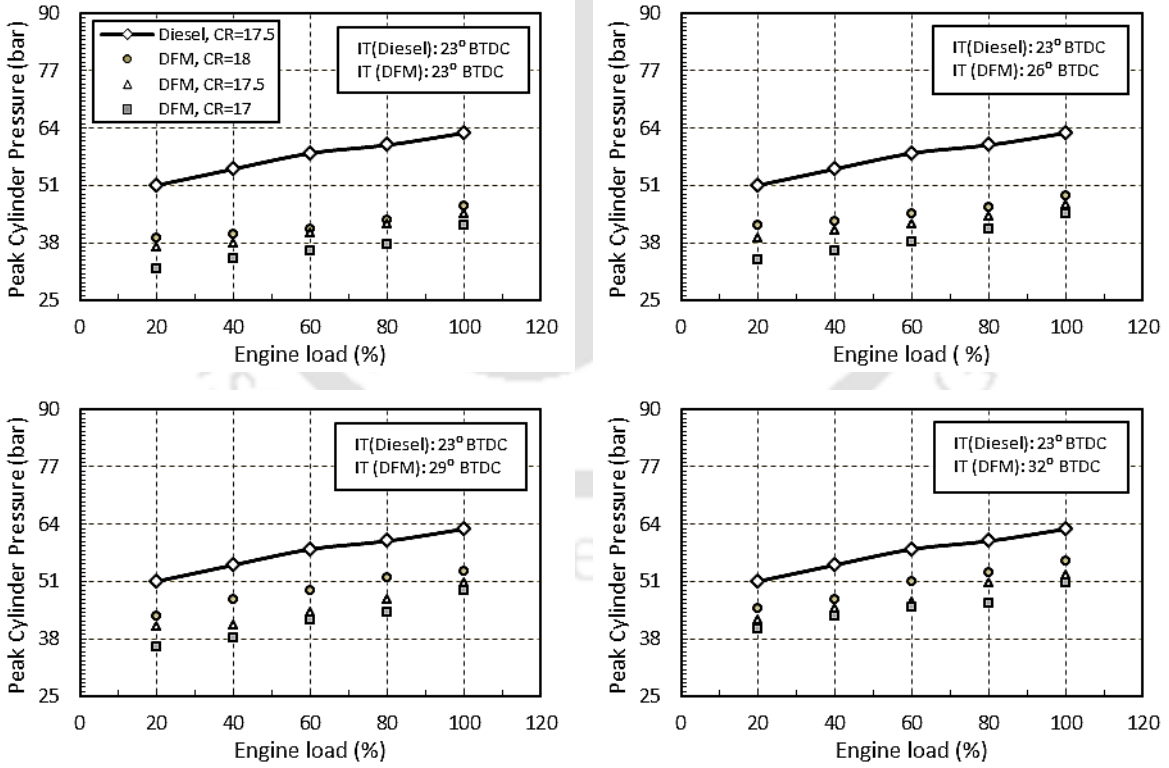

Fig. 8.8 Variation of PCP with load, CR and IT

However, the maximum NHRR were found to be 42.8 J/deg.CA, 37 J/deg.CA and 35.4 J/deg.CA for CRs of 18, 17.5 and 17, respectively at 32° BTDC. For CRs of 18, 17.5 and 17,

with 100% load, the crank angle corresponding to PCP is found to be 8°, 9° and 10° ATDCs at 26° BTDC in comparison to 8°, 9° and 9° ATDCs at 29° BTDC. However, the crank angle corresponding to PCP is found to be 7°, 7° and 9° ATDCs for CRs of 18, 17.5 and 17, respectively at 32° BTDC. Thus, it can be observed that there is a shift of the pressure curve towards top dead centre (TDC) with the advancement of IT. For CRs of 18, 17.5 and 17, the PCP drops by 22.13%, 25.86% and 32.48% at 26° BTDC in comparison to 15.13%, 22.28%, and 27.19% at 29° BTDC. However, at 32° BTDC, the PCP decreases by 12.42%, 17.75%, and 21.62% for CRs of 18, 17.5 and 17, respectively. Analogous trend of increase of ID and rise of both NHRR and PCP with advancement of IT for different test fuels was reported previously (Papagiannakis, 2007; Agarwal, 2013; Debnath, 2014a).

8.5 Emission Analysis

The samples are investigated inside the flue gas analyzer and visualize the respective concentrations of CO, CO_2, HC and NO_X emissions on the display of control unit.

8.5.1 Effect of Compression Ratio

In this investigation, CO_2 emission is higher in DFM in comparison to diesel mode as found in Fig. 8.9. This is due to the presence of a large amount of CO_2 (i.e. around 40% by volume) in raw biogas. The CO_2 emission increases at high CR. As CR increases, the clearance volume decreases, which in turn surges the temperature and pressure of the charge during the end of the compression stroke. The increased temperature causes a better combustion of fuel, which results in the increase of CO_2 emission. There is an increase of 23.45% in CO_2 emission while increasing the CR from 17 to 18 at 23° BTDC. In this study, CO emission is higher under DFM in comparison to diesel mode as shown in Fig. 8.10. The CO emission decreases for high CR. High CR results more growth of temperature during the compression stroke which results in better combustion. Further, the microexplosion of emulsified pilot fuel becomes faster with the rise of CR which expedites the combustion process. This leads to lower formation of CO for higher CR. There is a reduction of 17.60% in CO emission by increasing the CR from 17 to 18 at 23° BTDC. This goes well with the findings on CO emission with the change of CR as reported by the researcher (Sharma and Murugan, 2015). In this analysis, the lower flame velocity of biogas contributes to the formation of HC more under DFM in comparison to diesel mode as observed in Fig. 8.11. The HC emission

decreases with the increase of CR. This is due to the fact that the temperature of combustion rises with the increase of CR.

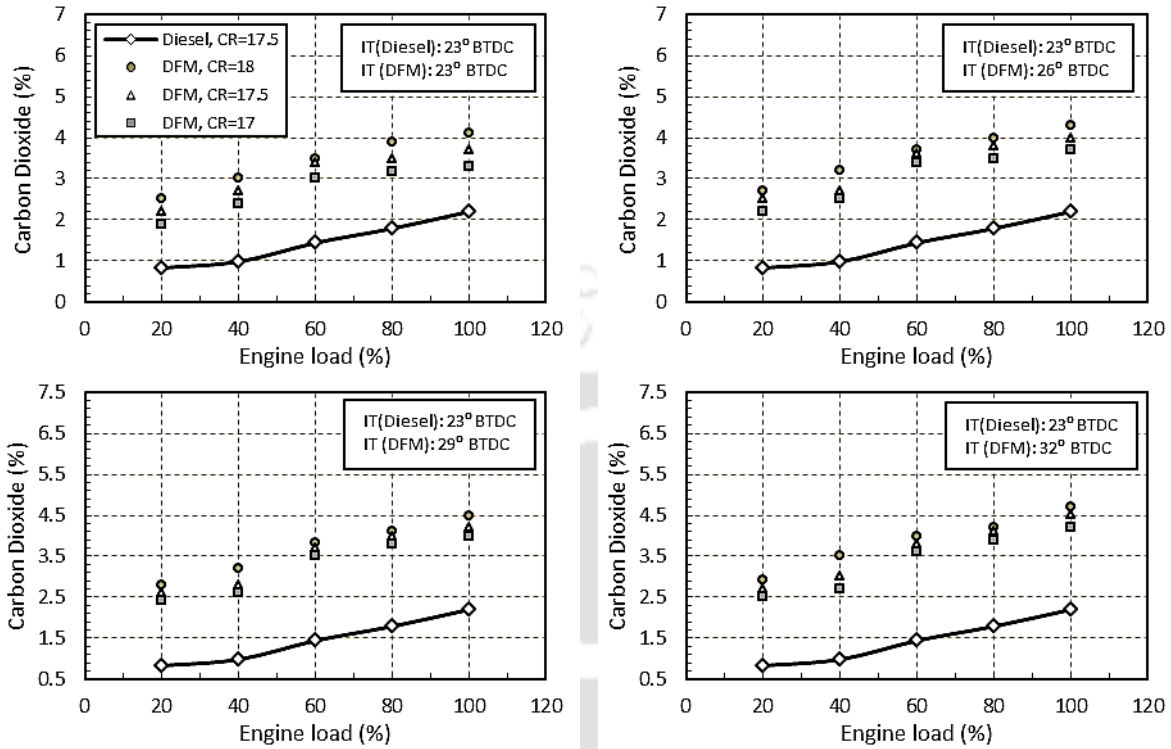

Fig. 8.9 Variation of CO_2 emission with load, CR and IT

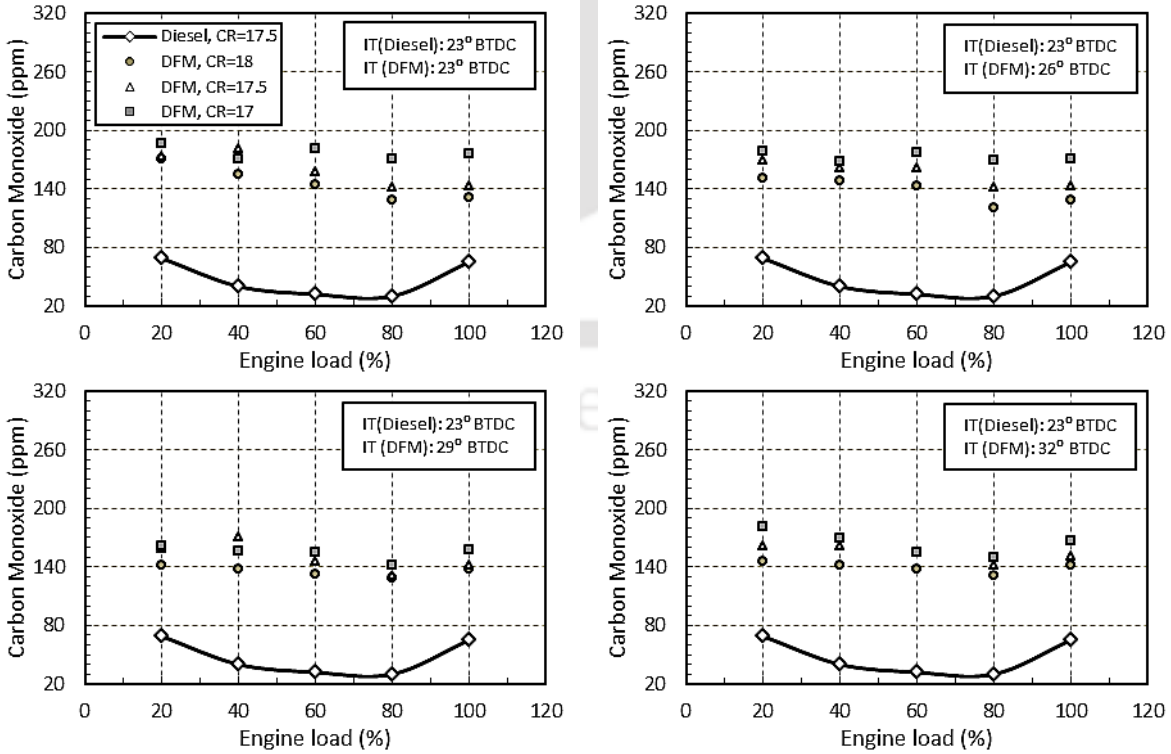

Fig. 8.10 Variation of CO emission with load, CR and IT

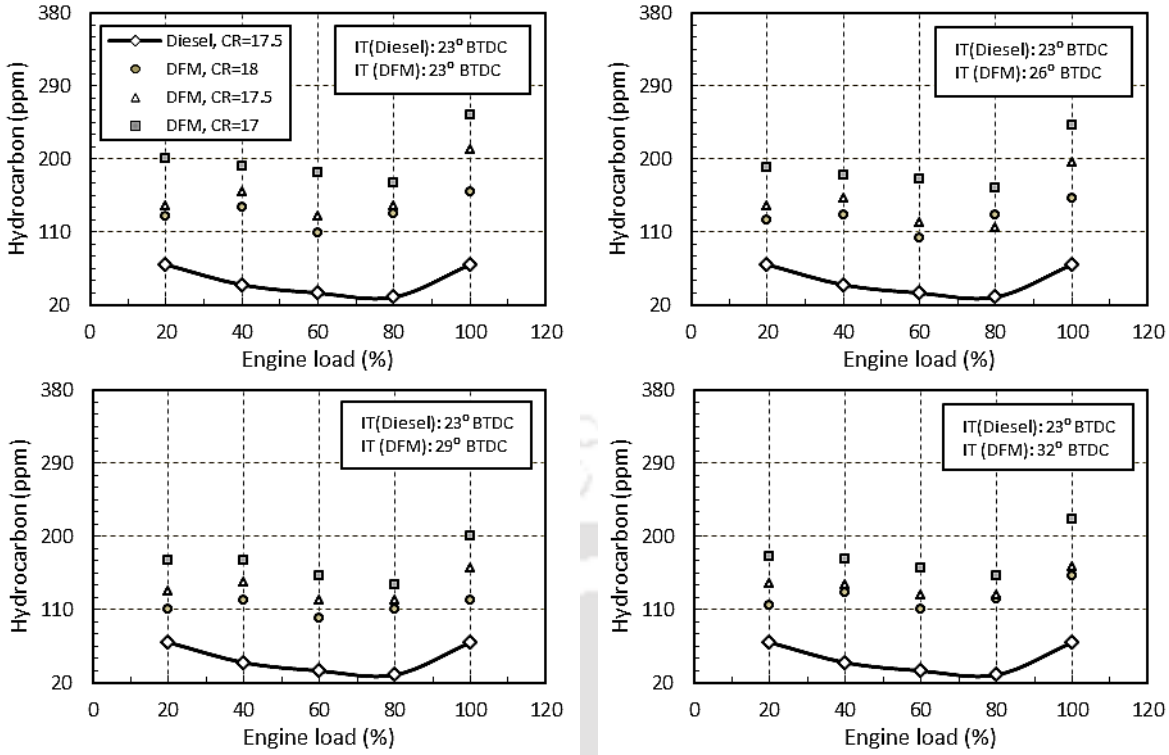

Fig. 8.11 Variation of HC emission with load, CR and IT

The higher rate of microexplosion phenomena due to rise temperature triggered early ignition of pilot fuel, which resulted in a better combustion of biogas. There is a reduction of 32.8% in HC emission is achieved by increasing the CR from 17 to 18 at 23° BTDC. The explanation for these findings is similar to that of CO emission. In this study, the NO_X emission for all the test cases under DFM is much higher than diesel mode as depicted in Fig. 8.12. This is because; the formation of NO_X depends on the temperature of the combustion chamber. The combustion chamber temperature in case of diesel is much more as diesel has a high calorific value as compared to biogas. Moreover, the presence of inert CO_2 in raw biogas and phenomena of microexplosion of water droplets due to emulsified pilot fuel resulted in lowering the temperature of the combustion chamber. The NO_X emission increases for high CR. On an average, an increase of 40.98% in NO_X emission is resulted by increasing the CR from 17 to 18 at 23° BTDC. Similar result of increased NO_X emission with the increase of CR was reported earlier (Jindal *et al*., 2010).

8.5.2 Effect of Injection Timing

It is found that advancing IT resulted in better combustion of biogas which caused an increase of CO_2 emission. Therefore, there is an increase of 13.76% in CO_2 emission on advancing IT from 23° to 32° BTDC for CR of 18. For the same range of IT, there is an

increase of 16.89% and 23.02% respectively in CO_2 emission for CR of 17.5 and 17. The CO emission decreases with advancement of IT. This resulted from the increase of CO oxidation mechanism which is due to the increased time interval during the expansion stroke for which high temperature persists in the cylinder. This resulted in more complete oxidation of CO. There is a reduction of 4.79% in CO emission on advancing IT from 23° to 32° BTDC for CR of 18. For the same range of IT, there is a reduction of 3.27% and 7.34% respectively in CO emission for CR of 17.5 and 17. Similar trend of CO emission with variation of IT was reported earlier (Sayin *et al.*, 2008).

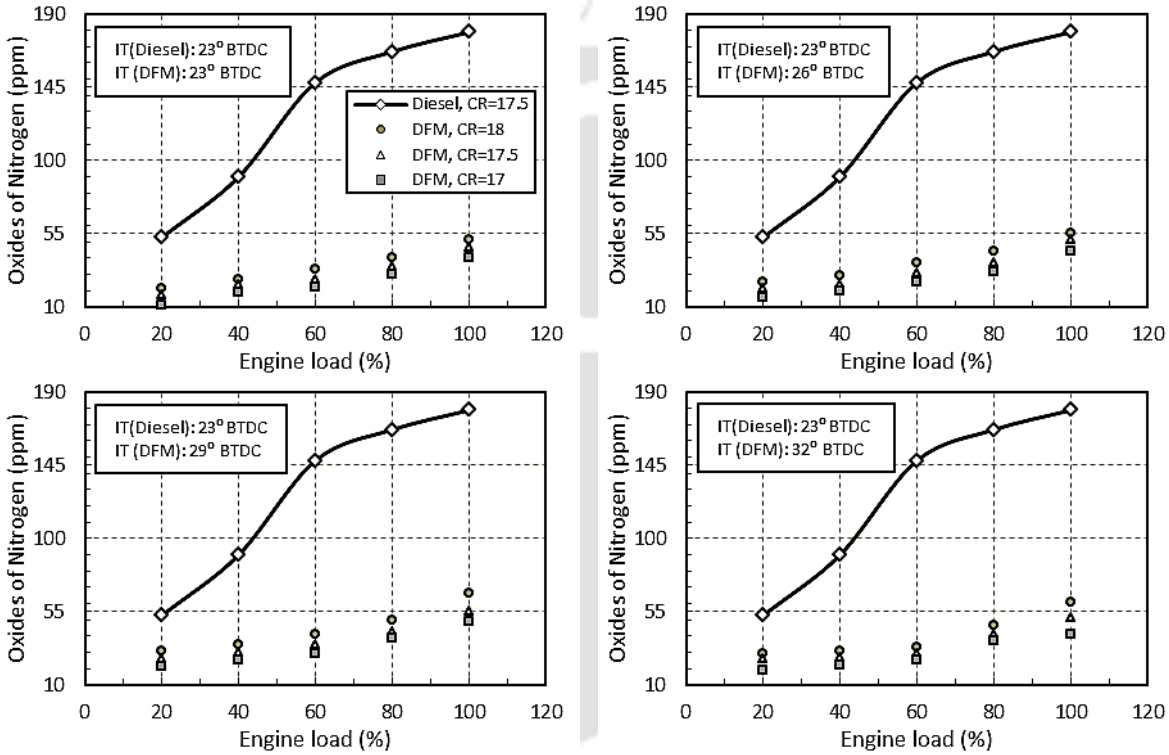

Fig. 8.12 Variation of NO_X emission with load, CR and IT

Advancing the IT causes earlier start of combustion relative to the TDC. This results in a relatively higher combustion chamber temperature as the charge being compressed as the piston moves to the TDC and lowers the HC emissions. There is a reduction of 6.23% in HC emission is achieved on advancing IT from 23° to 32° BTDC for CR of 18. For the same range of IT, there is a reduction of 11.96% and 13.5% respectively in HC emission for CRs of 17.5 and 17. Analogous results on HC emission with the variation of IT was reported earlier (Sayin and Gumus, 2011). The combustion chamber temperature increased with the advancement of IT due to better combustion of biogas. This resulted in higher emission of NO_X. There is an increase of 16.26% in emission is achieved on advancing IT from 23° to 32° BTDC for CR of 18. For the same range of IT, there is increase of 16% and 18.03%

respectively in NO_X emission for CR of 17.5 and 17. This goes well with the previous findings (Sayin *et al.*, 2008; Ryu, 2013).

8.6 Summary

- The BTE of the WIRBB-biogas run dual engine is found to be increase with the use of high CR of 18. The performance improves further with the advancement of pilot fuel IT. The maximum BTE of 23.62% is obtained for a combination of CR=18 and IT=29° BTDC.

- The BSEC is found to be decrease with the use of high CR of 18. Conversely, with the advancement of pilot fuel IT, the BSEC drops up to a particular IT. The maximum drop in BSEC of 19.66% is obtained for a combination of CR=18 and IT=29° BTDC.

- The use of high CR and advancement of IT results in a drop of EGT. The maximum drop of EGT is obtained for the combination of CR=18 and IT=32° BTDC.

- There is an average reduction in BFR by 15.84% for increasing the CR from 17 to 18. On advancing IT from 23° to 32° BTDC for CR of 18, there is a reduction of BFR by 11.21%. For the same range of IT, there is a drop of 8% and 11.7% in BFR at CRs of 17.5 and 17, respectively.

- At 23° BTDC with 100% load, the LFR is found to be 79.25%, 77.77% and 76.79% for CRs of 18, 17.5 and 17, respectively. For the same loading conditions at CRs of 18, 17.5 and 17, the LFR is found to be 79.47%, 78.27% and 78.21% at 26° BTDC in comparison to 82.22%, 80.24% and 79.25% at 29° BTDC. However, the LFR is found to be 80.24%, 79.25% and 75.46% for CRs of 18, 17.5 and 17, respectively at 32° BTDC.

- The average fall in ID with the rise of CR from 17 to 17.5 and 17.5 to 18 are 1.7% and 3.5%, respectively. The advancement of IT by 3°, 6° and 9° resulted in an average rise of IDs by about 20.42%, 22.22% and 22.68% for CR of 18, 17.5 and 17, respectively.

- The maximum NHRR and the PCP increases with use of high CR and advancement of IT of pilot fuel. The maximum NHRR and the PCP is attained for a combination of CR=18 and IT=32° BTDC.

- There is an average rise in CO_2 emission by 24.45% on increasing the CR from 17 to 18 at 23° BTDC. Therefore, there is a rise of 13.76% in CO_2 emission on advancing IT from 23° to 32° BTDC for CR of 18. For the same range of IT, on an average, there is an increase of 16.89% and 23.02% in CO_2 emission for CR of 17.5 and 17, respectively.

- There is an average drop in CO emission by 17.6% on increasing the CR from 17 to 18 at 23° BTDC. There is a reduction of 4.7% in CO emission on advancing IT from 23° to 32° BTDC for CR of 18. For the same range of IT, on an average, there is a reduction of 3.27% and 7.34% in CO emission for CR of 17.5 and 17, respectively.

- There is an average reduction in HC emission by 32.8% on increasing the CR from 17 to 18 at 23° BTDC. On an average, there is a reduction of 6.23% in HC emission is achieved on advancing IT from 23° to 32° BTDC for CR of 18 under DFM. For the same range of IT, on an average, there is a reduction of 11.96% and 13.5% in HC emission for CRs of 17.5 and 17, respectively.

- There is an average increase in NO_X emission by 40.98% on increasing the CR from 17 to 18 at 23° BTDC. There is an increase of 16.26% in emission is achieved on advancing IT from 23° to 32° BTDC for CR of 18 under DFM. For the same range of IT, there is a rise of 16% and 18.03% in NO_X emission for CR of 17.5 and 17, respectively.

Based on the above results, it can be concluded that the optimum combination for a biogas run dual fuel diesel engine using emulsified rice bran biodiesel as pilot fuel is found to be CR=18 and IT=29° BTDC.

Chapter-9

Analysis at Optimized Operating Condition

Overview:

Biogas is a potentially renewable, cheaply producible and environment friendly fuel. However, it is known fact that biogas has lesser heating value than neat diesel. That is the reason why, at standard diesel setting, biogas run dual fuel engine produces inferior performance. However, proper adjustment of the operating parameters can enhance the performance of a biogas run dual fuel diesel engine. Thus, the Compression ratio (CR) and Injection timing (IT) of pilot fuel are two very important parameters as far as proficient dual fuel combustion is concerned. The CR can be increased by reducing the clearance volume of the cylinder. Therefore, the pressure and temperature raises with increase of CR. Again, at the advanced IT, the pilot fuel sprayed earlier than into the biogas-air mixture and thereby, giving sufficient time to pilot fuel to interact with the biogas-air mixture. The advancement of IT is helpful in reducing the late combustion phenomenon that is evident in case of biogas run dual fuel diesel engine. Thus, the combination of high CR and advanced IT of pilot fuel ensures a better performance and emission characteristic for a biogas run dual fuel diesel engine. The objective of the this chapter is carry out a comparative analysis of diesel-biogas, RBB-biogas and WIRBB-biogas run dual fuel diesel engines at optimized conditions.

Chapter Outline:

9.1 Optimized Operating Parameters

The study on performance and emission characterises of a biogas run dual fuel diesel engine were carried out in chapters 5, 6 and 8. This chapter discusses and compares the results obtained at the optimized operating parameter of the biogas run dual fuel diesel engine using diesel, rice bran biodiesel (RBB) and emulsified rice bran biodiesel (WIRBB) as pilot fuel with respect to the neat diesel data at standard settings (CR=17.5 and IT=23º BTDC). The optimized operating parameters corresponding to diesel-biogas, RBB-biogas and WIRBB-biogas run dual fuel engine are found to be CR=18, IT=29º BTDC; CR=18, IT=32º BTDC; and CR=18, IT=32º BTDC, respectively. Alongside, this study also attempts to unravel the effect of different genre of pilot fuels on the performance of a biogas run duel fuel diesel engine. The comparison has been segregated into performance, combustion and emission analysis. The performance analysis evaluated are brake thermal efficiency (BTE), brake specific energy consumption (BSEC), exhaust gas temperature (EGT), biogas flow rate (BFR) and liquid fuel replacement (LFR). The combustion analysis include the cylinder pressure variation, ignition delay (ID), peak cylinder pressure (PCP) and net heat release rate (NHRR). Finally, emission analysis is performed by measuring carbon dioxide (CO_2), carbon monoxide (CO), hydrocarbon (HC) and oxides of nitrogen (NO_X).

9.2 Performance Analysis

The BTE increases with the increase in load for both diesel and dual fuel mode (DFM) as indicated in Fig. 9.1(a). However, BTEs are found to be lower for all three cases of dual fuel mode at their respective optimized setting in comparison to diesel mode mainly due to low calorific value of biogas. At 100% load, the BTEs are found to 25.44%, 25.88% and 23.62% for diesel-biogas, RBB-biogas and WIRBB-biogas, respectively under DFM as compared to 27.76% for diesel mode. Therefore, the use of biodiesel as pilot fuel for a biogas run dual fuel engine resulted in a slightly improved BTE in comparison to the other pilot fuels tested. This is due to the presence of oxygen (around 11%) in RBB, which resulted in a better combustion of biogas. Analogous result of improvement of BTE with biodiesel-biogas in comparison to diesel-biogas was reported earlier (Yoon and Lee, 2011). The BSEC reduces with increase of load for diesel and DFM as depicted in Fig. 9.1(b). However, the BSEC for all the three cases of dual fuel mode are higher in comparison to diesel mode. On an average, the BSEC increased by 58.59%, 52.36% and 60.9% for diesel-biogas, RBB-biogas and WIRBB-biogas, respectively under DFM as compared to diesel mode. The EGT increases linearly with the

increase of load. The EGT for all cases of DFM is found to be higher than diesel mode as observed in Fig. 9.1(c). This is due to late combustion of biogas which shortens the duration of extraction of power. As a result, the combustion products in the form of gases come out at higher temperature. On an average, there is an increase of 7.10%, 5.4% and 10.12% for diesel-biogas, RBB-biogas and WIRBB-biogas, respectively under DFM in compared to that of diesel mode. The BFR and LFR increases with the increase in load for diesel-biogas, RBB-biogas and WIRBB-biogas, respectively under DFM as depicted in Fig 9.1 (d). At 100% load, the BFR is found to be 2.02 kg/h, 2.22 kg/h and 2.24kg/h for diesel-biogas, RBB-biogas and WIRBB-biogas, respectively. For the same loading condition, the maximum LFR is found to be 82.67%, 82.75% and 82.11% for diesel-biogas, RBB-biogas and WIRBB-biogas, respectively.

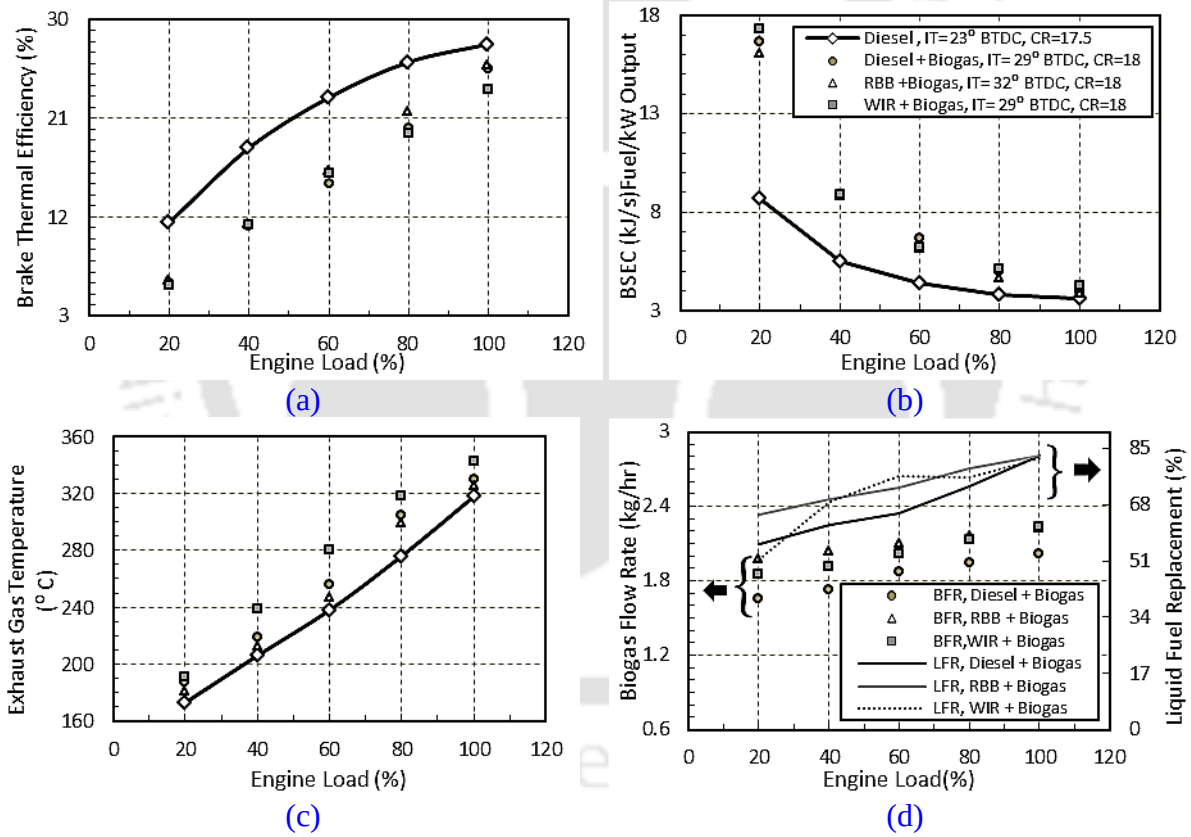

Fig. 9.1 Performance analysis of a biogas run dual fuel diesel engine using diesel, RBB and WIRBB as pilot fuel at optimum setting

9.3 Combustion Analysis

The ID gradually decreases as load increases for both diesel and DFM as observed in Fig. 9.2(a). However, the ID under the DFM is found to be longer than the diesel mode. The reason behind this prolonged ID for DFM is due to the presence of larger amount of biogas

fuel in the intake and compression processes. As biogas has a high overall heat capacity, therefore, it results in more lowering of the charge temperature as compared to diesel mode. This delays the ignition of pilot fuel significantly. On an average, the ID is found to increase by 69.33%, 77.33% and 69.33% for diesel-biogas, RBB-biogas and WIRBB-biogas, respectively under DFM in comparison to that of diesel mode. The heat release is more in diesel mode in comparison to DFM. This is due to high calorific value of diesel with respect to biogas. At 100% load, the maximum NHRR is found to be 48.41 J/deg.CA, 42.86 J/deg.CA and 36.56 J/deg.CA for diesel-biogas, RBB-biogas and WIRBB-biogas, respectively under DFM in comparison to 82.02 J/deg.CA in diesel mode as indicated in Fig. 9.2(b).

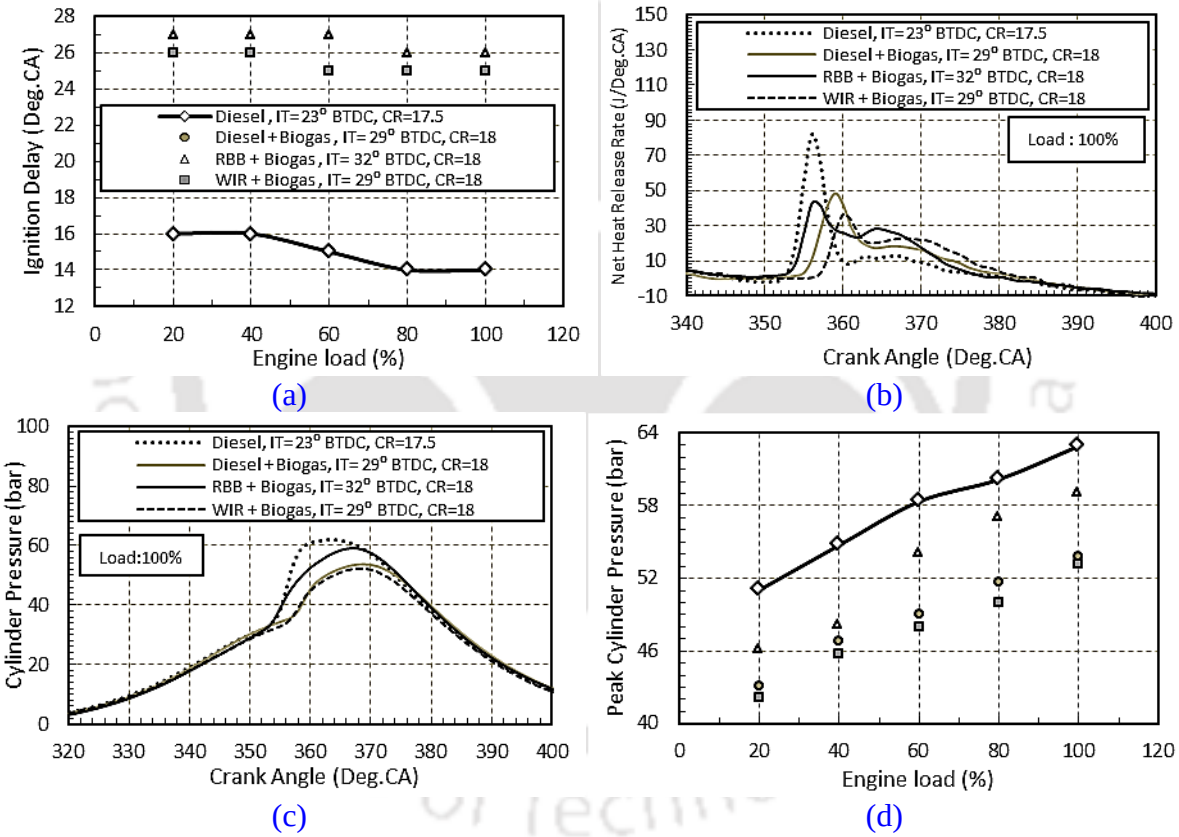

Fig. 9.2 Combustion analysis of a biogas run dual fuel diesel engine using diesel, RBB and WIRBB as pilot fuel at optimum setting

The PCP increases with the increase in load for both diesel and DFM as indicated in Fig. 9.2(c). However, the rise of pressure under all the three cases of DFM is less than diesel mode. On an average, the drop in PCP is found to be 14.9%, 8% and 15.13% for diesel-biogas, RBB-biogas and WIRBB-biogas, respectively under DFM in comparison to that of diesel mode. It can be observed from the *P-Θ* diagram analysis that there is a shift of PCP away from TDC in dual fuel mode as observed in Fig. 9.2(d). At 100% load, the crank angle

corresponding to PCP is found to be 8° ATDC, 6° ATDC and 8° ATDC for diesel-biogas, RBB-biogas and WIRBB-biogas, respectively under DFM in comparison to 3°ATDC in diesel mode.

9.4 Emission Analysis

The concentration of CO emissions are high at low loads, which then decreases at medium load, and again increases at high load as indicated in Fig. 9.3(a). However, the CO emissions are higher for all the three cases of DFM in comparison to diesel mode. On an average, there is a higher emission of CO by 77.03% and 74.93% for diesel-biogas and WIRBB-biogas, respectively in comparison to RBB-biogas.The CO_2 emission increases with the increase of load for both diesel and DFM as observed in Fig. 9.3(b). However, CO_2 emission is higher for all the three cases of dual fuel mode in comparison to diesel mode. This is because of presence of large amount of CO_2 (i.e. around 40% by volume) in biogas. On an average, there is a lower emission of CO_2 by 46.95% and 38.22% for diesel-biogas and WIRBB-biogas, respectively in comparison to RBB-biogas.

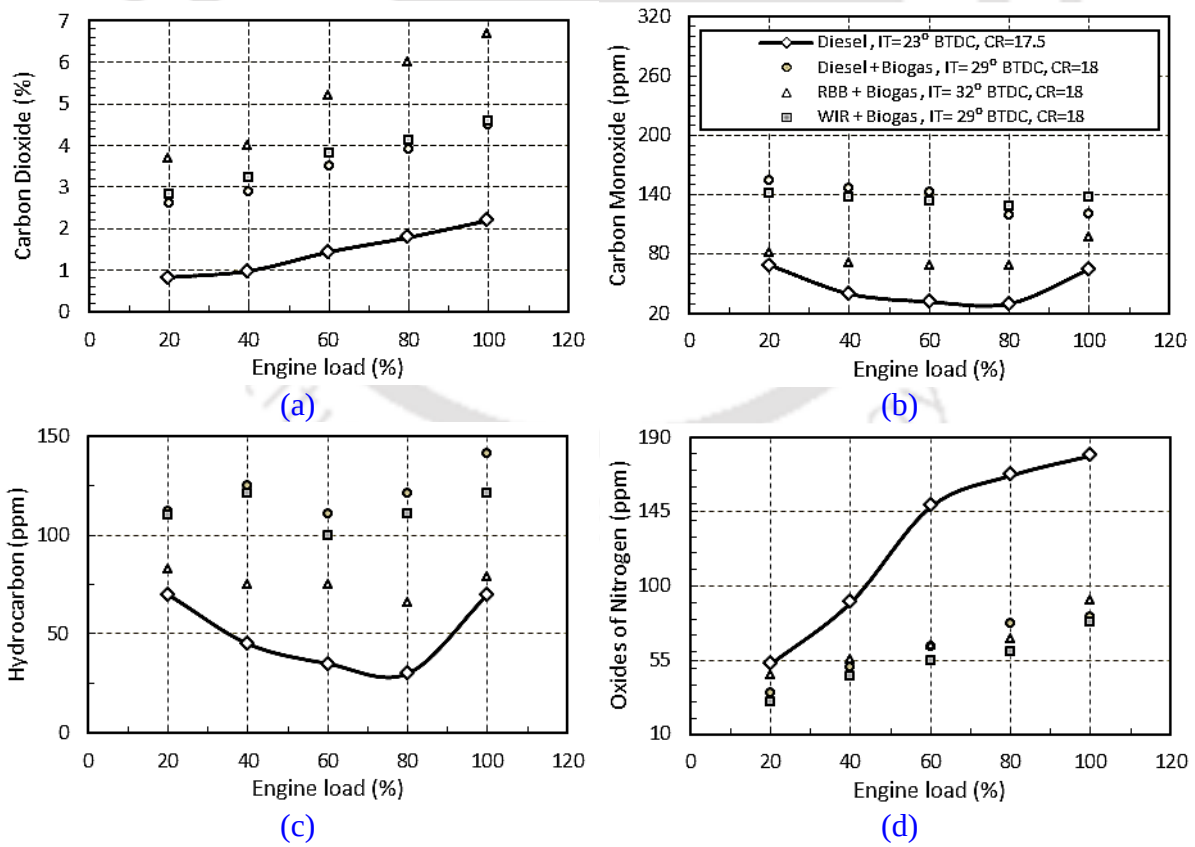

Fig. 9.3 Emission analysis of a biogas run dual fuel diesel engine using diesel, RBB and WIRBB as pilot fuel at optimum setting

In this study, the HC emission follows a similar trend to that CO emission with the increase of load as observed in Fig. 9.3(c). The HC is more in all the cases of DFM in comparison to diesel mode due to the low flame velocity of biogas. On an average, there is a higher emission of HC by 61.37% and 32.86% for diesel-biogas and WIRBB-biogas, respectively in comparison to RBB-biogas. The factor responsible for low CO and HC emissions and high CO_2 emissions in case RBB-biogas is due to the presence of oxygen (around 11%) in biodiesel which expedites the oxidation process. This results in a comparatively better combustion of biogas. In this investigation, the NOx emission increases with the increase of load as more amount of fuel needs to be supplied with increase of load which results in increase of temperature of combustion chamber. However, the NO_X emission in the diesel mode is much higher in comparison to all the three cases of DFM as depicted in Fig. 9.3(d). This is because the temperature of the combustion chamber in case of diesel is much more as diesel has a high calorific value as compared to biogas. Moreover, the presence of inert CO_2 in biogas results in lowering the temperature of combustion chamber. On an average, there is a higher emission of NO_X by 14.55% and 19.77% for diesel-biogas and RBB-biogas, respectively in comparison to WIRBB-biogas. The reason behind the reduction of NO_X emission in case of emulsified pilot fuel (WIRBB) is due to the decrease of the temperature of the combustion chamber as result of the vaporization of water present in the emulsified fuel.

9.5 Summary

The present chapter carries out a comparison study of a biogas run dual fuel diesel engine using three different types of pilot fuel, namely, diesel, rice bran biodiesel and emulsified rice bran biodiesel functioning at their respective optimized operating conditions. The main findings of this investigation are summarized below:

- The RBB-biogas produced the maximum brake thermal efficiency (25.44%) and least CO and HC emissions in comparison to diesel-biogas and WIRBB-biogas. This was due the oxygenated nature of RBB, which resulted in a better combustion biogas.

- The NO_X emission is found to be least for WIRBB-biogas in comparison to diesel-biogas and RBB-biogas. This is due to the presence of microexplosion phenomenon in case of WIRBB pilot fuel which lowered the combustion chamber temperature and thereby, reducing the NO_X emission.

- The optimum advancement of IT in case of biogas run dual fuel engine depends on the physical and chemical characteristics of the pilot fuel used.

- The advancement of IT of pilot fuel along with the use of high CR seems one of the panacea in lowering the late combustion phenomenon commonly observed in case of biogas run dual fuel diesel engines. This is mainly due to the difference of flame velocity between the pilot fuel and primary fuel.

Chapter-10

Energy and Exergy Analysis

Overview:

In general, the first law of thermodynamics is used for analyse of the engine performance parameters; however it does not consider the quality of energy content of a system. It is well understood that the first law often fails to give a good insight into the engine's operation. Therefore, the first and the second law analyses should be applied to the engine process simultaneously. In recent years, energy and exergy analysis method has been widely used in design, simulation and performance assessment of various types of engines for identifying the losses and thereby, improving efficiencies. However, the thermodynamic analysis of a biogas run dual fuel diesel engine is rare in open literature. It is observed that biogas has different physical and chemical properties than diesel. Hence, the energy and availability distribution of biogas run dual fuel diesel engine will not be identical to that of a diesel engine run at standard settings. To enlighten this ambiguous fact of literature, this chapter provides energy and exergy analysis of a biogas run dual fuel diesel engine using diesel, rice bran biodiesel (RBB) and water emulsified RBB (WIRBB).

Chapter Outline:

10.1 Thermodynamic Analysis

In view of the decreasing energy sources, optimization of the operating parameters of internal combustion (IC) engine is a must for effectual utilisation of fuel energy. For optimization of the operating parameters, it has long been understood that traditional first law analysis often fails to give the engineer the best insight into the IC operation (Rakopoulos and Giakoumis, 2009). In order to evaluate the inefficiencies associated with the various processes, second law analysis must be applied (Moran and Shapiro, 1995). The key concept of the second law analysis is 'availability or exergy' was first introduced by Gibbs. The availability or exergy of a process represents a quantitative measure of the quality or usefulness of this process (Caton, 2000). Unlike energy, availability can be destroyed, which is a result of some phenomena such as combustion, friction, mixing, throttling, etc. The destruction of availability is a source for insufficient use from fuel availability to produce useful mechanical work in an IC engine. The reduction of irreversibilities can lead to better engine performance through a more efficient exploitation of fuel (Rakopoulos and Giakoumis, 2006; Giakoumis, 2007). The first studies of IC engines operation that included exergy balance in the calculations were around 1960, the works of Traupel (1957), and Patterson and Van Wylen (1963). Many studies concerning to the second law application, thereafter, have been conducted in various types of spark ignition engines, diesel engines, homogeneous compression charge ignition engines and dual fuel engines. In Chapter 2, the literature review on dual fuel diesel engines highlights that the effect of operating parameters on the energy and exergy distributions of a biogas run dual fuel diesel engine has not been reported. This is important as the combustion characteristic of biogas is totally different from diesel. Therefore, such an investigation on operating parameters will make biogas run dual fuel engines more energy efficient.

Keeping this vista in mind, the thermodynamic analysis of the biogas run dual fuel diesel engine for the variation of CR and IT using different types of pilot fuel is carried out in the upcoming sections. The pilot fuel includes diesel, rice bran biodiesel (RBB) and water emulsified rice bran biodiesel (WIRBB). The equations for this study are included in Appendix-D. The energy analysis includes the fuel energy supplied per unit time (Q_{in}), shaft energy per unit time (Q_s), energy transferred to the cooling water per unit time (Q_w), energy loss through the exhaust gas per unit time (Q_e), uncounted energy loss per unit time (Q_u), brake thermal efficiency (BTE), brake specific energy consumption (BSEC), exhaust gas temperature (EGT), biogas flow rate (BFR), liquid fuel replacement (LFR), peak cylinder

pressure (PCP) and peak heat release rate (PHRR). The exergy analysis includes input availability of fuel (A_{in}), shaft energy availability (A_s), cooling water availability (A_c), exhaust gas availability (A_e), availability destroyed (A_d), exergetic efficiency (η_{II}) and entropy generation.

10.2 Energy and Exergy Distributions of the Diesel -Biogas Run Dual Fuel Engine

The energy and exergy distributions of a biogas run dual fuel engine using diesel as pilot fuel is discussed in the upcoming section discusses. The experimental matrix consists of sixteen combinations of CRs 16, 17, 17.5, and 18; and ITs of 23º, 26º, 29° and 32º BTDCs at full loading condition as discussed in Chapter 5.

10.2.1 Energy Analysis

The distribution of energy per unit time through different process at different combinations of CR and IT at full load is given in Table 10.1.

Table 10.1 Results of energy analysis for different combination of ITs and CRs at 100% load

Mode	CR	IT	Q_{in} (kW)	Q_s (kW)	Q_w (kW)	Q_e (kW)	Q_u (kW)
Diesel	17.5	23	12.64	3.51	5.02	3.04	1.05
Dual	18	23	17.48	3.57	5.24	7.06	1.6
	17.5	23	19.14	3.49	5.67	7.98	1.99
	17	23	19.73	3.51	5.75	8.28	2.32
	16	23	21.68	3.56	6.36	9.13	2.62
	18	26	15.77	3.55	4.91	5.89	1.40
	17.5	26	16.91	3.55	5.23	6.59	1.54
	17	26	19.15	3.53	5.76	7.81	2.04
	16	26	20.49	3.5	6.1	8.42	2.46
	18	29	13.77	3.52	4.42	4.64	1.19
	17.5	29	15.25	3.5	4.77	5.34	1.64
	17	29	17.79	3.54	5.49	6.72	2.02
	16	29	19.44	3.57	6.11	7.6	2.15
	18	32	14.60	3.49	4.59	5.27	1.25
	17.5	32	16.79	3.57	5.2	6.52	1.49
	17	32	18.31	3.46	5.74	7.12	1.98
	16	32	19.97	3.59	6.25	7.81	2.32

Effect of CR on Energy Distributions

To study the effect of CR on various energy distributions under dual fuel mode (DFM), the values of four ITs are averaged and included in Fig. 10.1(a). When the CR is increased from 16 to 18 at 23° BTDC, the shaft energy and the energy transferred to the cooling water, on an average, increases by 32.37% and 2.32% respectively. However, for the same setting, the energy loss through exhaust gas and uncounted energy losses decreases by 8.57% and 24.64%, respectively. This is due to the fact that with the rise of CR, the pressure and temperature inside the cylinder increases which ensures an improved combustion of biogas. Thus, the fuel energy supplied per unit time gets reduced with the increase of CR. This, in turn, increases the shaft energy and the energy transferred to the cooling water and lowers the energy loss through exhaust gas and uncounted energy losses. The BTEs are found to be 20.42%, 18.25%, 17.79% and 16.42% for CRs of 18, 17.5, 17 and 16, respectively at IT of 23° BTDC as depicted in Fig. 10.1(b). On an average, there is a drop of BSEC and BFR by 24.02% and 24.55% respectively on increasing the CR from 16 to 18 as indicated in Figs. 10.1(c) and 10.1(d). Upon increasing the CR from 16 to 18, there is an increase in PCP and PHRR by 25.64% and 17.94%, respectively as depicted in Fig. 10.1(e). The high temperature environment inside the combustion chamber at higher CR causes the fuel to burn more efficiently. This results in more release of energy from the fuel, which increases both PCP and PHRR as observed in the present study. At 23° BTDC, the LFR is found to be 79.46%, 79.1%, 74.73% and 72.43% for CRs of 18, 17.5 17 and 16, respectively as observed from Fig. 10.1(f). On an average, there is a drop of 9.74% in EGT on change of CR from 16 to 18 as indicated in Fig. 10.1(g). With the increase of CR, the energy loss through the exhaust gas reduces. This results in lowering of EGT.

Effect of IT on Energy Distributions

To study the effect of IT on various energy distributions under DFM, the values of four CRs are averaged and included in Fig. 10.1(h). With the advancement of IT from 23° BTDC to 32° BTDC, on an average, the shaft energy and energy transferred to the cooling water rises by 13.91% and 5.93%, respectively. On the other hand, for the same setting, the energy loss through exhaust gas and uncounted energy losses drops by 7.97% and 8.42%, respectively. For CRs of 18, 17.5, 17 and 16, the BTEs is found to be 22.51%, 20.99%, 18.42% and 17.12% at 26° BTDC in comparison to 25.57%, 22.99%, 19.89% and 18.36% at 29° BTDC.

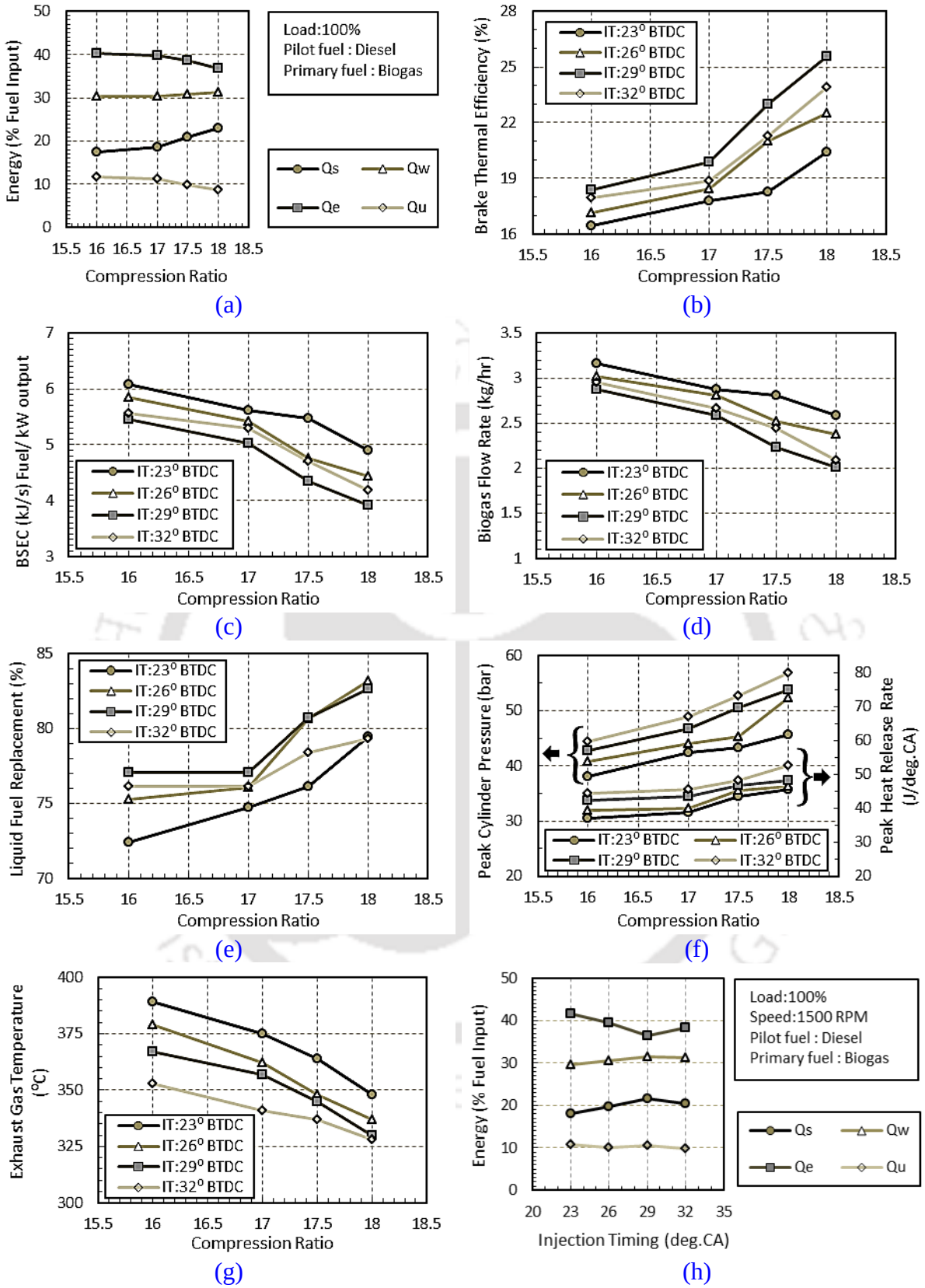

Fig. 10.1 Effect of CR and IT on energy analysis of a diesel-biogas run dual fuel engine

Further advancement of IT by 3°, the BTEs is found to be 23.9%, 21.25%, 18.86 and 17.96% for CRs of 18, 17.5, 17 and 16, respectively. From the above analysis, it is quite clear that the

shaft energy or BTE of the biogas run dual fuel diesel engine improves with the advancement of IT of pilot fuel. This is because when IT is advanced; diesel is injected earlier into the combustion chamber than the one at standard IT, thereby giving sufficient time for biogas-air mixture to burn efficiently. Thus, the fuel energy supplied per unit time gets reduced with the advancement of IT. This leads to increase of the shaft energy and the energy transferred to the cooling water and lowers the energy loss through exhaust gas and uncounted energy losses.The advancement of IT from 23° BTDC to 32° BTDC, on an average, exhibits a drop in BSEC, BFR and EGT by 10.54%, 11.32% and 7.92%, respectively. However, for the same setting, on an average, there is an increase in PCP and PHRR by 19.58% and 15.6%, respectively. For CRs of 18, 17.5, 17 and 16, the LFR is found to be 83.17%, 80.67%, 76.05% and 75.22% at 26° BTDC in comparison to 82.68%, 80.7%, 77.02% and 77% at 29° BTDC. For same loading condition, the LFR is found to be 79.32%, 78.4%, 76.11% and 76% for CRs of 18, 17.5, 17 and 16, respectively at 32° BTDC.

10.2.2 Exergy Analysis

The distribution of exergy per unit time through different process at different combinations of CR and IT at full load is given in Table 10.2.

Effect of CR on Exergy Distributions

To study the effect of CR on various exergy distributions under DFM, the values of four ITs are averaged and included in Fig. 10.2(a). The shaft energy availability increases by 32.27% for increase in CR from 16 to 18 at 23° BTDC. However, for the same setting, the exhaust gas availability decreases by 28.61%. The average cooling water availability and average availability destroyed are found to be around 0.93% and 67.35%, respectively. Similar value of cooling water availability for a biogas run dual fuel diesel engine at standard diesel setting was reported by Sahoo *et al.* (2012b). When CR is increased from 16 to 18, the entropy generation decrease by 25.87% as indicated in Fig. 10.2(b). On an average, the exergetic efficiency improved by 1.25% when CR is increased from 16 to 18 as depicted in Fig. 10.2(c). Analogous trends of variation of entropy generation and exergetic efficiency with CR have been reported by Debnath *et al.* (2013a, 2014a). Thus, it is quite evident from above investigation that the combustion improves at high CR owing to the raise in temperature of the combustion chamber. This causes an increase in shaft availability and low entropy generation due to reduction in heat transfer availability losses.

Table 10.2 Results of exergy analysis for different combination of ITs and CRs at 100% load

Mode	CR	IT	A_{in} (kW)	A_s (kW)	A_w (kW)	A_e (kW)	A_d (kW)	η_{II} (%)
Diesel	17.5	23	13.07	3.51	0.11	1.04	8.39	35.74
Dual	18	23	17.80	3.57	0.14	2.30	11.79	33.77
	17.5	23	19.5	3.49	0.15	2.64	13.22	32.22
	17	23	20.1	3.51	0.23	2.82	13.54	32.67
	16	23	22.08	3.56	0.22	3.27	15.03	31.92
	18	26	16.06	3.55	0.16	1.72	10.63	33.81
	17.5	26	17.23	3.55	0.15	1.96	11.57	32.84
	17	26	19.51	3.53	0.19	2.68	13.11	32.79
	16	26	20.88	3.5	0.23	3.13	14	32.91
	18	29	14.02	3.52	0.14	1.24	9.13	34.91
	17.5	29	15.54	3.5	0.15	1.53	10.35	33.41
	17	29	18.13	3.53	0.18	2.4	12	33.77
	16	29	19.8	3.57	0.17	2.93	13.13	33.67
	18	32	14.88	3.49	0.16	1.53	9.7	34.81
	17.5	32	17.1	3.57	0.17	2.11	11.25	34.21
	17	32	18.67	3.46	0.15	2.65	12.42	33.56
	16	32	20.35	3.58	0.18	3.1	13.47	33.79

Effect of IT on Exergy Distributions

To study the effect of IT on various exergy distributions under DFM, the values of four CRs are averaged and included in Fig. 10.2(d). On an average, the shaft energy availability increases by 12.47% on advancement of IT from 23° BTDC to 32° BTDC. For the same change of IT, on an average, the exhaust gas availability and availability destroyed decreases by 5.76% and 2.15%, respectively. The increase of cooling water availability is very marginal (i.e. around 0.17%) for the same combination of IT and CR. On advancement of IT from 23° to 32° BTDC, the entropy generation decreases by 12.61%. Therefore, it can be inferred that the combustion process improves with the advancement of IT, which results in the reduction of both fuel exergy input and entropy generation. Exergy analysis has shown around 33.44% of the fuel energy is converted to useful means of energy. The trends of exergy efficiency are found almost reciprocal to the entropy generation. This analysis highlights a vital point that

for the effectual utilisation of available energy of fuel, the standard diesel IT is not the optimum IT for the biogas run dual fuel diesel engine.

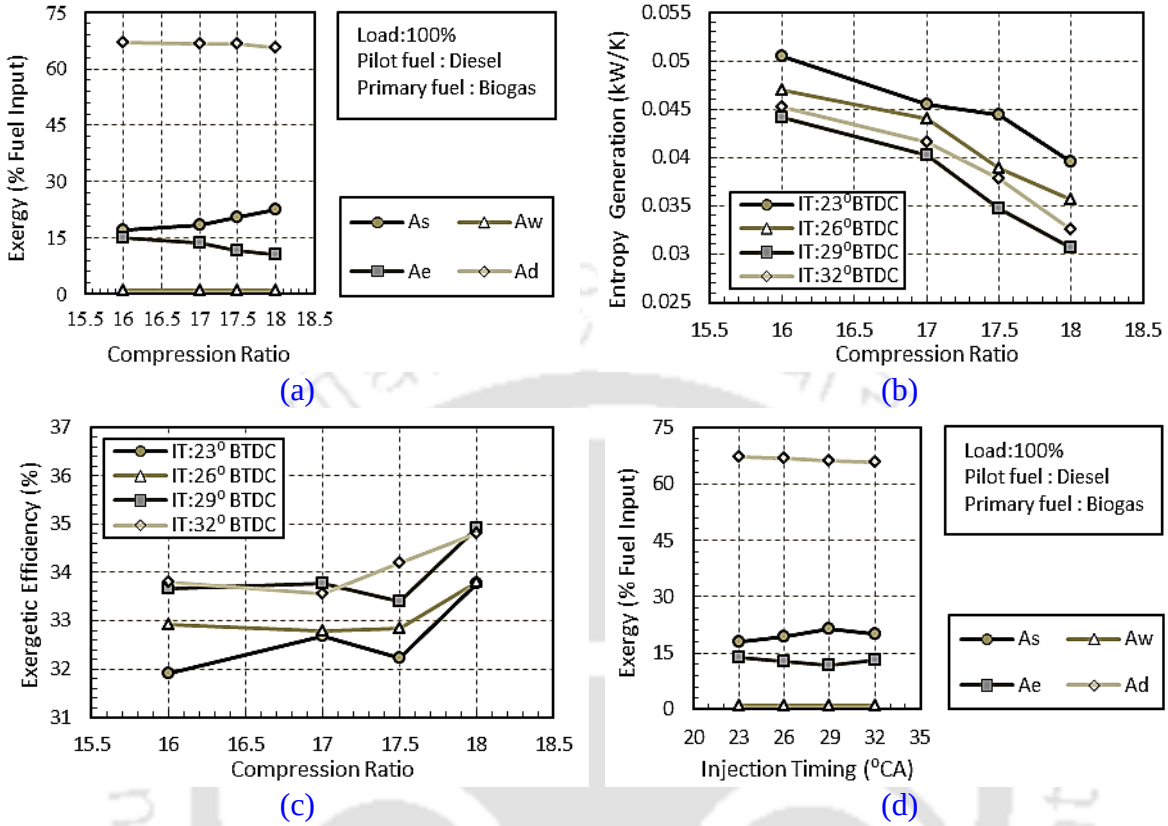

Fig. 10.2 Effect of CR and IT on exergy analysis of a diesel-biogas run dual fuel engine

10.3 Energy and Exergy Distributions of the RBB - Biogas Run Dual Fuel Engine

The upcoming section discusses the energy and exergy distributions of a biogas run dual fuel engine using RBB as pilot fuel. The experimental matrix consists of twelve combinations of CRs 17, 17.5, and 18; and ITs of 23º, 26º, 29° and 32º BTDCs at full loading condition as discussed in Chapter 6.

10.3.1 Energy Analysis

The distribution of energy per unit time of a biogas run dual fuel engine using RBB as pilot fuel through different process for different combinations of CR and IT at full load is given in Table 10.3.

Table 10.3 Results of energy analysis for different combination of ITs and CRs at 100% load

Mode	CR	IT	Q_{in} (kW)	Q_s (kW)	Q_w (kW)	Q_e (kW)	Q_u (kW)
Diesel	17.5	23	12.64	3.51	5.02	3.04	1.05
Dual	18	23	16.96	3.51	5.15	6.79	1.51
	17.5	23	18.05	3.57	5.32	7.55	1.85
	17	23	19.41	3.46	5.23	7.89	2.83
	18	26	15.71	3.46	4.88	5.99	1.37
	17.5	26	17.33	3.51	5.22	6.82	1.77
	17	26	17.93	3.48	5.1	7.32	2.04
	18	29	15.08	3.52	4.8	5.34	1.42
	17.5	29	16.65	3.52	5.12	6.32	1.69
	17	29	17.59	3.53	5.22	7.01	1.83
	18	32	13.57	3.51	4.5	4.32	1.24
	17.5	32	14.9	3.58	4.8	5.2	1.32
	17	32	17.37	3.66	5.4	6.77	1.53

Effect of CR on Energy Distributions

To investigate the influence of CR on various energies distribution under DFM, the values of four ITs are averaged and included in Fig. 10.3(a). On an average, the shaft energy and the energy taken away by the coolant increases by 16.63% and 7.96%, respectively for the increase of CR from 17 to 18 at 23° BTDC. However, for the same setting, the energy taken away by the exhaust and uncounted energy losses decreases by 10.04% and 14.62%, respectively. The BTEs are found to be 20.71%, 19.97% and 18.38% for CRs of 18, 17.5 and 17, respectively at IT of 23° BTDC as depicted in Fig. 10.3(b). On an average, there is a decrease of BSEC and BFR by 11.34% and 9.61%, respectively on increasing the CR from 17 to 18 as indicated in Figs. 10.3 (c) and 10.3 (d). The LFR is found to be 80%, 79% and 78.26% for CRs of 18, 17.5 and 17, respectively at IT of 23° BTDC as observed from Fig. 10.3(e). On increasing of CR from 17 to 18, there is a rise in PCP and PHRR by 14.13% and 29.87%, respectively as depicted in Fig. 10.3(f). On an average, there is a drop of 7% in EGT on change of CR from 17 to 18 as indicated in Fig. 10.3(g).

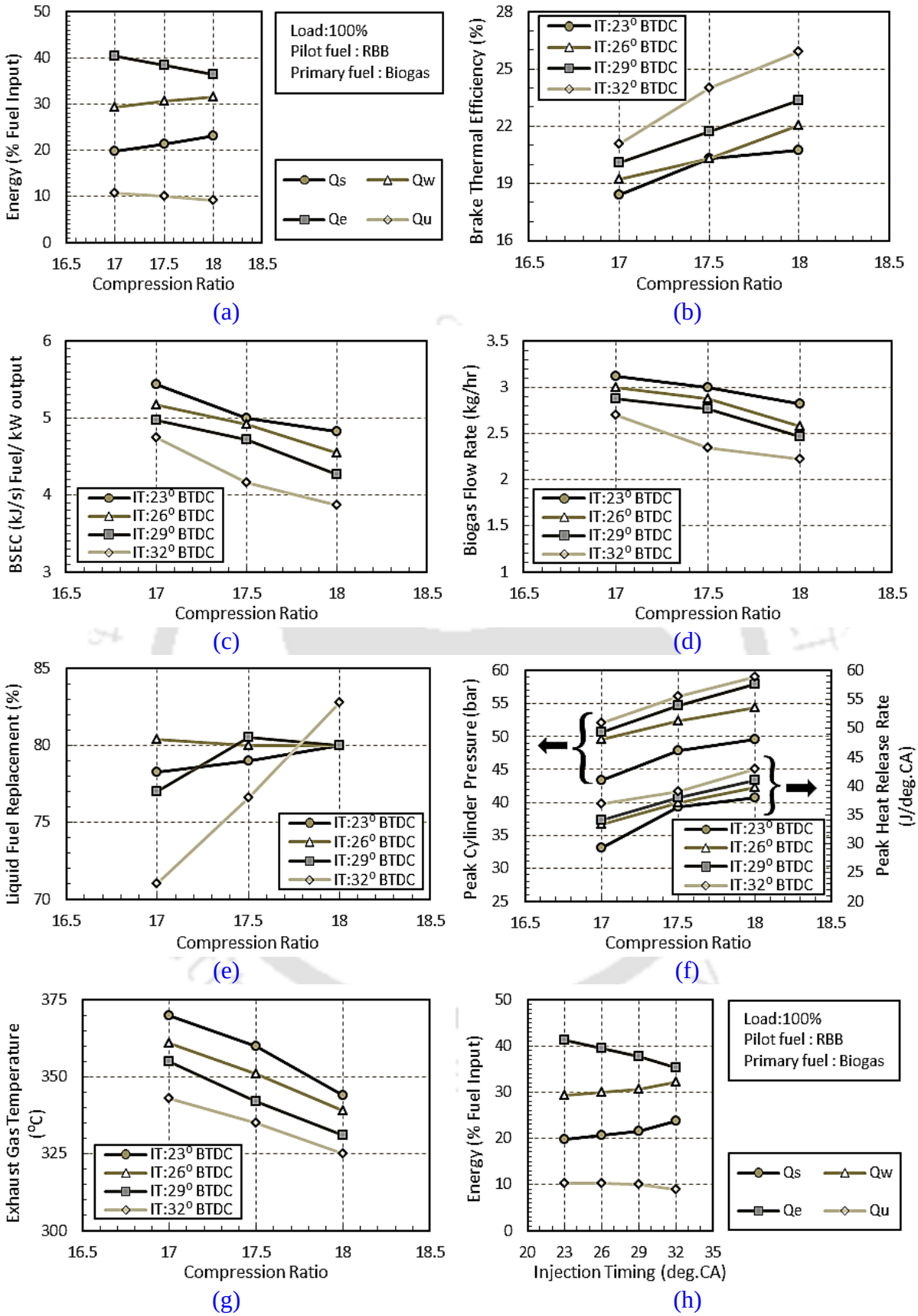

Fig. 10.3 Effect of CR and IT on energy analysis of a RBB-biogas run dual fuel engine

Effect of IT on Energy Distributions

To investigate the effect of IT on various energies distributions under DFM, the values of three CRs is averaged and included in Fig. 10.3(h). With the advancement of IT from 23° BTDC to 32° BTDC, on an average, the shaft energy and energy taken away by the coolant increases by 20.16% and 10.02%, respectively. On the other hand, for the same setting, the energy taken away by the exhaust and uncounted energy losses drop by 14.63% and 13.02%, respectively. For CRs of 18, 17.5, and 17, the BTEs is found to be 22.04%, 20.3% and 19.19% at 26° BTDC in comparison to 23.36%, 21.7% and 20.09% at 29° BTDC. Further advancement of IT by 3°, the BTEs is found to be 25.88%, 24% and 21.08% for CRs of 18, 17.5 and 17, respectively. The advancement of IT from 23° BTDC to 32° BTDC, on an average, displays a drop in BSEC, BFR and EGT by 16.61%, 18.79% and 6.61%, respectively. However, for the same setting, on an average, there is an increase in PCP and PHRR by 18.82% and 14.51%, respectively. The LFR increases marginally with the advancement of IT particularly for CR of 18. For CRs of 18, 17.5, and 17, the LFR is found to be 80%, 80% and 80.25% at 26° BTDC in comparison to 80.51%, 80.51% and 77.71% at 29° BTDC. For same loading condition, the LFR is found to be 82.75%, 72.51% and 71% for CRs of 18, 17.5 and 17, respectively at 32° BTDC.

10.3.2 Exergy Analysis

The findings for exergy analysis for different combinations of CR and IT at full load are included in Table 10.4.

Effect of CR on Exergy Distributions

To investigate the influence of CR on various exergies distribution under DFM, the values of four ITs are averaged and included in Fig. 10.4(a). On an average, the shaft energy availability increases by 16.67% for increase in CR from 17 to 18 at 23° BTDC. However, for the same setting, the exhaust gas availability drops by 24.35%. The average cooling water availability and average availability destroyed is found to be around 1.04% and 66%, respectively. The entropy generation rises by 14.37% for increase in CR from 17 to 18 at 23° BTDC as depicted in Fig. 10.4(b). For all combinations, the CR =18 irrespective of IT produced the maximum exergetic efficiency as indicated in Fig. 10.4(c).

Table 10.4 Results of exergy analysis for different combination of ITs and CRs at 100% load

Mode	CR	IT	A_{in} (kW)	A_s (kW)	A_w (kW)	A_e (kW)	A_d (kW)	η_{II} (%)
Diesel	17.5	23	13.07	3.51	0.11	1.04	8.39	35.74
Dual	18	23	16.87	3.51	0.15	1.94	11.26	33.19
	17.5	23	17.95	3.57	0.16	2.09	12.08	32.42
	17	23	19.19	3.46	0.16	2.42	13.15	31.47
	18	26	15.63	3.46	0.16	1.59	10.42	33.38
	17.5	26	17.23	3.51	0.15	1.98	11.57	32.84
	17	26	17.82	3.48	0.17	2.29	11.88	33.31
	18	29	15.02	3.52	0.15	1.29	10.03	33.17
	17.5	29	16.56	3.52	0.15	1.79	11.09	33.02
	17	29	17.52	3.53	0.16	2.22	11.58	33.86
	18	32	13.51	3.51	0.14	1.01	8.84	34.56
	17.5	32	14.89	3.58	0.18	1.32	9.79	34.21
	17	32	17.36	3.66	0.15	1.99	11.54	33.48

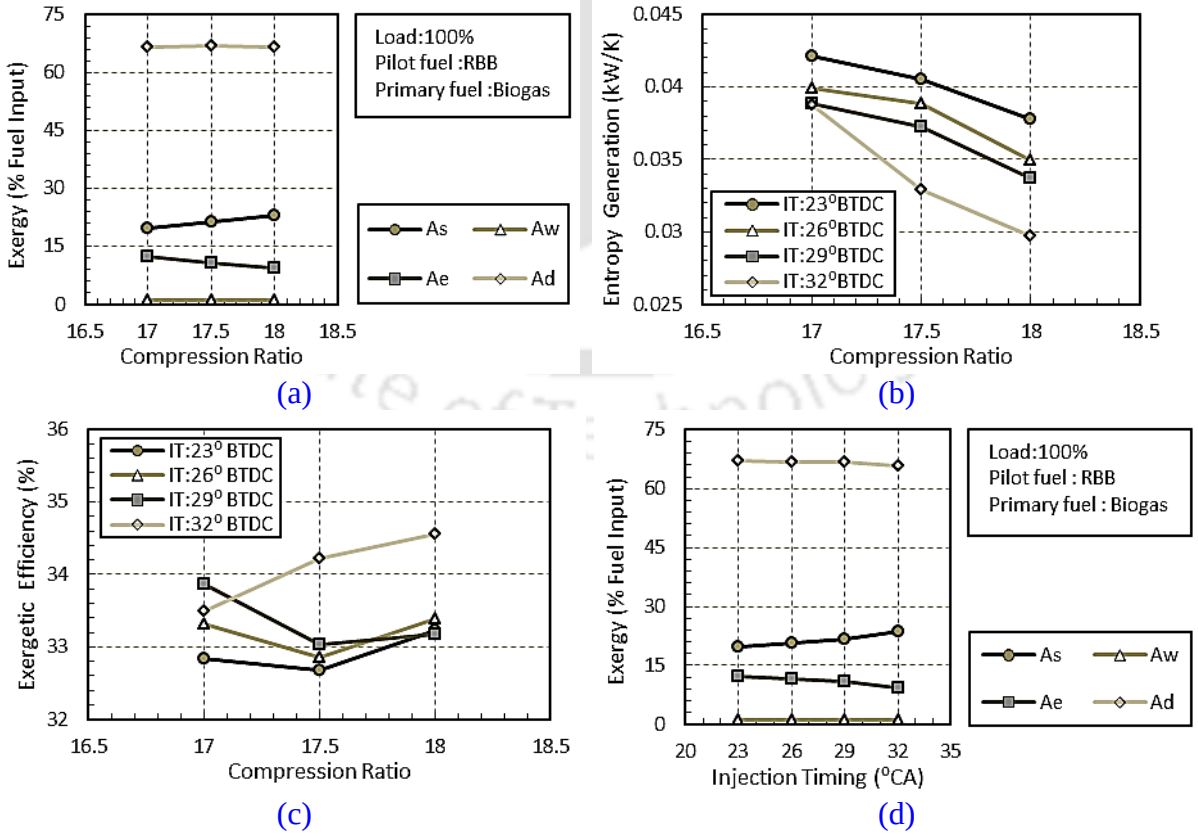

Fig. 10.4 Effect of CR and IT on exergy analysis of a RBB-biogas run dual fuel engine

Effect of IT on Exergy Distributions

To study the effect of IT on various exergies distribution under DFM, the values of three CRs are averaged and included in Fig. 10.4(d). On an average, the shaft energy availability rises by 19.72% on advancement of IT from 23° BTDC to 32° BTDC. For the same change of IT, on an average, the exhaust gas availability and availability destroyed drops by 22.69% and 1.75%, respectively. The increase of cooling water availability is very minimal (i.e. around 0.1%) for the same combination of IT and CR. On advancement of IT from 23° to 32° BTDC, the entropy generation decreases by 9.97%.Among the range of operating parameters tested, the IT = 32° BTDC and CR=18 gives the best better second law efficiency. This also means that the entropy generation ids least for this particular combination.

10.4 Energy and Exergy Distributions of the WIRBB-Biogas Run Dual Fuel Engine

The upcoming section discusses the energy and exergy distributions of a biogas run dual fuel engine using WIRBB as pilot fuel. The experimental matrix consists of twelve combinations of CRs 17, 17.5, and 18; and ITs of 23º, 26º, 29° and 32º BTDCs at full loading condition as discussed in Chapter 8.

10.4.1 Energy Analysis

The distribution of energy per unit time through various processes at different combinations of CR and IT at full load is given in Table 10.5.

Effect of CR on Energy distributions

To analyse the effect of CR on various energy distributions under DFM, the values of four ITs are averaged and included in Fig. 10.5(a). At 23° BTDC, on an average, the shaft energy and the energy transferred to the cooling water increased by 17.59% and 3.83%, respectively for the change of CR from 17 to 18. However, for the same setting, the energy transferred to the exhaust gas and uncounted energy losses decreases by 5.67% and 19.35%, respectively. At IT of 23° BTDC, the BTEs are found to be 19.84%, 18.07%, and 17.4% for CRs of 18, 17.5 and 17, respectively as depicted in Fig. 10.5(b). This can be attributed to the fast occurrence of microexplosion due to the rise of temperature and the pressure with the increase in CR. This initiates the earlier ignition of pilot fuel, thereby giving sufficient time

for the combustion of biogas. On an average, on increasing CR from 17 to 18, the exergetic efficiency increases by 3.32%

Table 10.5 Results of energy analysis for different combination of ITs and CRs at 100% load

Mode	CR	IT	Q_{in} (kW)	Q_s (kW)	Q_w (kW)	Q_e (kW)	Q_u (kW)
Diesel	17.5	23	12.64	3.51	5.02	3.04	1.05
Dual	18	23	17.75	3.52	5.50	7.12	1.61
	17.5	23	19.49	3.52	5.74	8.12	2.1
	17	23	20.23	3.52	5.63	8.49	2.58
	18	26	16.7	3.56	5.24	6.39	1.5
	17.5	26	18.49	3.56	5.57	7.44	1.92
	17	26	19.44	3.56	5.92	7.92	2.04
	18	29	14.9	3.52	4.73	5.38	1.27
	17.5	29	17.01	3.56	5.23	6.49	1.72
	17	29	17.75	3.52	5.52	6.92	1.78
	18	32	15.75	3.52	4.89	5.94	1.39
	17.5	32	17.69	3.52	5.48	6.79	1.89
	17	32	18.82	3.49	5.87	7.46	1.99

On an average, there is a decrease of BSEC and BFR by 14.52% and 14.76%, respectively on increasing the CR from 17 to 18 as indicated in Figs. 10.5(c) and 10.5(d). At 23° BTDC, the LFR is found to be 79.25%, 77.77% and 76.79% for CRs of 18, 17.5 and 17, respectively as observed from Fig. 10.5(e). Upon increasing the CR from 17 to 18, there is an increase in PCP and PHRR by 9.52% and 21.35%, respectively as depicted in Fig. 10.5(f). On an average, there is a drop of 6.18% in EGT on change of CR from 17 to 18 as indicated in Fig. 10.5 (g). This is due to the increase in burning velocity of the biogas air mixture with the increase of CR. Therefore, there is reduction in time for the complete combustion, and this result in lowering the EGT. Alongside, the occurrence of micro-explosion phenomenon due to emulsified pilot fuel also instrumental in lowering of EGT.

Effect of IT on Energy Distributions

To analyse the effect of IT on various energy distributions under DFM, the values of four CRs are averaged and included in Fig. 10.5(h). With the advancement of IT from 23° BTDC

to 32° BTDC, on an average, the shaft energy and energy transferred to the cooling water rises by 9.95% and 5.67%, respectively.

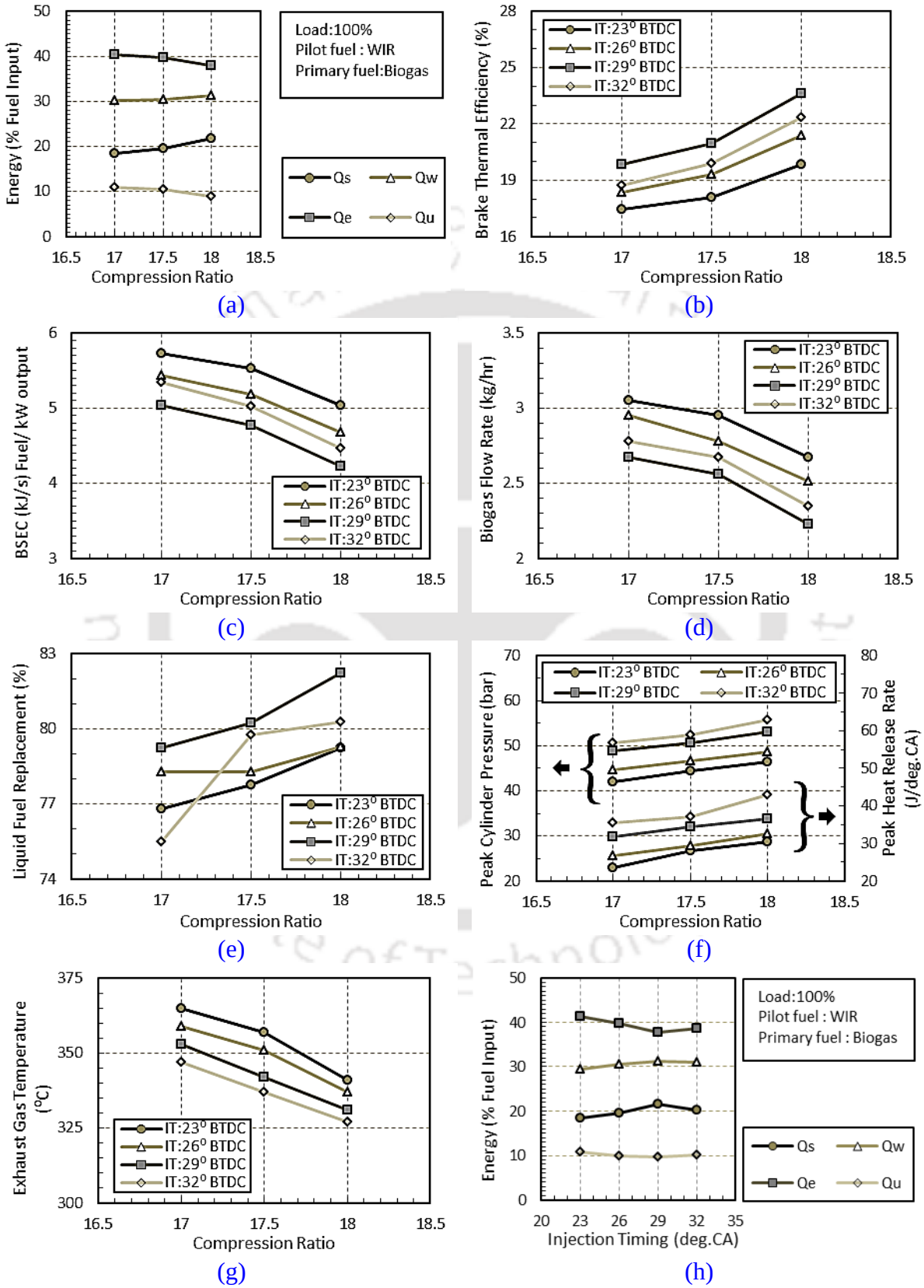

Fig. 10.5 Effect of CR and IT on energy analysis of a WIRBB-biogas run dual fuel engine

On the other hand, for the same setting, the energy transferred to the exhaust gas and uncounted energy losses reduces by 6.87% and 7.81%, respectively. For CRs of 18, 17.5 and 17, the BTEs are found to be 21.36%, 19.29% and 18.35% at 26° BTDC in comparison to 23.62%, 20.97% and 19.89% at 29° BTDC. Further advancement of IT by 3°, the BTEs are found to be 22.36%, 19.91%, and 18.27% for CRs of 18, 17.5 and 17, respectively. This analysis highlights important findings that that there is an improvement of BTE with the advancement of IT of pilot fuel up to a particular IT. This is because IT advancement results in injection of WIRBB earlier into the combustion chamber than standard IT. This gives sufficient time for the WIRBB to form a homogeneous mixture with air and biogas, thereby the biogas burns more efficiently. The advancement of IT from 23° BTDC to 32° BTDC, on an average, exhibits a drop in BSEC, BFR and EGT by 9.01%, 10.03% and 4.89%, respectively. However, for the same setting, on an average, there is a rise in PCP and PHRR by 19.67% and 40.72%, respectively. For CRs of 18, 17.5 and 17, the LFR is found to be 79.47%, 78.27% and 78.21% at 26° BTDC in comparison to 82.22%, 80.24% and 79.25% at 29° BTDC. For same loading condition, the LFR is found to be 80.24%, 79.75% and 75.46% for CRs of 18, 17.5 and 17, respectively at 32° BTDC.

10.4.2 Exergy Analysis

The distribution of exergy per unit time through various processes at different combinations of CR and IT at full load is given in Table 10.6.

Effect of CR on Exergy Distributions

To investigate the effect of CR on various exergy distributions under DFM, the values of four ITs are averaged and included in Fig. 10.6(a). The shaft energy availability increases by 17.55% for increase in CR from 17 to 18 at 23° BTDC. However, for the same setting, the exhaust gas availability decreases by 19.73%. The average cooling water availability and average availability destroyed are found to be around 1.02% and 67.52%, respectively. On increasing CR from 17 to 18, the entropy generation decreases by 15.74% as indicated in Fig. 10.6(b). Among CRs tested, the compression ratio =18 irrespective of IT produces maximum exergetic efficiency as observed in Fig. 10.6(c).

Table 10.6 Results of exergy analysis for different combination of ITs and CRs at 100% load

Mode	CR	IT	A_{in} (kW)	A_s (kW)	A_w (kW)	A_e (kW)	A_d (kW)	η_{II} (%)
Diesel	17.5	23	13.07	3.51	0.11	1.04	8.39	35.74
Dual	18	23	17.59	3.52	0.16	2.02	11.89	32.42
	17.5	23	19.31	3.52	0.18	2.25	13.36	30.83
	17	23	20.05	3.52	0.21	2.56	13.75	31.4
	18	26	16.55	3.56	0.18	1.72	11.08	33.05
	17.5	26	18.33	3.56	0.18	2.14	12.45	32.07
	17	26	19.26	3.56	0.18	2.49	13.03	32.34
	18	29	14.77	3.52	0.15	1.34	9.76	33.92
	17.5	29	16.86	3.56	0.16	1.81	11.32	32.84
	17	29	17.59	3.52	0.17	2.28	11.63	33.89
	18	32	15.63	3.52	0.19	1.49	10.42	33.29
	17.5	32	17.53	3.52	0.22	1.92	11.87	32.25
	17	32	18.67	3.49	0.17	2.2	12.8	31.41

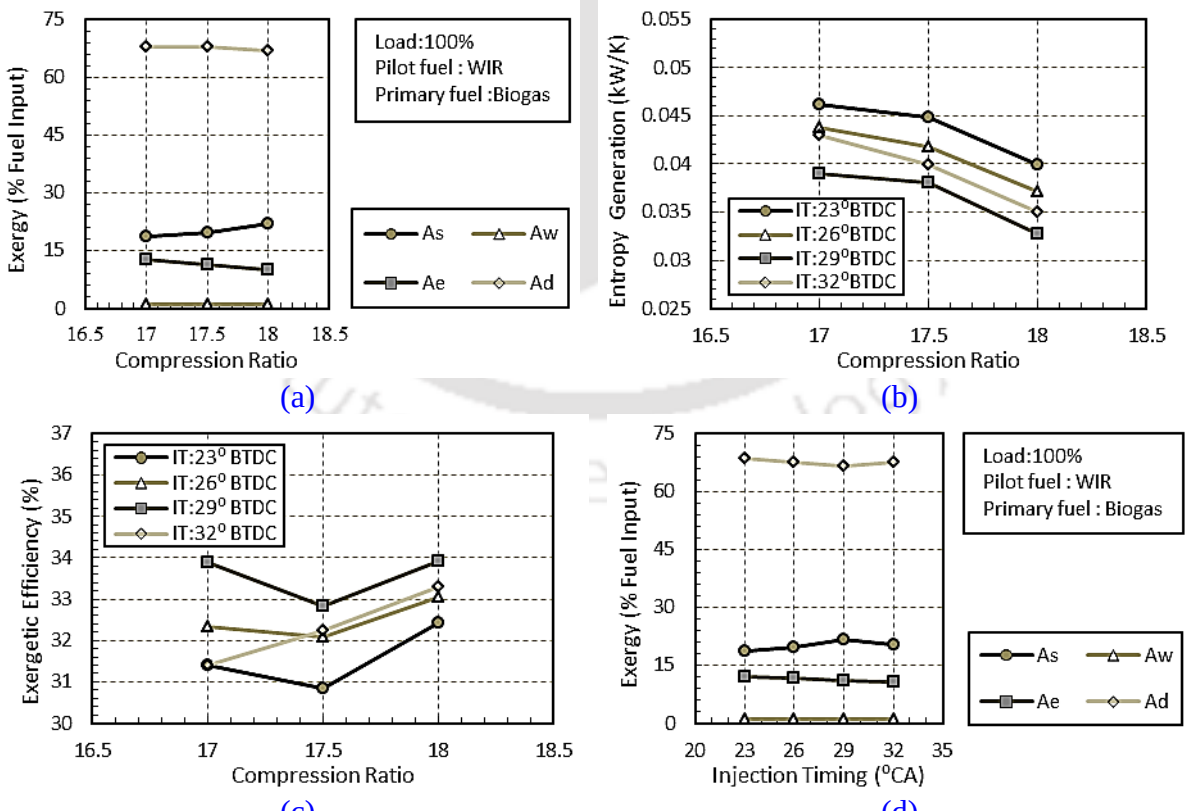

Fig. 10.6 Effect of CR and IT on exergy analysis of a WIRBB-biogas run dual fuel engine

Effect of IT on Exergy Distributions

To study the effect of IT on various exergy distributions under DFM, the values of four CRs are averaged and included in Fig. 10.6(d). On an average, the shaft energy availability and cooling water availability rises by 9.86% and 16.59%, respectively on advancement of IT from 23° BTDC to 32° BTDC. For the same change of IT, on an average, the exhaust gas availability and availability destroyed decrease by 10.27% and 1.12%, respectively. Exergy analysis has shown a conversion of fuel energy by 32.47% to useful means of energy. For advancement of IT from 23° to 32° BTDC, the entropy generation decreases by 9.97%. Among ITs tested, the pilot fuel injection timing =29° BTDC irrespective of CR produces maximum exergetic efficiency.

10.5 Summary

The details of energy and exergy analysis of a biogas run dual fuel diesel engine using diesel, RBB and WIRBB as pilot fuel for different combinations of CR and at full load condition summarizes following key points**.**

- The energy analysis demonstrated that biogas run dual fuel diesel engine using diesel as pilot fuel can recover around 20.12% of the energy supplied by the fuel. Rest of the energy is flown through the cooling water, exhaust gas and other uncounted losses. The increase in CR cause decrease in fuel supply for same BP or shaft power. Therefore, shaft power per unit fuel supply is increased. The study revealed that the CR=18 and pilot fuel IT=29° BTDC were found to be optimum for this particular diesel engine, which produced a BTE of 25.44% along with a LFR of 82.11%.

- The exergy analysis of the biogas run dual fuel diesel engine using diesel as pilot fuel showed that around 33.44% of the fuel exergy input can be converted in useful means of energy or exergy. The shaft availability is increased with the increase of CR, and advancement of IT. However, cooling water and exhaust gas availability is found to be very low for both CR and IT variation.

- The energy analysis indicated that biogas run dual fuel diesel engine using RBB as pilot fuel can recover around 21.46% of the energy supplied by the fuel. The optimum

combination is found to be CR=18 and pilot fuel IT=32° BTDC, which produced a BTE of 25.44% along with a LFR of 82.75%.

- The exergy analysis of biogas run dual fuel diesel engine using diesel as pilot fuel revealed that around 33.24% of the fuel exergy input can be converted in useful means of energy or exergy.

- The energy analysis exhibited that biogas run dual fuel diesel engine using WIRBB as pilot fuel can recover around 19.94% of the energy supplied by the fuel. The investigation indicated that the CR=18 and pilot fuel IT=29° BTDC were found to be optimum for this particular diesel engine, which produced a BTE of 23.68% along with a LFR of 82.22%.

- The exergy analysis of biogas run dual fuel diesel engine using WIRBB as pilot fuel showed that around 32.47% of the fuel exergy input can be converted in useful means of energy or exergy. The exergy destruction is reduced with the rise in CR and advancement of pilot fuel IT irrespective of the pilot fuel used in the biogas run dual fuel diesel engine.

Based on the above investigation, biogas run dual fuel engine should be operated at a high compression ratio and advanced injection timing of pilot fuel for effective utilization of fuel. However, the exact advancement of the injection timing depends on the type of pilot fuel used, which can be found out through experimentation.

Chapter-11

Conclusion and Future Scopes

Overview:

At present, diesel engines are the most fuel efficient combustion engines and diesel fuel is the dominant fuel used in the commercial transportation, industrial and transport sectors. However, the diesel engines suffer from high smoke and oxides of nitrogen emissions. The more stringent governmental regulation on the exhaust emissions and the fast of worldwide petroleum reserves provides a strong encouragement to search for alternative renewable fuels. Biogas, one such renewable fuel, can be successfully used in diesel engines under dual fuel mode. However, biogas run dual fuel engine produces inferior performance at standard diesel setting mainly due to the low calorific value of biogas. On the other hand, proper adjustment of the operating parameters can enhance the performance of a biogas run dual fuel diesel engine. The present study attempts to standardize the operating parameters, namely, compression ratio and injection timing for a biogas run dual fuel diesel engine for stationary applications using different test pilot fuels. The main aim of this chapter is to analyse the contribution of the present work, application potential and future scope.

Chapter Outline:

11.1 Contribution of the Present Work

The main contribution of this study is standardization of the operating parameters of a biogas run dual fuel diesel engine for stationary applications using different types of pilot fuel. The operating parameters considered for this investigation are compression ratio (CR) and injection timing (IT). Keeping in vista of current fuel crisis, at first, a comparative analysis of different types of biodiesel as pilot fuel is carried out to assess the best pilot fuel for this particular composition of raw biogas. This is followed by enhancement of performance of a biogas run dual fuel diesel engine through standardization of the operating parameters for different types of pilot fuel, namely, diesel, RBB and emulsified RBB as pilot fuel. Thirdly, a thermodynamic analysis of the biogas run dual fuel engine using diesel, RBB and emulsified RBB as pilot fuel is carried out to unravel the effect of operating parameters on the exergy and energy distribution. For experimentation, a 3.5 kW single cylinder, direct injection, water cooled, variable compression ratio diesel engine into biogas run dual fuel diesel engine by connecting a venturi gas mixer at its inlet manifold and installing a fuel control mechanism.

11.1.1 Pilot Fuel Study

The main objective of pilot fuel study is to carry out a comparative analysis among the three biodiesels is carried out to evaluate the best pilot fuel on the basis of performance, combustion and emission analysis of a biogas run dual fuel diesel engine at standard diesel setting. Three biodiesels namely, rice bran biodiesel (RBB), pongamia biodiesel (POBD) and palm biodiesel (PBD) based on the availability were considered for the investigation. The main findings of this work are discussed below

- The pilot fuel study indicated that RBB-biogas produced a maximum brake thermal efficiency (BTE) of 19.97% in comparison to 18.4% and 17.4% for POBD-biogas and PBD-biogas, respectively at 100% load.

- At 100% load, the maximum liquid fuel replacement (LFR) is found to be 79%, 78% and 77% for RBB-biogas, POBD-biogas and PBD-biogas, respectively.

- There is an increase of carbon monoxide (CO) emission by 25.74% and 32.58% for POBD-biogas and PBD-biogas, respectively in comparison to RBB-biogas.

- The hydrocarbon (HC) emissions for POBD-biogas and PBD-biogas increased by 11.73 % and 16.27 %, respectively in comparison to that of RBB-biogas.

- There is a decrease in oxides of nitrogen (NOx) emission by 5.8% and 14% for POBD-biogas and PBD-biogas, respectively in comparison to RBB-biogas.

- The carbon dioxide (CO_2) emission for POBD-biogas and PBD-biogas decreased by 23.1% and 31.83%, respectively in comparison to that of RBB-biogas.

Based on the above analysis, it can be concluded that RBB proved to be the best pilot fuel for a biogas run dual fuel diesel engine among the liquid fuels tested.

11.1.2 Standardisation of Operating Parameters for a Biogas Run Dual Fuel Engine

The operating parameters namely, compression ratio (CR) and injection timing (IT), were standardised on the basis performance and emission characteristic for a biogas run dual fuel diesel engine using three different types of pilot fuel. The pilot fuel includes diesel, RBB and emulsified RBB (WIRBB). The main findings of this study are discussed below

For Diesel Pilot Fuel:

- The BTE of the biogas run dual engine is found to be increase with the use of high CR of 18. However, with the advancement of pilot fuel IT, the performance improves up to a particular IT. The maximum BTE of 25.44% is obtained for a combination of CR=18 and IT=29° BTDC.

- At 23° BTDC with 100% load, the LFR is found to be 79.46%, 76.1%, 74% and 72% for CRs of 18, 17.5, 17 and 16, respectively. For CRs of 18, 17.5, 17 and 16, the LFR is found to be 83.17%, 80.67%, 76.06% and 75.22%, respectively at 26° BTDC in comparison to 82.67%, 80.70%, 76.06 and 75.22% at 29° BTDC. However, at 32° BTDC, the LFR is found to be 79.32%, 78.4%, 76.13% and 76.1% for CRs of 18, 17.5, 17 and 16, respectively.

- On an average, there is an increase of 23.23% in CO_2 emission on advancing IT from 23° to 32° BTDC for CR of 18. For the same range of IT, there is an increase of 18.18%, 15.37% and 14.97% in CO_2 emission for CR of 17.5, 17 and 16, respectively.

- Therefore, there is an increase of 27.18% in CO_2 emission while increasing the CR from 16 to 18 at 23° BTDC.

- There is a reduction of 26.22% in CO emission by increasing the CR from 16 to 18 at 23° BTDC. There is a reduction of 5.59% in CO emission on advancing IT from 23° to 32° BTDC for CR of 18. For the same range of IT, there is a reduction of 6.56%, 8.64% and 10.7% in CO emission for CR of 17.5, 17 and 16, respectively.

- There is a reduction of 41.97% in HC emission is achieved by increasing the CR from 16 to 18 at 23° BTDC. There is reduction of 9.54% in HC emission is achieved on advancing IT from 23° to 32° BTDC for CR of 18. For the same range of IT, on an average, there is a reduction of 10.03%, 13.83% and 8.98% in HC emission for CRs of 17.5, 17 and 16, respectively.

- There is an increase of 38.81% in NO_X emission is resulted by increasing the CR from 16 to 18 at 23° BTDC. there is an increase of 15.91% in emission is achieved on advancing IT from 23° BTDC to 32° BTDC for CR of 18. For the same range of IT, there is increase of 10.76%, 9.7% and 4.2% in NO_X emission for CR of 17.5, 17 and 16, respectively.

For RBB Pilot Fuel:

- The BTE of the RBB-biogas run dual engine is found to be increase with the use of high CR of 18. The performance improves further with the advancement of pilot fuel IT. The maximum BTE of 25.88% is obtained for a combination of CR=18 and IT=32° BTDC.

- At 23° BTDC with 100% load, the LFR is found to be 80%, 79% and 78.26% for CRs of 18, 17.5 and 17, respectively. For the same loading conditions at CRs of 18, 17.5 and 17, the LFR is found to be 80%, 80% and 80.25% at 26° BTDC in comparison to 80.51%, 80.51% and 77.71% at 29° BTDC. However, the LFR is found to be 82.75%, 72.51% and 71% for CRs of 18, 17.5 and 17, respectively at 32° BTDC.

- There is an average rise in CO_2 emission by 13.78% on increasing the CR from 17 to 18 at 23° BTDC. Therefore, there is a rise of 17.43% in CO_2 emission on advancing IT from 23° to 32° BTDC for CR of 18. For the same range of IT, on an average, there is

an increase of 17.14% and 12.21% in CO_2 emission for CR of 17.5 and 17, respectively.

- There is an average drop in CO emission by 17.67% on increasing the CR from 17 to 18 at 23° BTDC. There is a reduction of 11.64% in CO emission on advancing IT from 23° to 32° BTDC for CR of 18. For the same range of IT, on an average, there is a reduction of 6% and 3.38% in CO emission for CR of 17.5 and 17, respectively.

- There is an average reduction in HC emission by 17.67% on increasing the CR from 17 to 18 at 23° BTDC. On an average, there is a reduction of 15.24% in HC emission is achieved on advancing IT from 23° to 32° BTDC for CR of 18 under DFM. For the same range of IT, on an average, there is a reduction of 13.14% and 14.27% in HC emission for CRs of 17.5 and 17, respectively.

- There is an average increase in NO_X emission by 42% on increasing the CR from 17 to 18 at 23° BTDC. There is an increase of 39% in emission is achieved on advancing IT from 23° to 32° BTDC for CR of 18 under DFM. For the same range of IT, there is a rise of 41.42% and 52.14% in NO_X emission for CR of 17.5 and 17, respectively.

For Emulsified RBB Pilot Fuel:

A two-phase stable WIRBB emulsion was prepared in the laboratory using by optimizing the factors such as water content (5%and 10%), surfactants (3%), and hydrophilic lipophilic balance (HLB) values. The prepared WIRBB was then characterized by means of droplet diameter measurement and stability study. The results of this study are summarized as follows

- The values of mean droplet diameter (1.64 µm for 5% water WIRBB) fall within the acceptable range of maximum (20 µm) and minimum (0.1 µm) values.

- The longer the emulsification time, lower is the mean droplet diameter.

- Higher the surfactant quantity, lower is the mean droplet diameter.

- Increase in water quantity increases droplet size.

- Larger water quantity increases separation and sedimentation.

The prepared WIRBB is tested as a pilot fuel in a biogas run dual fuel engine for a set of combinations of CRs and ITs at different loading conditions. The results of the analysis are discussed below

- The BTE of the WIRBB-biogas run dual engine is found to be increase with the use of high CR of 18. The performance improves further with the advancement of pilot fuel IT. The maximum BTE of 23.62% is obtained for a combination of CR=18 and IT=29° BTDC.

- At 23° BTDC with 100% load, the LFR is found to be 79.25%, 77.77% and 76.79% for CRs of 18, 17.5 and 17, respectively. For the same loading conditions at CRs of 18, 17.5 and 17, the LFR is found to be 79.47%, 78.27% and 78.21% at 26° BTDC in comparison to 82.22%, 80.24% and 79.25% at 29° BTDC. However, the LFR is found to be 80.24%, 79.25% and 75.46% for CRs of 18, 17.5 and 17, respectively at 32° BTDC.

- There is an average rise in CO_2 emission by 24.45% on increasing the CR from 17 to 18 at 23° BTDC. Therefore, there is a rise of 13.76% in CO_2 emission on advancing IT from 23° to 32° BTDC for CR of 18. For the same range of IT, on an average, there is an increase of 16.89% and 23.02% in CO_2 emission for CR of 17.5 and 17, respectively.

- There is an average drop in CO emission by 17.6% on increasing the CR from 17 to 18 at 23° BTDC. There is a reduction of 4.7% in CO emission on advancing IT from 23° to 32° BTDC for CR of 18. For the same range of IT, on an average, there is a reduction of 3.27% and 7.34% in CO emission for CR of 17.5 and 17, respectively.

- There is an average reduction in HC emission by 32.8% on increasing the CR from 17 to 18 at 23° BTDC. On an average, there is a reduction of 6.23% in HC emission is achieved on advancing IT from 23° to 32° BTDC for CR of 18 under DFM. For the same range of IT, on an average, there is a reduction of 11.96% and 13.5% in HC emission for CRs of 17.5 and 17, respectively.

- There is an average increase in NO_X emission by 40.98% on increasing the CR from 17 to 18 at 23° BTDC. There is an increase of 16.26% in emission is achieved on

advancing IT from 23° to 32° BTDC for CR of 18 under DFM. For the same range of IT, there is a rise of 16% and 18.03% in NO_X emission for CR of 17.5 and 17, respectively.

11.1.3 Energy and Exergy Distributions of a Biogas Run Dual Fuel Engine

This section describes the energy and exergy distribution of diesel-biogas, RBB-biogas and WIRBB-biogas run dual fuel diesel engine under variable CR-IT and full load conditions. The key findings of this investigation are summarized below

For Diesel Pilot Fuel:

- On an average, the energy analysis demonstrated that biogas run dual fuel diesel engine using diesel as pilot fuel can recover around 20.12% of the energy supplied by the fuel. Rest of the energy is flown through the cooling water, exhaust gas and other uncounted losses. The increase in CR cause decrease in fuel supply for same BP or shaft power. When the CR is increased from 16 to 18 at 23° BTDC, the shaft energy and the energy transferred to the cooling water increases by 32.37% and 2.32% respectively. However, for the same setting, the energy loss through exhaust gas and uncounted energy losses decreases by 8.57% and 24.64%, respectively. With the advancement of IT from 23° BTDC to 32° BTDC, the shaft energy and energy transferred to the cooling water rises by 13.91% and 5.93%, respectively. On the other hand, for the same setting, the energy loss through exhaust gas and uncounted energy losses drops by 7.97% and 8.42%, respectively.

- The exergy analysis of the biogas run dual fuel diesel engine using diesel as pilot fuel showed that around 33.44% of the fuel exergy input can be converted in useful means of energy or exergy.

- The shaft energy availability increases by 32.27% for increase in CR from 16 to 18 at 23° BTDC. However, for the same setting, the exhaust gas availability decreases by 28.61%. The average cooling water availability and average availability destroyed are found to be around 0.93% and 67.35%, respectively. On an average, the shaft energy availability increases by 12.47% on advancement of IT from 23° BTDC to 32° BTDC. For the same change of IT, on an average, the exhaust gas availability and

availability destroyed decreases by 5.76% and 2.15%, respectively. The increase of cooling water availability is very marginal (i.e. around 0.17%) for the same combination of IT and CR.

- When CR is increased from 16 to 18, the entropy generation decrease by 25.87%. On advancement of IT from 23° to 32° BTDC, the entropy generation decreases by 12.61%.

For RBB Pilot Fuel:

- On an average, the energy analysis indicated that biogas run dual fuel diesel engine using RBB as pilot fuel can recover around 21.46% of the energy supplied by the fuel. On an average, the shaft energy and the energy taken away by the coolant increases by 16.63% and 7.96%, respectively for the increase of CR from 17 to 18 at 23° BTDC. However, for the same setting, the energy taken away by the exhaust and uncounted energy losses decreases by 10.04% and 14.62%, respectively. With the advancement of IT from 23° BTDC to 32° BTDC, on an average, the shaft energy and energy taken away by the coolant increases by 20.16% and 10.02%, respectively. On the other hand, for the same setting, the energy taken away by the exhaust and uncounted energy losses drop by 14.63% and 13.02%, respectively.

- The exergy analysis of biogas run dual fuel diesel engine using diesel as pilot fuel revealed that around 33.24% of the fuel exergy input can be converted in useful means of energy or exergy.

- On an average, the shaft energy availability increases by 16.67% for increase in CR from 17 to 18 at 23° BTDC. However, for the same setting, the exhaust gas availability drops by 24.35%. The average cooling water availability and average availability destroyed is found to be around 1.04% and 66%, respectively. On an average, the shaft energy availability rises by 19.72% on advancement of IT from 23° BTDC to 32° BTDC. For the same change of IT, on an average, the exhaust gas availability and availability destroyed drops by 22.69% and 1.75%, respectively. The increase of cooling water availability is very minimal (i.e. around 0.1%) for the same combination of IT and CR.

- The entropy generation rises by 15.74% for increase in CR from 17 to 18. On advancement of IT from 23° to 32° BTDC, the entropy generation decreases by 9.97%.

For Emulsified RBB Pilot Fuel:

- On an average, the energy analysis exhibited that biogas run dual fuel diesel engine using WIRBB as pilot fuel can recover around 19.94% of the energy supplied by the fuel. At 23° BTDC, on an average, the shaft energy and the energy transferred to the cooling water increased by 17.59% and 3.83%, respectively for the change of CR from 17 to 18. However, for the same setting, the energy transferred to the exhaust gas and uncounted energy losses decreases by 5.67% and 19.35%, respectively. With the advancement of IT from 23° BTDC to 32° BTDC, on an average, the shaft energy and energy transferred to the cooling water rises by 9.95% and 5.67%, respectively. On the other hand, for the same setting, the energy transferred to the exhaust gas and uncounted energy losses reduces by 6.87% and 7.81%, respectively.

- The exergy analysis of biogas run dual fuel diesel engine using WIRBB as pilot fuel showed that around 32.47% of the fuel exergy input can be converted in useful means of energy. The exergy destruction is reduced with the rise in CR and advancement of pilot fuel IT irrespective of the pilot fuel used in the biogas run dual fuel diesel engine.

- The shaft energy availability increases by 17.55% for increase in CR from 17 to 18 at 23° BTDC. However, for the same setting, the exhaust gas availability decreases by 19.73%. The average cooling water availability and average availability destroyed are found to be around 1.02% and 67.52%, respectively. On an average, the shaft energy availability and cooling water availability rises by 9.86% and 16.59%, respectively on advancement of IT from 23° BTDC to 32° BTDC. For the same change of IT, on an average, the exhaust gas availability and availability destroyed decrease by 10.27% and 1.12%, respectively. For advancement of IT from 23° to 32° BTDC, the entropy generation decreases by 9.97%.
- On increasing CR from 17 to 18, the entropy generation decreases by 15.74%. For advancement of IT from 23° to 32° BTDC, the entropy generation decreases by 9.97%.

Table 11.1 Performance and emission characteristic of the biogas run dual fuel diesel engine at the optimum operating parameters

Pilot Fuel	Optimised IT	CR	BTE	Emission			
				CO_2 (%)	CO (ppm)	HC (ppm)	NO_X (ppm)
Diesel	29° BTDC	18	25.44%	4.59	121	141	53.77
RBB	32° BTDC	18	25.88%	6.7	97	79	59
Emulsified RBB	29° BTDC	18	23.62%	4.51	137	121	53.16

11.2 Application Potential

The research engine considered for this investigation is commonly available in rural areas, which is used for power generation or for water pumping. Nowadays, most of the renowned genset manufacturing companies like Cummins, Wartsila, and such others rebuilds the old diesel engines to cut down the cost. The present research could be implemented especially to these types of engines with minor modification to convert them to biogas run dual fuel engines, which can solve the problem of power generation in rural areas.

11.3 Future Scopes

In the present investigation, an attempt has been made to revolutionise the biogas technology through enhancement of the performance and emission characteristics of a biogas run dual fuel diesel engine. The findings of the present study have been already discussed in section 11.1. However, further improvement can be done to make the biogas run dual fuel diesel engine more efficient. In this connection, some scope and suggestions for future studies are highlighted here.

- The effect of injection pressure of pilot fuel on the performance and emission characteristic has not been reported in any open literature. The adjustment of the optimum injection pressure of the pilot fuel may enhance the efficiency of the biogas run dual fuel diesel engine.

- The energy and exergy analysis of the present investigation unravels that a considerable amount of exergy of the biogas run dual fuel diesel engine is lost through exhaust gas. Therefore, a means such as heat exchanger to utilize the potential of exhaust gases which can be used in preheating the biogas. The influence of preheating of both liquid fuel and biogas on the performance of the biogas run dual fuel diesel engine has not been reported. This may enhance the performance of the biogas run dual fuel diesel engine particularly at low load.

- In this present study, the investigations were done by conducting short-term tests. However, long term tests should be done to examine the problems like corrosion of engine components, carbon deposits on engine surfaces, engine lubrication, and wear of fuel pump, etc. Thus, to promote biogas run dual fuel diesel engines commercially, long-term test is essential.

- A comprehensive economic analysis of the biogas run dual fuel diesel engines needs to be carried out for promotion of biogas as the alternative fuel for diesel engines. Therefore, a cost analysis of the dual fuel operations can be executed by considering various economic terms such as the fuel cost per kW power production. The performance and emissions study along with the economic assessment can provide a perfect competitive characteristic of biogas as the alternative fuels for diesel engines.

- The study on scrubbed biogas run dual fuel diesel engine is limited. The use of scrubbed biogas may enhance the performance in terms of efficiency and emission characteristics. Besides, the use of scrubbed biogas will prevent the corrosion of engine components.

- Thermodynamic modeling of combustion of biogas run dual fuel engines is also lacking in the literature. The combustion of pilot fuel and subsequently the combustion of primary fuel are complex phenomena. Further, the use of different types of pilot fuel like diesel, biodiesel and emulsified fuel. The assistance of zero, two or three-dimensional modeling can be implemented to know the effect of dual fuel combustion in varying load conditions. Further, software like ANSYS and CHEMKIN PRO can be used to estimate the combustion temperature, ignition delay, heat release rate, combustion duration, etc. This will allow optimizing the rigorous experimentation, and will save a lot of time, effort and money.

References

Abu-Zaid M, (2004), Performance of single cylinder, direct injection diesel engine using water fuel emulsions, *Energy Conservation and Management*, Vol. 45, No. 45, pp. 697-705.

Agarwal AK, (2007), Biofuels (alcohols and biodiesel) applications as fuels for internal combustion engines, *Progress in Energy and Combustion Science*, Vol. 33, No. 3, pp. 233–271.

Agarwal AK, Srivastava DS, Dhar A, Maurya RK, Shukla PC, and **Singh AP**, (2013), Effect of fuel injection timing and pressure on combustion, emissions and performance characteristics of a single cylinder diesel engine, *Fuel*, Vol. 111, pp. 374–383.

Alahmer A, (2013), Influence of using emulsified diesel fuel on the performance and pollutants emitted from diesel engine, *Energy Conversion and Management*, Vol. 73, pp. 361–369.

AL-Najem NM, and **Diab JM**, (1992), Energy-exergy analysis of a diesel engine, *Heat Recovery Systems & CHP*, Vol. 12, No. 6, pp. 525–529.

Banapurmath NR, **Tewari PG, Yaliwal VS, KambalimathS**, and **Basavarajappa YH,** (2009) Combustion characteristics of a 4-stroke CI engine operated on Honge oil, Neem and Rice Bran oils when directly injected and dual fuelled with producer gas induction, *Renewable Energy*, Vol. 34, No.7, pp. 1877–1884.

Bari S, (1996), Effect of carbon dioxide on the performance of biogas/diesel duel-fuel engine, *Renewable Energy*, Vol. 9, No. 1-4, pp. 1007-1010.

Barik D, and **Murugan S**, (2014a), Simultaneous reduction of NOx and smoke in a dual fuel DI diesel engine, *Energy Conversion and Management*, Vol. 84, pp. 217–226.

Barik D, and **Murugan S**, (2014b), Investigation on combustion performance and emission characteristics of a DI (direct injection) diesel engine fuelled with biogas - diesel in dual fuel mode, *Energy*, Vol. 72, No. 1, pp. 760-771.

Becher P, (1965), Emulsions: theory and practice. 2nd edition, USA: Chemical Rubber Co., Cleveland, Ohio.

Bedoya ID, Arrieta AA, and **Cadavid FJ**, (2009), Effects of mixing system and pilot fuel quality on diesel – biogas dual fuel engine performance, *Bioresource Technology*, Vol. 100, No. 24, pp. 6624-6629.

Bedoya ID, Saxena S, Cadavid FJ, and **Dibble RJ**, (2012), Exploring strategies for reducing high intake temperature requirements and allowing optimal operational conditions in a biogas fuelled HCCI Engine for power generation, *ASME Journal of Engineering for Gas Turbines and Power*, Vol. 134, pp. 1-9.

BP Energy Outlook 2035 Report, http://www.bp.com/en/global/corporate/about-bp/energy-economics/energy-outlook.html [Accessed on 19th June, 2015].

.**Buehler Ltd.**, *Buehler Analyst Section***,** USA, 1993**.**

Cacua K, Amell A, and **Cadavid F**, (2012), Effects of oxygen enriched air on the operation and performance of a diesel-biogas dual fuel engine, *Biomass and Bioenergy*, Vol. 45, pp. 159-167.

Caliskan H, Tat ME, and **Hepbasli A**, (2009), Performance assessment of an internal combustion engine at varying dead (reference) state temperatures, *Applied Thermal Engineering*, Vol. 29, No. 16, pp. 3431–3436.

Caton JA, (2000), On the destruction of availability (exergy) due to combustion process—with specific application to internal-combustion engines, *Energy*, Vol. 25, No. 11, pp. 1097–1117.

Chen Z, Wang X, Pei Y, Zhang C, Xi M, and **He J**, (2015), Experimental investigation of the performance and emissions of diesel engines by a novel emulsified diesel fuel, *Energy Conversion and Management*, Vol. 95, pp. 334–341.

Cheng J, (2010), *Biomass to renewable energy processes*, CRC Press, Boca Raton, USA, pp. 151-208.

Cheng-qiu J, Tian-wei L, and **Jian-li Z**, (1989), A study on compressed biogas and its application to the compression ignition dual-fuel engine, *Biomass*, Vol. 20, No. 1-2, pp. 53-59.

Chintala V, and **Subramanian KA**, (2014), Assessment of maximum available work of a hydrogen fuelled compression ignition engine using exergy analysis, *Energy*, Vol. 67, No. 1, pp. 162–175.

Costa YJRD, Lima AGBD, Filho CRB, and **Liman, LDA**, (2012), Energetic and exergetic analyses of a dual-fuel diesel engine, *Renewable and Sustainable Energy Reviews*, Vol. 16, No. 7, pp. 4651–4660.

Crookes RJ, Kiannejad F, and Nazha MAA, (1997), Systematic assessment of combustion characteristics of biofuels and emulsions with water for use as diesel engine fuels, *Energy Conservation and Management*, Vol. 38, No. 15-17, pp. 1785– 1795.

Debnath BK, (2013), *Experimental and theoretical routes towards assessing the potential of emulsified palm biodiesel as an alternative to diesel fuel*, Ph.D thesis, Mechanical Engineering Department, IIT Guwahati, India.

Debnath BK, Sahoo N, and **Saha UK**, (2013a),Thermodynamic analysis of a variable compression ratio diesel engine running with palm oil methyl ester, *Energy Conversion and Management*, Vol. 65, pp. 147–154.

Debnath BK, Saha UK, and **Sahoo N**, (2013b), Adjusting the operating characteristics to improve the performance of an emulsified palm oil methyl ester run diesel engine, *Energy Conversion and Management*, Vol. 69, pp.191-198.

Debnath BK, Saha UK, and **Sahoo N**, (2014a), Theoretical Route toward the Estimation of Second Law Potential of an Emulsified Palm Biodiesel Run Diesel Engine, *ASCE Journal of Energy Engineering*, Vol. 140, pp. A4014007-1–A4014007-10.

Debnath BK, Saha UK, and **Sahoo N**, (2014b), An experimental way of assessing the application potential of emulsified palm biodiesel toward alternative to diesel, *ASME Journal of Engineering for Gas Turbines and Power*, Vol. 136, No. 2, pp. 021401–021412.

Duc PM, and **Wattanavichien K**, (2007), Study on biogas premixed charge diesel dual fuelled engine. *Energy Conversion and Management*, Vol. 48, No. 8, pp. 2286-2308.

Ebiana AB, Savadekar RT, and **Patel KV**, (2005), Entropy generation/availability energy loss analysis inside MIT gas spring and 'two space' test rigs, Paper No. AIAA2005-5675, *Proceeding of Third International Energy Conversion Engineering Conference (IECEC*), San Francisco, American Institute of Aeronautics and Astronautics, Reston, VA.

El_Kassaby M, and **Nemit_allah M**, (2013), Studying the effect of compression ratio on a engine fuelled with waste oil produced biodiesel/diesel fuel, *Alexandria Engineering Journal*, Vol. 52, No. 1, pp. 1-11.

Flynn PF, Hoag KL, Kamel MM, and **Primus, RJ**, (1984), A new perspective on diesel engine evaluation based on second law analysis, *Society of Automotive Engineers*, Paper No. 840032.

Ganesan V, (2012), *Internal Combustion Engines*, 4th edition, Tata McGraw Hill Education Private Limited, New Delhi, India**.**

Ghazikhani M, Feyz ME, and **Joharchi A**, (2010), Experimental investigation of the exhaust gas recirculation effects on irreversibility and brake specific fuel consumption of indirect injection diesel engines, *Applied Thermal Engineering*, Vol. 30, No. 13, pp. 1711–1718.

Ghazikhani M, Hatami M, Ganji DD, Gorji-Bandpy M, Behravana A, and **Shahi G,** (2014), Exergy recovery from the exhaust cooling in a DI diesel engine for BSFC reduction purposes, *Energy*, Vol. 65, pp. 44–51.

Ghojel J, Honnery D, and **Al-khaleefi K**, (2006), Performance, emissions and heat release characteristics of direct injection diesel engine operating on diesel oil emulsion, *Applied Thermal Engineering*, Vol. 26, No. 17-18, pp. 2132-2141.

Giakoumis EG, (2013), A statistical investigation of biodiesel physical and chemical properties and their correlation with the degree of unsaturation, *Renewable Energy*, Vol. 50, pp. 858-878.

Giakoumis EG, (2007), Cylinder wall insulation effects on the first- and second-law balances of a turbocharged diesel engine operating under transient load conditions, *Energy Conversion and Management*, Vol. 48, No. 11, pp. 2925–2933

Gorjibandpy M, and **Sangsereki MK**, (2010), Computational Investigation of Air-Gas Venturi Mixer for Powered Bi-Fuel Diesel Engine, *World Academy of Science , Engineering and Technology*, Vol. 4, pp. 11 – 22.

Government of India, Ministry of New and Renewable Energy, National Policy on Biofuels, pp. 1-18. http://www.mnre.gov.in/policy/biofuel-policy.pdf [Accessed on 1st Sept., 2014].

Greeves G, Khan IM, and **Onion G**, (1977), Effects of water introduction on diesel engine combustion and emissions, *Symposium (International) on Combustion*, Vol. 16, No. 1, pp.321-336.

Griffin WC, (1949), Classification of Surface-Active agents by HLB, *Journal of the Society of Cosmetic Chemists*, Vol. 1, pp. 311–320.

Guo X, Rong Z, and **Ying X**, (2006), Calculation of hydrophile–lipophile balance for polyethoxylated surfactants by group contribution method, *Journal of Colloid and Interface Science*, Vol. 298, No. 1, pp. 441–450.

Hatami M, Ganji DD, and **Gorji-Bandpy M**, (2015), Experimental and thermodynamical analyses of the diesel exhaust vortex generator heat exchanger for optimizing its operating condition, *Applied Thermal Engineering*, Vol. 75, pp. 580–591.

Henham A, and **Makkar MK**, (1998), Combustion of simulated biogas in a dual-fuel diesel engine, *Energy Conversion and Management*, Vol. 39, No. 16-18, pp. 2001-2009.

Heywood JB, (1988), *Internal Combustion Engine Fundamentals*, McGraw-Hill Book Company, New York, USA.

Hosseinzadeh A, Saray RK, and **Mahmoudi SMS**, (2010), Comparison of thermal, radical and chemical effects of EGR gases using availability analysis in dual-fuel engines at part loads, *Energy Conversion and Management*, Vol. 51, No. 11, pp. 2321–2329.

Jafarmadar S, (2014), Exergy analysis of hydrogen/diesel combustion in a dual fuel engine using three-dimensional model, *International Journal of Hydrogen Energy*, Vol. 39, No. 17, pp. 9505–9514.

Jemni MA, Kantchev G, and **Abid MS**, (2011), Influence of intake manifold design on in-cylinder flow and engine performances in a bus diesel engine converted to LPG gas fuelled, using CFD analyses and experimental investigations, *Energy*, Vol. 36, No. 5, pp. 2701 – 2715.

Jena J, and **Misra RD**, (2014), Effect of fuel oxygen on the energetic and exergetic efficiency of a compression ignition engine fuelled separately with palm and karanja biodiesels, *Energy*, Vol. 68, pp. 411–419.

Jindal S, Nandwana BP, Rathore NS, and **Vashistha V**, (2010), Experimental investigation of the effect of the compression ratio and injection pressure in a direct engine running on jatropha methyl ester, *Applied Thermal Engineering*, Vol. 30, No. 5, pp. 442-448.

Junior RFB, and **Martins CA**, (2015), Emission analysis of a Diesel Engine Operating in Diesel–Ethanol Dual-Fuel mode, *Fuel*, Vol. 148, pp. 191-201.

Kannan GR, and **Anand R**, (2011), Experimental investigation on diesel engine with diestrol-water micro emulsions, *Energy*, Vol. 36, No. 3, pp. 1680-1687.

Kline SJ, and **McClintock FA**, (1953), Describing uncertainties in single-sample experiments, *Mechanical Engineering*, Vol. 75, pp. 3–8.

Korakianitis T, Namasivayam AM, and **Crookes RJ**, (2010), Hydrogen dual-fuelling of compression ignition engines with emulsified biodiesel as pilot fuel, *International Journal of Hydrogen Energy*, Vol. 35, No. 24, pp. 13328-13344.

Korakianitis T, Namasivayam AM, and **Crookes RJ**, (2011), Diesel and rapeseed methyl ester (RME) pilot fuels for hydrogen and natural gas dual-fuel combustion in compression–ignition engines, *Fuel*, Vol. 90, No. 7, pp. 2384–2395.

Kotas TJ, (1985), *The exergy method of thermal power plant analysis*, London, UK: Butterworths.

Kumar MS, and **Jaikumar M**, (2014), Studies on the effect of hydrogen induction on performance, emission and combustion behaviour of a WCO emulsion based dual fuel engine, *International Journal of Hydrogen Energy*, Vol. 39, No. 32, pp. 18440-18450.

Lata DB, Misra A, and **Medhekar S**, (2012), Effect of hydrogen and LPG addition on the efficiency and emissions of a dual fuel diesel engine, *International Journal of Hydrogen Energy*, Vol. 37, No. 7, pp. 6084-6096.

Lei J, Shen L, Bi Y, and **Chen H**, (2012), A novel emulsifier for ethanol-diesel blends and its effect on performance and emissions of diesel engine, *Fuel*, Vol. 93, pp. 305-311.

Lin C, and **Chen L**, (2006), Engine performance and emission characteristics of three-phase diesel emulsions prepared by an ultrasonic emulsification method, *Fuel*, Vol. 85, No. 5-6, pp. 593-600.

Lin C, and **Lin H**, (2007), Engine performance and emission characteristics of a three –phase emulsion of biodiesel produced by peroxidation, *Fuel Processing Technology*, Vol. 88, No. 1, pp. 35-41.

Lin CY, and **Chen LW**, (2008), Comparison of fuel properties and emission characteristics of two- and three-phase emulsions prepared by ultrasonically vibrating and mechanically homogenizing emulsification methods, *Fuel*, Vol. 87, No. 10-11, pp. 2154–2161.

Lin C-Y, and **Wang KH**, (2003), The fuel properties of three-phase emulsions as an alternative fuel for diesel engines, *Fuel*, Vol. 82, No. 11, pp. 1367–1375

Lin CY, and **Wang KH**, (2004), Diesel engine performance and emission characteristic using three-phase emulsions as fuel, *Fuel*, Vol. 83, No. 4-5, pp. 537-545.

Lopez I, Quintana CE, Ruiz JJ, Cruz-Peragon F, and **Dorado MP**, (2014), Effect of the use of olive–pomace oil biodiesel/diesel fuel blends in a compression ignition engine: Preliminary exergy analysis, *Energy Conversion and Management*, Vol. 85, pp. 227-233.

Luijten CM, and **Kerkhof E**, (2011), Jatropha oil and biogas in a dual fuel CI engine for rural electrification, *Energy Conversion and Management*, Vol. 52, No. 2, pp. 1426-1438.

Maizonnasse M, Plante JS, Oh D, and **Laflamme CB**, (2013), Investigation of the degradation of a low-cost untreated biogas engine using preheated biogas with phase separation for electric power generation, *Renewable Energy*, Vol. 55, pp. 501-513.

Makareviciene V, Sendzikiene E, Pukalskas S, Rimkus A, and **Vegneris R**, (2013), Performance and emission characteristics of biogas used in diesel engine operation, *Energy Conversion and Management*, Vol. 75, pp. 224-233.

Mansour C, Bounif A, Aris A, and **Gaillard F**, (2001), Gas diesel (dual-fuel) modelling in diesel environment, *International Journal of Thermal Sciences*, Vol. 40, No.4, pp. 409-424.

Mital KM, (1996), *Biogas Systems: Principles and Applications*, New Age International (P) Ltd., New Delhi, India

Moffat RJ, (1982), Contributions to the theory of single-sample uncertainty analysis, *ASME Journal of Fluids Engineering*, Vol. 104, pp. 250-264.

MohamedMusthafa M, Sivapirakasam SP, and **Udayakumar M**, (2011), Comparative studies on fly ash coated low heat rejection diesel engine on performance and emission characteristics fueled by rice bran and pongamia methyl ester and their blend with diesel, *Energy*, Vol. 36, No. 5, pp. 2343-2351.

Moran MJ, and **Shapiro HN,** (1995), *Fundamentals of Engineering Thermodynamics*, John Wiley and Sons Inc., USA.

Morsy MH, (2015), Assessment of a direct injection diesel engine fumigated with ethanol/water mixtures, *Energy Conversion and Management*, Vol. 94, pp. 406–414.

Mustafi NN, Raine RR, and **Verhelst S**, (2013), Combustion and emissions characteristics of a dual fuel engine operated on alternative gaseous fuels, *Fuel*, Vol. 109, pp. 669-78.

Nakonieczny K, (2002), Entropy generation in a diesel engine turbocharging system, *Energy*, Vol. 27, No. 11, pp. 1027–1056.

Namasivayam AM, Korakianitis T, Crookes RJ, Bob-Manuel KDH, and **Olsen J**, (2010), Biodiesel, emulsified biodiesel and dimethyl ether as pilot fuels for natural gas fuelled engines, *Applied Energy*, Vol. 87, No.3, pp. 769-778.

Nazha MAA, and **Crookes RJ**, (1985), Effect of water content on pollutant formation in a burning spray of water-in-diesel fuel emulsion, *Twentieth Symposium (International) on Combustion/ The Combustion Institute*, Vol. 20, No.1, pp. 2001-2010.

Nijaguna BT, (2002), Biogas Technology, New Age International (P) limited, New Delhi, India.

Ozkan M, Ozkan DB, Ozener O, and **Yilmaz H**, (2013), Experimental study on energy and exergy analyses of a diesel engine performed with multiple injection strategies: Effect of pre-injection timing, *Applied Thermal Engineering*, Vol. 53, No. 1, pp. 21–30.

Pandey A, (2009), *Biodiesel from rice bran oil handbook of plant-based biofuels*, CRC Press, Taylor & Francis Group, Boca Raton, Florida, U.S.A., pp. 241-254.

Papagiannakis RG, Hountalas DT, and **Rakopoulos CD**, (2007), Theoretical study of the effects of pilot fuel quantity and its injection timing on the performance and emissions of a dual fuel diesel engine, *Energy Conversion Management*, Vol. 48, No.11, pp. 2951-2961.

Parlak A, (2005), The effect of heat transfer on performance of the Diesel cycle and exergy of the exhaust gas stream in a LHR Diesel engine at the optimum injection timing, *Energy Conversion and Management*, Vol. 46, No. 2, pp. 167–179.

Parlak A, Yasar H, and **Eldogan O**, (2005), The effect of thermal barrier coating on a turbo-charged Diesel engine performance and exergy potential of the exhaust gas, *Energy Conversion and Management*, Vol. 46, No.3, pp. 489–499.

Patterson D, and **Van Wylen G**, (1963), A digital computer simulation for spark-ignited engine cycles, *SAE Paper*, No. 630076.

Polk AC, Carpenter CD, Srinivasan KK, and **Krishnan SR**, 2014, An investigation of diesel–ignited propane dual fuel combustion in a heavy-duty diesel engine, *Fuel*, Vol. 132, pp. 135–148.

Pollution control, Know the exhaust Standard, http://www.delhi.gov.in/wps/wcm/connect /doit_transport/Transport/Home/Pollution+Control/Know+the+Exhaust+Emission+Standards

Pulkrabek WW, (2004), *Engineering Fundamentals of the Internal Combustion Engine*, 2nd edition, Pearson Education, New Delhi, India.

Pullen J, and **Saeed K**, (2014), Factors affecting biodiesel engine performance and exhaust emissions Part I: Review, *Energy*, Vol. 72, pp. 1–16.

Pundir BP, (2010), *IC Engines Combustion and Emissions*, Narosa Publishing House Private Limited, New Delhi, India.

Qi DH, Chen H, Matthews RD, and **Brian YZH**, (2010), Combustion and emission characteristics of ethanol-biodiesel-water micro-emulsions used in a direct injection compression ignition engine, *Fuel*, Vol. 89, No. 5, pp. 959-964.

Raheman H, and **Ghadge SV**, (2008), Performance of diesel engine with biodiesel at varying compression ratio and ignition timing, *Fuel*, Vol. 87, No. 12, pp. 2659-2666.

Rakopoulos CD, and **Giakoumis EG**, (1997a), Development of cumulative and availability rate balances in a multi-cylinder turbocharged indirect injection diesel engine, *Energy Conversion and Management*; Vol. 38, No. 4, pp. 341-369.

Rakopoulos CD, and **Giakoumis EG**, (1997b), Simulation and exergy analysis of transient diesel-engine operation, *Energy*, Vol. 22, No. 9, pp. 875-885.

Rakopoulos CD, and **Giakoumis EG**, (1997c), Speed and load effects on the availability balances and irreversibilities production in a multi-cylinder turbocharged diesel engine, *Applied Thermal Engineering*, Vol. 17, No. 3, pp. 299–313.

Rakopoulos CD, and **Giakoumis EG**, (2006), Second-law analyses applied to internal combustion engines operation, *Progress in Energy and Combustion Science*, Vol. 32, No. 1, pp. 2-47.

Rakopoulos CD, and **Giakoumis EG**, (2009), *Diesel Transient Operation: Principles of Operation and Simulation Analysis*, Springer –Verlag London Limited, UK, pp. 277-304.

Rakopoulos CD, and **Kyritsis DC**, (2001), Comparative second-law analysis of internal combustion engine operation for methane, methanol, and dodecane fuels. *Energy*, Vol. 26, No. 7, pp. 705-722.

Rakopoulos CD, and **Kyritsis DC**, (2006), Hydrogen enrichment effects on the second law analysis of natural and landfill gas combustion in engine cylinders, *International Journal of Hydrogen Energy*, Vol. 31, No. 10, pp. 1384–1393.

Rakopoulos CD, Scott MA, Kyritsis, DC, and **Giakoumis EG**, (2008), Availability analysis of hydrogen/natural gas blends combustion in internal combustion engines, *Energy*, Vol. 33, No.2, pp. 248–255.

Rakopoulos DC, Rakopoulos CD, Giakoumis EG, Papagiannakis RG, and **Kyritsis DC**, (2014), Influence of properties of various common bio-fuels on the combustion and emission characteristics of high-speed DI (direct injection) diesel engine: Vegetable oil, bio-diesel, ethanol, n-butanol, diethyl ether, *Energy*, Vol. 73, No.14, pp. 354-366.

Ryu K, (2013), Effects of pilot injection timing on the combustion and emissions characteristics in a diesel engine using biodiesel–CNG dual fuel, *Applied Energy*, Vol. 111, pp. 721-730.

Sadhik Basha J, and **Anand, RB**, (2010), An experimental investigation in a diesel engine using carbon nanotubes blended water-diesel emulsion, *Proc. IMechE Part A: Journal of Power and Energy*, Vol. 225, pp. 279-288.

Sahoo BB, (2011), *Clean development mechanism potential of compression ignition diesel engines using gaseous fuel in dual fuel mode*, Ph.D thesis, Centre for Energy, IIT Guwahati, India.

Sahoo BB, Saha UK, and **Sahoo N**, (2011a), Theoretical performance limits of a syngas-diesel fuelled compression ignition engine from second law analysis, *Energy*, Vol. 36, No. 2, pp. 760–769.

Sahoo BB, Saha UK, and **Sahoo N**, (2011b), Effect of load level on the performance of a dual fuel compression ignition engine operating on syngas fuels with varying H_2/CO content, *ASME Journal of Engineering for Gas Turbines and Power*, Vol. 133, No. 12, pp. 122802–122812.

Sahoo BB, Saha UK, and **Sahoo N**, (2012), Diagnosing the effects of pilot fuel quality on exergy terms in a biogas run dual fuel diesel engine, *International Journal of Exergy*, Vol. 10, No. 1, pp. 77-93.

Saravanan S, and **Nagarajan G**, (2014)**,** Comparison of influencing factors of diesel with crude rice bran oil methyl ester in multi response optimization of NOx emission, *Ain Shams Engineering Journal*, Vol.5, No. 4, pp.1241–1248.

Saravanan S, Nagarajan G, and **Rao GLN**, (2009), Feasibility analysis of crude rice bran oil methyl ester blend as a stationary and automotive diesel engine fuel, *Energy for Sustainable Development*, Vol. 13, No.1, pp. 52–55.

Saravanan S, Nagarajan G, Rao GLN, and **Sampath S**, (2010), Combustion characteristics of a stationary diesel engine fuelled with a blend of crude rice bran oil methyl ester and diesel, *Energy*, Vol. 35, No.1, pp. 94–100.

Sayin C, and **Canakci M**, (2009), Effects of injection timing on the engine performance and exhaust emissions of a dual-fuel diesel engine, *Energy Conversion and Management*, Vol. 50, No. 1, pp. 203-213.

Sayin C, and **Gumus M**, (2011), Impact of compression ratio and injection parameters on the performance and emissions of a DI diesel engine fueled with biodiesel-blended diesel fuel, *Applied Thermal engineering*, Vol. 31, No. 16 pp. 3182-3188.

Sayin C, Iihan M, Canakci M, and **Gumus M**, (2009), Effects of injection timing on the exhaust emissions of a diesel engine using diesel –methanol blends, *Renewable Energy*, Vol. 34, No. 5, pp. 1261-1269.

Sayin C, Uslu K, and **Canakci M**, (2008), Influence of injection timing on the exhaust emissions of a dual-fuel CI engine, *Renewable Energy*, Vol. 33, No. 6, pp. 1314-1323.
Science, Vol. 298, pp. 441–450.

Selim MYE, (2004), Sensitivity of dual fuel engine combustion and knocking limits to gaseous fuel composition, *Energy Conversion Management*, Vol. 45, No. 3, pp. 411-425.

Sharma A, and **Murugan S**, (2015), Potential for using a tyre pyrolysis oil-biodiesel blend in a diesel engine at different compression ratios, Energy Conversion and Management, Vol. 93, pp. 289–297.

Sjogren A, (1977), Burning of water-in oil emulsions, *Symposium (International) on Combustion*, Vol. 16, No.1, pp. 297-305.

Som SK, and **Datta A**, (2008), Thermodynamic irreversibilities and exergy balance in combustion process, *Progress in Energy and Combustion Science*, Vol. 34, No.3, pp. 351-376.

Stepanov VS, (1995), Chemical energies and exergies of fuels, *Energy*, Vol. 20, No. 3, pp. 235–242.

Stone R, (1985), *Experimental facilities: Introduction to Internal combustion engines*, 2nd edition, London: The Macmillan Press Limited, Hampshire, London, pp. 506-509.

Stewart J, Clarke A, and **Chen R, (2007)**, An Experimental Study of the Dual-Fuel Performance of a Small Compression Ignition Diesel Engine Operating with Three Gaseous Fuels, *Proc. of the Institution of Mechanical Engineers Part D: Journal of Automobile Engineering*, Vol. 221, pp. 943 – 956.

Tat ME, (2011), Cetane number effect on the energetic and exergetic efficiency of a diesel engine fuelled with biodiesel, *Fuel Processing Technology*, Vol. 92, No. 7, pp. 1311–1321.

Testo India, Flue gas analysis in industry: Practical guide for emission and process measurements, 2012, http://www.testointernational.com/online/embedded/Sites/INT/main

Navigation/SectorsAndProducts/emission/Unterthema_Fibel.pdf) [Accessed on 19th Sept., 2012].

Thipse SS, (2010), *Alternative Fuels: Concepts, Technologies and Developments*, Jaico Publishing House, India.

Tippayawong N, Promwungkwa A, and **Rerkkriangkrai P**, (2007), Long-term operation of a small biogas/diesel dual-fuel engine for on-farm electricity generation, *Biosystems Engineering*, Vol. 98, No. 1, pp. 26-32.

Traupel W, (1957), Reciprocating Engine and Turbine**,** *Proceedings of the International Congress of Combustion Engines (CIMAC),* Zurich, Switzerland.

Umesh KS, Pravin VK, Rajagopal K, and **Veena PH**, (2012), Development of a CFD 3D model to determine the effect of the mixing quality on the CNG-diesel engine performance, *International Journal of Engineering Research & Technology (IJERT)*, Vol.1, No. 5, pp. 1 - 12.

von-Mitzlaff K, (1988), *Engines for Biogas - Theory, Modification, Economic Operation*, A publication of Deutsches Zentrum fur Entwicklungstecknologien, GTZ Gate.

Walsh JL, Ross CC, Smith MS, and **Harper SR**, (1989), Utilization of biogas, *Biomass*, Vol. 20, No. 3-4, pp. 277- 290.

Yaliwala VS, Banapurmath NR, Gireesh NM, and **Tewari PG**, (2014), Production and utilization of renewable and sustainable gaseous fuel for power generation applications: A review of literature, *Renewable and Sustainable Energy Reviews*, Vol. 34, pp. 608-627.

Yoon SH, and **Lee CS**, (2011), Experimental investigation on the combustion and exhaust emission characteristics of biogas – biodiesel dual-fuel combustion in a CI Engine, *Fuel Processing Technology*, Vol. 92, No. 5, pp. 992-1000.

Yusaf T, and **Zamri M**, (2000), Development of A 3D CFD Model to Investigate the Effect of the Mixing Quality on the CNG-Diesel Engine Performance, *Proceeding of the International Conference and Exhibition and Natural Gas Vehicles*, Yokohama, Japan

Zhang W, Chen Z, Shen Y, ShuG, Chen G, Xu B, and **Zhao W,** (2013), Influence of water emulsified diesel & oxygen-enriched air on diesel engine NO-smoke emissions and combustion characteristics, *Energy*, Vol. 55, pp. 369-377.

Zheng J, and **Caton JA**, (2012), Second law analysis of a low temperature combustion diesel engine: Effect of injection timing and exhaust gas recirculation, *Energy*, Vol. 38, No. 1, pp. 78–84.

Zullaikah S, Lai CC, Vali SR, and **Ju YH**, (2005), A two-step acid-catalyzed process for the production of biodiesel from rice bran oil, *Bioresource Technology*, Vol. 96, No. 17, pp.1889–1896.

Appendix-A

Equations used for Performance and Combustion Analysis

I. Performance Analysis

(i) Brake power (*BP*)

$$BP = (2 \times \Pi \times N \times W \times r)/(60 \times 1000), kW \quad \text{Eq. (A1)}$$

where N, W and r are the speed of the engine (rpm), engine load (kg-m/s^2) and dynamometer arm radius (m), respectively.

(ii) Brake thermal efficiency (*BTE)*

For diesel mode,

$$BTE = (BP \times 3600 \times 100)/(\dot{m}_{di} \times LHV_{di}), \% \quad \text{Eq. (A2)}$$

For dual fuel mode,

$$BTE = (BP \times 3600 \times 100)/(\dot{m}_{p} \times LHV_{p} + \dot{m}_{bg} \times LHV_{bg}), \% \quad \text{Eq. (A3)}$$

where $\dot{m}_{di}(kg/s)$, $\dot{m}_{p}$ (kg/s) and $\dot{m}_{bg}$ (kg/s) are the diesel, pilot fuel and biogas flow rate respectively, and LHV_{di} (kJ/kg), LHV_{p} (kJ/kg) and LHV_{bg} (kJ/kg) are the lower heating values of diesel, pilot fuel and gaseous fuel respectively.

(iii) Air flow rate (AFR)

$$AFR = C_d \times (\Pi/4) \times d^2 \times 3600 \times A_{den} \times \sqrt{(2gh \times W_{den})/(A_{den})}, kg/h \quad \text{Eq. (A4)}$$

where C_d, d, h, W_{den} and A_{den} are coefficient of discharge, diameter of the orifice of air flow (m), manometer reading across orifice (m), water density (kg/m^3) and the density of ambient air (kg/m^3), respectively.

(iv) Volumetric efficiency *(Π_{vol})*

$$\eta_{vol} = (AFR)/\{(\Pi/4) \times D^2 \times L \times (N/n) \times 60 \times K \times A_{den}\} \times 100, \% \qquad \text{Eq. (A5)}$$

where *D*, *L*, *n* and *K* are engine cylinder diameter (m), engine stroke length (m), number of . revolution per cycle (2 for four stroke engine), number of cylinders

(v) Brake specific energy consumption *(BSEC)*

$$BSEC = \left\{\sum (\dot{m}_f \times LHV_f)\right\}/BP, (kJ/s)/kW \qquad \text{Eq. (A6)}$$

where $\dot{m}_f$ (kg/s) and LHV_f are fuel flow rate and he lower heating values of fuel respectively

(vi) Liquid fuel replacement (Z)

$$Z = \{(\dot{m}_{di} - \dot{m}_p) \times 100\}/\dot{m}_d, \% \qquad \text{Eq. (A7)}$$

II. Combustion Analysis

(i) Ignition delay (ID)

$$ID = \theta_{IN} - \theta_{CS} \qquad \text{Eq. (A8)}$$

where θ_{IN} is the standard fuel injection Timing which is obtained from the manufacturer specifications i.e. 23ºBTDC and θ_{CS} the crank angle at which combustion starts and is obtained from the $\frac{dP}{d\theta}$ diagram as it changes its concavity when combustion starts.

(ii) Net heat release rate

The calculation of net heat release rates for both diesel and dual fuel run engines needs the instantaneous *P-V* data recorded during experiments. The crank angle encoder connected to the engine shaft detects each degree (1º) rotation of the crank for each cycle. Hence, for a particular cycle, a total of 720 data for both cylinder pressure and volume are recorded at each load. Each heat release calculations at a particular load are calculated by considering ten cycles. The equation used for the net heat release rate (NHRR) is obtained from the first law

analysis (Heywood, 1988) by implementing the rate of pressure rise and rate of volume change, which is given below

$$\frac{dQ_n}{d\theta} = (\gamma \times P \times \frac{dV}{d\theta})/(\gamma - 1) + (V \times \frac{dP}{d\theta})/(\gamma - 1) \quad \text{Eq. (A9)}$$

where $\frac{dQ_n}{d\theta}$, γ, P and V are net heat release rate (J/ºCA), ratio of specific heats, instantaneous cylinder pressure (N/m^2) and cylinder volume (m^3), respectively. The value of γ is considered as 1.35 based on the ranges of Heywood (1988), Pundir (2010).

(iii) Pressure correction

The DAD can record cylinder pressure variation with each degree of crank angle change. Differentiating the raw pressure data shows a noisy trend between successive values. Therefore, after treatment of these pressure data in the form of smoothing becomes necessary. The equation A8 is used for the smoothing of the instantaneous pressure data (Stone, 1997).

$$P_n = \{(P_{n-1}) + 2(P_n) + (P_{n+1})\}/4 \quad \text{Eq. (A10)}$$

The values of change of volume per unit change of crank angle ($\frac{dV}{d\theta}$) are calculated from the instantaneous volume change data recorded during experiments. The values of change of pressure per unit change of crank angle ($\frac{dP}{d\theta}$) are evaluated by using the first order finite difference equation with fourth order accuracy (Stone, 1997).

$$\frac{dP}{d\theta} = \{(P_{n-2}) - 8(P_{n-1}) + 8(P_{n+1}) - (P_{n+2})\}/\{12(\Delta\theta)\} \quad \text{Eq. (A11)}$$

Appendix-B

Design of Gas Mixer and Fuel Control Mechanism

B1. Gas Mixer Design:

For converting a diesel engine to dual fuel mode, the major modification needed is to connect a gas mixer to the inlet manifold (Sahoo, 2011). The gas mixer is very important in dual-fuel engine, as it provides a combustible mixture of fuel gas and air in the required quantity and quality for efficient operation of the engine under all conditions (Yusaf and Zamri, 2000). According to the performance required, the flow of fuel gas can be varied. It also enables to supply a sufficient amount of air at maximum load and speed at the actual pressures of fuel gas and air. The maximum air to fuel ratio should not be less than 1.5 in order to ensure combustion even for the pilot fuel. The design of a gas mixer for a particular engine mainly depends on its rated power, specific fuel consumption, speed, and volumetric efficiency, swept volume, and manifold connection diameter (von Mitzlaff, 1988).

B1.1 Existing Design of the Gas Mixer

In most of the cases, a T-junction gas mixer is used when a diesel engine is modified to a dual fuel mode. The existing design of the gas mixer consists of a channel having a T-junction. It has two inlets, one each for air and gas, and an outlet for air-gas mixture (Fig. B.1). The gas inlet is fixed at 90º with air inlet. The exit of the mixture is coupled to the engine intake manifold.

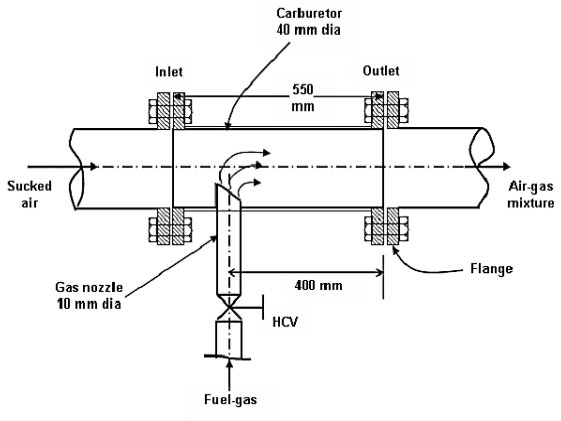

Fig. B.1 T-junction gas mixer proposed by von Mitzlaff (1988)

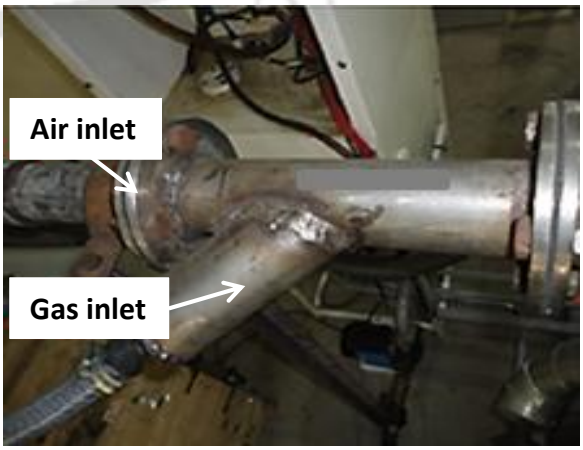

Fig. B.2 T-junction gas mixer proposed by Sahoo (2011)

However, this simple design creates a huge energy loss when air and gas stream collide with each other at high velocities. In order to reduce this loss of collision and to increase the additional shear mixing, recently, a gas mixer is designed and developed (Sahoo, 2011). This gas mixer has a gas inlet inclined at 45º with the air inlet as shown in Fig. B.2.However, this design is unable to overcome the asymmetrical mixing of air and gaseous fuel at the mixing region and further downstream. This finally destined the charge to become nonhomogeneous and hence, needs a close investigation.

B1.2 Modified Design of the Gas Mixer

The proposed design of the gas mixer uses the concept of venturimeter and is known as 'venturi gas mixer' (Fig. B.3). The venturi gas mixer comprises of two gas inlets, one air inlet and one air-gas outlet. It consists of a smooth contraction section and an expansion section which reduce the prominence of irreversible pressure loss.

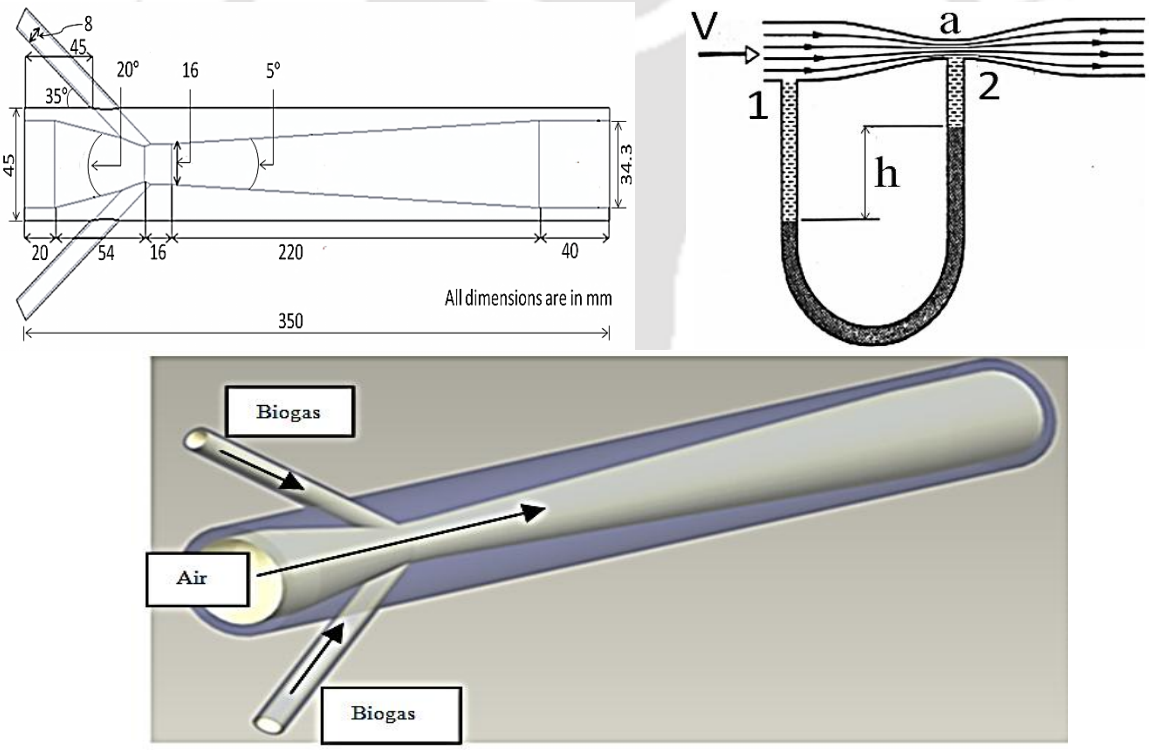

Fig. B.3 Design and dimensions of the venturi gas mixer

The function of the converging section is to increase the velocity of the fluid and lower its static pressure. This low pressure region will drag in more gas and enriches the turbulence mixing with air. Thus, there will be a pressure difference created between the inlet and the throat.

Using Bernoulli equation, this pressure difference can be expressed in terms of rate of flow

$$P_1 - P_2 = \frac{{V_2}^2 - {V_1}^2}{2}\rho \qquad \text{Eq. (B.1)}$$

Applying continuity equation to Eq. (B.1)

$$P_1 - P_2 = \frac{{A_1}^2 - {A_2}^2}{{A_1}^2 \times {A_2}^2}\rho Q \qquad \text{Eq. (B.2)}$$

where suffix '1' and '2' represent the inlet and throat conditions

From Eq. (B.2), it can be understood that, pressure drop is inversely proportional to the square of the area when all other parameters being kept constant. Hence, at the throat region the pressure and velocity are minimum and maximum, respectively. There are four main designing parameters namely converging angle (θ_1), diverging angle (θ_2), nozzle angle (θ_n) and β (ratio between the diameters of throat and inlet manifold). The values of θ_1, θ_2, θ_n and β are considered as 20°, 5°, 35°and 0.46, respectively as shown in (Fig. B.3). These geometric values are dictated by past simulation studies. The throat diameter, inlet manifold and biogas inlet diameter are 16 mm and 34.3 mm and 8 mm, respectively. The diameter of biogas inlet nozzle is found to 8 mm be based on the methodology as suggested by von Mitzlaff (1988). According to Stewart *et al.* (2007), the length of the diverging section should be 10 times the inlet manifold diameter. However, considering the diverging angle of 5° the length of the same is found to be 220 mm with respect to the manifold diameter of 34.3 mm. All this design parameters of the gas mixer is based on a diesel engine with rated power of 3.5 kW. The volumetric efficiency and speed of the engine are considered as 90% and 1500 rpm. The maximum diesel substitution by biogas in this engine is taken as 80% (von Mitzlaff, 1988).

B1.3 Methodology

The Computational Fluid Dynamics (CFD) analysis has been carried out in FLUENT software, which is available in ANSYS Workbench 14. The analysis has been performed for the existing gas mixtures with gas nozzles inclined at 45° and 90°, as well as the proposed design of gas mixer. The design of the gas mixers are first modeled in Pro/Engineer and then analyzed in Fluent. The governing equations of the dynamics of air and gas mixture are the conservation and the thermodynamics laws. Simulation is based on the turbulence model of

the non-stationary 3D flow. Gases are considered as compressible viscous fluid. The standard *k-ε* model is used to solve the flow problems reigning inside the gas mixer for the three inlets; one is air inlet and the other two for fuel biogas inlet. The equations governing the inflow model, including the conservation equations of mass, momentum and energy are summarized in the conservative form of the Navier-Stokes equations (Jemni *et al.*, 2011).

$$\frac{\partial \rho}{\partial t} + \frac{\partial y}{\partial x}(\rho U_i) = 0 \qquad \text{Eq. (B.3)}$$

$$\frac{\partial}{\partial t}(\rho U_i) + \frac{\partial}{\partial x_i}(\rho U_i U_j) + \frac{\partial P}{\partial x_i} = \frac{\partial}{\partial x_i}\left(t_{ij} + {t_{ij}}^R\right) + S_{ij}, \qquad i = 1,2,3 \qquad \text{Eq. (B.4)}$$

where 'S_i' is an external force per unit mass, 'h' is the thermal enthalpy, 'Q_H' is a heat source or sink per unit volume, 'S_{ij}' is the viscous shear stress tensor, 'q_i' is the diffusive heat flux. The subscripts are used to denote summation over the three coordinate directions.

$$\frac{\partial}{\partial t}(\rho H) + \frac{\partial}{\partial x_j}(\rho U_i H) = \frac{\partial}{\partial x_i}\left(U_j(t_{ij} + {t_{ij}}^R) + q_i\right) + \frac{\partial P}{\partial t} - {t_{ij}}^R \frac{\partial U_i}{\partial X_j} + \rho\varepsilon + S_i U_i + Q_H \qquad \text{Eq. (B.5)}$$

$$H = h + \frac{U^2}{2} \qquad \text{Eq. (B.6)}$$

$$\frac{\partial}{\partial t}(\rho E) + \frac{\partial \rho U_i}{\partial X_i}\left(E + \frac{P}{\rho}\right) = \frac{\partial}{\partial X_i}\{U_j\left(t_{ij} + {t_{ij}}^R + q_i\right)\} - {t_{ij}}^R \frac{\partial U_i}{\partial U_j} + \rho\varepsilon + S_i U_i + Q_H \qquad \text{Eq. (B.7)}$$

$$E = e + \frac{U^2}{2} \qquad \text{Eq. (B.8)}$$

where 'e' is the internal energy

For an ideal gas at constant specific heat ratio, $\gamma = \frac{C_P}{C_V}$, the pressure is given by the state law of perfect gases

$$P = \rho RT = (\gamma - 1)\rho \qquad \text{Eq. (B.9)}$$

B1.4 Model of Turbulence

The turbulence modeling is found to have more significance while modeling combustion in Internal Combustion engines (Jemni *et al.*, 2011). In fact, turbulence directly affects the mixing, the mixture homogenization and combustion in an engine. The adequate prediction of the turbulence behavior is necessary for a better comprehension of these phenomena in order to improve engine performances and to reduce emissions. In the majority of the multidimensional computer codes developed till date have numerous key characteristics of velocity. These are directly related to the scales of turbulence in the models corresponding to the admission, combustion and heat transfer processes. These processes would be modeled correctly if the modeling and the prediction of turbulence are also precise. In this paper, turbulence model is considered according to the *k-ε* turbulence model (Umesh *et al.*, 2012). The Reynolds-stress tensor used in this model is defined as

$$t_{ij}{}^{R} = \mu_t \left(\frac{\partial U_i}{\partial X_j} + \frac{\partial U_j}{\partial X_i} - \frac{2}{3}\delta_{ij}\frac{\partial y}{\partial x} \right) - \frac{2}{3}\rho K \delta_{ij} \qquad \text{Eq. (B.10)}$$

'δ_{ij}' is equal to unity when i=j, and zero otherwise, 'μ' is the dynamic viscosity coefficient, 'μ_t' is the turbulent eddy viscosity coefficient and 'k' is the turbulent kinetic energy. In the frame of the k-ε turbulence model, 'μ_t' is defined using, turbulent viscosity factor 'f_μ'.

$$\mu_t = \frac{f_\mu C_\mu \rho K^2}{\varepsilon} \qquad \text{Eq. (B.11)}$$

B1.5 Boundary and Initial Condition for the Model

The boundary conditions are used for CFD analysis is represented in Fig. B.3. The intensity of turbulence is specified as 3% (Jemni *et al.*, 2011). The species model used to calculate various species formation during combustion is non–premixed combustion model. The velocities of biogas and air are considered as 20 m/s and 5.82 m/s, respectively based on a study done on the same specification of a biogas run dual fuel diesel engine (Sahoo, 2011).

B1.6 Results and Discussion

The CFD analyses for the three different gas mixer designs are discussed in this section. The designs investigated are the existing gas mixtures with gas nozzles inclined at 45° and 90° along with the proposed venturi gas mixer. The analyses are executed on the basis of pressure, turbulence intensity and mass fraction of methane at different cross sectional planes.

The planes are made at equidistant from the entry of biogas into the air stream to find out the optimum design.

B1.6.1 Pressure Analysis

Figures B.4(a), B.4(b) and B.4(c) shows the pressure contours of existing T-junction design gas mixer with single nozzle inclined at angle of 45°, 90° and venturi gas mixer. Figures B.4(a) and B.4(b) display that, the existing T-junction gas mixers with single nozzle inclined at an angle of 45° and at an angle 90° give very less pressure drop at the entry. This hampers in effective fuel suction. As a result, the mixing of the fuel gas and air in the gas mixer is not appropriate.

Fig. B.4(a) Pressure contour of T-junction design gas mixer with nozzle inclined at an angle of 90°

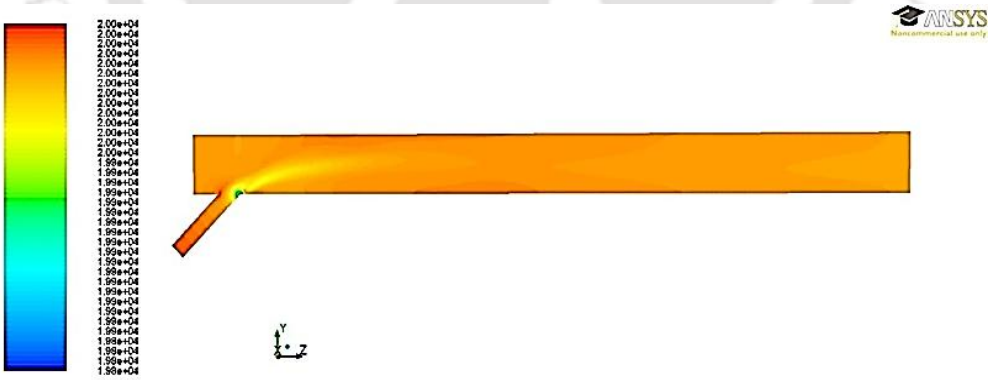

Fig. B.4(b) Pressure contour of T-junction design gas mixer single nozzle inclined at an angle of 45°

In addition, the mixing of the fuel biogas and air is non-uniform as there is a pressure drop at one side of the current T-junction gas mixers with the single nozzle. On the other hand, for the venturi gas mixer, the mixing of the fuel biogas and air would be proper if the pressure drop is uniform throughout the throat section of the gas mixer. However, in the proposed

venturi type design, the pressure drop at the entry at the throat area is found to be higher as compared to existing gas mixer. This enhanced pressure drop owing to the geometry of the venturi type mixer provides in better suction of the biogas intruding through the small pipes. This led to the superior mixing of the fuel biogas and air which would result a proper combustion of air fuel mixture. Similar patterns of pressure distributions for venturi gas mixers of different designs for other gaseous fuel have been reported in the literature (Umesh *et al.*, 2012; Gorjibandpy and Sangsereki, 2010).

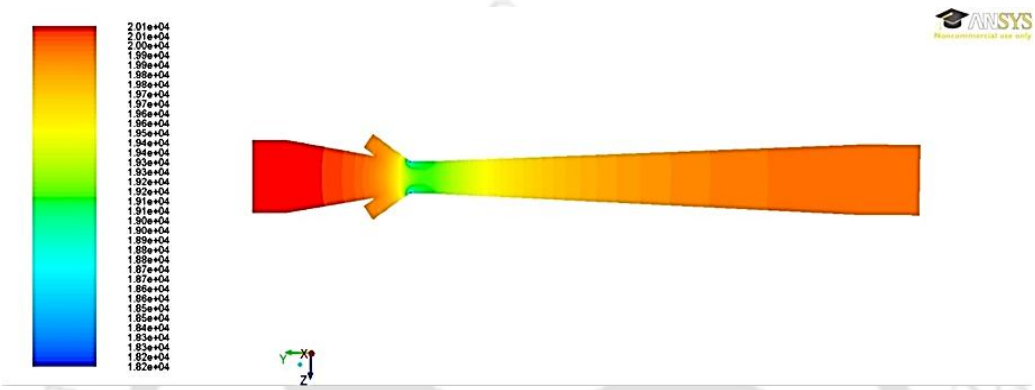

Fig. B.4(c) Pressure contour of venturi gas mixer

B.1.6.2 Turbulence Intensity Analysis

The contours of turbulence of existing T-junction design gas mixer with single nozzle inclined at angle of 45°, 90° and venturi gas mixer are shown in Figs. B.5(a), B.5(b) and B.5(c).

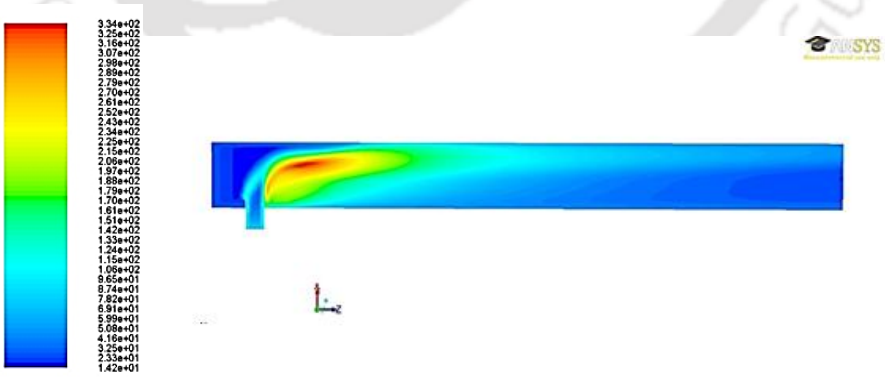

Fig. B.5(a) Turbulence intensity of T-junction design gas mixer with nozzle inclined at an angle of 90°

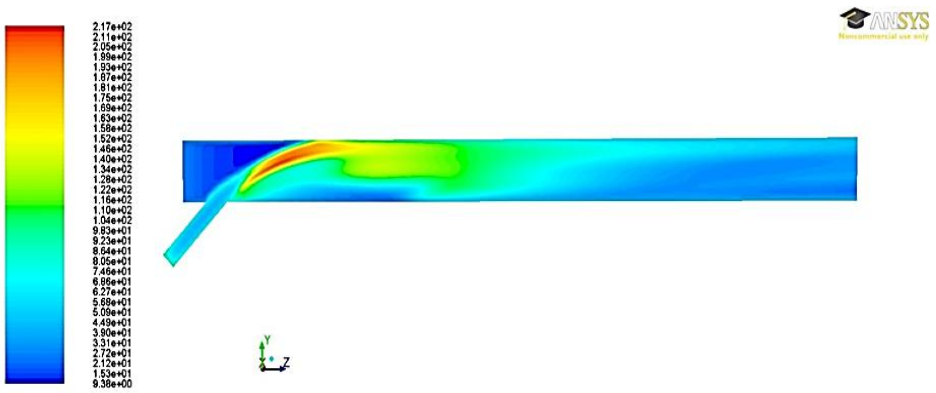

Fig. B.5(b) Turbulence intensity of T-junction design gas mixer single nozzle inclined at an angle of 45°

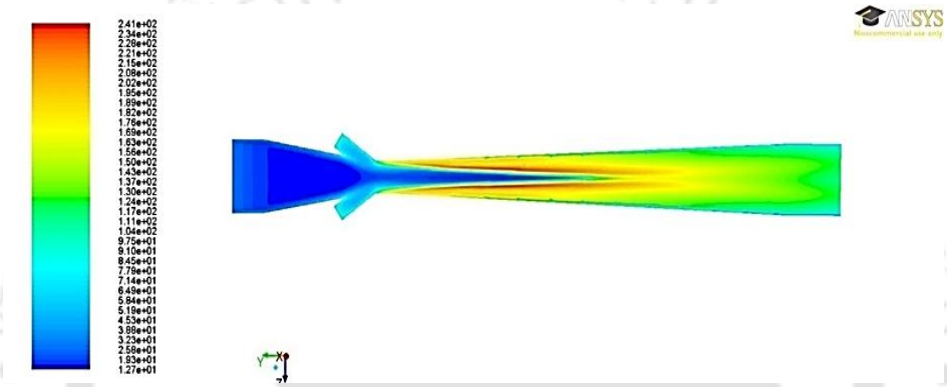

Fig. B.5(c) Turbulence intensity of venturi gas mixer

In order to have a better combustion, the biogas and air requires to be mixed at a molecular level. The turbulence enhances the mixing of biogas and air. On analyzing the turbulence contour of the various designs, the existing T-junction gas mixers with single nozzle inclined at an angle of 45° and at an angle 90° as illustrated in Figs. B.5(a) and B.5(b) exhibits a non-uniform turbulence which results in non-uniform mixing of the biogas and air mixture. Figures B.5(c) expresses the turbulence contour of the venturi type gas mixture. It can be clearly understood from the figure that a wide zone of uniform turbulence is generated at the diverging segment of the gas mixture. This will cause a healthier mixing of biogas and air, which results a homogeneous combustion and reducing the effective consumption of fuel as reported earlier (Jemni *et al.*, 2011; Gorjibandpy and Sangsereki, 2010).

B.1.6.3 Analysis of Mass Fraction of Methane

Figures B.6(a), B.6(b) and B.6(c) express the contours of methane for the existing T-junction design gas mixer with single nozzle inclined at angle of 45°, 90° and venturi gas mixer. For superior combustion, the mixing of the fuel biogas and air should be homogeneous and

uniform. The study of the methane contours in case of existing design with single nozzle, the methane distribution along the span of the gas mixer is not even, with one side being rich and other side being lean as illustrated in Figs. B.6(a) and B.6(b).

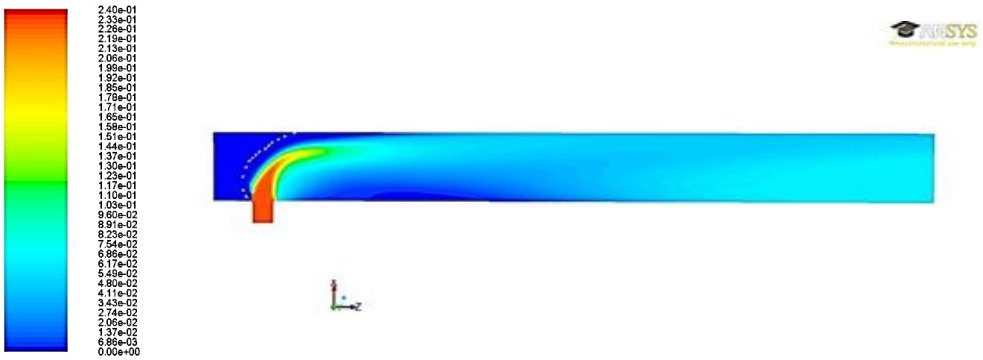

Fig. B.6(a) Methane contours of T-junction design gas mixer single nozzle inclined at an angle of 90°

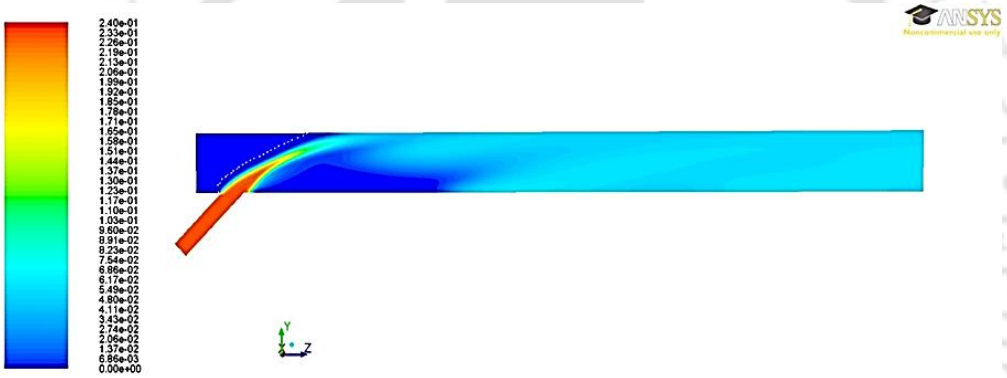

Fig. B.6(b) Methane contours of T-junction design gas mixer single nozzle inclined at an angle of 45°

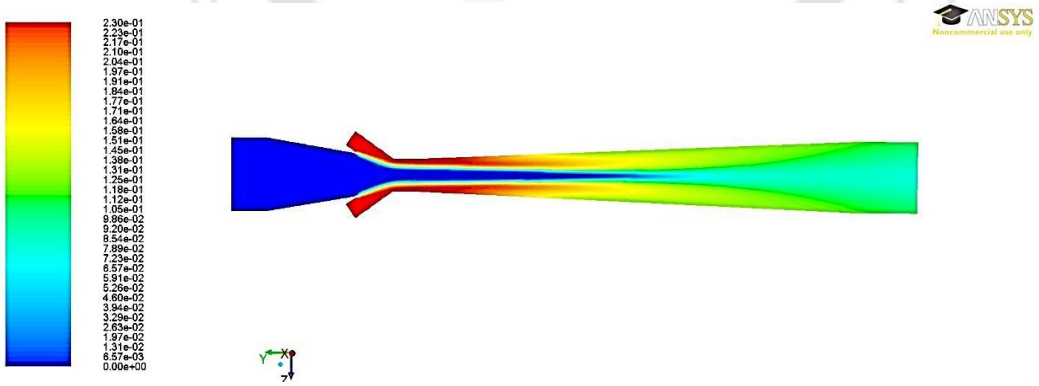

Fig. B.6(c) Methane contours of venturi gas mixer

This trend indicates that the mixing of biogas with air is made more uniform and homogeneous in case of venturi gas mixer than the existing T-junction gas mixers with single nozzle inclined at an angle of 45° and at an angle 90°. The methane contours in case of

venturi gas mixer indicates that at the throat there are two distinct stream of biogas which slowly disappears in the diverging section and the distribution of biogas turn out to be more uniform as shown in Fig. B 6(c). Figures B.7(a), B.7(b) and B.7(c) demonstrates the mixing of the biogas with air along the length of all the three types of gas mixer. These contours are produced by making cross section planes at equidistant length starting from entry of the gas mixer. The red and blue zone represents the biogas and air at the inlet in the cross section plane 1.

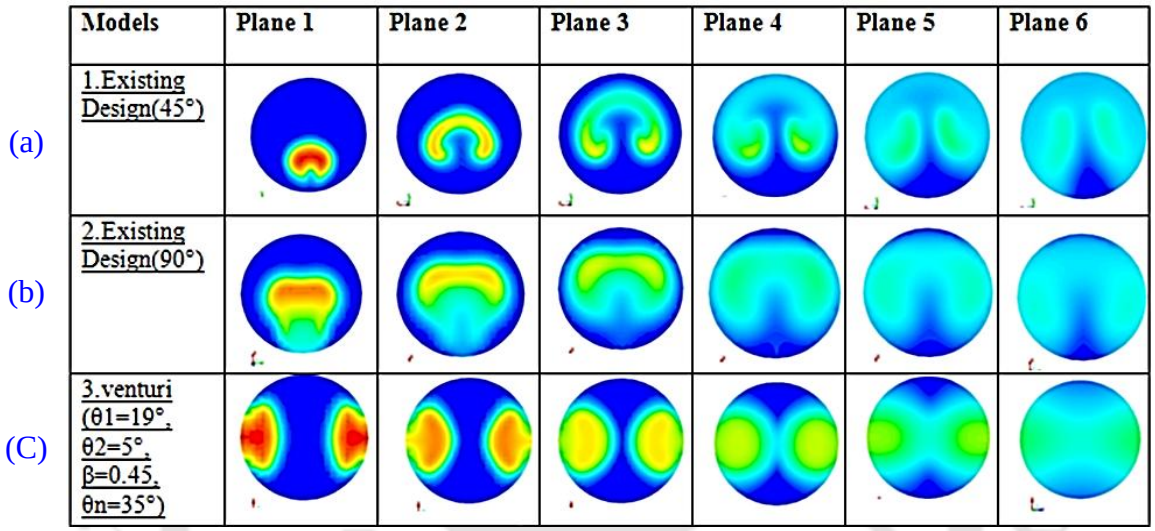

Fig. B.7 depicts the cross section planes from 1 to 6 for existing T-junction design gas mixers and venturi gas mixer

Figures B.7(a) and B.7(b)demonstrate the cross section planes from 1 to 6 for existing T-junction design gas mixers with single nozzle. There are zones where there is no mixing between air and fuel biogas. However, in case of venturi gas mixer, there is a gradual mixing of air and biogas to take place. The mixing neighborhood is progressively develops even though moving from one plane to other as presented in Fig. B.7(c). This recognizes an appropriate mixing amongst the biogas and air. Thus, it is clear that the mixing is healthier in case of venturi gas mixer than the designs proposed by von Mitzlaff (1988) or Sahoo (2011). Therefore, it can be concluded that the venturi type design provides a higher pressure drop at the throat region and ensures a better suction of biogas which ultimately boosts the mixing. This design further provides the flow to be converged at the throat, and thereafter, scatters in the diverging section covering a larger volume with a uniform concentration of methane. As the cross sectional area increases in the diverging section, the mixing zone of biogas, especially methane gradually covers a larger area. The difference between maximum and minimum concentration reduces, thereby ensuring more even distribution of methane. Thus,

the venturi type gas mixer seems to provide far better mixing of fuel biogas and air than the existing T-junction gas mixers developed earlier.

B2. Fuel Control Mechanism:

The fuel control mechanism (FCM) helps to calculate the amount of the liquid fuel replacement at any specific load corresponding to any particular speed. The FCM mainly consist of a spindle, shaft and a sleeve as depicted in Fig. B.8. The spindle is connected to the one end of the shaft and sleeve is attached to the other end of the shaft. The sleeve is mounted on the control lever of the fuel pump, which limits the liquid fuel supply. The rotation of spindle moves the shaft linearly forward which then pushes the sleeve connected to the fuel control valve and thereby, limiting the liquid fuel supply. The procedure for finding out liquid fuel replacement is as follows: Initially, the rpm and fuel consumption corresponding to a particular load in diesel mode is noted down. During dual fuel operation, biogas supply is slowly open. As both diesel and biogas undergo combustion, therefore, more energy is released. This increases the rpm of the engine. After certain duration, the governor slowly reduces the rpm by reducing the liquid fuel supply. However, to perfectly match the rpm of the diesel mode, the control lever connect to the fuel shut off valve limits the fuel further. This control lever marginally pushes the fuel control shut valve connected to the fuel pump. The least count of the fabricated FCM is found to be 1rpm.

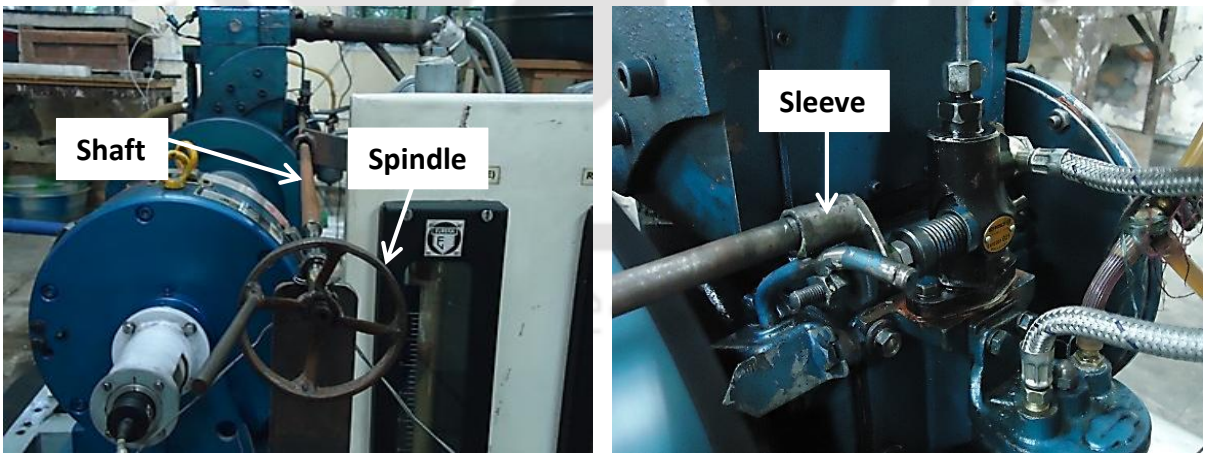

Fig. B.8 Fuel control mechanism

Appendix-C

Measurement of Uncertainty Analysis

Every experiment is associated with some uncertainty due presence of error. The uncertainties of the parameters are calculated by using the sequential perturbation technique brought by Kline and McClintok (1953) and Moffat (1982). The method is described as follows. If N is a dependant is a dependant measuring parameter which is a function of independent variables $x_1, x_2, x_3, \ldots\ldots x_n$. Therefore,

$$N = N(x_1, x_2, \ldots\ldots\ldots, x_n) \qquad \text{Eq. (C1)}$$

If ΔN is the uncertainty created due to the individual uncertainties of the independent parameters termed as ΔN_1, ΔN_2, ΔN_3,…….. ΔN_n. Then the uncertainty of the dependant variable can be written as

$$\Delta N = \left[\left(\frac{\partial N}{\partial x_1}\Delta N_1\right)^2 + \left(\frac{\partial N}{\partial x_2}\Delta N_2\right)^2 + \cdots + \left(\frac{\partial N}{\partial x_n}\Delta N_n\right)^2\right]^{1/2} \qquad \text{Eq. (C2)}$$

The calculated uncertainties of each of the measured independent parameters are shown in Table C1. The uncertainties of the dependent performance parameters are included in Table C2. A sample calculation is shown for better understanding of the concept.

Brake power (*BP*)

$$BP = (2 \times \Pi \times N \times W \times r)/(60 \times 1000), kW \qquad \text{Eq. (C3)}$$

Here, r is a constant; N and W are independent variable. The uncertainties associated of N and W are 1.2 % and 0.1% respectively. Therefore, the uncertainty associated with BP measurement is

$$\Delta BP = (0.012^2 + 0.001^2)^{1/2}$$
$$= \pm 0.01204$$
$$= \pm 1.2\%$$

Similarly, uncertainties of other dependent parameters are calculated.

Appendix-D

Equations Related to Thermodynamic Study

In Internal Combustion (IC) engines, the energy released by the fuel gets divided mainly into three parts: shaft power (brake power), heat taken away by coolant and heat taken away by the exhaust gases and of course, some amount of uncounted loses due to radiation, friction, heat transfer to the surrounding. For better utilization of energy, the heat taken away by coolant and exhaust gases should be optimum so that most of energy can be utilized in generation of power. Thus, first and second law of thermodynamics can be helpful in giving a clear insight into the utilization of energy in the IC engines. The first law and second law give the quantity and quality of the energy. The quality can be defined in terms of exergy or available energy which is the maximum useful work that could be obtained from the system at a given state. During various processes in IC engines, availability is destroyed by irreversibilities. In order to maximize efficiency, the irreversibilities should be minimized. About 80% of the combustion irreversibilities occur during heat transfer process between the reacting gases and yet unburned mixture.

2.4.1 Energy analysis

The energy input (Q_{in}) required for powering the internal combustion engines is contained in its fuel. In such engines, the chemical energy of the fuel is mainly converted to shaft energy (BP), energy transferred to the cooling water (Q_w), energy transferred to the exhaust gases (Q_e) and uncounted losses (Q_u) due to radiation, friction, heat transfer to the surrounding, etc.

For diesel mode:

Fuel energy supplied per unit time can be expressed as

$$Q_{in} = [\dot{m}_{di} \times LHV_{di}], kW \qquad \text{Eq. (D1)}$$

Brake power (BP) is given by

$$\text{BP} = [(2 \times \Pi \times N \times W \times r)/(60 \times 1000)], kW \qquad \text{Eq. (D2)}$$

Brake thermal efficiency (*BTE)* is calculated from

$$\text{BTE} = [(BP \times 3600 \times 100)/Q_{in}]\ \% \qquad \text{Eq. (D3)}$$

Brake specific energy consumption (BSEC) can be evaluated from

$$\text{BSEC} = [\sum(\dot{m}_f \times LHV_f)]/\text{BP}, (kJ/s)/kW \qquad \text{Eq. (D4)}$$

Energy in the cooling water per unit time is measured by

$$Q_c = [\dot{m}_{we} \times C_{pw} \times (T_{woe} - T_{wie})], kW \qquad \text{Eq. (D5)}$$

Energy in the by the exhaust gases per unit time is given by

$$Q_e = [(\dot{m}_a + \dot{m}_{di}) \times C_{pe} \times (T_{eic} - T_{amb})], kW \qquad \text{Eq. (D6)}$$

Specific heat of the exhaust gas is evaluated from energy balance of exhaust gas calorimeter as given

$$C_{pe} = \left[\dot{m}_{wic} \times C_{pw} \times (T_{wco} - T_{wic})\right]/[(\dot{m}_a + \dot{m}_{di}) \times (T_{eic} - T_{eoc})], kJ/KgK \qquad \text{Eq. (D7)}$$

Uncounted energy loses per unit time is found from

$$Q_u = [Q_{in} - (Q_s + Q_c + Q_e)], kW \qquad \text{Eq. (D8)}$$

For dual fuel operation:

Fuel energy supplied per unit time is measured by

$$Q_{in} = [(\dot{m}_p \times LHV_p) + (\dot{m}_{bg} \times LHV_{bg})], kW \qquad \text{Eq. (D9)}$$

Brake thermal efficiency (*BTE)* is calculated from

$$\text{BTE} = [(BP \times 3600 \times 100)/(\dot{m}_p \times LHV_p + \dot{m}_{bg} \times LHV_{bg})], \% \qquad \text{Eq. (D10)}$$

Energy in the by the exhaust gases per unit time is given by

$$Q_e = [(\dot{m}_a + \dot{m}_{bg} + \dot{m}_p) \times C_{pe} \times (T_{eic} - T_{amb})], kW \qquad \text{Eq. (D11)}$$

Specific heat of the exhaust gas is measured from

$$C_{pe} = \left[\dot{m}_{wic} \times C_{pw} \times (T_{woe} - T_{wie})\right]/[(\dot{m}_a + \dot{m}_{bg} + \dot{m}_p) \times (T_{eic} - T_{eoc})], kJ/KgK \quad \text{Eq. (D12)}$$

Liquid fuel replacement rate (LFR) is evaluated from

$$\text{LFR} = [\{(\dot{m}_{di} - \dot{m}_p) \times 100\}/\dot{m}_{di}], \% \quad \text{Eq. (D13)}$$

2.4.2 Exergy analysis

In internal combustion engines, the availability input (A_{in}) which is contained in the chemical availability of fuel is converted into shaft availability or useful work (A_s), availability transferred to the cooling water (A_w), availability transferred to the exhaust gases (A_e) and uncounted availability destruction (A_d) due to radiation friction, heat transfer to the surrounding, etc. The availability terms are evaluated on the basis of second law of thermodynamics as explained by Flynn (1984), Kotas (1985), Stepanov (1995), Ebiana *et al.* (2005), Sahoo *et al.* (2011, 2012) and Debnath *et al.* (2013a, 2014b).

Input availability is given by

$$A_{in} = [(1.0338 \times \dot{m}_{di} \times LHV_{di})/3600], \text{kW} \quad \text{Eq. (D14)}$$

Shaft availability is found from

$$A_s = Brake\ power, kW \quad \text{Eq. (D15)}$$

Cooling water availability is evaluated from

$$A_w = [Q_c - \dot{m}_{cw} \times C_{pw} \times T_{amb} \times ln(T_{woe}/T_{wie})], kW \quad \text{Eq. (D16)}$$

Exhaust gas availability is calculated from

$$A_e = Q_e + \left[(\dot{m}_a + \dot{m}_{di}) \times T_{amb} \times \{C_{pe} \times ln(T_{amb}/T_{eic}) - R_e \times ln(P_{amb}/P_e)\}\right], kW \quad \text{Eq. (D17)}$$

where R_e is the specific gas constant of the exhaust gas in kJ/kg K. It is calculated from the thermodynamic relation R_e=(R/molecular weight). R is the universal gas constant in

kJ/kmol.K and the molecular weight (kg/kmol) of the combustion products is calculated considering complete combustion.

Destructed Availability is evaluated by

$$A_d = [A_{in} - (A_s + A_w + A_e)], kW \quad \text{Eq. (D18)}$$

Exergy efficiency is given by

$$\eta_{II} = [1 - (A_d/A_{in})] \times 100\% \quad \text{Eq.(D19)}$$

Entropy generation is measured by

$$S = A_d/T_{amb}\,, kW/K \quad \text{Eq. (D20)}$$

For dual fuel operation:

Input availability is calculated from

For pilot fuel diesel and primary fuel biogas:

$$A_{in} = \left[(1.0338 \times \dot{m}_{pdi} \times LHV_{di}) + \left(0.95 \times \dot{m}_{bg} \times HHV_{bg}\right)\right]/3600, kW \quad \text{Eq. (D21)}$$

For pilot fuel RBB and primary fuel biogas:

$$A_{in} = \left[(0.975 \times \dot{m}_{bd} \times HHV_{bd}) + \left(0.95 \times \dot{m}_{bg} \times HHV_{bg}\right)\right]/3600, kW \quad \text{Eq. (D22)}$$

For pilot fuel WIRBB and primary fuel biogas:

$$A_{in} = \left[(0.975 \times \dot{m}_{WIR} \times HHV_{WIR}) + \left(0.95 \times \dot{m}_{bg} \times HHV_{bg}\right)\right]/3600, kW \quad \text{Eq. (D23)}$$

Exhaust gas availability is given by

$$A_e = Q_e + \left[\left(\dot{m}_a + \dot{m}_{bg} + \dot{m}_p\right) \times T_{amb} \times \{C_{pe} \times ln(T_{amb}/T_{eic}) - R_e \times ln(P_{amb}/P_e)\}\right], kW \quad \text{Eq. (D24)}$$

List of Publications

Journals:

1. **Bora BJ**, and Saha UK, (2016), Optimization of injection timing and compression ratio of a raw biogas run dual-fuelled diesel engine, *Applied Thermal Engineering,* Vol. 92, pp.111-121.

2. **Bora BJ**, and Saha UK, (2016), Estimating the theoretical performance limits of a biogas powered dual fuel diesel engine using emulsified rice bran biodiesel as pilot fuel, *ASME Journal of Energy Resources Technology,* Vol. 138, pp. 021801-1–021801-10.

3. **Bora BJ,** and Saha UK, (2016), Experimental evaluation of a rice bran biodiesel- biogas run dual fuel diesel engine at varying compression ratios, *Renewable Energy*, Vol. 87, pp. 782-790.

4. **Bora BJ**, and Saha UK, (2015), Theoretical performance limits of a biogas–diesel powered dual fuel diesel engine for different combinations of compression ratio and injection timing, *ASCE Journal of Energy Engineering*, Vol. 140, pp. E4015001-1 – E4015001-9.

5. **Bora BJ**, and Saha UK, (2015), Improving the performance of a biogas powered dual fuel diesel engine using emulsified rice bran biodiesel as pilot fuel through adjustment of compression ratio and injection timing, *ASME Journal of Engineering for Gas Turbines and Power*, Vol. 137, No. 9, pp. 091505-1–091505-14.

6. **Bora BJ**, and Saha UK, (2015), Comparative assessment of a biogas run dual fuel diesel engine with rice bran oil methyl ester, pongamia oil methyl ester and palm oil methyl ester as pilot fuels, *Renewable Energy*, Vol. 81, pp. 490-498.

7. **Bora BJ**, and Saha UK, (2014), Effect of compression ratio on performance, combustion and emission characteristics of a dual fuel diesel engine run on raw biogas, *Energy Conversion and Management*, Vol. 87, pp. 1000 – 1009.

8. **Bora BJ**, Debnath BK, Gupta N, Saha UK, and Sahoo N, (2013), Investigation on the flow behaviour of a venture type gas mixer for dual fuel diesel engines, *International Journal of Emerging Technology and Advanced Engineering*, Vol. 3, pp. 202 - 209.

Conferences:

1. **Bora BJ**, Saha UK, Chatterjee S, and Veer V, (2014), Effect of load level on the performance and emission characteristics of a biogas run dual fuel diesel engine, *5th International (& 41st National) Conference on Fluid Mechanics and Fluid Power*, December 12-14, IIT Kanpur, India.

2. **Bora BJ**, and Saha UK, (2014), On the attainment of optimum injection timing for pilot fuel in a dual fuel diesel engine run on biogas, Paper No**.** ESDA2014-20162, *ASME 12th Biennial Conference on Engineering Systems Design and Analysis*, June 25–27, Copenhagen, Denmark**.**

3. Verma VS, **Bora BJ**, Sarkar A, and Saha UK, (2014), Experimental investigation of a dual fuel diesel engine run on scrubbed biogas using the method of adsorption, Paper No**.** ESDA2014-20164, *ASME 12th Biennial Conference on Engineering Systems Design and Analysis*, June 25–27, Copenhagen, Denmark**.**

4. **Bora BJ**, and Saha UK, (2013), Energy and exergy analysis of a dual fuelled diesel engine run on biogas, *4th International Conference on Advances in Energy Research*, ICAER-2013, December 10-12, IIT Bombay, India.